Exploring the Roles of the Centrosomal RASSF Proteins, RASSF1A & RASSF7, in Stem Cells & Cancer

Leanne Bradley
St Anne's College



Thesis submitted to the University of Oxford for the degree of Doctor of Philosophy

Michaelmas Term 2017

Supervisor: Prof. Eric O'Neill (University of Oxford)





St Anne's College

The work presented in this thesis was performed at the CRUK/MRC Oxford Institute for Radiation Oncology, Department of Oncology, University of Oxford. Leanne Bradley is funded by a Medical Sciences Graduate School Studentship from the Medical Research Council and Department of Oncology. Eric O'Neill is funded by Cancer Research UK and the Medical Research Council

Abstract

Exploring the Roles of the Centrosomal RASSF Proteins, RASSF1A & RASSF7, in Stem Cells & Cancer

Submitted for the Degree of Doctor of Philosophy

Leanne Bradley, St Anne's College, Michaelmas Term 2017

The Ras – Association Domain Family (RASSF) is a group of ten structurally related proteins that have been linked to a series of human pathologies. RASSF1A is the most widely studied member of this group and is a *bona fide* tumour suppressor gene that has been reported as the most frequently epigenetically silenced gene in human sporadic malignancies. Loss of *RASSF1A* expression is linked to poor prognosis and a more aggressive clinical phenotype. Recently, RASSF1A has been linked to the regulation of pluripotency via modulation of the Hippo pathway and the transcriptional output of YAP associated genes. Here, we present evidence that the asymmetric localisation and subsequent inheritance of RASSF1A can influence the fate determination of differentiating stem cells. We propose that this event is the molecular basis of the clinical observation that RASSF1A loss leads to increased stem cell signatures in patient tumours. We also demonstrate that the asymmetry of RASSF1A is correlated to centrosome age and describe for the first time a role for RASSF1A in the assembly of the primary cilium, an important sensory organelle involved in signal transduction and development. Furthermore, we present an explorative study of RASSF7 function. RASSF7 is a widely-underexplored member of the RASSF group. It functions typically as an oncogene, yet relatively little is known about its molecular role. We show that RASSF7 interacts with the Hippo core kinase MST2 and has an important role in its subcellular localisation. This thesis focuses primarily on further establishing the molecular roles of RASSF1A and RASSF7 to determine how their deregulation leads to tumourigenesis.

For my wonderful family and very best friend

Acknowledgements

To my supervisor, Eric, thank you for giving me the opportunity to work on this project and your help over the years. I am particularly grateful for your understanding when it came to some difficult times, and for being able to drop into your office for a bit of craic!

I would like also to thank my examiners for taking the time to read and examine my thesis.

A huge thank you to the O'Neill Lab Members past and present who have made my DPhil studies such an enjoyable experience. Nikola, Aswin, Ali, Daniela & Jelte, thanks for all the laughs! Asmita, thanks for being such a doll and all your help over the past while and thank you to Michael for all your bioinformatics help and sense of humour! Also, thank you to others in the department who made this whole experience that bit more fun, especially Ella, Neele, Greg, GG and Luiza as well as Sibyl, thanks for always being around for a chat! Thanks also to Graham and Rhod for all your help with imaging over the years!

I would especially like to thank three very special ladies without whom my DPhil experience would have been very different! Firstly, I would like to thank the queen of our lab, Dafni! Thank you for your guidance in the lab and friendship everywhere else. Maria-Laura, our Italian sweetheart, thank you for always being there for me no matter what. Last but certainly not least, a huge thank you to Delia who has been an exceptional housemate, colleague and friend over the last four years. I don't know what I would have done without you (literally in some cases following the ops), I feel like I have gained another sister in you.

Thank you to my Stanners; Nat, Christina, Ben, Kristen, Hillary, Hannah & Henri - who made coming to Oxford at the start much less scary!

To my wonderful family & friends – Thank you to my parents for all their support, without which I would never be able to have done this – thank you especially to my Mammy for always believing in me. Thank you to all my siblings and nieces and nephews for being such a source of joy. Thank you to Áine & Darran who made home seem a bit closer over here and I would like to especially thank Nicola, who always made sure I was doing alright! All the facetimes with you and your amazing children helped me more than I think you could ever know.

Finally, I would like to thank you, Jonny. Without your unending support, love and faith – I could not have done this.

Go raibh míle maith agaibh go léir, ó bhun mo chroí.

Contents

Contents

Abstract I
Acknowledgements III
Contents IV
List of Figures XI
List of Tables XIV
Abbreviations XV
Chapter 1 1

Introduction 1
1. Introduction 1
1.1 Cancer 1
1.2 Stem Cells 3
1.2.1 Mouse Embryonic Stem Cells 4
1.2.2 Totipotency & Pluripotency 4
1.2.3 Differentiation 5
1.2.4 Asymmetric Cell Division and Fate Determination 5
1.2.5 Stem Cells & Cancer 7
1.3 Centrosomes & Cilia 9
1.3.1 Centrosomes 9
1.3.2 Cilia 14
1.3.3 Centrosome & Cilia Function 20

1.3.4 Centrosomes & Cilia in Human Pathology 25

1.4 RASSF1A & RASSF7 28

1.4.1 Ras Signalling: The Oncoproteins and their Effectors 28

1.4.2 The Ras-Association Domain Family 29

1.4.3 RASSF1A 30

1.4.4 RASSF1A & Cancer 31

1.4.5 Hippo Signalling 33

1.4.6 RASSF1A & Apoptosis 35

1.4.7 RASSF1A & Genome Integrity 36

1.4.8 RASSF1A in Stem cells 36

1.4.9 RASSF1A in Mitosis and Cell Cycle Control 37

1.4.10 RASSF1A in Cancer 40

1.4.11 RASSF7 42

1.4.12 RASSF7 & Cancer 44

1.5 Aims of this Work 46

Chapter 2 47

Methods & Materials 47

2.1 General Laboratory Reagents 47

2.2 Cell Culture 47

2.2.1 Mouse ESC Differentiation 48

2.2.2 Transient (Forward) Transfection 48

2.2.3 Transient (Reverse) Transfection 49

2.2.4 Drug Treatment 49

2.2.5 Induction of Ciliogenesis 49

2.3 Chemicals 50

2.4 Buffers 51

2.5 RNAi Sequences 51

2.6 Primary Antibodies for Immunofluorescence 52

2.7 Primary Antibodies for Western Blot 53

2.8 Secondary Antibodies 53

2.9 Molecular Biology 54

2.9.1 Molecular Cloning 54

..... 54

2.9.2 Bacterial Transformation 54

2.9.3 Plasmid Isolation 56

2.10 Biochemistry 56

2.10.1 Cell Lysate Extraction & Quantification 56

2.10.2 Immunoprecipitation 56

2.10.3 Immunoblotting 57

2.10.4 Immunofluorescence 58

2.11 Microscopy 59

2.11.1 Confocal 59

2.11.2 Live Imaging..... 59

2.12 Image Analysis 60

2.12.1 Zen..... 60

2.12.2 Image J – Quantification of Fluorescence Intensity 60

2.12.3 Image J – Cilia Length 60

2.12.4 Image J - Nuclear Size and Scoring 61

2.13 Computational Biology 61

2.13.1 Gene Set Enrichment Analysis..... 61

2.13.2 Kaplan Meier Curves 63

2.14 Statistics..... 63

Chapter 3..... 64

Results I 64

3.1 Introduction 64

3.2 RASSF1A Expression Correlates with a Differentiation Phenotype..... 65

3.3 RASSF1A Localises to the Centrosomes of mESCs 69

3.4 RASSF1A is Asymmetric at the Centrosomes of mESCs & may Function in Asymmetric Cell Division 71

3.5 RASSF1A Expression Affects the Pluripotent Status of Cancer Cells..... 79

3.6 Discussion 82

Chapter 4..... 85

Results II 85

4.1 Introduction 85

4.2 RASSF1A Localises with the more mature centrosome and centriole in mESCs 86

4.3 RASSF1A Localises with the Mother Centriole and Basal Body of ARPE19 cells 90

4.4 RASSF1A Depletion Leads to Defects in Ciliogenesis 93

4.5 RASSF1A Effect on Ciliation Levels Correlates with Changes in αTubulin Acetylation Independently of HDAC6 95

4.6 RASSF1A Depletion Leads to Defective Cilium Assembly Induction 101

4.7 RASSF1A Expression in LUAD Cell Lines Correlates with Ciliation..... 104

4.8 Discussion 106

Chapter 5..... 109

Results III 109

5.1 Introduction 109

5.2 RASSF7 Dynamics..... 110

5.3 RASSF7 is Not Associated with the Endosome..... 114

5.4 Exploring RASSF7 at the Nuclear Periphery 118

5.5 RASSF7 and Cancer 125

5.6 Discussion 129

Chapter 6..... 132

Discussion..... 132

6.1 RASSF1A & Pluripotency 132

6.1.1 Remaining Questions 135

6.2 RASSF1A and the Cilium 139

6.2.1 Remaining Questions 144

6.3 Connecting the Dots 145

6.4 RASSF7 145

6.4.1 Remaining Questions 149

6.5 Concluding Remarks 151

Chapter 7 – Appendices 152

7.1 Appendix I 152

7.2 Appendix II 166

7.3 Appendix III – Original Copyright Notices 167

Figure 1.1 167

References 174

Declaration

I declare that this thesis was composed by myself and the work presented herein is wholly my own, except where explicitly stated otherwise. No portion of this work has been submitted previously for any other degree or qualification at this or any other University.

Nomenclature

Human gene symbols are denoted in upper case italics (e.g. *RASSF1*) whilst mouse genes are italicised with the first letter in uppercase and the remaining letters in lowercase (e.g. *Rassf1*). Human and mouse protein symbols are denoted in upper case lettering (e.g. RASSF1). Species are denoted in italic lettering (e.g. *Drosophila Melanogaster*).

List of Figure

FIGURE 1. 1 THE HALLMARKS OF CANCER 2

FIGURE 1. 2 ASYMMETRIC CELL DIVISION CAN LEAD TO THE DETERMINATION OF DIFFERENTIAL CELL FATES. 6

FIGURE 1. 3 CENTROSOME STRUCTURE..... 10

FIGURE 1. 4 THE CENTROSOME CYCLE. 12

FIGURE 1. 5 THE PRIMARY CILIUM. 15

FIGURE 1. 6 THE RASSF PROTEIN FAMILY. 30

FIGURE 1. 7 THE MAMMALIAN HIPPO SIGNALLING PATHWAY. 33

FIGURE 2. 1 PZSGREEN PLASMID MAP..... 54

FIGURE 2.2 DNA RESTRICTION DIGEST SHOWING THE SUCCESSFUL INTEGRATION OF RASSF7 CDNA INTO A PZSGREEN BACKBONE 55

FIGURE 3. 1 ENDOGENOUS RASSF1A LOCALISATION..... 66

FIGURE 3. 2 RASSF1A EXPRESSION INCREASES AS MESCS DIFFERENTIATE. 67

FIGURE 3. 3 RASSF1A KNOCKDOWN CAUSES AN INCREASED ‘STEMNESS’ PHENOTYPE 68

FIGURE 3. 4 ZSRASSF1A LOCALISES WITH THE CENTROSOMES OF MITOTIC MESCS 70

FIGURE 3. 5 OVEREXPRESSION OF RASSF1A DOES NOT AFFECT MITOTIC INDEX OR CENTRIOLE NUMBERS IN MESCS 71

FIGURE 3. 6 ZSRASSF1A CAN LOCALISE AT THE CENTROSOMES ASYMMETRICALLY AND SYMMETRICALLY. 73

FIGURE 3. 7 ENDOGENOUS RASSF1A ASSOCIATES WITH THE CENTROSOME SYMMETRICALLY AND ASYMMETRICALLY 74

FIGURE 3. 8 ZSRASSF1A IS ACTIVELY ASYMMETRICALLY DISTRIBUTED DURING MITOSIS OF MESCS..... 75

FIGURE 3. 9 RASSF1A IS POLARISED TO THE CELL PERIPHERY IN DIFFERENTIATING STEM CELLS 77

FIGURE 3. 10 RASSF1A IS SYMMETRICALLY AND ASYMMETRICALLY INHERITED WITH THE FATE DETERMINANT NUMB. 78

FIGURE 3. 11 ZSRASSF1A ASYMMETRICALLY LOCALISES WITH THE CENTROSOMES OF MITOTIC CANCER CELLS..... 80

FIGURE 3. 12 ZSRASSF1A OVEREXPRESSION LEADS TO A DECREASE IN PLURIPOTENCY MARKER EXPRESSION IN CANCER CELLS. 81

FIGURE 3. 13 LOSS OF RASSF1A IN GBM COHORT CORRELATES WITH AN INCREASE IN STEM CELL SIGNATURE EXPRESSION 82

FIGURE 4. 1 RASSF1A LOCALISES PREFERENTIALLY WITH THE MORE MATURE CENTRIOLE..... 87

FIGURE 4. 2 RASSF1A LOCALISES WITH THE MATURE CENTRIOLE MARKER CEP164 IN MESCS 88

FIGURE 4. 3 RASSF1A LOCALISES SYMMETRICALLY AND ASYMMETRICALLY WITHIN THE CENTROSOMES 89

FIGURE 4. 4 RASSF1A LOCALISES WITH THE CENTROSOMES OF HUMAN ARPE19 CELLS..... 91

FIGURE 4. 5 RASSF1A LOCALISES AT THE BASAL BODY OF THE PRIMARY CILIUM. 92

FIGURE 4. 6 RASSF1A DEPLETION LEADS TO A DECREASE IN CILIA NUMBERS. 93

FIGURE 4. 7 RASSF1A DEPLETION CAUSES ANOMALIES IN CILIARY SHAPE AND PROTEIN LEVELS..... 94

FIGURE 4. 8 REDUCTION OF RASSF1A EXPRESSION LEADS TO A DECREASE OF ACETYLATED αTUBULIN SIGNAL..... 96

FIGURE 4. 9 RASSF1A IS ASSOCIATED WITH ACETYLATED α-TUBULIN 97

FIGURE 4. 10 HDAC6 LOCALISATION IS INDEPENDENT OF RASSF1A 98

FIGURE 4. 11 TUBACIN MEDIATED INHIBITION OF HDAC6 DOES NOT RESCUE THE RASSF1A INDUCED PHENOTYPE DURING CILIOGENESIS 100

FIGURE 4. 12 RASSF1A AND IFT88 COLOCALISE AT THE BASAL BODY OF THE CILIUM 102

FIGURE 4. 13 RASSF1A DOES NOT AFFECT CILIATION LEVELS OR CILIUM LENGTH POST-ASSEMBLY..... 103

FIGURE 4. 14 EXPRESSION OF RASSF1A CORRELATES WITH CILIATION IN LUAD CELL LINES 105

FIGURE 5. 1 ZSRASSF7 DISPLAYS A DYNAMIC STAINING PATTERN THROUGHOUT THE CELL CYCLE. 111

FIGURE 5. 2 ENDOGENOUS RASSF7 LEVELS VARY WITH THE CELL CYCLE..... 113

FIGURE 5. 3 ZSRASSF7 VESICLES ARE MOTILE..... 116

FIGURE 5. 4 ZSRASSF7 DOES NOT LOCALISE WITH TESTED MVB MARKERS 117

FIGURE 5. 5 RASSF7 LOCALISES AT THE PERIPHERY OF THE NUCLEAR ENVELOPE 119

FIGURE 5. 6 RASSF7 DEPLETION DOES NOT AFFECT NUCLEAR ENVELOPE INTEGRITY 121

FIGURE 5. 7 RASSF7 & MST2 ARE ASSOCIATED WITH ONE ANOTHER..... 123

FIGURE 5. 8 DEPLETION OF RASSF7 REMOVES MST2 FROM THE NUCLEAR PERIPHERY..... 124

FIGURE 5. 9 RASSF7 EXPRESSION CORRELATES DIFFERENTIALLY WITH OVERALL SURVIVAL IN DIFFERENT CANCERS 126

FIGURE 5. 10 RASSF7 EXPRESSION IN STAD & PAAD CORRELATES WITH CHANGES IN SEVERAL TYPES OF GENE SIGNATURES 128

FIGURE 6. 1 HYPOTHETICAL MODEL OF RASSF1A AND NUMB ASSOCIATIONS DURING DIFFERENTIATION. 136

FIGURE 6. 2 MODEL OF RASSF1A LOCALISATION WITHIN THE CENTROSOME 140

FIGURE 6. 3 MODEL OF RASSF1A IN THE FORMATION OF THE PRIMARY CILIUM. 143

FIGURE 6. 4 HYPOTHESISED MODELS OF ACTION FOR RASFF7 MEDIATED REGULATION OF MST2 PROTEIN LEVELS AND LOCALISATION 148

FIGURE 7. 1. OVERALL ASYMMETRY OF ENDOGENOUS RASSF1A IN MITOTIC MESCS. APPROX. 20 MITOSES COUNTED PER EXPERIMENT, P = 0.001383 152

FIGURE 7. 2 RASSF1A DOES NOT EXHIBIT ANY OBVIOUS CORRELATION OR LOCALISATION WITH ENDOSOMAL MARKERS 153

FIGURE 7. 3 MST2 LOCALISES WITH HP1A AT THE NUCLEAR PERIPHERY 154

FIGURE 7. 4 RASSF7 EXPRESSION DATA ACROSS HUMAN TUMOUR TYPES 155

FIGURE 7. 5 PRASSF1A SER131, CAN TRAVERSE THE CILIARY AXONEME. 164

FIGURE 7. 6 RASSF7 LOCALISES AT THE MIDBODY RING OF CYTOKINETIC CELLS, AS MARKERD WITH THE CENTRALSPINDLIN COMPONENET MKLP1 165

List of Tables

TABLE 4. 1 LUAD LINES AND THEIR RESPECTIVE LEVELS OF RASSF1A RNA AND PROMOTER METHYLATION. 104

TABLE 7. 1 DESCRIPTION OF THE NUCLEAR ENVELOPE PHENOTYPES ANALYSED IN FIGURE 5.6 154

TABLE 7. 2 TOP 50 GO CELLULAR COMPONENT GENE SETS ENRICHED WITH HIGH RASSF7 EXPRESSION IN STAD. 159

TABLE 7. 3 TOP 50 GO CELLULAR COMPONENT GENE SETS ENRICHED WITH HIGH RASSF7 EXPRESSION IN PAAD. 163

Abbreviations

APC/Cdc-20	Anaphase promoting complex/Cdc20
Approx.	Approximately
ATM	Ataxia-telangiectasia mutated
ATR	Ataxia-telangiectasia – and Rad3 – related
AURKA	Aurora - A
Bax	BCL2 Associated X, Apoptosis Regulator
BMP	Bone Morphogenic Protein
CACNA2D2	Calcium Voltage-Gated Channel Auxiliary Subunit $\alpha 2\delta 2$
CC	Cancer cell
CDK	Cyclin Dependent Kinase
CDK2	Cyclin-dependent kinase 2
CEP164	Centrosomal Protein 164
Cep97	Centrosomal Protein 97
cm	Centimetre
CHMP1B	Charged Multivesicular Body Protein 1B
CP110	Centriolar coiled-coil protein of 110 kDa
CPLANE	Ciliogenesis and Planar Polarity effectors
CSC	Cancer Stem Cell
C-terminal	Carboxyl-terminal
CYB561D2	Cytochrome B561 Family Member D2
DAVs	Distal appendage vesicles
DAXX	Death Domain- Associated Protein 6
DDR	DNA Damage Response
DISC1	Disrupted in schizophrenia 1
DMEM	Dulbecco's Modified Eagle's Medium
DMSO	Dimethyl Sulfoxide
DNA	Deoxyribonucleic Acid
DTC	Distal Tip Cell
E#	Embryonic Development Day #
EDTA	Ethylenediaminetetraacetic acid
EEA1	Early Endosome Antigen 1
ESCRT-III	Endosomal Sorting Complex Required for Transport 3
FBS	Foetal Bovine Serum
FCS	Foetal Calf Serum
FSG	Fish Skin Gelatin
FUS1	FUS (Fusion) RNA Binding Protein
GATA1	GATA binding protein 1
Gli	Glioblastoma associated transcription factor
GSC	Germline Stem Cell
GSC	Germline Stem Cell
GSEA	Gene Set Enrichment Analysis

GTP	Guanosine triphosphate
GTPase	Guanosine triphosphatase
h	Hour
HDAC6	Histone deacetylase 6
HEF1	Human Enhancer of Filamentation 1
hESCs	Human embryonic stem cells
Hh	Hedgehog
HRC1	HRas cluster 1
HYAL2	Hyaluronoglucosaminidase 2
IBD	Inflammatory bowel disease
ICM	Inner Cell Mass
IDD	Intervertebral Disc Degeneration
IF	Immunofluorescence
IFT	Intraflagellar transport
K40	Lysine 40
Kif24	Kinesin Family Member 24
Kif2a	Kinesin Family Member 2a
KIF7	Kinesin family member 7
KM-Plot	Kaplan-Meier Plot
LATS	Large Tumour Suppressor
LB	Lysogeny Broth
LIF	Leukaemia Inhibitory Factor
LOH	Loss of Heterozygosity
LSM	Light scanning microscope
LUCA2	Lung Carcinoma Protein 2
MAP1	Microtubule Associated Protein 1
MAPK	Mitogen activated protein kinase
MAPs	Microtubule Associated Proteins
MEFs	Mouse embryonic fibroblasts
mESC	Mouse embryonic stem cells
min	Minute
MIP	Maximum Intensity Projection
MKK7	Mitogen-activated protein kinase kinase 7
μm	Micrometre
MST	Mammalian sterile 20-like kinase
MST	Mammalian sterile 20-like protein
MT	Microtubule
MTOC	Microtubule organising centre
MVB	Multivesicular body
NB	Neuroblast
NCI	National Cancer Institute
NDR1/2	Nuclear dbf2-related kinases 1/2
NEDD9	Neural Precursor Cell Expressed, Developmentally Down-Regulated

nM	Nanomolar
NORE1	Novel Ras Effector 1
NPRL2	Nitrogen permease regulator 2-Like protein
NSCLC	Non-small cell lung carcinoma
N-terminal	Amino-terminal
NuMA	Nuclear Mitotic Apparatus Protein
ºC	Degrees Centigrade
ODF2	Outer Dense Fibre of Sperm Tails 2
P/S	Pen/strep
PBS	Phosphate Buffered Saline
PCM	Pericentriolar material
PCP	Planar cell polarity
PDAC	Pancreatic ductal adenocarcinoma
Pen/Strep	Penicillin/Streptomycin
PI3K	Phosphatidylinositol-4,5-bisphosphate 3-kinase
PL6	Placental protein 6,
Plk1	Polo-like kinase 1
PTCH1	Patched-1
PTM	Post translational modification
R1A	RASSF1A
RA	Ras Association
RABP1	RASSF1A-binding protein 1
RAF	Rapidly Accelerated Fibrosarcoma
Ras	Rat Sarcoma
RASSF	Ras Association Domain Family
RASSF1A	Ras Association Domain Family member 1A
RASSF7	Ras Association Domain Family member 7
RB	Ras Binding
Rb	Retinoblastoma
RG	Radial Glial
RTK	Receptor tyrosine kinase
SARAH	Sav – RASSF – Hpo
Sas4	Spindle assembly abnormal 4 orthologue
SAV1	Salvador 1
SC	Stem Cell
Ser	Serine
SIRT1	Sirtuin 1
SIRT2	Sirtuin 2
SMO	Smoothened
SOX2	SRY (sex determining region Y) - box 2
STK3/4	Serine/threonine-protein kinase 3/4
STLC	S-trityl-L-cysteine
Sufu	Suppressor of fused
TAZ	Transcriptional Co-activator with PDZ-binding Motif

TF	Transcription Factor
TGFβ	Transforming growth factor β
TIC	Tumour initiating cell
TSG	Tumour suppressor gene
TTBK2	Tau tubulin kinase 2
TUBA	Tubacin
TUSC2	Tumour suppressor candidate 2
TUSC4	Tumour suppressor candidate 4
TZ	Transition Zone
v/v	Volume to Volume Ratio
VZ	Ventricular Zone
WHO	World Health organisation
Wnt	Wingless-related integration site
WT	Wild type
XPA	Xeroderma Pigmentosum Complementation Group A
YAP	Yes-associated protein
ZMYND10	Zinc Finger Myeloid, Nervy, DEAF1 Domain-Containing Protein 10
ZsGreen	ZsGreen - Empty Vector
ZsR1A	ZsGreen RASSF1A

Chapter 1

Introduction

1. Introduction

1.1 Cancer

Cancer is a term used to define a broad range of neoplastic diseases which are generally characterised by the uncontrollable and defective growth of cells. These aberrant cells have the potential to spread throughout the body and disrupt normal cellular function, leading ultimately to death. According to the World Health Organisation (WHO), cancer is the second leading cause of death in the world and is a major strain on worldwide health providers. In the United Kingdom, breast, lung, prostate, and bowel cancers are the most common of over 200 cancer types (Cancer Research UK).

Cancer is a multifactorial disease, and across the broad spectrum of tumour types there are several intra- and extracellular changes that are frequently observed – typically referred to as the 'Hallmarks of Cancer' (Figure 1.1). These features allow disease progression, and include the ability of cancers to replicate continuously, evade cell death and harbour genome instability (Hanahan and Weinberg, 2011). Together, these features allow the progression of tumourigenesis. Importantly, these traits can each be

accounted to the disruption of proper and normal cellular function, highlighting the need to understand their basis on a molecular level to improve cancer therapies.

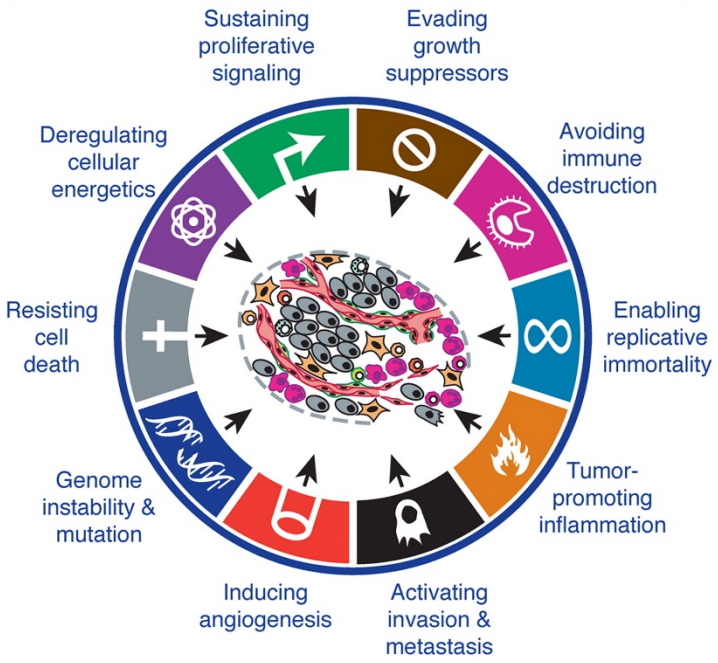


Figure 1. 1 The Hallmarks of Cancer *There are a number of unifying traits observed in human malignancies which promote tumour progression. (Adapted from Hanahan and Weinberg, 2011).*

The majority of cancers are caused by acquired genetic changes. These can be sporadic or caused by carcinogens and other risk factors including tobacco and alcohol (WHO). The two major types of cancer related genes are oncogenes and tumour suppressor genes (TSGs). Oncogenes are often upregulated in cancer, with their expression causing cellular transformation. Typically, these genes exist in a regulated manner in normal cells, ensuring that cells grow normally and maintain homeostasis. However, upon cellular insult, such as a mutation, the function of these genes proceeds uncontrollably. Conversely, TSGs normally have roles in the suppression of cell proliferation and growth and their expression is often found to be lost in malignancy.

The way in which oncogenes are activated or TSGs suppressed can occur through direct changes to the DNA, known broadly as mutations, or via indirect changes such as epigenetic alterations, i.e. DNA methylation. In both cases the result is inappropriate gene expression. Obesity is another factor that can increase the risk of cancer development; however, this has not been shown to be a result of genetic changes. Instead, obesity is thought to cause tumourigenesis by deregulating several cellular processes via improper control of aggravating factors including inflammation and growth hormones (Font-Burgada et al., 2016).

1.2 Stem Cells

Stem cells (SCs) are an undifferentiated, unspecialised cell type with the potential to divide asymmetrically and differentiate or divide symmetrically to self-renew or terminally differentiate. Stem cells were originally described in the embryo but soon after adult stem cells, which reside in certain tissues of developed organisms, were identified. Whilst embryonic stem cells are clearly important in development, adult SCs were quickly associated with several important roles, particularly in maintaining cell populations (as seen in the haematopoietic system) or in tissue repair and regeneration (as seen during wound healing). The unique replicative and differential characteristics of SCs means that they offer an intriguing potential to open new avenues of regenerative medicine, which could lead to treatments for diseases such as diabetes and heart disease.

1.2.1 Mouse Embryonic Stem Cells

Embryonic SCs (ESCs) are those derived from the embryo. Scientists initially isolated and cultured mouse ESCs (mESCs) from the inner cell mass (ICM) of a mouse blastocyst in 1981 (Evans and Kaufman, 1981). Many years were spent trying to establish the factors that would maintain pluripotency in cultured mESCs as initially they required maintenance in foetal calf serum (FCS) on a layer of mouse embryonic fibroblast (MEF) 'feeder' cells. However, in these conditions, it was difficult to maintain the SCs in a pluripotent state and eventually the 'pluripotency factor' was discovered to be the cytokine, leukaemia inhibitory factor (LIF) (Williams et al., 1988). Nowadays, there is a carefully defined medium for mESC culture (however, there remains some unknown factors in FCS) which includes LIF. To induce differentiation, one simply needs to withdraw LIF from the culture medium.

1.2.2 Totipotency & Pluripotency

Totipotency is defined as the ability of a cell to form all cell types in an organism, including the extra-embryonic tissue. The SCs of the ICM are pluripotent, meaning they have lost the ability to form extra-embryonic tissue but still have the capacity to form every cell type from each germ layer. Extensive research has been conducted to establish what gives such staggering potential to SCs and it is now understood that a set of core transcription factors (TFs) mediate this characteristic. These TFs include NANOG (NANOG homeobox) and OCT4A (Octamer Binding Protein 4/POU Class 5 Homeobox 1). The pluripotency TFs regulate a plethora of genes, either activating or repressing their expression as appropriate. In 2006 it was shown that overexpression of what are now

known as the Yamanaka factors can reverse the differentiated phenotype of mouse fibroblasts, reprogramming them to an ESC-like state.

1.2.3 Differentiation

Understanding the differentiation process, particularly of lineage specific differentiation, is essential if regenerative medicine is to reach its full potential. The onset of differentiation is accompanied by extensive changes in gene expression. Included in this change is the suppression of the pluripotency promoting genes which can be silenced by methylation, as is seen in the case of Nanog and OCT4A (Bernstein et al., 2006; Mikkelsen et al., 2007). During differentiation, stem cells must commit to a specific lineage. Lineage specification is governed by the action of specific transcription factors (TFs). GATA-1 (GATA Binding Protein 1), for example, was one of the first to be identified as an essential erythro-megakaryocytic TF which mediates the specification of certain blood cells (Evans and Felsenfeld, 1989; Tsai et al., 1989). These TFs cause commitment by upregulating the expression of lineage specific genes and facilitate the formation of the three germ layers.

1.2.4 Asymmetric Cell Division and Fate Determination

Differentiation is often referred to as fate specification. One way in which cells can ensure diverging fates in daughter cells following division is through the asymmetric distribution of cell fate determinants (Figure 1.2), in other words, through asymmetric cell division (ACD).

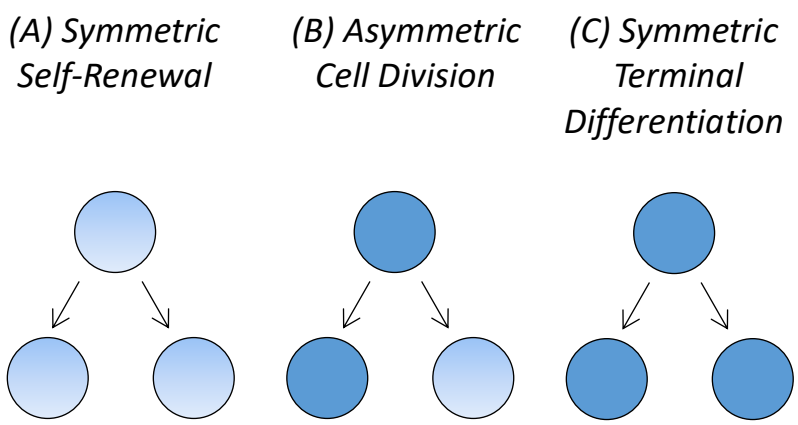


Figure 1. 2 Asymmetric Cell Division can lead to the determination of differential cell fates. (A) Stem cells can self-renew by symmetric cell division, with both daughter cells retaining a stem cell phenotype. (B) Asymmetric cell division is determined by the segregation of fate determinants (dark blue). The cell that inherits the fate determinant will have a different fate to the other daughter cell, such as differentiation. (C) A third option is symmetric terminal differentiation, where a differentiating fate determinant is distributed between both daughter cells that then go on to differentiate. In this scenario, the stem cell is depleted.

ACD can be achieved through extrinsic or intrinsic mechanisms. In the first scenario, signals from the external microenvironment (the stem cell niche) act on the cell. The SC niche is important in maintaining a stem-like fate as it provides biochemical, structural and mechanical signals which modulate the activity of cells within its proximity. An example of a SC niche was first described in *C. elegans*, where it was shown that the mesenchymal distal tip cell (DTC) of the gonad was necessary in the proper differentiation of germ-line stem cells (GSCs) to adult tissue cells (Kimble and White, 1981). The DTC maintains the SC like character of the proximal GSC via Notch signalling, an important regulator of SC behaviour (Pepper et al., 2003; Liu et al., 2010).

During intrinsically directed ACD, regulators of cell fate are physically localised asymmetrically which results in differential inheritance. The asymmetric inheritance of cell fate determinants leads to divergences in the way two daughter cells will proceed to function. The first reported segregating fate determinant, Numb, was discovered in

Drosophila (Rhyu et al., 1994). Numb has been found to function primarily through inhibition of Notch signalling by endocytosis and ubiquitination of the Notch-1 receptor (Frise et al., 1996; McGill and McGlade, 2003; Couturier et al., 2012) – the loss Notch signalling is then permissive to differentiation. The relevance of Numb function in the mammalian system was demonstrated in 2002, when it was shown that asymmetric inheritance of Numb is essential for proper ACD during mouse cerebral cortical development (Shen et al., 2002). Knowledge of ACD in vertebrates is lacking, with information existing primarily on ACD in *Drosophila* and *C. elegans.* However, ACD has been implicated in development and is regarded as an important regulator of tissue maintenance in homeostasis and injury, highlighting the need for further investigation.

1.2.5 Stem Cells & Cancer

Cancer cells (CCs) and SCs harbour many similarities. First and foremost, both cell types have the shared capability of being replicatively immortal – this prompted further study into the similarities between the two and led to the cancer stem cell (CSC) hypothesis. Cancer cells often display ESC-like phenotypes, with the first tumour 'stem cells' being described in 1971. The CSC theory proposes that tumours are fuelled by a sub-population of CSCs or 'tumour initiating' cells (TICs). Extensive research has been carried out into this field, and CSCs have been identified in leukaemia (Lapidot et al., 1994; Bonnet and Dick, 1997), as well as tumours of the brain (Singh et al., 2004), breast (Al-Hajj et al., 2003), colon (O'Brien et al., 2007; Ricci-Vitiani et al., 2007), pancreas and others (Li et al., 2007).

The interest fuelling investigations into CSCs lies in their therapeutic implications. Current models of tumour cell populations pertain that the heterogeneity observed in cancers is the result of a 'tumour hierarchy'. The CSC is hypothesised to fuel tumour growth and is the parent cell of the hierarchy, capable of self-renewal. Importantly, CSCs display resistance to current chemo- and radiotherapy treatments which leads to disease relapse. Therefore, effort is being made to target and eliminate these CSCs from tumours as a treatment avenue. To effectively design such treatments, it is important that we understand how this stem-like phenotype arises and persists. This can be achieved through a combinational approach whereby normal SC pathways are unravelled and studied in parallel in CCs.

ACD is an essential feature of CSCs, as it is needed to allow tumour expansion whilst retaining the parent SC. However, it has been suggested that such cells have a limited capacity for terminal differentiation, further fuelling the SC-phenotype of the cancer (Driessens et al., 2012). Deregulation of ACD regulators in *Drosophila* has been linked to the onset of tumourigenesis following the mutation of several important cell fate directing genes, including *numb*. Loss of these regulators led to massive overexpansion of *Drosophila* neuroblasts, which were also able to invade other tissues and displayed typical cancerous phenotypes (Caussinus and Gonzalez, 2005).

Deregulation of ACD has been identified in human cancers. The fate determinant Numb has been described as a tumour suppressor that promotes the normal function of the major TSG p53 (Colaluca et al., 2008). Further, Numb depleted breast cancers are phenotypically aggressive and found to have upregulated Notch signalling (Pece et al., 2004), typically associated with an increased SC character. Similar findings in Chronic

Myelogenous Leukaemia (CML) have implicated Numb in disease progression, showing that its expression is repressed by another cell fate determinant, Musashi2 (Msi2). Msi2 functions as a promoter of SC characteristics and its expression in CML is an indicator of poor prognosis. Re-expression of Numb *in vivo* restores the ACD and differentiation capacity of CML cells and impairs advanced stage disease (Ito et al., 2010). Loss of ACD has also been reported in oligodendrogliomas, which results in excessive numbers of aberrantly self-renewing oligodendrocyte progenitor cells that are differentiation defective and promote tumour expansion (Sugiarto et al., 2011).

Taken together, ACD function is playing an important role in tissue homeostasis. Improper regulation of this process leads to a poorly differentiated clinical phenotype in many cancers and promotes tumour expansion. Notably, this deregulation has been reported across several tumour types, highlighting the importance of ACD and fate determination in proper tissue growth and maintenance in several tissues.

1.3 Centrosomes & Cilia

1.3.1 Centrosomes

The centrosome is a eukaryotic organelle that acts as the primary microtubule organising centre (MTOC) of most animal cells. They consist of two centrioles, surrounded by the pericentriolar material (PCM) (Figure 1.3). The centriole is a cylindrical, symmetrical arrangement of nine MT triplets around a central cartwheel structure, and the pair are connected by linker fibres at their proximal ends. The PCM is an amorphous matrix of proteins (Andersen et al., 2003; Alves-Cruzeiro et al., 2014) in

which the centrioles are embedded. The PCM is important for MT nucleation and seems to provide a scaffold onto which important centrosomal components such as γ-tubulin can be assembled (Gould and Borisy, 1977; Moritz et al., 1995).

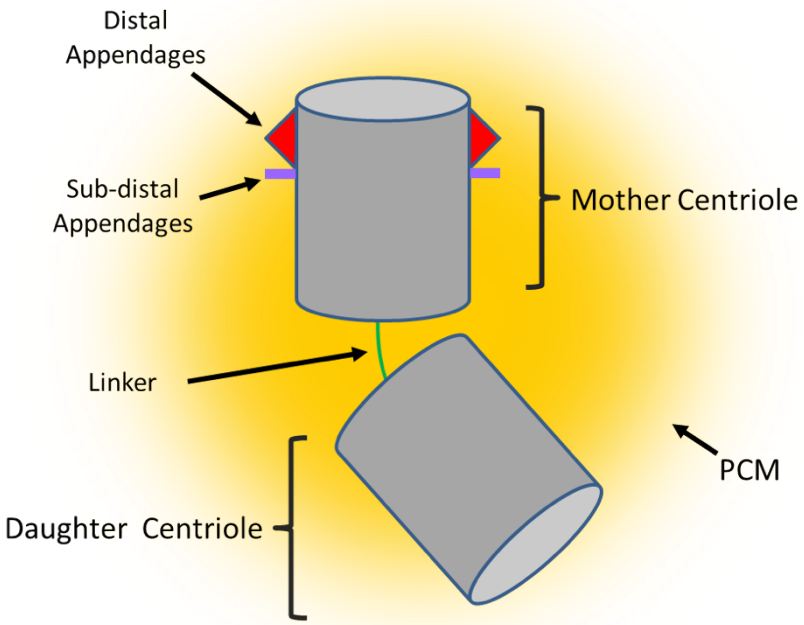


Figure 1. 3 Centrosome Structure. Centrosomes are comprised of two centrioles (grey) surrounded by the proteinaceous pericentriolar material (PCM, yellow). The centrioles are connected by a linker protein fiber (green) and possess different levels of maturity, with the more mature 'mother' centriole possessing distal (red) and sub-distal (purple) appendages.

Centrosomes possess an inherent asymmetry, with each centriole displaying different age and maturity as well as differing behaviour and functionality. The more mature centriole is referred to as the 'mother' centriole and can be identified by the presence of distal and sub-distal appendages (Figure 1.3) which are not present on the younger, 'daughter' centriole. These include the distal appendage protein CEP164 (Graser et al., 2007a) and the sub-distal appendage protein ODF2 (Nakagawa et al., 2001). In the decades since the centrosome was first described by Boveri and van Beneden (Boveri,

1887; van Beneden and Neyt, 1887), the centrosome has been intensely studied given its seemingly important role which is visible in mitosis.

Centrioles and centrosomes are comprised of hundreds of proteins that are important in the assembly, maintenance and function of this fascinating organelle. Initially, a core set of proteins were discovered in *C. elegans* (Pelletier et al., 2006) that were essential in the assembly mechanism. Since then, this has been found to be a highly conserved process, with the functional homologues shown in several publications to have parallel roles in the sequential assembly of the centriole in *Drosophila* (Blachon et al., 2008; Dzhindzhev et al., 2010; Feng et al., 2017) and humans (Hatch et al., 2010; Cizmecioglu et al., 2010; Kitagawa et al., 2011; van Breugel et al., 2011; Sonnen et al., 2013; Kim et al., 2013b).

At the beginning of the cell cycle, one centrosome/centriole pair exists, this centrosome must be duplicated for two centrosomes to be available for cell division. To achieve this a centrosome cycle (Figure 1.4), which is tightly linked to the cell cycle, exists. The existence of this cycle gives rise to the asymmetries observed between and within centrosomes (Vorobjev and Chentsov YuS, 1982).

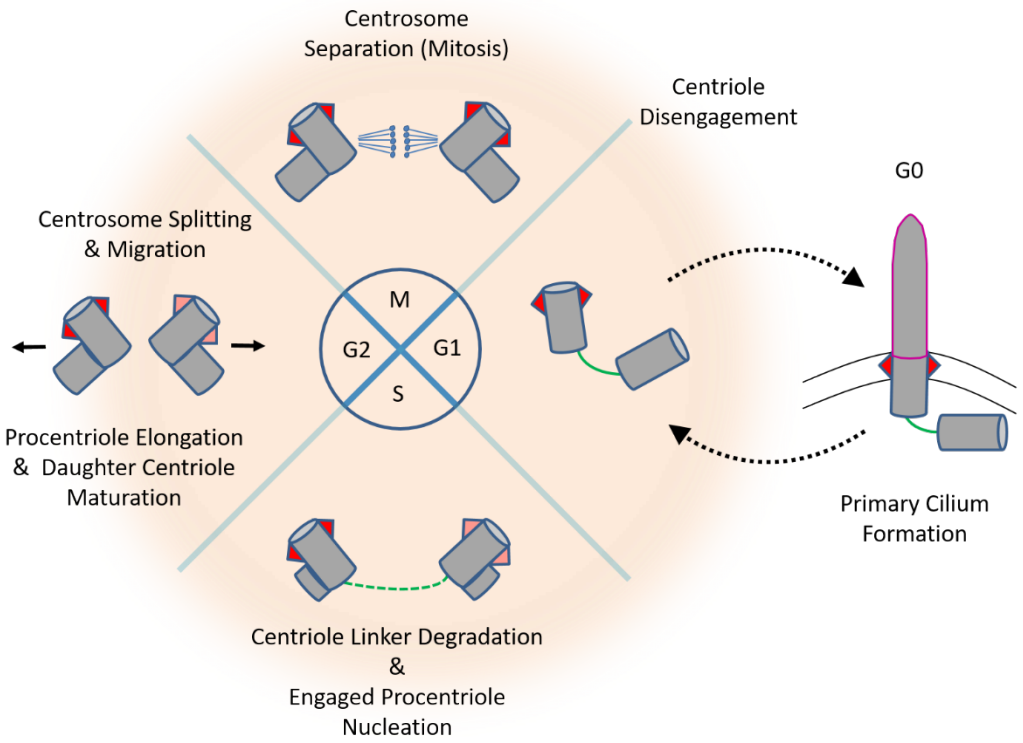


Figure 1. 4 The Centrosome Cycle. The Centrosome Cycle is tightly linked with cell cycle stage (central circle). In G1, two centrioles (individual grey cylinders) exist connected by a proteinaceous linker (green line between centrioles). As cells progress through the cell cycle, each centriole nucleates a new daughter centriole (procentriole) perpendicular to itself. The procentriole and its parent centriole are said to be engaged as they are physically interacting with one another. As cells pass from S phase to G2 phase, the linker between the original centrioles is gradually degraded (dashed green line). Also during this time, the original daughter centriole begins to mature and gains distal and sub-distal appendage proteins (red triangles). Throughout G2 phase, daughter centriole maturation continues and the procentrioles lengthen whilst the linker is abolished in an event termed 'centrosome splitting', resulting in two independent centrosomes. The centrosomes migrate away from one another (arrows) to opposite poles of the cell in preparation for mitosis. In M-phase, the mitotic spindle is assembled, and the cells divide, leaving each daughter cell with an engaged centriole pair. The disengagement of the centrioles is essential for cell cycle progression. This includes the separation of the centrioles and is facilitated by the assembly of a new linker. In quiescent cells, the centrosome can migrate to the plasma membrane where the mother centriole docks via its distal appendage proteins and nucleates another organelle, the primary cilium (pink outline). During this time, the daughter centriole remains attached to the mother centriole via the linker but is not docked. The primary cilium is typically disassembled to permit progression of the cell cycle.

To ensure that this duplication occurs only once per cell cycle this process is tightly regulated. At the beginning of the cell cycle, just one centrosome exists in close proximity to the nuclear envelope. As cells progress into S-phase, the mother and daughter centrioles each nucleate a new procentriole from their proximal ends (Habedanck et al., 2005; Bettencourt-Dias et al., 2005). The newly formed centrioles are engaged with their parental centriole via strong proteinaceous connections.

As the cell progresses through S phase and into G_2, the new centrioles continue to lengthen and mature (Spektor et al., 2007; Schmidt et al., 2009). Simultaneously, the original daughter centriole matures and becomes a new mother (herein, mother) centriole, and the linker fibres between the old mother (herein, 'grandmother') and the new mother centriole are severed (Tsou et al., 2009). This results in two new, engaged and independent centriole pairs – i.e. two new centrosomes. These centrosomes also display differences in maturity due to the differing maturity between the mother and grandmother centrioles present. They can now continue to mature and accumulate essential components of the PCM.

As prophase commences, the centrosomes begin to generate spindle fibres and migrate to opposite sides of the cell and form the bipolar spindle seen in metaphase. The following cell division then results in each daughter cell receiving one centriole pair containing centrosome each. At the end of mitosis, the mother and daughter centrioles within each centrosome are disengaged and the linker fibres that connect them more loosely are established – this disengagement is a prerequisite for the initiation of a new cycle (Mayor et al., 2000; Bahe et al., 2005; Graser et al., 2007b). The need for this cycle to be regulated at each stage is of paramount importance to the cell, as errors here can

lead to several issues, including chromosome segregation errors and the establishment of multipolar spindles, both of which can lead to tumourigenesis (Nigg and Raff, 2009).

Another important stage exists in the centrosome cycle that is only observed in quiescent (at the G_0 phase of the cell cycle) cells. In this stage the mother centriole migrates to the plasma membrane and initiates one of the most important functions of the centrosome, the formation of the primary cilium (Figure 1.4).

1.3.2 Cilia

The primary cilium is a thin, solitary projection that emanates from the cell surface. Once thought to be a vestigial organelle, the past decade of research has revealed that instead, the cilium is a specialised structure with vital roles in signalling pathways, homeostasis and development. As mentioned, the mother centriole is responsible for the initiation of primary cilium formation, however, recent data suggests that it is dispensable for ciliary maintenance and maturation (Serwas et al., 2017). Initially, the mother centriole docks at the plasma membrane and transitions to a structure known as the basal body. From here the core of the cilium, the axoneme, is nucleated. The axoneme contains nine doublet MTs which extend from those within the basal body (abbreviated as 9+0), and these are surrounded by a specialised ciliary membrane which is continuous with the plasma membrane and contains specific proteins such as ARL13B (Cevik et al., 2010) (Figure 1.5). Interestingly, motile cilia, contain an additional single central MT pair (9+2) which are absent from primary cilia.

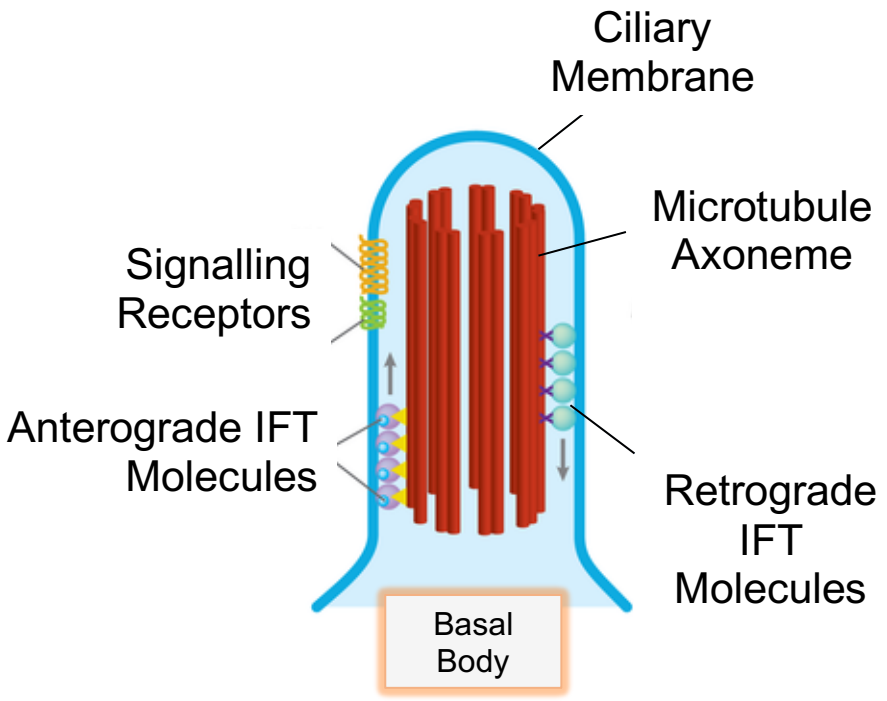


Figure 1. 5 The Primary Cilium. The primary cilium in a membrane bound organelle that extends from the basal body. It consists of a central core axoneme that is comprised of microtubule doublets. Intraflagellar transport (IFT) proteins traffic within the cilium in both directions and are essential for its assembly. Signalling pathway receptors can be detected on the ciliary membrane. (Adapted from open access article, Bodle JC, Rubenstein CD, Phillips ME, Bernacki SH, Qi J, Banes AJ, et al. (2013) Primary Cilia: The Chemical Antenna Regulating Human Adipose-Derived Stem Cell Osteogenesis. PLoS ONE 8(5): e62554. https://doi.org/10.1371/journal.pone.0062554).

Assembly of the primary cilium, or ciliogenesis, is a tightly orchestrated event which has been found to involve the function of several proteins and remains only partially understood. Ciliogenesis involves dramatic remodelling of the distal appendages of the mother centriole. Distal appendage vesicles (DAVs) form a cap known as the ciliary vesicle on the distal end of the mother centriole (Basiri et al., 2014). The ciliary vesicle works in concert with a number of Rab GTPases to accommodate the extension of the ciliary membrane around the extending axoneme (Westlake et al., 2011). During the early stages of ciliogenesis, there are extensive changes within the basal body itself. CP110 is a centriole duplication and length regulating protein which is located at the distal end of the centrioles and interacts with Cep97, together they have been reported

to suppress cilium assembly (Spektor et al., 2007). Studies have demonstrated that the asymmetric destruction of CP110 on the mother centriole is necessary to allow ciliary assembly to begin and this is regulated by the opposing functions of the $SCF^{Cyclin\ F}$ ubiquitin ligase complex and the deubiquitinating enzyme USP33 (D'Angiolella et al., 2010; Li et al., 2013a).

The extension of the axoneme occurs once the basal body docks in the plasma membrane, this docking is mediated by the distal appendage protein CEP164 (Schmidt et al., 2012). How the axoneme extends is not entirely understood, but it requires MT nucleation as well as the addition of new axoneme components to the distal tip of the forming cilium. Typically 5 – 10 μm in length, the major component of the axoneme is tubulin and the α/β–tubulin dimers of the cilium are modified in several ways.

Axoneme formation and maintenance depends heavily on two intraflagellar transport (IFT) complexes, IFT-A and IFT-B, which are responsible for the shuttling of cargo to and from the ciliary tip (Figure 1.5). These are recruited to the distal appendages of the mother centriole through CEP164 dependent enlistment of Tau tubulin kinase 2 (TTBK2) (Deane et al., 2001; Čajánek and Nigg, 2014). Upon removal of CP110, the transition zone (TZ) is formed, this acts as a regulatory gate through which the IFT complexes shuttle proteins. IFT is highly conserved and considered the key way in which proteins are transported to and within the cilium. It was first reported in *Chlamydomonas reinhardtii*, when Kozminski et al. reported the bidirectional movement of 'particles' within its flagellum (Kozminski et al., 1993). Cargo important for ciliary extension and maintenance is transported along the axoneme, associated with IFT-A/B by the IFT motors kinesin-2 and dynein 1b.

Certain cell types are multiciliated meaning that they can form several cilia, however, their assembly differs from that of the primary cilium. Whilst healthy cycling cells typically tightly regulate and restrict centriole duplication, multiciliated cells must amplify their centriole numbers massively to facilitate multiciliogenesis. To achieve this, they also employ an 'acentriolar' mechanism, with *de novo* basal body generation being templated from a proteinaceous structure termed the 'deuterosome' instead of the mother centriole (Sorokin, 1968). This *de novo* centriole amplification is a post-mitotic event, uncoupled from the cell cycle and controlled by a distinct set of proteins to the mother centriole-dependent pathway (Tang, 2013).

Ciliary disassembly is also an area of intense research interest, and much less is known about this process than assembly. It has been proposed that this occurs in two 'waves', with the first in G1 phase and full disassembly achieved before mitosis (Pugacheva et al., 2007). Destabilisation and depolymerisation of MTs within the axoneme is a recurrent theme in the ciliary disassembly mechanisms uncovered thus far. At the base of the cilium, Aurora-A is activated by HEF1/NEDD9 and calcium calmodulin. The active Aurora-A in turn phosphorylates HDAC6 which is responsible for the de-acetylation of acetylated α-Tubulin in the axoneme, causing destabilisation of the MTs (Pugacheva et al., 2007; Plotnikova et al., 2012). MT depolymerising kinesins, namely Kif2a and Kif24, have also been implicated in initiating cilium disassembly. Kif2a is activated by Plk1, which is an important mitotic kinase – this proliferative signal causes Kif2a to trigger depolymerisation of ciliary MTs, whilst a similar result is achieved by Nek2 mediated phosphorylation of Kif24 (Kim et al., 2015b). A mechanism not involving tubulin dynamics has also been described, with the cilium being abscised from the basal body

during mouse and chick neurogenesis by actin-myosin contraction (Das and Storey, 2014).

Post-translational modifications (PTMs) have important roles in the integrity of ciliary function and structure, forming specific patterns which facilitate specific activities. The best known ciliary tubulin PTM is acetylation of α-tubulin at K40, which is often used as a marker to visualise the cilia (Piperno and Fuller, 1985). Acetyl-K40 is the only known PTM of tubulin known to occur inside of the ciliary lumen and it is mediated by the conserved enzyme MEC-17/ATAT1 (Akella et al., 2010; Shida et al., 2010; Kalebic et al., 2013) and may be promoted by the presence of LiCl (Nakakura et al., 2015). The presence of acetyl-K40 is considered a marker for mature, stable MTs, which has been suggested to promote cohesion between MT filaments in the axoneme (Cueva et al., 2012). Acetylated α-tubulin dynamics have been described in the disassembly programme, where deacetylation is performed by HDAC6 (Hubbert et al., 2002) and SIRT2 (North et al., 2003). Absence of these deacetylation proteins has been shown to result in an increased cilia frequency and length, suggesting that this modified tubulin is important in stabilising the axoneme. However, conflicting reports exist as to the importance of this PTM, especially following the discovery that *Atat1* knock out mice can assemble cilia without the acetyl-K40 tubulin mark (Kim et al., 2013a) and that cilia with deacetylated tubulin have no major structural differences (Howes et al., 2014).

Other PTMs observed on ciliary tubulin include glutamylation, tyrosination and glycylation; the functionality of these PTMs at the cilium are not well understood. The B-tubules of the cilia axoneme are enriched for detyrosination, the reversible removal of a gene encoded tyrosine from the C-terminal of α-tubulin (Arce and Barra, 1983).

During IFT, anterograde movement of cargo occurs on the B-tubules and is driven by kinesin-2; detyrosination has been found to amplify the speed of kinesin-2, thus improving IFT and making detyrosination considered a generally stabilising mark for cilia.

Glutamylation and glycylation of tubulin (the addition of a glutamate or glycine residue) has been reported to occur at many sites on α- and β-tubulin. Recently, glycylation of axonemal MTs was found to be an important modulator of cilia length – with more glycylation observed as cilia elongate (Gadadhar et al., 2017b). Glutamylation has been reported to be non-essential to the cilium (Wloga et al., 2008) but is present in all studied cilia (Janke et al., 2005). Glutamylation has been mostly linked to an important role in motile cilia, particularly mammalian sperm, where it has been shown that glutamylation promotes ciliary assembly and stability (Campbell et al., 2002; Regnard et al., 2003; Konno et al., 2016). The stabilising effects of glutamylation may also be linked to increased IFT efficacy, as polyglutamylation of β-tubulin is associated with enhanced kinesin-2 activity (Sirajuddin et al., 2014). In contrast, excessive glutamylation has also been linked to ciliary shortening, usually observed when cilia are destabilised. This has been linked to the stimulation of Katanin which severs the axoneme in *C. elegans* (Sharma et al., 2007; O'Hagan and Barr, 2012). Glycylation and glutamylation of tubulin are competitive marks and their balance is considered to be an important factor in ciliary function (Rogowski et al., 2009; Wloga et al., 2009).

Taken together, this suggests there is a fine-tuning of PTMs which is important in balancing cilia assembly and disassembly. The overall PTMs on tubulin have been proposed to result in a 'tubulin code' which may be important in functional regulation

of the MTs under consideration – but this is a relatively new theory that requires considerable research to be confirmed (Gadadhar et al., 2017a).

1.3.3 Centrosome & Cilia Function

Extensive investigation has been carried out into the function of the centrosomes and the cilia. Since their discovery, centrosomes have been implicated in the assembly of the mitotic spindle and MT nucleation given their conspicuous ability to nucleate MTs (Boveri, 1887). However, not all cells contain centrosomes but can still assemble a spindle (Khodjakov et al., 2000; Hornick et al., 2011), and *Drosophila* were found to be able to develop almost entirely normally in the *Sas4*$^{-/-}$ mutant which can assemble a spindle (albeit more slowly) despite lacking centrioles (Basto et al., 2006). This indicates that a) the spindle can assemble without centrosomes and b) that the major defects seen upon centriolar loss must occur due to a loss of different functions. Subsequent studies have demonstrated that important roles of the centrosome during mitosis include spindle positioning (Yamashita et al., 2003; Rebollo et al., 2007) and assembly efficiency and integrity (Hornick et al., 2011). In this way they function in maintaining genomic integrity by ensuring proper chromosome segregation, particularly in vertebrates (Habedanck et al., 2005; Sir et al., 2013).

Arguably the most important role of the centrioles is the formation of the primary cilia. This is demonstrated in the study previously mentioned by Basto et al. (2006), that showed that whilst *Sas4*$^{-/-}$ flies can develop fairly well, they cannot survive until adulthood as they cannot form a primary cilium (Basto et al., 2006). Oftentimes, the cilia and centrosomes display interrelated functions.

Both the centrosome and cilium are regarded as signalling 'hubs'. The concentration of signalling pathway components that localise at the centrosome, coupled with their mobility, make them attractive candidates for research into how signalling can be co-ordinated spatially within the cell. Several signalling events have been reported to occur at, and depend on, centrosomal association, particularly those linked to cell cycle progression. This includes the activation of Cdk1/Cyclin B (Jackman et al., 2003). Essentially every protein that has been found to be involved in mitotic progression signalling is found at the centrosome at least transiently during the life cycle of a vertebrate cell; including Aurora-A, Cyclin B and Plk1 (Golsteyn et al., 1995; Gopalan et al., 1997; Jackman et al., 2003).

Another compelling relationship that has been studied in this regard is that between centrosomes and the DNA damage response (DDR), as many of the major DDR proteins also associate with the centrosomes, including ATM dependent localisation of p53 (Tritarelli et al., 2004). A link between centrosomes and the guardian of the genome was suggested when it was reported that loss of p53 led to centrosome amplification (Fukasawa et al., 1996), which is thought to be a result of defective cell division, leading to tetraploidy (Meraldi et al., 2002). Interplay between the centrosome and p53 signalling was further highlighted when it was demonstrated that defects in centrosomal structure could lead to p53 dependent cell cycle arrest (Mikule et al., 2007).

Whilst the centrosome remains a candidate for facilitating signalling, the primary cilium has been proven to do so, and is broadly acknowledged as a sensory organelle that mediates responses to external stimuli (Shah et al., 2009). In fact, the cilium is required

for proper Sonic Hedgehog (Hh) signalling (Huangfu et al., 2003). Differential localisation of the Hh signalling components is witnessed at the cilium, and the cascade is interlinked with IFT (Goetz and Anderson, 2010). Beyond Hh signalling, the cilium has also been implicated in Wnt (Otto et al., 2003; Watanabe et al., 2003; Simons et al., 2005) and RTK (Schneider et al., 2005) signalling, as well as having roles in mechanosensation (Praetorius and Spring, 2001; Nauli et al., 2003; Khayyeri et al., 2015; Delling et al., 2016).

Both the cilium and centrosome have roles in cell polarity, which is important during development. Centrosomes have been demonstrated to provide signals that directly induce polarisation of the cell, in processes particularly well analysed in *C. elegans* (Cowan and Hyman, 2004; Bienkowska and Cowan, 2012; Feldman and Priess, 2012). The position of the centrosome has been found to have an important link to polarisation, with non-polarised cells often having their centrosome close to the cell centre through association with the nucleus. In several tissues, both the centrosome and cilia are polarised to the apical surface of the cells (e.g., epithelial cells in the mammary gland (Dylewski and Keenan, 1984)). This polarisation of the centrosomes means that radial MT organisation is lost and an apical-basal array of MTs is established, which is important in cilia assembly and in intracellular vesicular transport (Müsch, 2004). The primary cilium has been linked to planar cell polarity (PCP) signalling, with important ciliary proteins (e.g. IFT88) being shown to be necessary in the establishment of PCP in the epithelia of the cochlear duct in mice (Ross et al., 2005; Jones et al., 2008; May-Simera et al., 2015). In fact, there has recently been the classification of a protein module known as CPLANE (ciliogenesis and planar polarity effectors), which includes

several conserved PCP proteins with roles in vertebrate ciliogenesis, suggesting extensive interconnection between the two processes (Toriyama et al., 2016).

Interestingly, recent studies have implicated both the centrosome and cilia in the regulation of differentiation, mainly in the context of asymmetric inheritance. This is a controversial topic, with species and tissue specificity regarded as particularly important. Asymmetric cell division, as previously mentioned, is important in the determination of cell fate. Given the inherent asymmetry of the centrosome, one could argue that all cell divisions are indeed, asymmetric, as each daughter cell will inherit a centrosome of differing age and therefore differing functionality.

The phenomenon of a link between centrosome inheritance and fate determination in eukaryotes was first reported in *Drosophila*, where it has been shown to factor in the fate specification of male germline stem cells (GSCs) (Yamashita et al., 2007) and in larval neuroblasts (NBs) (Conduit and Raff, 2010; Januschke et al., 2011). Whilst the inheritance of a particular centrosome was persistently seen in these studies, it was apparent that the centrosome itself didn't infer fate specification, as the mother centrosome was retained in the GSCs, but the daughter was retained in NBs. However, they support the theory that there is a correlation between centrosome age and fate determination in self-renewing stem cell divisions.

Asymmetric centrosome inheritance has also been explored as an important mechanism of fate determination in mammalian systems. Using the mouse neocortex as a model to examine fate determination, it was shown that centrosome maturity regulates differential behaviour in the daughter cells. Radial glial (RG) progenitors reside in the ventricular zone (VZ), these cells are capable of self-renewing or producing

differentiating cells, which will migrate to form the neocortex. As in the male GSCs of *Drosophila*, the self-renewing RG progenitor retains the mother centrosome, whilst the daughter is inherited by the differentiating cell – loss of maturity related proteins also disrupted these ACDs and caused a depletion of progenitor cells (Wang et al., 2009). ACD and centrosome inheritance has been recorded in human neuroblastoma cells also, with the daughter centrosome observed to be asymmetrically inherited alongside the important ACD protein, NuMA (Izumi and Kaneko, 2012). Elegant studies on mESCs suggested that specific signalling pathways can also exert an effect on ACD, with an oriented Wnt signal shown to induce ACD. The cell proximal to Wnt signals retain the hallmarks of pluripotency alongside the mother centrosome (Habib et al., 2013; Lowndes et al., 2016). In the mammalian systems discussed, the mother centrosome seems to correlate with a stem-like phenotype, however, in other systems this is not consistent. It will be interesting to determine if the centrosome age and pluripotency correlations in mammals are also tissue specific or there is a global consensus.

Recent studies have also began to shed light on the role of the cilium in cell fate determination as the older centrosome is better primed to form a cilium post-mitosis, but this wasn't definitively shown until 2009 (Anderson and Stearns, 2009). In fact, since then it has been shown that the cilium may not even be fully disassembled in cycling stem and cancer cells. Ciliary markers often persist at the mother centrosome in these cells, ensuring speedy reassembly post-mitosis in the stem cell character retaining cells (Paridaen et al., 2013). The prevailing theory is that the cilium may be important in fate determination given the differential response ability of cells that do or do not possess this organelle.

Cilia have been identified on a number of stem cell types (Kiprilov et al., 2008; Plaisant et al., 2009; Nathwani et al., 2014) and appear to decrease in number as adipose SCs differentiate (Plaisant et al., 2009). It has also been proposed that the cilium is important in lineage commitment, with cilia related protein depletion in mesenchymal and adipose SCs leading to a disruption of differentiation cues (Tummala et al., 2010; Bodle et al., 2013; Arrighi et al., 2017). The role of the cilium in differentiation is often linked to its association with Hh signalling, which is a crucial signalling hub during differentiation and development (Goetz and Anderson, 2010). During vertebrae neurogenesis, it has been shown that the cilia are abscised, removing the ability of the cells to receive Hh ligand and permitting proper differentiation (Das and Storey, 2014). Further to this was the finding that the primary cilium is required to control Hh signalling in the differentiation of skeletal muscle cells (Fu et al., 2014). The importance of cilia and centrosomes in proper differentiation is highlighted by the developmental and pathological defects seen in cases where abnormalities exist in these organelles.

1.3.4 Centrosomes & Cilia in Human Pathology

Important cellular roles for the centrosome and cilia means that disruption to their functionality can result in severe consequences for the organism. The centrosome has been extensively linked to disease, including neurodegenerative disorders such as Parkinson's Disease (Zhao et al., 2003) and developmental defects such has hereditary spastic paraplegia (Trotta et al., 2004) and Miller-Dieker syndrome (Wynshaw-Boris and Gambello, 2001). Deficiency in ciliary function, maintenance and (dis-)assembly can also cause a wide range of pathologies, with the diseases collectively termed ciliopathies. Ciliopathies are frequently developmental disorders linked to signalling deregulation

and display a wide range of pathologies including polycystic kidney disease (Pazour et al., 2000), polydactyly, learning difficulties, obesity and heart disease.

Centrosome amplification has been reported alongside centrosomal aberrations (such as excessive centriole number or length) in several types of cancer and is associated genomic instability thought to arise from chromosome segregation errors (Lingle et al., 2002; Pihan et al., 2003). One leading theory behind these observations was that multiple centrosomes would lead to multipolar spindles and, therefore, aneuploidy. However, it was shown that multiple centrosomes preferentially cluster to avoid this and can still assemble a bipolar spindle (Quintyne et al., 2005). Despite this, subsequent studies have shown that these 'clustered' bipolar spindles are problematic in themselves, and lead to a greater incidence of lagging chromosomes and merotelic attachment errors, ultimately causing chromosomal instability (Ganem et al., 2009).

Large-scale analysis of several tumour types have shown that mutations and changes to centrosomal proteins are much rarer than originally expected, given the widespread belief that centrosome aberrations drive tumour progression (Zack et al., 2013; Lawrence et al., 2014). However, it is necessary that this is further explored as these studies encompassed exome sequencing alone and it is possible that centrosomal defects result from other genomic changes, including epigenetic alterations or changes to regulatory elements. RASSF1A is a fitting example of this; it is a *bona fide* TSG considered a centrosomal protein, but it is not frequently mutated in cancer, instead subjected to hypermethylation that silences gene expression (Dammann et al., 2003b).

Whilst supernumerary centrosomes can drive a cancer phenotype in flies (Basto et al., 2008), to date the same can't be seen in mammals. Instead, amplification of centrosome

number in the developing mouse brain and primary microcephaly patients has been linked to the development of microcephaly following inappropriate apoptosis (Marthiens et al., 2013; Arquint and Nigg, 2014). Despite being in the spotlight as a cancer driver for over a century, the role of the centrosome in cancer progression remains unclear.

Recently, the primary cilium has come under the spotlight as also being a key player in cancer progression. Cilia have been reported to be lost in a number of cancers, including breast cancer (Reilova-Velez and Seiler, 1984; Yuan et al., 2010) and renal cell carcinoma (Schraml et al., 2009), with cilia assembly defects observed in rhabdomyosarcomas (Fu et al., 2014). Conversely, in pancreatic cancers the re-emergence of cilia expression is associated with a progression to worse prognosis (Emoto et al., 2014). The most prevalent reasoning behind a link between cilia and cancer is due to the importance of the cilium as a signalling hub, as signalling pathways are hugely disrupted in tumourigenesis. Interestingly, cilia have been shown to have a dual role in certain cancer subtypes. In both medulloblastoma and basal cell carcinoma, the presence of cilia has been shown as a prerequisite for Hh signalling dependent cancers, but not those driven by Gli2 activation (Han et al., 2009; Wong et al., 2009).

Taken together, it is clear that deregulation of the primary cilium is an enabling phenotype in several cancer types. Extensive research is still required on the subject as a direct link between cilia and cancer remains elusive. However, given reports to date, it is evident that there is a complicated, tumour specific interplay between the cilium and cancer progression.

1.4 RASSF1A & RASSF7

1.4.1 Ras Signalling: The Oncoproteins and their Effectors

The RAS oncoproteins are a superfamily of related proteins that orchestrate a diverse range of signalling outputs, such as cell proliferation, death and differentiation (Rajalingam et al., 2007). The RAS proteins are evolutionarily conserved small guanosine triphosphatases (GTPases) and the founding members of the family are HRAS, NRAS and KRAS. There are currently more than 150 known human members in the family which are divided into five major branches defined by the similarities between protein sequence and function; namely, Ras, Rho, Rab, Ran and Arf (Wennerberg et al., 2005). The RAS family proteins have enjoyed decades of intense study given their importance in human malignancies. They are generally referred to as oncogenes/oncoproteins, with approximately 16 % of all human tumours displaying activating mutations in RAS proteins. However, this mutation incidence is much higher in certain cancers, with mutations found in more than 30 % of large intestine and biliary tract tumours, whilst this is increased further in pancreatic cancers, with an incidence of 63 % (Prior et al., 2012).

Ras proteins function as molecular switches, with the active form of the protein being GTP-bound. When active, the RAS proteins can bind to their downstream signalling partners, collectively termed RAS effector proteins. To date, several Ras effectors have been identified and grouped based on the presence of a RAS-interaction mediating domain. One of the main groups of Ras effector proteins contain a Ras binding (RB) domain. The first RB containing effector identified was RAF1, a protein kinase that initiates the MAPK (mitogen activated protein kinase) cascade (Morrisont et al., 1988)

and important in the regulation of several cellular outputs, including cell cycle progression and proliferation (Kolch et al., 1991; Meloche and Pouysségur, 2007; Zhang and Liu, 2002). Since then, several more RB domain proteins have been identified, with RAF (particularly B-RAF) and PI3-K (Phosphatidylinositol-4,5-bisphosphate 3-kinases) being the best studied due to their far reaching implications in human pathologies including cancer and developmental birth defects (Leicht et al., 2007; Mansour et al., 1994; Fruman and Rommel, 2014; Fruman et al., 2017). Another major group of Ras effector proteins contain a different domain that mediates Ras interaction, this is the Ras association (RA) domain and proteins containing this motif have been classified into a sub-class of Ras effector proteins known as the Ras-association domain family (RASSF).

1.4.2 The Ras-Association Domain Family

The RASSF group of proteins consists of 10 members (termed RASSF1 – 10) that all share the RA domain motif, the position of which is used to classify each member as a classical/C – or N – terminal RASSF protein (Figure 1.6). The first identified RASSF protein was RASSF5 (previously known as NORE1) (Vavvas et al., 1998), quickly joined by RASSF1 (Dammann et al., 2000). These are the best characterised of the family. The RASSF members have gained interest due to their links with human disease and have been found to display an increasingly broad range of functions including cell cycle control, apoptosis and microtubule stabilisation, which implicates them in cancer progression (Richter et al., 2009). Another unifying feature of the classical RASSF proteins is the presence of a SARAH (Sav – RASSF – Hpo) domain (Figure 1.6) which is a coiled-coil structure that mediates crucial interactions between RASSF 1-6 and other signalling molecules.

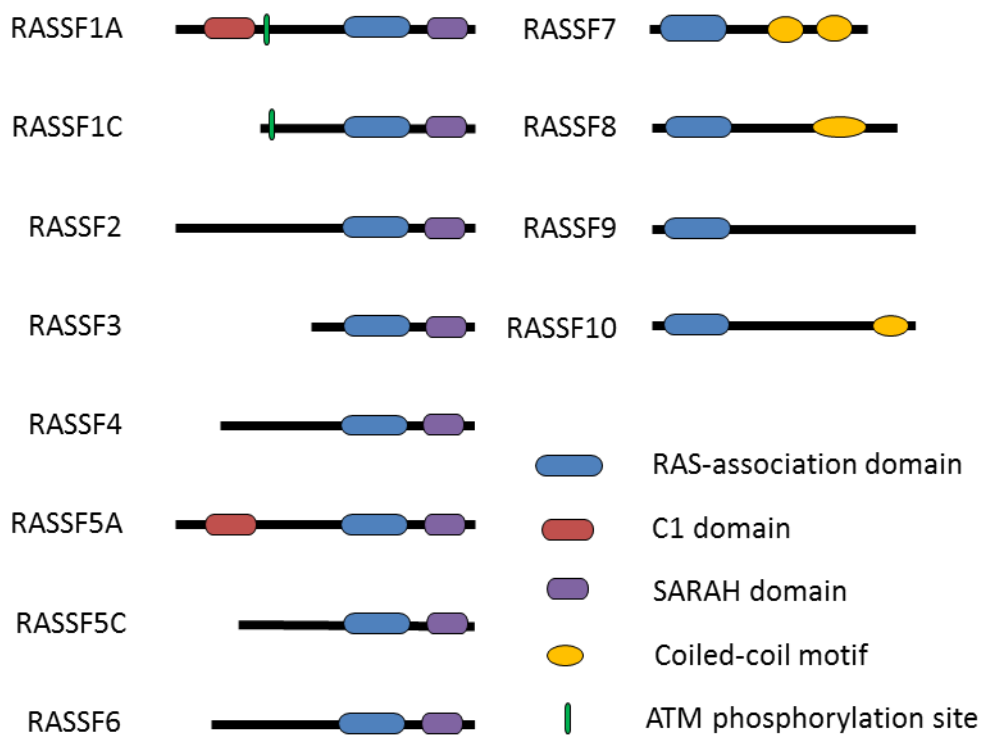


Figure 1. 6 The RASSF Protein Family. The RASSF protein family consists of ten structurally related proteins that all share the presence of an RA-domain (blue). They can be sub-divided into the C-terminal (RASSF1 - 6, left) and N-terminal class of RASSF protein (RASSF7 – 10, right), based on the localisation of their RA domain. Other structurally important domains are illustrated, including the SARAH domain (purple) and the coiled coil domains (yellow). These domains have roles in protein-protein interaction.

1.4.3 RASSF1A

RASSF1 (Ras association domain family member 1) is the most studied member of the family and was initially identified as part of loss of heterozygosity (LOH) studies in lung, breast and kidney cancers. These indicated several loci that were suspected to harbour at least one important TSG on chromosome 3p. Of interest was region 3p.21.3 because of a high incidence of instability here detected in lung and breast cancers (Hung et al., 1995; Kok et al., 1997; Sekido et al., 1998; Sundaresan et al., 1992; Wistuba et al., 2000). Within this region eight candidates were discovered; *CACNA2D2, PL6, CYB561D2/101F6, TUSC4/NPRL2/G21, ZMYND10/BLU, RASSF1/123F2, TUSC2/FUS1,* and *HYAL2/LUCA2* (Sekido et al., 1998; Lerman and Minna, 2000). However, none of these eight genes

displayed the expected high mutation rate typical of a TSG. Around the same time, another group isolated cDNA that encoded a novel protein that interacted with the DNA damage repair protein, XPA (Xeroderma Pigmentosum Complementation Group A). This sequence was located in the region 3p21.3 and was found to have high homology (approx. 55 %) with the C – terminus of the already known NORE1 protein, and so they characterised it as the Ras effector homologue (RASSF1) (Dammann et al., 2000).

Several isoforms of RASSF1 exist, with the A, B and C transcripts being identified first (Dammann et al., 2000). The *RASSF1* gene can generate eight isoforms (A-H) via alternative splicing and promoter usage, it contains eight exons and spans around 11 kb of the human genome. Interestingly, *RASSF1* contains two CpG islands in its promoters. The first is located within the promoter region for isoforms RASSF1A, D, E, F, G and H, whilst the second CpG island spans the promoter region for RASSF1B and C. The major isoforms of RASSF1 are RASSF1A and RASSF1C, they are ubiquitously transcribed in normal tissue (Dammann et al., 2000) whilst the other isoforms are tissue specific or unclassified (Donninger et al., 2007). The roles of *RASSF1A* and *RASSF1C* are still being elucidated with many studies suggesting that they can perform differing and even opposing functions in a number of scenarios (Estrabaud et al., 2007; Vlahov et al., 2015; Reeves et al., 2013). However, *RASSF1A* has been most extensively studied given its links to human cancer.

1.4.4 RASSF1A & Cancer

RASSF1A silencing is one of the most frequent events in human sporadic malignancies, with gene silencing occurring via hypermethylation of the *RASSF1A* promoter CpG island

(Donninger et al., 2007; Hesson et al., 2007; Weyden and Adams, 2007). Widespread *RASSF1A* expression loss in cancer has led to its classification as a *bona fide* TSG and its epigenetic inactivation may serve as a diagnostic and therapeutic biomarker given its frequent occurrence (Grawenda and O'Neill, 2015). The RASSF1A protein performs many roles typical of a tumour suppressive function and has been found to modulate several signalling outputs.

RASSF1A is a major upstream regulator of the Hippo pathway (Figure 1.7), a highly conserved signalling cascade with roles in tissue growth (Dong et al., 2007; Zhao et al., 2007), apoptosis and proliferation (Wu et al., 2003; Harvey et al., 2003; Udan et al., 2003), stem cell function (Hong et al., 2005; Varelas et al., 2008; Lian et al., 2010; Mo et al., 2014) and regeneration in several tissue types (Ren et al., 2010; Shaw et al., 2010; Zhang et al., 2010; Lee et al., 2008; Schlegelmilch et al., 2011; Elbediwy et al., 2016; Bai et al., 2012; Lee et al., 2016; Lin et al., 2014; Park et al., 2016; Huang et al., 2016). Many of the Hippo pathway functions are dependent on RASSF1A action. It has been shown that RASSF1A regulates Hippo signalling via its interaction with the MST kinases and Salvador (SAV1/WW45) in mammals (Guo et al., 2007) as well as the *Drosophila* system (Scheel and Hofmann, 2003).

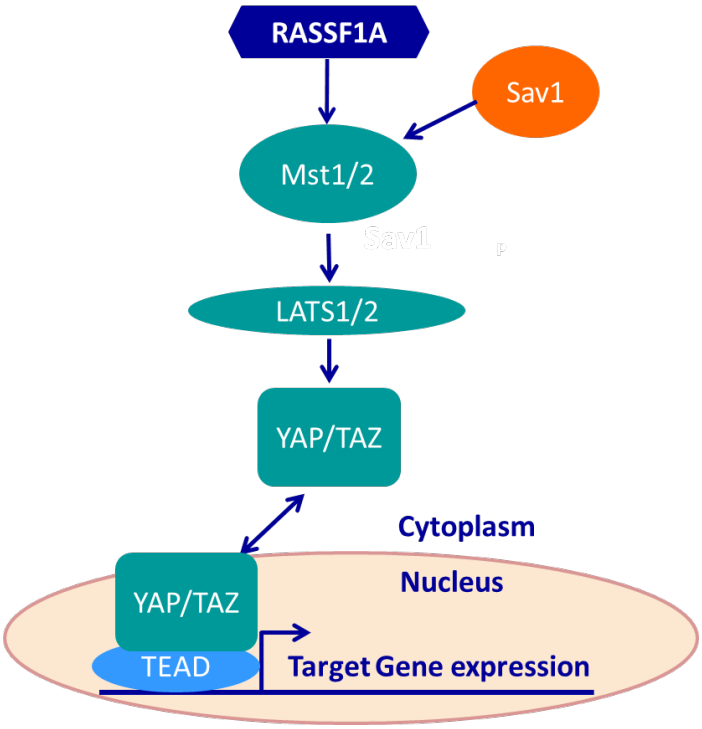


Figure 1. 7 The Mammalian Hippo Signalling Pathway. RASSF1A is a major upstream regulator of the Hippo signalling cascade. The pathway has two core kinases, MST1/2 & LATS1/2, which modulate activity of the pathway effector, YAP. YAP can shuttle between the nucleus and the cytoplasm and regulate gene expression through differential transcription factor binding.

1.4.5 Hippo Signalling

The Hippo signalling pathway has been linked to the balance between pluripotency and differentiation in stem cells, particularly via the effector YAP. YAP has been shown to be critical during embryogenesis, with *Yap*$^{-/-}$ embryos arresting around E8.5 (Morin-Kensicki et al., 2006). YAP's importance in development comes from its role as a transcriptional regulator, meaning that it associates with certain TFs and controls their activity. The TEAD (TEA-Domain) family of TFs is one of the major YAP targets. TEADs are some of the earliest activated genes during embryonic development and are important in lineage specification (Yagi et al., 2007; Sawada et al., 2008) in often YAP-

dependent mechanisms (Nishioka et al., 2009). Importantly, YAP/TEAD complexes can modulate the expression of the master pluripotency factors Nanog and OCT4 (Lian et al., 2010). The Hippo pathway has also been linked to CSCs. In breast cancer, TAZ activity has been shown to be upregulated in poorly differentiated tumours, and induces a more malignant, stem-like phenotype in low-grade breast cancer cell lines (Cordenonsi et al., 2011). Increased TAZ expression has also been correlated with high-grade glioblastoma (Bhat et al., 2011).

Interestingly, recent studies have also linked Hippo signalling to the primary cilium. The cilia related protein NPHP4 negatively regulates Hippo signalling by binding LATS1 and inhibiting its kinase activity on YAP, thereby decreasing the activity of the pro-proliferative YAP target genes (Habbig et al., 2011). Conversely, other cilia-related proteins including NPHP9 and NPHP3 have been found to interact with and activate TAZ, translocating to the nucleus to transcribe TAZ target genes (Frank et al., 2013). The cilium also provides an ideal platform through which crosstalk between different pathways can occur, which can be exemplified by the upregulation of YAP transcription and activity by Hh signalling (Fernandez-L et al., 2009).

The core Hippo kinase, MST1/2 interacts with SAV1 to promote ciliogenesis in two ways. Firstly, the kinases mediate phosphorylation of Aurora-A, causing dissociation of the Aurora-A/HDAC6 disassembly complex and the MST1/2-SAV1 complex can interact with the TZ to promote the localisation of ciliary proteins (Kim et al., 2014). Interestingly, the nexus between Hippo signalling and the cilia has been linked to actin dynamics. It was reported that YAP/TAZ expression had no effect on ciliogenesis (Kim et al., 2014), but subsequent studies have challenged this. These suggest that YAP/TAZ overexpression

and nuclear retention can suppress ciliogenesis via the upregulation of disassembly proteins. YAP/TAZ target genes can be modulated by actin remodelling factors, proposing that the actin cytoskeleton can regulate ciliogenesis (Kim et al., 2015a). This has been further supported by a recent report in which jasplakinolide (which induces actin polymerisation) can induce ciliogenesis by inactivating YAP (Nagai and Mizuno, 2017). These initial links between Hippo signalling and the primary cilium suggest that a complicated relationship exists at several levels.

1.4.6 RASSF1A & Apoptosis

RASSF1A is a proapoptotic protein. Apoptosis describes the carefully regulated and programmed death of a cell; it is often triggered in response to cellular deregulation and is a pathway frequently disabled in carcinogenesis. RASSF1A was found to associate with MST1 (Praskova et al., 2004) and promote death receptor mediated apoptosis via the kinases NDR1/2 (Vichalkovski et al., 2008; Oh et al., 2006). The RASSF1A/MST2 interaction also leads to apoptosis. In 2007, Matallanas et al. demonstrated that RASSF1A induces *PUMA* mediated proapoptotic gene expression. It does so by causing phosphorylation of MST2 and LATS1, which leads to the phosphorylation of YAP and causes it to change its transcriptional partner to p73 (Matallanas et al., 2007). RASSF1A can also promote apoptosis through a non-Hippo linked mechanism via interaction with MAP1 and activation of the proapoptotic protein Bax (Baksh et al., 2005; Vos et al., 2006). This integral role for RASSF1A in the regulation of programmed cell death is one of the reasons that its loss in human malignancy is detrimental.

1.4.7 RASSF1A & Genome Integrity

Another important function of RASSF1A that lends to its tumour suppressive role, is the protection of genome stability. ATM (ataxia-telangiectasia mutated) is an upstream DDR protein that is activated upon the onset of DNA damage (Bakkenist and Kastan, 2003). When ATM is activated it phosphorylates and activates RASSF1A on Ser131, this stimulates the interaction between RASSF1A and the MST2 kinase, leading to increased activation of LATS1 and formation of the YAP/p73 transcriptional complex (Hamilton et al., 2009) which regulates expression of proapoptotic genes (Strano et al., 2005). ATR (ataxia-telangiectasia – and Rad3 – related) can also phosphorylate RASSF1A in response to DNA damage (Pefani et al., 2014). RASSF1A was initially identified as an interactor of the DNA damage repair protein XPA (Dammann et al., 2000) and in 2015, a non-Hippo signalling oriented role of RASSF1A in genome stability was identified. Donninger et al. showed that RASSF1A can directly influence DNA repair by complexing with XPA and facilitating its nucleotide excision repair activity by modulating its acetylation by SIRT1 (Sirtuin 1) (Donninger et al., 2015). RASSF1A was also observed to block activated K-Ras genomic instability (Vos et al., 2004).

1.4.8 RASSF1A in Stem cells

An emerging role for RASSF1A in stem cells has been identified and is linked to RASSF1A's modulation of the Hippo pathway. Recently, we demonstrated that RASSF1A has a role in differentiation (Papaspyropoulos et al., 2018). Our data suggests that RASSF1A is important in early mESC fate specification, and that an increase in *Rassf1a* expression promotes differentiation by modulating the transcriptional partners of YAP. Instead of YAP complexing with β-catenin/TCF (which is important in maintaining

pluripotency (Sato et al., 2004; Ying et al., 2008; ten Berge et al., 2011)), RASSF1A expression leads to YAP instead binding to p73, enabling the activation of a differentiation promoting transcriptional programme. Of note, the activation of *Rassf1a* was found to be under the control of the master transcription factor GATA1. Taken together, these studies demonstrate that RASSF1A may act as a barrier to self-renewal. This is particularly important in the cancer context, where an increase in stem-like properties is frequently associated with poor prognosis and increased invasiveness (Hochedlinger et al., 2005; Ben-Porath et al., 2008; Chang, 2016). RASSF1A is being considered to play an increasingly pivotal role in the balance between pluripotency and malignancy, with epigenetic inactivation of RASSF1A in human mesenchymal stem cells being sufficient to give them a cancerous phenotype (Teng et al., 2011).

1.4.9 RASSF1A in Mitosis and Cell Cycle Control

Overall, however, RASSF1A has been most heavily linked to the regulation of the cell cycle and mitosis through a number of mechanisms. It has been claimed that cell cycle control by RASSF1A is more important than its apoptotic role in the suppression of tumourigenesis (Donninger et al., 2014). RASSF1A has shown the ability to arrest the cell cycle in each of its phases, and is generally viewed as a restrictor of cell cycle progression (Rong et al., 2004). In the transition from G_1-S phase, RASSF1A engages the Rb (Retinoblastoma) cell cycle checkpoint and inhibits the accumulation of Cyclin D1 which usually permits the progression of the cycle to S-phase (Shivakumar et al., 2002). RASSF1A expression was further shown to inhibit the cell cycle only transiently in G_1 phase, whilst also inducing arrest at the G_2/M interface in a MT interaction dependent manner (Rong et al., 2004; Donninger et al., 2014). Further elucidation of RASSF1A's

control over the cell cycle in G_1 was demonstrated when it was shown that RASSF1A can induce both cell cycle arrest and senescence by regulating the expression of the CDK inhibitor $p21^{Cip1/Waf}$ (Thaler et al., 2009). Moreover, RASSF1A expression was also shown to block JNK (c-Jun-NH_2-kinase) signalling in lung cancer cells, impeding their growth with a G_1 arrest resulting from a down-regulation of Cyclin D1 (Whang et al., 2005).

RASSF1A has exhibited the ability to allow cells to exit mitosis when mitotic stress is encountered via a transient M-phase interaction with DAXX (Death Domain- Associated Protein 6) – an important precursor to appropriate apoptosis in abnormal cells (Giovinazzi et al., 2012). Studies also suggest that APC/Cdc20 dependent mitotic progression may be under the control of RASSF1A. The APC (anaphase promoting complex) facilitates progress through and out of M-phase by targeting mitotic proteins, such as cyclin B, for degradation (King et al., 1995; Peters, 2006). Cdc20 is an activating co-factor of the APC with which RASSF1A has been shown to interact, and inhibit (Sup Song et al., 2004a). However, a follow up study disputed this claim (Limin Liu, Katrin Baier, 2007), and so it is clear that more work is required to fully understand RASSF1A's role in mitotic progression.

Aurora-A is a major mitotic kinase that localises with the centrosomes and is necessary for their maturation (Gopalan et al., 1997; Roghi et al., 1998; Hannak et al., 2001) and for maintaining mitotic integrity and progression (Meraldi et al., 2002; Fu et al., 2007). Regulation of RASSF1A in mitosis seems to be under the control of Aurora-A. Aurora-A has been shown to directly phosphorylate and activate RASSF1A (Rong et al., 2007), thus directly regulating the ability of RASSF1A to arrest the cell cycle. Furthermore, the Aurora-A dependent phosphorylation of RASSF1A at Ser203 has been shown to be

necessary to allow prometaphase progression by suppressing the inhibitive action of RASSF1A on the APC (Song et al., 2009). Interestingly, RASSF1A has also been suggested to act as a scaffold that facilitates the phosphorylation and activation of Aurora- A (Liu et al., 2008). This suggests that there may be feedback loop operating between the two proteins, ensuring a delicate balance between their functions to maintain proper cell-cycle progression whilst avoiding tumourigenic errors.

RASSF1A mediated control of the cell cycle is impaired upon ablation of its ability to interact with MTs (Donninger et al., 2014), perhaps demonstrating that the ability of RASSF1A to interact with and modulate MT dynamics is one of its most important roles. Indeed, the loss of RASSF1A's MT stabilising action in *Rassf1a*$^{-/-}$ mice seems to be the driving cause of increased tumourigenesis observed in these mice, and not deregulated apoptosis (Weyden et al., 2005; Tommasi et al., 2005).

The amino acid positions D120 – S288 of RASSF1A represent a positively charged basic domain which is responsible for the interaction of RASSF1A with MTs (Liu et al., 2003; Rong et al., 2004) and contains both the RA domain and ATM/ATR phosphorylation sites of RASSF1A. Also, RASSF1A has been reported to immunoprecipitate with MAPs (microtubule associated proteins) which also interact with and regulate MT stability and functionality (Dallol et al., 2004). The association of RASSF1A with MTs leads to their stabilisation and protects them from MT destabilising agents such as nocodazole, this stability has been linked to an increase in α–tubulin acetylation (Liu et al., 2003; Vos et al., 2004; Dallol et al., 2004) which may be the result of RASSF1A mediated inactivation of HDAC6 (Histone deacetylase 6), an important tubulin deacetylating protein (Jung Hae-Yun Jung Jun Seok, 2013).

RASSF1A's interaction with MTs is likely largely facilitated by its localisation with the centrosome. RABP1 (RASSF1A-binding protein 1) is required for RASSF1A localisation with the centrosomes, with its ablation leading to accelerated mitosis (Sup Song et al., 2004b). RASSF1A has been reported to interact with RAN-GTPase at the spindle poles, and this interaction is thought to be crucial in the induction of MT hyperstability by RASSF1A (Dallol et al., 2009). Importantly, RASSF1A binds specifically and stably to distinct segments of the MTs that are non-dynamic. These sites mark the location of MT rescue and, therefore, the promotion of polymerisation which is coupled with the ability of RASSF1A to bundle the MTs – all of which lead to MT stabilisation (Arnette et al., 2014). Arnette et al., further show that the presence of RASSF1A on the MTs is essential for proper polarity establishment.

RASSF1A has been thus extensively described as a major player in the regulation of mitosis and the cell cycle. Interestingly, many of these roles are Hippo pathway independent, demonstrating a vast functionality for RASSF1A beyond Hippo signalling.

1.4.10 RASSF1A in Cancer

Emerging studies have shown that RASSF1A inactivation leads to early cancer onset. For example, the single nucleotide polymorphic (SNP) variant of RASSF1A (RASSF1 c.397G>T, pAla133SER, rs2073498) cannot be phosphorylated by ATM or ATR, leading to defects in DDR and early cancer onset (Kanzaki et al., 2006; Gao et al., 2008; Bergqvist et al., 2010). Despite this, somatic mutations of RASSF1A are uncommon (Dammann et al., 2003b). However, as previously mentioned, epigenetic inactivation of *RASSF1A* is perhaps the most frequent event in sporadic human malignancy. Epigenetic regulation has been identified as a mediator of expression for several *RASSF* genes, specifically in

the form of CpG island methylation at the promoters. This methylation and silencing of *RASSF1A* is considered to be one of the most common and earliest events in human cancer (Klajic et al., 2013). Epigenetic silencing of *RASSF1A* has been detected in other diseases including certain types of inflammatory bowel disease (IBD) (Wahab et al., 2011) and pancreatitis (Dammann et al., 2003a), where RASSF1A loss has been correlated to colorectal and pancreatic cancer onset, respectively. This supports the notion that inactivation of RASSF1A expression may be one of the earliest steps leading to cancer.

Hypermethylation of the *RASSF1A* promoter has been reported in many cancers (Donninger et al., 2007; Volodko et al., 2014), with the event observed in as many as 88 % of small cell lung cancers (Grote et al., 2006) and 99 % of prostate cancers (Jerónimo et al., 2004). The loss of *RASSF1A* expression has been reported to correlate with poor prognosis, higher tumour grade and increased metastasis (Klajic et al., 2013; Duan et al., 2013).

The loss of RASSF1A's ability to stabilise tubulin is one of the major factors leading to tumourigenesis. Destabilised MTs can lead to cancer causing genomic instability during mitosis, when the MTs are heavily involved in proper chromosome segregation. Further, tubulin instability has been independently linked to an invasive/metastatic phenotype in cancer cells (Kaverina and Straube, 2011). Changes to the MT network are becoming an increasingly recognised feature in a range of cancers. Often in cancer, there are variations in tubulin post-translational modifications (PTMs) and alterations in the expression of MAPs as well as the different tubulin isoforms. In fact, a recent review summarised that the deregulation of tubulin dynamics leads to several complications in

homeostatic mechanisms, including errors in autophagy, apoptotic signalling and metabolism which ultimately causes disease progression and treatment resistance (Parker et al., 2014).

1.4.11 RASSF7

RASSF7 is arguably the first identified RASSF member, but when the gene was discovered in 1992 it was named *HRC1* (HRas cluster 1). The gene locus was located upstream of the *HRAS1* gene and from the initial study it was recognised that it may belong to a conserved gene family given the identified homology with other regions of the genome (Weitzel et al., 1992). Since then, the gene has been officially renamed as *RASSF7* and joined the ranks of the RASSFs (Sherwood et al., 2008).

RASSF7 is an N-terminus RASSF protein, with its RA domain at the N-terminus of the protein and lacking a C1 and SARAH domain, instead displaying two coiled-coil C-terminal domains (Figure 1.6). The gene is located on chromosome 11p15.5 and has three known splice variants, with isoform 1 considered the 'canonical' sequence on UniProt[1].

The function of RASSF7 has remained elusive. For many years following the *HRC1* discovery it was speculated that it may be involved in cell growth and differentiation, as well as having a potential link to carcinogenesis (Weitzel et al., 1992). However, the first molecular finding was the report that RASSF7 (referred to as 'carcinoma associated') was expressed in the early *Xenopus* embryo (Chalmers et al., 2006). This expression was confirmed (Sherwood et al., 2008) and also demonstrated in the mouse embryo (Recino

[1] http://www.uniprot.org/uniprot/Q02833

et al., 2010). This suggests that RASSF7 may have a role in development and studies indicate it is important specifically in brain development. In the developing *Xenopus* embryo, *RASSF7* was shown to be highly expressed in the neural tube and was crucial in maintaining tissue architecture there (Sherwood et al., 2008). In addition to this, it was recently reported that RASSF7 directly interacts with DISC1 (Disrupted in Schizophrenia 1), which is expressed ubiquitously in the brain and is important both in the adult and embryonic tissue (Schurov et al., 2004). This interaction is necessary for the activation of the RAS/MEK/ERK signalling pathway, which regulates genes involved in astrogenesis (Wang et al., 2016).

RASSF7, like RASSF1A, has also been shown to be an important regulator of mitosis and apoptosis, and it also localises with the centrosomes. The developmental defects observed in *RASSF7* depleted *Xenopus* neural tubes were found to be due to an inability to complete mitosis. RASSF7 expression was found to be important in MT organisation during M-phase and spindle formation and, interestingly, the localisation of RASSF7 at the centrosome was dependent on the presence of stable MTs (Sherwood et al., 2008). This mitotic role for RASSF7 was also confirmed in human cells, with knock down of expression leading to defective spindle formation and chromosome congression due to a failure to activate Aurora-B (Recino et al., 2010). Conversely to their studies in *Xenopus*, Recino et al. (2010) showed that RASSF7 centrosomal location in human cells is not mediated by MTs, as nocodazole treatment had no effect on the co-localisation. More recently, the same group showed that RASSF7's localisation with the centrosome is mediated by its coiled-coil domain, and not the RA domain. They also showed that a RASSF7 truncation observed in renal clear cell carcinoma can lead to centrosomal

defects, with the mutated cells displaying abnormally excessive RASSF7 centrosome association and high levels of γ-tubulin (Gulsen et al., 2016).

Similarly to RASSF1A, RASSF7 has been shown to regulate JNK signalling, however, it plays an anti-apoptotic role. Via its RA domain, RASSF7 interacts with NRas and MKK7 (mitogen-activated protein kinase kinase 7) and inhibits the pro-apoptotic pathway (Takahashi et al., 2011). This discovery has proven therapeutically promising for patients with intervertebral disc degeneration (IDD) which is thought to be linked to increased apoptosis. Degenerative IDD cells display a lower level of RASSF7, and overexpression of the protein leads to a lower rate of apoptosis (Liu et al., 2015). Recently, it has also been demonstrated that RASSF7 can interact with MST1/2, however, the biological relevance of this interaction remains underexplored (Chan et al., 2013).

1.4.12 RASSF7 & Cancer

In contrast to *RASSF1A*, *RASSF7* is typically considered an oncogene. It has been found to be overexpressed in endometrial cancer (Mutter et al., 2001), ovarian clear cell carcinoma (Tan et al., 2009), pancreatic ductal adenocarcinoma (PDAC) (Friess et al., 2003; Logsdon et al., 2003; Brandt et al., 2004), islet cell tumours (Lowe et al., 2007) and malignant thyroid neoplasms (Li et al., 2013b) . It is also upregulated in hypoxia (Recino et al., 2010), a common feature of solid tumours. RASSF7 was directly demonstrated to act as an oncogene in non-small cell lung carcinoma (NSCLC), with overexpression of the protein leading to increased tumour volume, weight and metastatic lesions in nude mice by inhibiting Hippo signalling (Zheng et al., 2017).

Interestingly, RASSF7 has also been found to be silenced in cancers, with promoter methylation reported in 16 % of chronic lymphocytic leukaemia cases (Shinawi et al.,

2012) and in a high proportion of neuroblastoma samples (Djos et al., 2012), suggesting that it may harbour some tumour suppressive functions. However, it is considered a much less frequent event than *RASSF1A* methylation.

Despite this, there is still limited understanding of the functional roles of RASSF7 and how this links to human pathology. Given the emerging disease related roles of RASSF7 and the extensive roles of the other RASSF members, it is likely that there is still a wealth of information to be uncovered.

1.5 Aims of this Work

It is clear that *RASSF1A* is an important TSG in human malignancies and that it is critical in maintaining cellular integrity. However, there remains much unknown about how this gene confers its detrimental phenotype, particularly in the stem cell context. Centrosomal localisation of RASSF1A is a widely-recognised aspect in RASSF1A functionality studies, but the implications of this in differential cell fate specification remain under-explored. In this thesis, our first aim was to determine the consequences of RASSF1A inheritance in mESCs and establish if it may be playing a role in asymmetric cell division.

As studies into the RASSF proteins progress, it is becoming increasingly clear that they perform a vast variety of important cellular functions. Bearing this in mind, we decided to investigate one of the N-terminal proteins, RASSF7, due to its centrosomal localisation, in the hope that we may further establish its cellular role.

Chapter 2

Methods & Materials

2.1 General Laboratory Reagents

Plastic ware was purchased from Sarstedt and Corning. Glassware was purchased from Fisher and VWR unless otherwise stated.

2.2 Cell Culture

All culture media/supplements are from Gibco® unless otherwise stated and cells were maintained in a humidified incubator with 5 % CO_2, at 37°C. All percentages stated are (v/v). Cancer Cell lines (HeLa, MCF7, HOP-92, EKVX, NCI-H460, NCI-H322M, PANC1 and H1299) were cultured in DMEM supplemented with 10 % FBS, 100U/mL Pen/Strep and 2mM Glutamine. ARPE19 Cells were cultured in DMEM/F12 supplemented with 10 % FBS. Mouse ESC line (E14) was maintained in DMEM supplemented with approximately 0.01μg/mL ESGRO® (LIF, Millipore), 10 % Knockout Serum Replacement (Invitrogen), 2 % ES-Grade FCS (Invitrogen), 1.25 % 200mM L-Glutamine, 1.25 % 10mM Non-essential amino acids and 4μL β–mercaptoethanol. Stem cells were cultured on plates coated with gelatin (Sigma Aldrich, 0.1 %). All cells were washed with sterile 1X PBS and passaged using 0.25 % Trypsin-EDTA solution.

To cryopreserve cells, they were passaged, pelleted and gently resuspended in freezing media. For the cancer cell lines and ARPE19 cells, freezing media was comprised of FBS

supplemented with 10% DMSO. Mouse ESCs were frozen in complete mESC culture media supplemented with 10 % DMSO. The cell suspension was transferred to cryogenic vials and initially frozen in Mr Frosty™ freezing containers (Sigma-Aldrich) at -80°C before being transferred to liquid nitrogen for long term storage.

2.2.1 Mouse ESC Differentiation

Mouse ESCs were differentiated by LIF withdrawal. Simply, mESCs were cultured in complete media, without LIF, to allow spontaneous differentiation.

2.2.2 Transient (Forward) Transfection

Transfection of cancer/ARPE19 cell lines was carried out with Lipofectamine 2000/3000 as the transfection agent and OptiMEM (Gibco) used as the diluent, per the manufacturer's protocols. Briefly, cells were seeded in P/S-free media the day before transfection was scheduled. Appropriate volumes of plasmid/siRNA were diluted in OptiMEM (depending on final medium volume) and Lipofectamine was diluted in OptiMEM, and incubated at room-temperature for 5 minutes. Following incubation, the plasmid/siRNA and Lipofectamine mixes were combined in a 1:1 ratio and incubated for 15 minutes at room temperature. The transfection mix was added dropwise to seeded cells. Media was changed 6 – 8 h later when Lipofectamine 2000 was used, and 24 h with Lipofectamine 3000. Cells were collected for processing 48 h post – transfection. For plasmid transfection 5 μg of plasmid was used for a 10 cm plate (or suitably scaled up/down for other sizes) and 100 nM of siRNA from a 100 μM stock was used for siRNA-mediated knock down.

2.2.3 Transient (Reverse) Transfection

Reverse transfection was used to improve the efficiency in mouse embryonic stem cells (mESC) and Lipofectamine 3000 was used as the transfection reagent and OptiMEM (Gibco) used as the diluent. Plasmid and siRNA transfection mixes were prepared as described for forward transfection, but cells were added to the transfection mix post-incubation. Media was then added directly to the cell/transfection mix on the plate. Cells were collected for processing 48 h post-transfection.

2.2.4 Drug Treatment

Cells were treated by relevant drugs (in this thesis Tubacin, 2 μm for 24 h, and S-Trityl-L-cysteine, 5 μm for 16 h) by addition of the drug to the medium in suitable concentration prior to addition of the media to cells.

2.2.5 Induction of Ciliogenesis

Ciliogenesis was induced by serum starvation. Briefly, cells were cultured as described but with 0.1 % FBS.

2.3 Chemicals

Reagent	**Provider**
1 kb DNA Ladder	New England Biolabs
2-Propanol	Fisher Scientific
4',6-diamidino-2-phenylindole dihydrochloride (DAPI)	Thermo Fisher Scientific
Agarose	Sigma-Aldrich UK
Dimethyl sulfoxide (DMSO)	Sigma-Aldrich UK
Dithiothreitol (DTT)	Sigma-Aldrich UK
Ethanol (EtOH)	Fisher Scientific
Formaldehyde (PFA)	Thermo Fisher Scientific
Glycine	Fisher Scientific
HiMark Pre-Stained Protein Standard	Life technologies
Hydrochloric acid	Fisher Scientific
LB Broth	Sigma-Aldrich UK
Lipofectamine 2000	Thermo Fisher Scientific
Lipofectamine 3000	Thermo Fisher Scientific
Methanol (MeOH)	Fisher Scientific
Milk powder	Marvel
NuPAGE MOPS SDS Running Buffer (20X)	Thermo Fisher Scientific
Phosphatase inhibitors	Roche
Phosphate buffered saline (PBS) tablets	Oxoid
Protease inhibitors	Roche
Sodium chloride	Fisher Scientific
Sodium deoxycholate	Sigma-Aldrich UK
Sodium dodecyl sulphate (SDS)	Sigma-Aldrich UK
S-Trityl-L-cysteine (STLC)	Sigma-Aldrich UK
Tris base	Fisher Scientific
Triton X 100	Sigma-Aldrich UK
Tween 20	Sigma-Aldrich UK
Tubacin	Sigma-Aldrich UK

2.4 Buffers

Buffer	Ingredients
4 x DNA Loading Buffer	50% (v/v) Glycerol 1 X TAE Orange G
5% Skimmed milk blocking solution	5% (w/v) skimmed milk powder in 1 x PBS-T
LB Broth	2% (w/v) LB broth in dH_2O
PBS (Phosphate-buffered Saline)	137 mM NaCl 2.7 mM KCl 10 mM Na_2HPO_4 1.76 Mm KH_2HPO_4 pH 7.4
PBS-T (PBS-Tween, 10 %)	PBS as above 0.1% (v/v) Tween 20
TAE Buffer	40 mM Tris 18 mM Glacial acetic acid 1mM EDTA pH 8.0
Transfer Buffer	25 mM Tris 190 mM Glycine 20% (v/v) Methanol

2.5 RNAi Sequences

SiRNA	Sequence (Sense Strand)	Supplier
MST2	CCUGUUGAAUCAGAUCUUCAGGGAAA	Eurofins MWG OPERON
Luciferase	CAUUCUAUCCUCUAGAGGAUG	Dharmacon
RASSF1A (Human)	GACCUCUGUGGCGACUUCA	Eurofins MWG OPERON
RASSF1A (Mouse) Stealth siRNA	CAGAACTCATTGAACTACGCGAGCT	Invitrogen
RASSF7 (Human), SMARTpool	UGCCAGCGAUGUCCAGUUU GAACGCUGCCUAAUUCGUG CGCACUAGCCCAAGCAAUA CAGCAGAGCGAGCCUUGCA	Eurofins MWG OPERON

2.6 Primary Antibodies for Immunofluorescence

Antibody	**Company**	**Species**	**Dilution**
Acetylated αTubulin	Thermo	Mouse	1:1000
ARL13B	PTG Labs	Rabbit	1:250
Centrin-3	Santa Cruz	Mouse	1:250
CEP164	Gift from Gislene Pierera	Guinea Pig	1:1000
γ-Tubulin	Thermo	Rabbit	1:1000
γ-Tubulin	Thermo	Mouse	1:1000
HDAC6	Abcam	Rabbit	1:100
IFT88	PTG Labs	Mouse	1:100
Lamin A	Cell Signalling Technologies	Mouse	1:500
Lamin A	Abcam	Rabbit	1:500
MST2	Abcam	Rabbit	1:100
Nanog (XP)	Cell Signalling Technologies	Rabbit	1:500
Numb	Abcam	Rabbit	1:100
ODF2	Gift from Gislene Pierera	Guinea Pig	1:500
pRASSF1A S131	Custom antibody; Hamilton et al., 2009	Rabbit	1:50
RASSF1A	eBioscience	Mouse	1:50
RASSF1A	Atlas	Rabbit	1:100
RASSF7 (C6)	Santa Cruz	Mouse	1:100

2.7 Primary Antibodies for Western Blot

Antibody	**Company**	**Species**	**Dilution**
Acetylated αTubulin	Thermo	Mouse	1:5000
Actin	Santa Cruz	Goat	1:1000
Cyclin A	Cell Signalling Technologies	Mouse	1:1000
Cyclin E	Cell Signalling Technologies	Rabbit	1:1000
GAPDH	Cell Signalling Technologies	Mouse	1:5000
HDAC6	Abcam	Rabbit	1:1000
IFT 88	PTG Labs	Mouse	1:1000
IFT81	PTG Labs	Rabbit	1:1000
LATS1	Abcam	Rabbit	1:1000
MST2	Abcam	Rabbit	1:1000
Nanog	Cell Signalling Technologies	Rabbit	1:1000
OCT4A	Abcam	Rabbit	1:1000
pHistone H3	Cell Signalling Technologies	Rabbit	1:1000
RASSF1A	Atlas	Rabbit	1:500
RASSF7 (C6)	Santa Cruz	Mouse	1:1000

2.8 Secondary Antibodies

Antibody	**Company**	**Dilution**
Alexa fluor® donkey anti-mouse 488nm	Thermo Fisher Scientific	1:500
Alexa fluor® goat anti-mouse 1gG1 488nm	Thermo Fisher Scientific	1:500
Alexa fluor® goat anti-rabbit 488nm	Thermo Fisher Scientific	1:500
Alexa fluor® donkey anti-goat 488nm	Thermo Fisher Scientific	1:500
Alexa fluor® donkey anti-mouse 594nm	Thermo Fisher Scientific	1:500
Alexa fluor® goat anti-mouse 1gG1 594nm	Thermo Fisher Scientific	1:500
Alexa fluor® goat anti-rabbit 594nm	Thermo Fisher Scientific	1:500
Alexa fluor® donkey anti-goat 594nm	Thermo Fisher Scientific	1:500
Alexa fluor® goat anti-guinea pig 594nm	Thermo Fisher Scientific	1:500
Alexa fluor® donkey anti-mouse 647nm	Thermo Fisher Scientific	1:500
Alexa fluor® goat anti-rabbit 647nm	Thermo Fisher Scientific	1:500
Alexa fluor® donkey anti-goat 647nm	Thermo Fisher Scientific	1:500
Anti-Goat IgG, HRP conjugated	Jackson Immuno Research	1:5000
Anti-Mouse IgG, HRP conjugated	Jackson Immuno Research	1:5000
Anti-Rabbit IgG, HRP conjugated	Jackson Immuno Research	1:5000

2.9 Molecular Biology

2.9.1 Molecular Cloning

The pZsGreen plasmid was used throughout this thesis, with different cDNA sequences cloned into the backbone (Figure 2.1). In this project, RASSF7 was cloned into the pZsGreen plasmid following restriction digest of the vector with HindIII and BamHI restriction enzymes for 1 h at 37 ^{o}C and ligated with the cDNA insert by incubation with the T4 DNA Ligase Buffer mix at room temperature for 10 min. The ligated ZsRASSF7 plasmid was then transformed into bacteria and the clones tested for integration by DNA digest and sequencing.

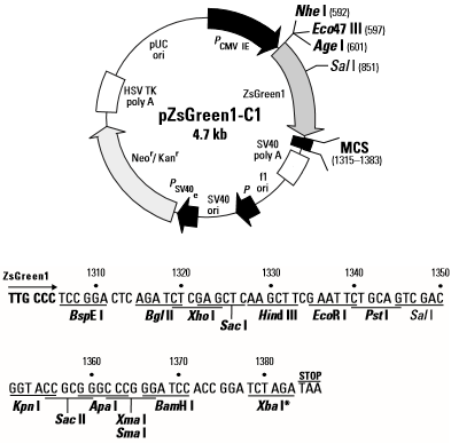


Figure 2. 1 pZsGreen Plasmid Map

2.9.2 Bacterial Transformation

LB agar plates and LB broth (both Sigma) were prepared prior to transformation. To achieve this 20g LB was dissolved in 500ml Milli Q water and 31g 2YT broth was dissolved in 1 L Milli Q Water. Autoclavation at 121 ^{o}C, 15 psi for 30min was used for the sterilisation process. The LB agar was then left to cool to approximately 50 ^{o}C before

adding the required antibiotics to a final concentration of 100 µg/mL. Once completed the agar was distributed into 10cm (Thermo Fisher Scientific) dishes and when it had solidified was then stored at 4 °C.

DNA constructs were transformed by heat shock (42 °C, 30 sec) into DH5α *E. coli* (Life Technologies) and plated onto agar plates containing an appropriate antibiotic selection agent. LB broth (1 Ml) was added to the bacteria then incubated at 37 °C for 1hr with shaking at 750rpm (Eppendorf heat block). Once complete the bacteria were spun down at 4500rpm then resuspended in 100 µl LB broth. Transformation reactions were spread onto LB agar plates which had been supplemented with appropriate antibiotics then incubated at 37 °C. Single clones were picked, and the DNA purified using a mini-prep kit (Qiagen). Correct insertion of the PCR product into the vector was tested by double restriction digest, to show reconstitution of the cut sites, and by Sanger sequencing (Source Biosciences).

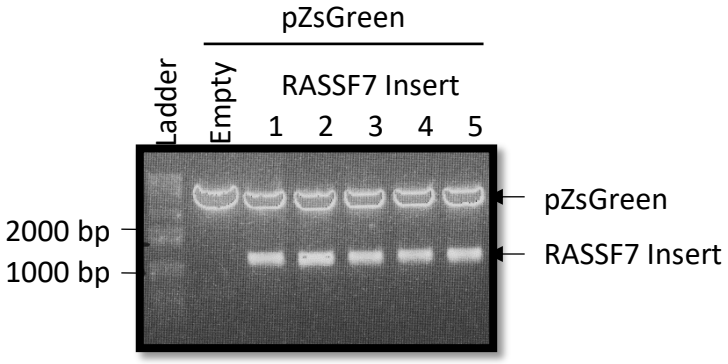


Figure 2.2 DNA Restriction Digest showing the successful integration of RASSF7 cDNA into a pZsGreen Backbone. All 5 isolated strains demonstrated successful insertion, BamHI and HindIII restriction endonucleases were used for DNA restriction.

2.9.3 Plasmid Isolation

A sterile pipette tip was used to pick colonies and transferred to 5ml LB broth. The LB broth contained the appropriate antibiotic in a round-bottom 14ml tube (Nunc™, Thermo Fisher Scientific). Incubation of the starter cultures was carried out for approximately 6-10hrs at 37 ^{o}C whilst shaking at 225rpm (Innova 44 Incubator). Overnight culture of 200ml LB broth, containing the appropriate antibodies, were inoculated with 500µL bacterial starter culture. Once the bacteria had grown they were harvested through centrifugation which occurred at 6000g for 15min at 4 ^{o}C. Isolation of the plasmid DNA was achieved using a QIAGEN Plasmid Maxi Kit. In brief, bacterial pellets were resuspended, lysed (buffer P1 and P2) and then precipitated (buffer P3). To bind plasmid DNA to the column, supernatant was applied to a Qiagen-tip 500. Once was washed with buffer QC, DNA was eluted with buffer QF and then precipitated using isopropanol. After centrifugation and washing with 70% (w/v) ethanol, the DNA was air-dried and resuspended in 200µl nuclease-free water.

2.10 Biochemistry

2.10.1 Cell Lysate Extraction & Quantification

Cell pellets were lysed in SDS lysis buffer (containing Na_3VO_4, β–mercaptoethanol, 50X protease inhibitors and sodium fluoride) and then boiled at 100^{o}C until dissolved. Protein concentration was determined using the Nanodrop™ machine.

2.10.2 Immunoprecipitation

Cells to be immunoprecipitated were lysed on ice using 500 µL NP40 lysis buffer (150 mM Sodium Chloride, 20 mM Hepes, 0.5 µM EDTA, 50 mM Sodium Fluoride, 10 mM b-

glycerophosphate, 0.5 % (v/v) NP40 and 0.5 mM Sodium orthovanidate). Lysates were incubated with end-over-end rotation for 15 min at 4 ^{o}C and sonicated for 2 secs before clearing by centrifugation (21,913 x g; 30 minutes, 4 ^{o}C). Cleared lysates were transferred to new, labelled 1.5 mL eppendorf tubes and 10 % volume was removed for input control. Lysate concentration was quantified using Bradford assay. Briefly, lysates were diluted 1:10 in 1 X PBS; 5 μL of diluted lysate was pipetted in triplicate into a 96 – well Sterilin Plate (Thermo Fisher) alongside known serial dilutions of Bovine serum albumin (BSA, Thermo Fisher) and a triplicate 1 X PBS control. Next, 250 μL of Commassie Reagent was added to each well and the absorbance measured at 595 nm, the lysate concentrations were calculated via normalisation to the known BSA standards. DynaBeads (Thermo Fisher) were used for immunoprecipitation, with 20 μL used for each condition, and were combined with 1 μg of antibody and equal quantities of cleared cell lysate (approx. 1 mg). Immunoprecipitation mixture was incubated end-over-end for 3 hr at 4 ^{o}C. Using a magnetic rack, the supernatant was discarded, and beads were washed end-over-end at 4 ^{o}C for 5 min, three times with NP40 lysis buffer. Wash buffer was discarded, and protein-bound beads were diluted in 70 μL of 1 X Laemelli loading dye supplemented with 100 nM DTT. Diluted beads were stored at – 20 ^{o}C until analysis by immunoblotting, before which they were boiled at 100 ^{o}C for 30 min to elute bound protein.

2.10.3 Immunoblotting

Normalised cell lysates in 4X loading buffer were loaded in equal quantities and separated by gel electrophoresis at 120 V using pre-cast gels (4-12 % and 10 % Bis-Tris; Invitrogen) alongside See Blue® plus 2 pre-stained marker (Thermo Fisher). The samples

were then transferred from the gel onto a methanol activated PVDF membrane (Immobilon™), sandwiched between Whatman paper, sponges and cassettes, using a BioRad mini gel blotting system. The transfer was performed in ice cold transfer buffer at 100 V for 80 minutes. Membranes were then blocked in 5 % milk (w/v) in PBS-T and then incubated in primary antibody at 4 ^{o}C overnight on a roller; they were washed in PBS-T before secondary antibody incubation at room temperature for 1.5 - 3 hours. To visualise protein bands, the membranes were soaked in ECL solution from Thermo or GE Healthcare and then exposed to Kodak film in a dark room and developed using a XoGraph processor (XoGraph Imaging Systems) before being scanned onto a computer. For multiple antibody probing, membranes were stripped, washed with PBS-T before re-blocking and incubation with the next primary antibody.

2.10.4 Immunofluorescence

Cells to be studied using IF were plated on 10 cm/6 well plates with glass cover slips (Fisher), They were then washed in 1X PBS before being fixed in ice-cold 100 % methanol for 15 mins at - 20 ^{o}C. Cover slips were blocked using 0.2 % (v/v) Fish Skin Gelatin (FSG, Thermo Fisher) (in 1 X PBS). Cells were then incubated in primary antibody in FSG overnight at 4 ^{o}C before being washed in 1X PBS and incubated in secondary antibody for 1 - 3 hours at RT. Cells were re-washed and then mounted onto microscope slides using Prolong® Gold anti-fade reagent with DAPI (Life Technologies). Cover slips were sealed with clear nail varnish.

2.11 Microscopy

2.11.1 Confocal

Confocal microscopy was performed using a Zeiss LSM 780 (with Airyscan fitted). 3-D Images were acquired using optimal slice distance and laser settings were maintained across samples in each experiment. To achieve higher resolution of images, the Airyscan detector was utilised. Airyscan imaging utilises a concentrically-arranged hexagonal detector array which acts as multiple, independent pinholes with positional information, allowing all photons can be collected during image acquisition (as opposed to the rejection of out-of-focus light by the pinhole in conventional confocal imaging). Thus, Airyscan imaging improves optical sectioning allowing for a higher resolution and signal-to-noise ratio, meaning that smaller objects, such as the centrosome, can be imaged with greater clarity.

2.11.2 Live Imaging

Time lapse imaging was performed using a Nikon TE2000 inverted microscope at 37 ^{o}C and 5 % CO_2. Cells were plated on Ibidi μ-slides or μ-dishes 24 h prior to image initiation and the media was changed to complete media without phenol red to enhance visualisation.

2.12 Image Analysis

2.12.1 Zen

Images acquired by Zeiss LSM 780 were processed using the Zen Blue/Black softwares. 3D images were compressed using the Maximum Intensity Projection Method on Zen Black.

2.12.2 Image J – Quantification of Fluorescence Intensity

Fluorescence intensity was determined from 3D reconstructions of cells. In images of cells growing as a colony, it was necessary to create subset images to ensure that Nanog expression from adjacent cells would not influence the read out. Furthermore, mitotic cells were excluded from measurements as NEBD renders them an unreliable readout of Nanog fluorescence. Intensity was calculated using ImageJ, the area, integrated density and mean gray values were measured for each nucleus as well as a 'background' region measurement where no nuclei were present. The corrected total cell fluorescence (CTCF) was calculated using the formula:

CTCF = Integrated Density – (Area of selected cell * Mean fluorescence of background readings)

Following calculation, the CTCF of mESCs per condition was plotted using Excel.

2.12.3 Image J – Cilia Length

To measure cilia length, ImageJ was first calibrated to the correct pixel size in micrometres. Next, the segmented line tool was used to measure individual cilia length

and the resulting data was plotted using Excel. Cilia length was measured using the ARL13B or acetylated α-Tubulin channel.

2.12.4 Image J - Nuclear Size and Scoring

ImageJ was used to measure nucleus size on the DAPI channel along the longest axis of the nucleus. Nuclei were scored as normal or abnormal based on their shape, with a smooth, oval/rounded nucleus considered normal, and irregularly shaped nuclei with visible structures such as micronuclei, nuclear blebs and chromatin bridges scored as abnormally shaped.

2.13 Computational Biology

2.13.1 Gene Set Enrichment Analysis

Gene Set Enrichment Analysis (GSEA) was performed using the GSEA 3.0 software (downloaded from http://software.broadinstitute.org/gsea/index.jsp). The normalised gene expression and isoform mRNAseq Archive data from selected tumour types available from TCGA was downloaded from FireBrowse (http://firebrowse.org/). Once data was downloaded, the gene expression data for RASSF7 or the isoform data for RASSF1A (uc003dae) expression was compiled with corresponding tumour sample mRNA expression. The data were converted to GSEA software compatible expression dataset and phenotype label files and the gene set databases used by the programme were selected using the Molecular Signatures Database (MSigDB, http://software.broadinstitute.org/gsea/msigdb/index.jsp) and the latest version available was utilised. Once all parameters were determined (Number of permutations,

1000; Collapse dataset to gene symbols, false; permutation type, gene set), the software was run and the GSEA results generated.

The GSEA results provide the computation of four values. First, the Enrichment Score (ES) represents the degree that a gene set is overrepresented at the top/bottom of a ranked gene list and is derived from the correlation of a gene with the phenotype. The size of the ES reflects the maximum deviation from zero for a gene set and this can be visualised on an enrichment plot for the top twenty enriched gene sets. Enrichment plots of gene sets linked to the phenotype in question often have a distinct 'peak' in their ES, at the beginning or end of the ranked gene list. The plots also contain information on the position of members of each gene set in the tanked list of genes, within this are the 'leading edge subset', or the members of the gene set which contribute most to the phenotype. The bottom of the plot represents the distribution of the genes in the gene set and their correlation with a phenotype; positive values in this region demonstrate a correlation with the first phenotype analysed whilst a negative value suggests correlation with the second phenotype. Secondly, GSEA also generates a Normalised Enrichment Score (NES). Normalisation of the ES accounts for differences in gene set sizes and in the calculated correlations, allowing for a direct comparison of analysis results from different gene sets. The False Discovery Rate (FDR) for the GSEA is the third statistic generated by the software, which estimates the probability that the calculated NES for a gene set is a 'false positive', values less than 0.25 are generally considered appropriate. Finally, a Nominal P Value is also calculated that represents the statistical significance of the ES for each gene set, however, as it is not corrected for gene set size, the FDR is generally considered a more reliable read-out of significance.

The results also generate a GSEA Report which provides detailed information on gene set enrichment for each analysed phenotype. The report contains a section for gene sets that have a positive enrichment score (i.e. gene sets that are enriched at the top of the ranked list) and a section for gene sets that have a negative enrichment score (i.e. gene sets that are enriched at the bottom of the ranked list). The report also clearly states the number of significant gene sets that have a FDR of less than 0.25 and those with a nominal p-value of less than 0.01 and 0.05. Further, the report contains the enrichment plots for the top NES results as well as links to the detailed enrichment results for each enriched gene set.

2.13.2 Kaplan Meier Curves

Kaplan-Meier plots were generated using the online tool KM-plotter (http://kmplot.com/analysis/index.php?p=background). For each tumour type analysed, the RASSF7 gene symbol (JetSet probes) was selected and survival curves were generated for overall survival using the 'Auto select best cut off' parameter.

2.14 Statistics

All experiments presented were performed for n = 3 unless otherwise stated. Data was plotted using Excel; the standard error of the mean (SEM) was used for error bars and p-values for significance were generated using the Student's T-Test.

Chapter 3

Results I

Investigating RASSF1A's Role at the Centrosome: Differentiation & Asymmetric Cell Division

3.1 Introduction

RASSF1A is an important tumour suppressor gene in humans, with roles in cell death and cell cycle control (Donninger et al., 2014). RASSF1A is a major, upstream regulator of the Hippo pathway and together, they have been implicated in the modulation of pluripotency. Our recent findings in the lab have identified RASSF1A as an important regulator of YAP transcriptional partners during the differentiation programme of mouse embryonic stem cells (mESCs) (Papaspyropoulos et al., 2018), with increased RASSF1A expression leading to differentiation. This is particularly important given our finding that tumours with decreased RASSF1A expression display significant upregulation of ESC-linked gene expression signatures (Pefani et al., 2016).

RASSF1A has been previously shown to display centrosomal localisation in cancer cells (Liu et al., 2003), however, this has not been reported in stem cells. Furthermore, preliminary data from our lab suggested that RASSF1A inheritance could be asymmetric and lead to the fate specification of dividing mESCs. Asymmetric cell division is an important mechanism via which cells can differentiate and has also recently been

implicated in tumourigenesis (Gómez-López et al., 2014). Given this, we hypothesised that RASSF1A's role at the centrosome might contribute to the differentiation phenotype observed upon RASSF1A expression in mESCs. To address this question, we decided to further explore the localisation and function of RASSF1A in mESCs and to see if RASSF1A expression in cancer cells has any impact on differentiation status.

3.2 RASSF1A Expression Correlates with a Differentiation Phenotype

To examine the physiological relevance of RASSF1A in mESCs, we optimised the protocol for RASSF1A staining in immunofluorescence (IF). Using siRNA mediated knockdown of RASSF1A, we were able to confirm that the used antibody was capable of specifically staining endogenous RASSF1A in mESCs (Figure 3.1).

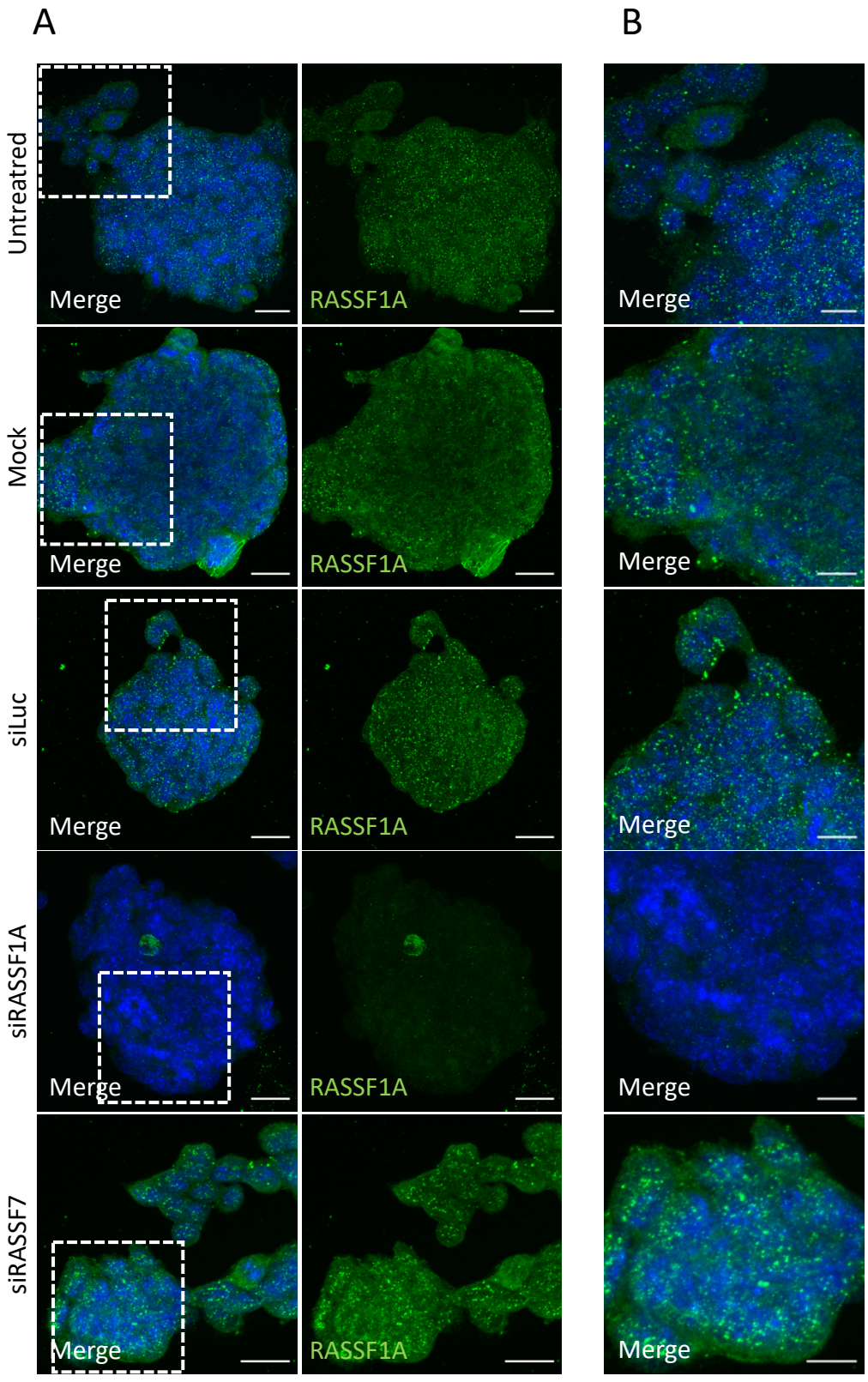


Figure 3. 1 Endogenous RASSF1A localisation. (A) The staining pattern of the RASSF1A eBioscience antibody was confirmed using siRNA mediated knockdown of RASSF1A. siRNAs targeting the Luciferase gene and RASSF7 were used as controls, scale = 20μm. (B) Zoomed regions from indicated areas in (A). DAPI is shown in blue, scale = 10μm.

Western blot and qPCR analysis had been previously used in our group to demonstrate an increase of RASSF1A expression in differentiating cells (Papaspyropoulos et al., 2018). However, prior to this study we had not achieved immunofluorescence confirmation of these findings. Using LIF withdrawal to induce differentiation and the antibody shown in Figure 3.1, we attempted to do so (Figure 3.2).

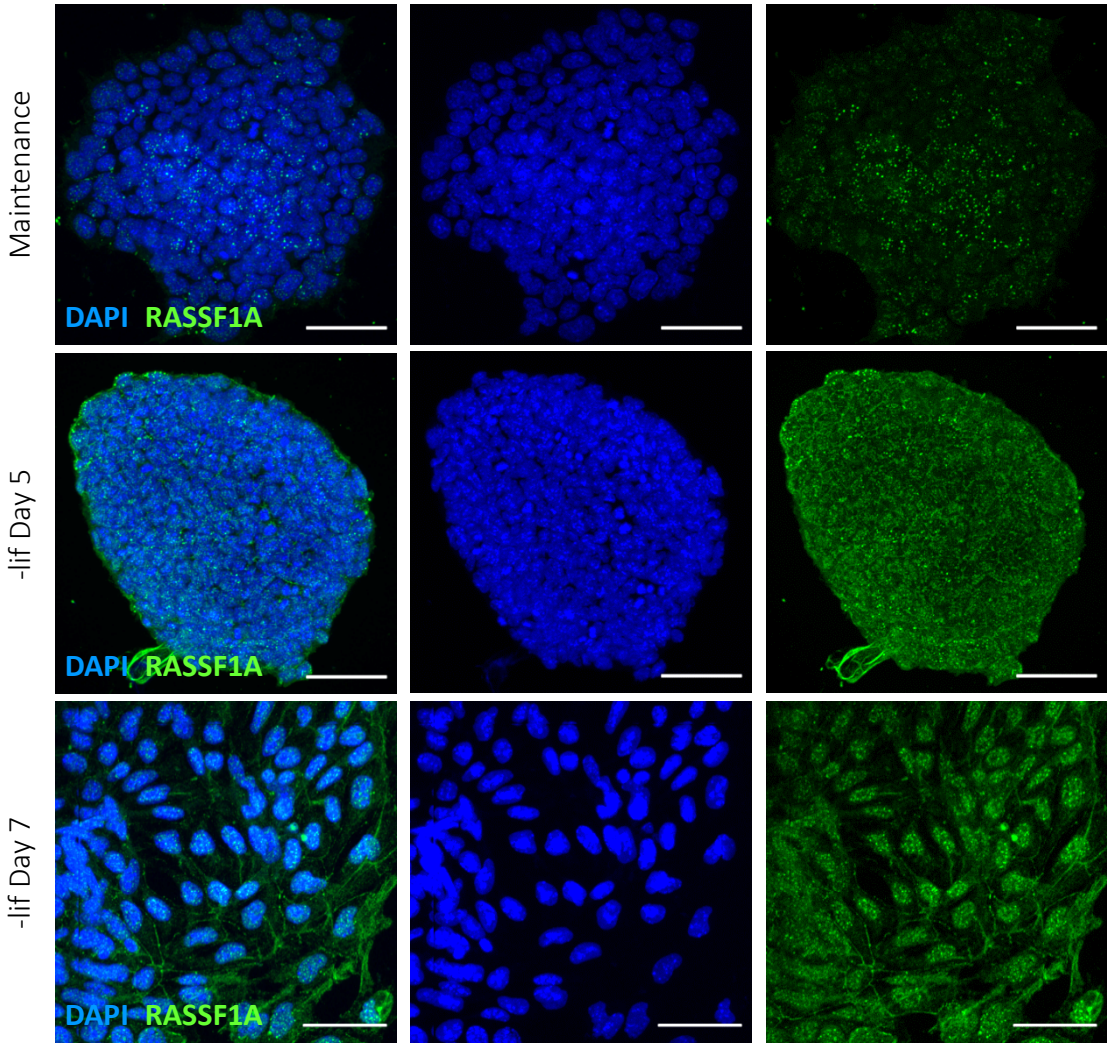


Figure 3. 2 RASSF1A expression increases as mESCs differentiate. Upon the withdrawal of LIF, the expression of RASSF1A was observed as mESCs differentiate. Scale = 50μm.

Concomitant with the findings of Papaspyropoulos et al., we observed an increase in RASSF1A expression as mESCs differentiate. Given these observations, we went on to test the effect of RASSF1A knock down in mESCs (Figure 3.3).

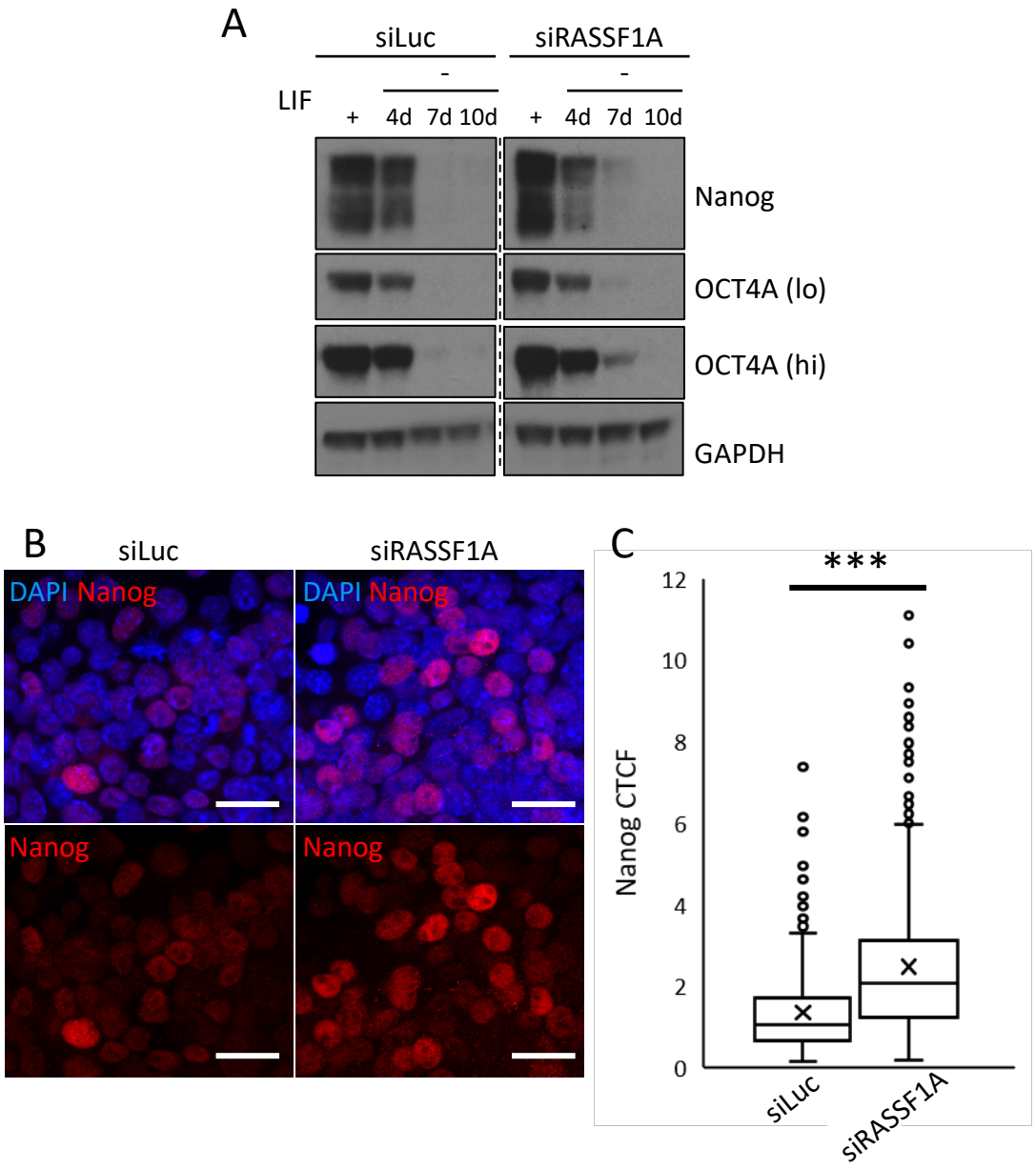


Figure 3. 3 RASSF1A knockdown causes an increased 'stemness' phenotype. (A) mESCs were transfected with the indicated siRNAs and Western Blot analysis was carried out with the antibodies indicated to observe pluripotency transcription factor expression. GAPDH was used as a loading control. (B) Nanog immunofluoresence levels in siRNA treated mESC. (C) Quantified Nanog corrected total cell fluorescence (CTCF) as a box and whisker plot, p = 0.000109. The cross (x) represents the mean CTCF value and the line inside the box represents the median value. Boxes indcate the 25th and 75th percentiles and the whiskers show the 1st – 99th percentile values. Hollow circles depict outliers from these parameters.

Using siRNA mediated depletion of RASSF1A in pluripotent mESCs, we observed an increase in the stem cell markers Nanog and Oct4A in +LIF medium conditions (Figure 3.3 A). This was accompanied by a delay in differentiation upon withdrawal of LIF, as is seen by the persistence of both Nanog and OCT4A at day 7 post-LIF withdrawal in the siRASSF1A treated cells, compared to the siLuc treated cells (Figure 3.3 A). In support of this, we also observed a marked increase in Nanog fluorescence intensity (Figure 3.3 B & C). Taken together, this data expands on previous work in the lab and demonstrates that depletion of RASSF1A causes an increase of 'stemness' in mESCs. This suggests that *Rassf1a* expression is important in mESC differentiation.

3.3 RASSF1A Localises to the Centrosomes of mESCs

As described earlier, the findings from our group by Papaspyropoulos et al. (2018) described a role for RASSF1A in differentiation via a transcriptional control mechanism. However, the expression pattern of RASSF1A during differentiation was quite striking and changed considerably throughout the process (see Figure 3.2). In fact, in some cases it seemed that RASSF1A may be inherited asymmetrically. We wondered, therefore, if RASSF1A may have a dual role in differentiation and also be involved in asymmetric cell division (ACD). ACD is an important method through which SCs can self-renew whilst also allowing one daughter cell to differentiate. Interestingly, the centrosome is a major player in many ACD processes described to date and given the well-known association of RASSF1A with the centrosome, we decided to investigate the possibility that there may be a link between the two in mESCs.

Firstly, to test if RASSF1A localises with the centrosomes of pluripotent mESCs, RASSF1A was overexpressed with a ZsGreen-tag to aid visualisation, hereby referred to as

ZsRASSF1A (Figure 3.4). The results from IF analysis confirmed our hypothesis and demonstrated that RASSF1A resides at the centrosomes of mESCs.

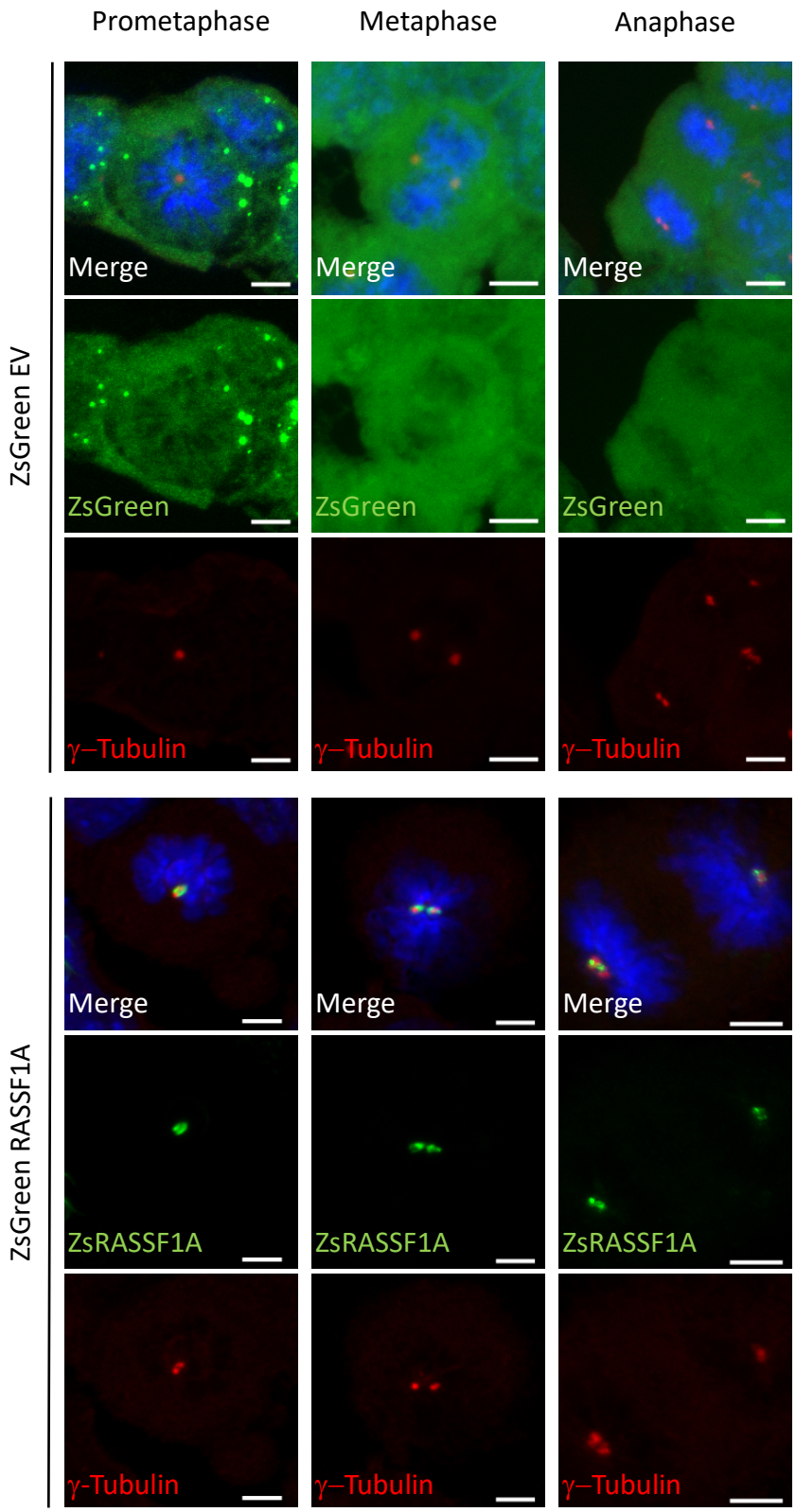


Figure 3. 4 ZsRASSF1A localises with the centrosomes of mitotic mESCS. . ZsRASSF1A overexpression demonstrates that RASSF1A localises at the centrosomes (γ-Tubulin, red) in mitotic mESCs. DAPI is shown in blue, scale = 5μm.

To the best of our knowledge, RASSF1A presence at the centrosome of mESCs has not been reported, so we assessed the effect of RASSF1A overexpression on mitotic index (MI) (Figure 3.5 A) and centriole number (Figure 3.5 B). In line with previous studies (Weyden et al., 2005), RASSF1A overexpression did not lead to any overt or significant changes in either MI or centriole numbers.

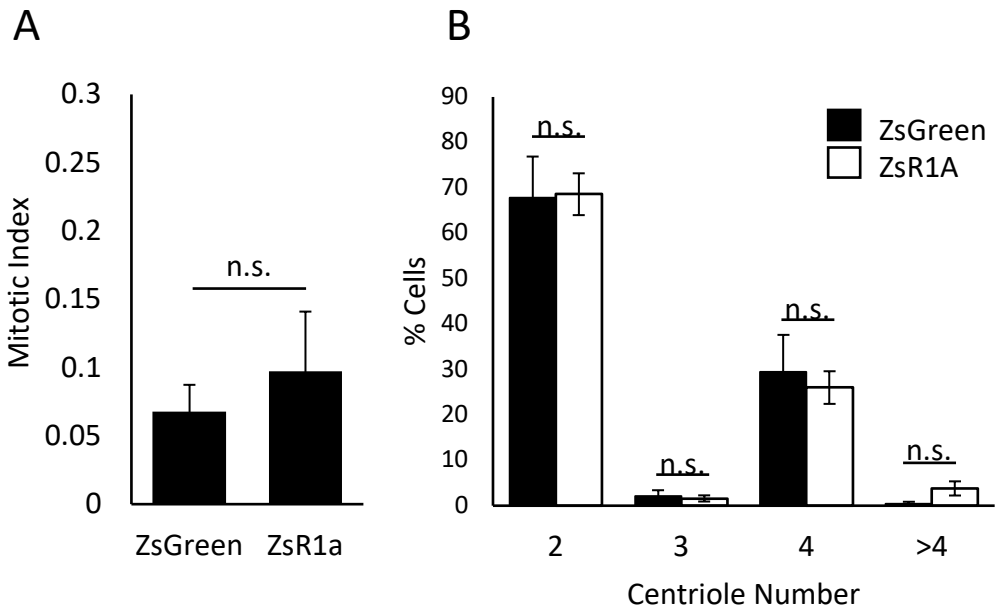


Figure 3. 5 Overexpression of RASSF1A does not affect Mitotic Index or Centriole Numbers in mESCs. (A) Mitotic index of mESCs with expression of ZsGreen or ZsRASSF1A, p = 0.2124. (B) Centriole numbers in mESCs with expression of ZsGreen or ZsRASSF1A. P-values between the centriole numbers for ZsGreen and ZsRASSF1A treated cells are as follows; 2 centrioles, p = 0.47819; 3 centrioles, p = 0.3808; 4 centrioles, p = 0.3853; >4 centrioles = 0.08308.

3.4 RASSF1A is Asymmetric at the Centrosomes of mESCs & may Function in Asymmetric Cell Division

Interestingly, we also noted that the accumulation of ZsRASSF1A on the centrosomes often appeared to be asymmetric (Figure3.6 A). To demonstrate the differences observed, the IMARIS software was used to render 3D-stacks of mitotic mESCs

expressing ZsRASSF1A (Figure 3.6 B) and the frequency of the asymmetry was quantified, demonstrating that a substantial number of mitotic cells had asymmetric RASSF1A levels at their centrosomes (Figure 3.6 C).

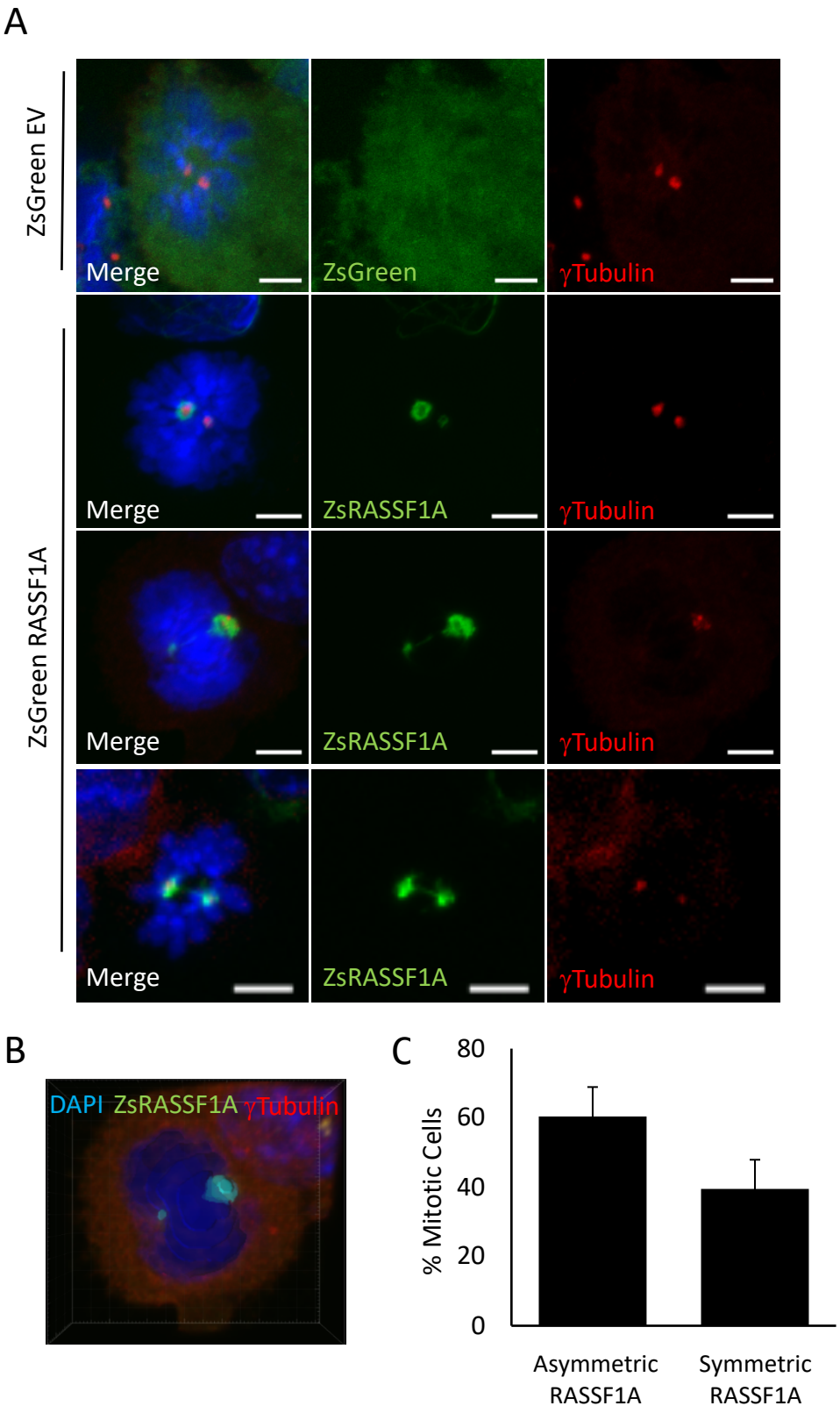


Figure 3. 6 ZsRASSF1A can localise at the centrosomes asymmetrically and symmetrically. (A) ZsRASSF1A was visualised at the centrosomes of mitotic mESCs. DAPI is shown in blue, scale = 5μm. In the ZsGreen RASSF1A panel, the top two rows illustrate the appearance of asymmetric RASSF1A accumulation at the centrosomes, whilst the bottom row exemplifies a symmetric event. (B) IMARIS 3D image reconstruction demonstrates the differences in ZsRASSF1A levels at the centrosomes. (C) The proportion of mitotic cells displaying asymmetric and symmetric levels of ZsRASSF1A at the bipolar centrosomes.

To test the physiological relevance of this observation, we then examined the localisation pattern of endogenous RASSF1A in mESCs. Maximum intensity projection (MIP) of our images showed that RASSF1A can accumulate at the centrosomes, both symmetrically and asymmetrically (Figure 3.7 A). We also quantified this in mitotic mESCs to determine the frequencies (Figure 3.7 B).

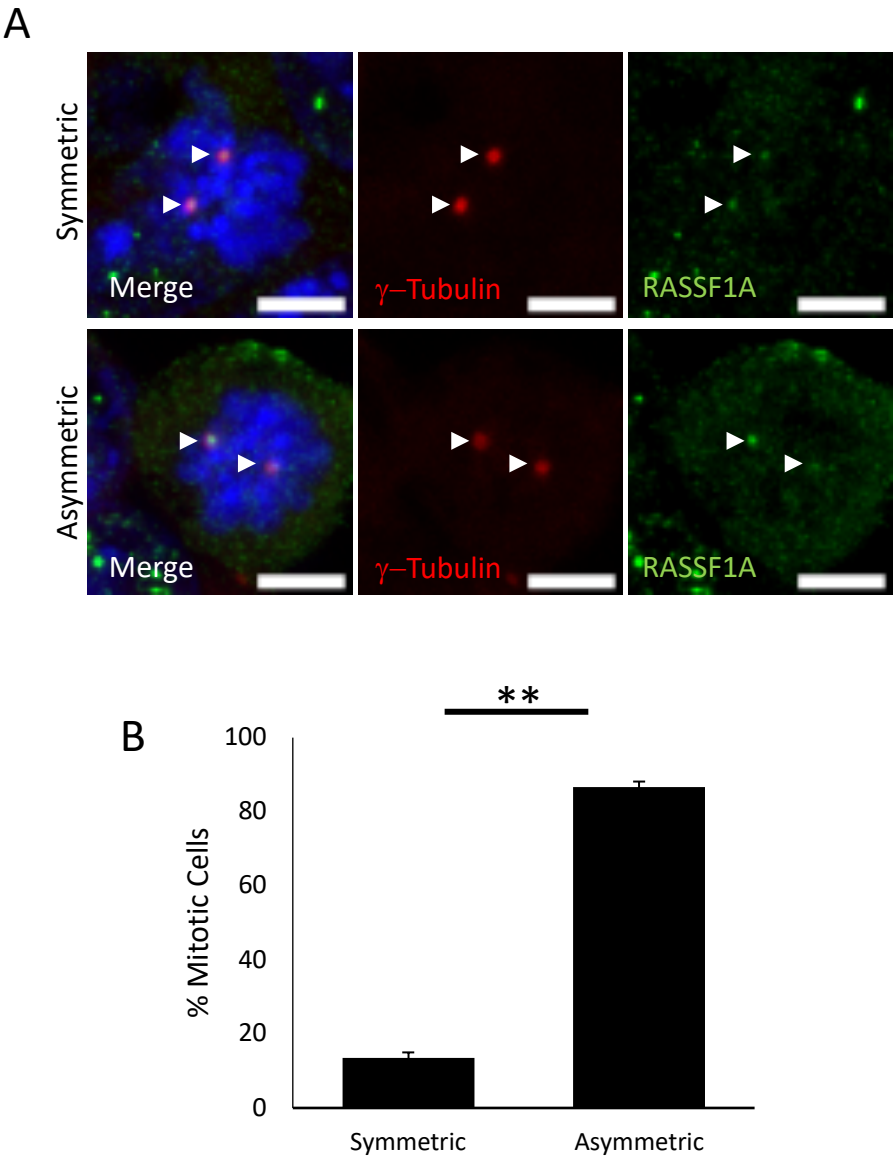


Figure 3. 7 Endogenous RASSF1A associates with the centrosome symmetrically and asymmetrically. (A) Representative immunofluorescence MIP images showing endogenous RASSF1A localisation at the centrosomes (γ-tubulin, red). DAPI is shown in blue, scale = 5 μm. (B) Quantification of asymmetry in approx. 20 mitoses over three biological replicates, p = 0.0014.

Whilst there was a much more pronounced difference in the amount of ZsRASSF1A present at each centrosome in the overexpression scenario, endogenous asymmetry at the centrosome appears to be a much more frequent event. It would be ideal to analyse more mitoses per experiment and achieve higher resolution of this event, but quantification across three experiments demonstrated a consistent and considerable difference.

Intrigued by this data, we wanted to determine if mESCs could asymmetrically distribute RASSF1A whilst actively dividing. We again employed the ZsGreen tagged RASSF1A construct alongside a H2B-RFP construct, to observe protein dynamics using live cell imaging. In doing so, we could show that ZsRASSF1A can be actively asymmetrically segregated in dividing mESCs (Figure 3.8).

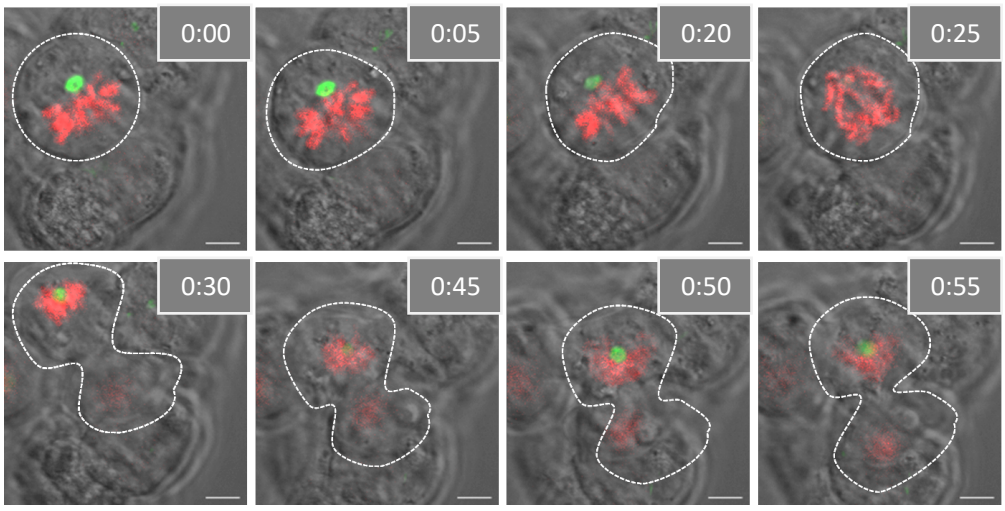


Figure 3. 8 ZsRASSF1A is actively asymmetrically distributed during mitosis of mESCs. Time lapse of live imaging used to examine the dynamics of asymmetric ZsRASSF1A inheritance in mESCs. ZsRASSF1A, green; H2B-RFP, red, to mark the DNA, red. Scale = 5 μm. Time from first frame and onset of metaphase is depicted as hh:mm in the top right-hand corner of each time frame.

As mentioned, we also observed that endogenous RASSF1A localisation changed dramatically as mESCs differentiated and became polarised at the cell periphery (Figure

3.9). This further encouraged our theory that RASSF1A may be involved in asymmetric cell division, as this staining pattern is typical of polarity regulators, which are instrumental in the establishment and direction of directional mitosis (Oozeer et al., 2017). It would be preferable to quantify this observation, but co-staining with a plasma membrane marker (e.g. with cadherin antibodies) would be necessary in order to confirm colocalisation.

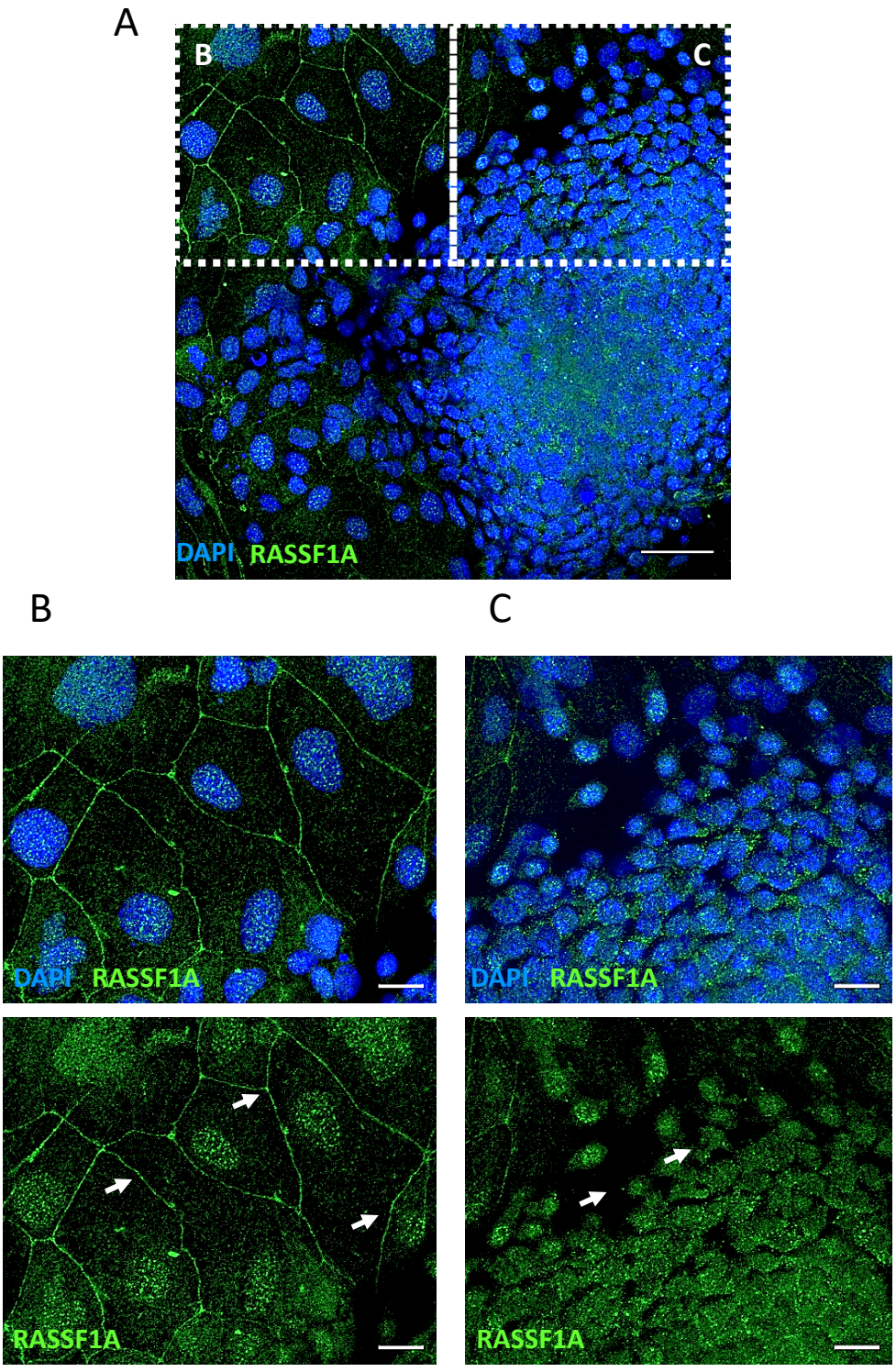


Figure 3. 9 RASSF1A is polarised to the cell periphery in differentiating stem cells. (A) RASSF1A's expression pattern alters in mESCs that spontaneously differentiate from the colony body, Scale = 50μm. Magnified regions show mESCs that have spontaneously differentiated (B) at the colony edge display a differential RASSF1A localisation pattern (arrows) to those that remain within the more pluripotent colony (C), Scale = 20μm.

We then decided to evaluate the inheritance and association of RASSF1A with important cell fate, polarity and ACD proteins, such as NuMA and Scrib (data not shown), but no obvious associations were observed. However, we did observe an association between RASSF1A and the cell fate determinant Numb (Figure 3.9).

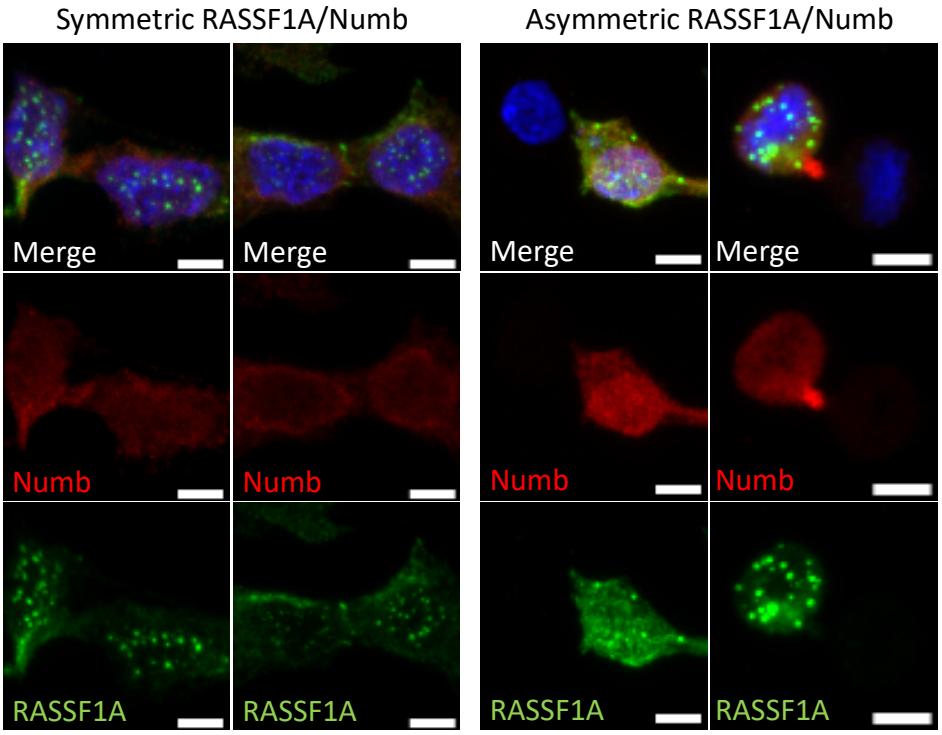


Figure 3. 10 RASSF1A is symmetrically and asymmetrically inherited with the fate determinant Numb. Representative images showing the symmetric and asymmetric division of stem cells. In a subset of cells, RASSF1A (green) is asymmetrically inherited with the fate determinant, Numb (red). DAPI is shown in blue, scale = 5μm. It is pertinent to note that quantification is not included here given the rarity of relevant mitotic events.

RASSF1A was seen to be either symmetrically inherited by both daughter cells, with low levels of symmetric Numb, or asymmetrically inherited with higher expression and corresponding asymmetry of Numb. Importantly, Numb is an inhibitor of the Notch signalling pathway, which is involved in maintaining SC character. This supports our previous findings that RASSF1A is a driver of differentiation in mESCs. Taken together, the data presented thus far suggests that the spatial localisation of RASSF1A may be

important in cell fate determination, however, further work is necessary to clarify these findings.

3.5 RASSF1A Expression Affects the Pluripotent Status of Cancer Cells

Stem-like characteristics have been correlated to poor disease prognosis in several cancers (Ginestier et al., 2007; Hermann et al., 2007; Hurt et al., 2008; Yang et al., 2010; Chiou et al., 2010). Given the tumour suppressive role of RASSF1A in cancer, as well as the data from our group suggesting that stem-like properties are enhanced in RASSF1A negative tumours (Pefani et al., 2016), we decided to evaluate the effect of RASSF1A expression in cancer cells. Upon expression of ZsRASSF1A, we could observe asymmetric localisation of the protein at the centrosomes, similarly to that seen in mESCs (Figure 3.11).

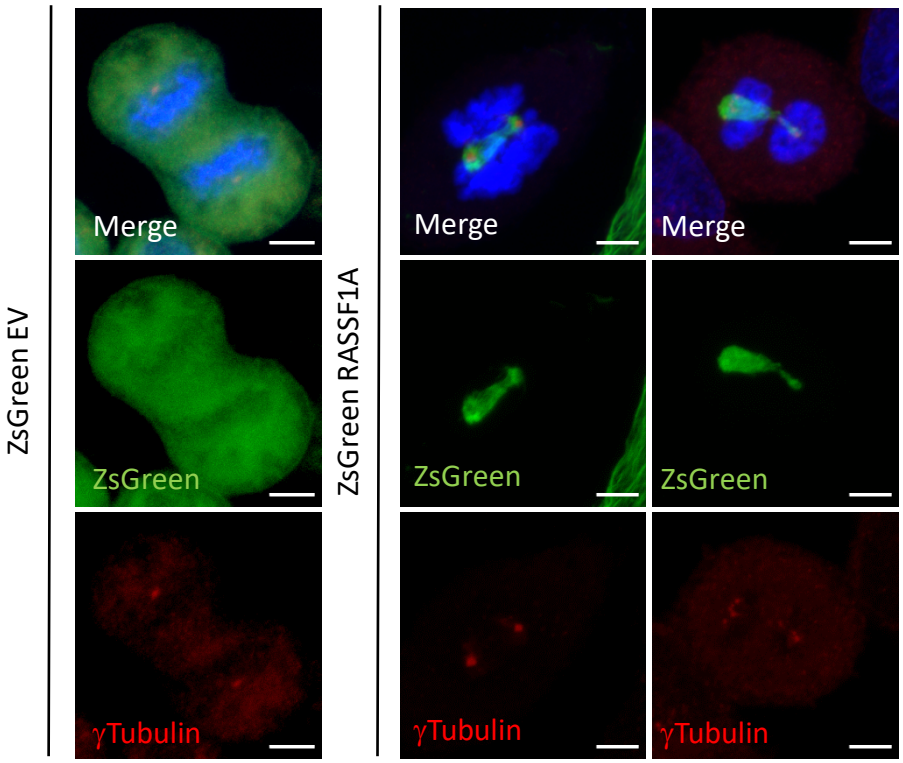


Figure 3. 11 ZsRASSF1A asymmetrically localises with the centrosomes of mitotic cancer cells. (A) When overexpressed in HeLa cervical cancer cells, ZsRASSF1A displays the ability to accumulate asymmetrically on the centrosome (γ-Tubulin, red), DAPI is shown in blue, scale = 5μm.

Interestingly, we also observed a complete ablation of Nanog in HeLa and MCF7 cells upon the overexpression of RASSF1A (Figure 3.12), suggesting that expression of RASSF1A can redirect cancer cells from their 'stem-like' phenotype.

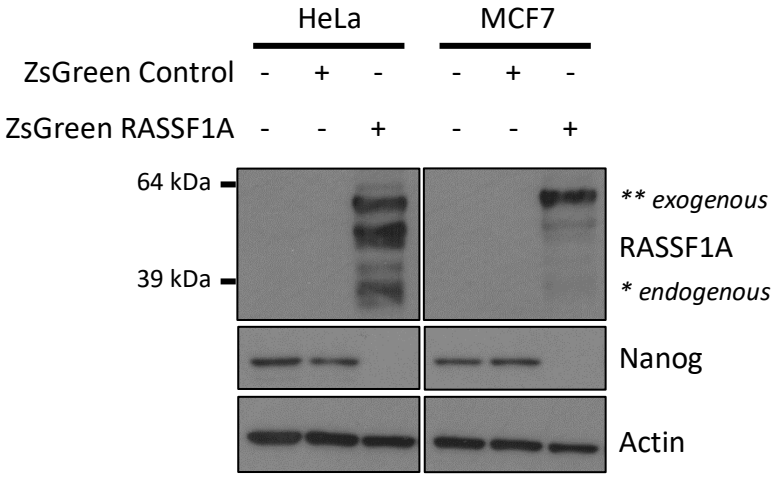


Figure 3. 12 ZsRASSF1A overexpression leads to a decrease in pluripotency marker expression in cancer cells. Expression of ZsRASSF1A in HeLa (left panel) and MCF7 (right panel) cancer cell lines, causes a marked decrease in Nanog expression. Western Blot analysis was carried out with the antibodies indicated to observe pluripotency transcription factor (Nanog) expression and Actin was used as a loading control. The relative position of the detection of endogenous (*) and tagged exogenous (**) RASSF1A is indicated.

To establish if these findings were relevant in clinical cohorts, we used Gene Set Enrichment Analysis (GSEA) to determine differences in the gene expression profiles of RASSF1A expressing and non-expressing tumour types. Due to the existence of cancer stem cells in Glioblastoma Multiforme (GBM), we initially analysed the publicly available TCGA data to compare the gene set changes in RASSF1A positive and negative GBM samples. Of these, only 21 % of the primary tumours exhibited RASSF1A expression and when we ran the GSEA, we found a clear upregulation of an embryonic stem cell gene set in the RASSF1A negative tumours (Figure 3.13).

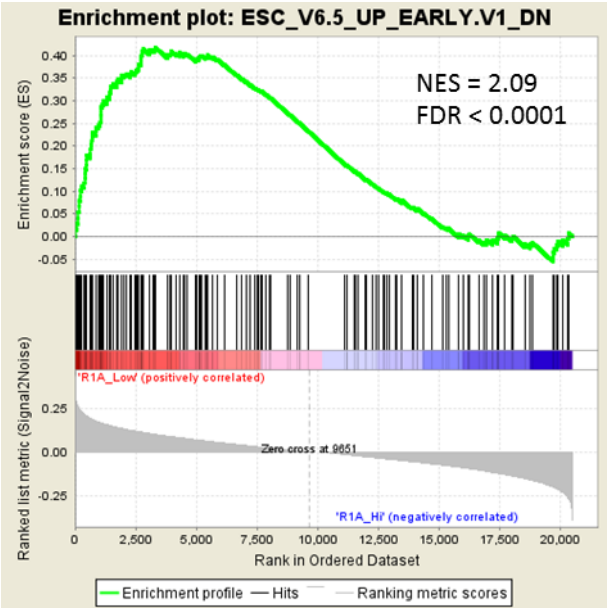


Figure 3. 13 Loss of RASSF1A in GBM cohort correlates with an increase in stem cell signature expression. In GBM, there is a significant increase in genes that are typically down-regulated in differentiation. NES = Normalised enrichment score; FDR = False discovery Rate

3.6 Discussion

In this chapter, we explored the role of centrosomal RASSF1A in ACD and fate determination. We demonstrate using immunofluorescence that endogenous RASSF1A expression increases as mESCs differentiate (Figure 3.2). Of note, we also consistently saw an increase in nuclear size as the mESCs differentiate (Figure 3.2). Extensive nuclear reorganisation has been reported to be necessary during differentiation and is important in the modulation of gene expression (Markiewicz et al., 2005; Therizols et al., 2014), which is the likely reason behind this observation. Furthermore, the differentiated mESCs grow in a monolayer as opposed to the colony growth of the pluripotent cells. This means they are subjected to distinct microenvironments and mechanical forces, both of which have been shown to direct differentiation (Vining and Mooney, 2017).

Our data demonstrates that transient knock down of RASSF1A can delay differentiation of mESCs and lead to an increase in pluripotency markers (Figure 3.3). To examine a spatial role for RASSF1A in mESCs, we considered that the localisation of RASSF1A at the centrosome might be important. In agreement with studies published in cancer cells, RASSF1A expression levels do not seem to impact the mitotic index or centriole number observed in mESCs (Figure 3.5). However, RASSF1A (overexpressed and endogenous) localisation is persistent and asymmetric at the centrosomes (Figures 3.4, 3.6 and 3.7). This asymmetry at the centrosome is relevant as we demonstrate using live imaging that mESCs can effectively segregate ZsRASSF1A during mitosis (Figure 3.8). The endogenous staining of RASSF1A during differentiation demonstrates a major change in localisation, with RASSF1A seeming to polarise as the cells lose pluripotency (Figure 3.9). Importantly, we demonstrate that RASSF1A can be asymmetrically inherited with the cell fate determinant, Numb (Figure 3.10). However, further work is necessary to determine this proposal. For instance, it is necessary to evaluate the effect of RASSF1A loss on ACD and Numb localisation. As is discussed in Chapter 6, this would require a suitable model system to achieve reliable analysis. Furthermore, rigorous validation of the asymmetric inheritance of RASSF1A with Numb is required as these events were too infrequent in the system used to obtain a reliable quantification. It may be helpful to optimise a synchronisation protocol for this cell line to enrich the population of cells in telophase. Also, it would be interesting to validate if the inheritance frequency is altered in pluripotent versus differentiating conditions.

Considering the widespread silencing of *RASSF1A* expression in human malignancies, we decided to explore the effect of RASSF1A in cancer cells. We demonstrate here that

RASSF1A can also accumulate asymmetrically on the centrosomes of CCs (Figure 3.11) and that overexpression can lead to a decrease in their SC characteristics (Figure 3.12). This suggests that, if RASSF1A can in fact regulate ACD in mESCs, this may also be important in differentiated cells. Furthermore, using GSEA we expand upon previous findings in Breast Cancer and Lung Adenocarcinoma (Pefani et al., 2016), and show that loss of RASSF1A in TCGA curated GBM tumours leads to an upregulation of stem cell signature genes (Figure 3.13).

In conclusion, the data in this chapter highlights an important role for RASSF1A in facilitating a differentiated phenotype. We show that RASSF1A's association with the centrosome does not overtly affect cell- or centrosome-cycle dynamics and may have a role in ACD.

Chapter 4

Results II

Investigating RASSF1A's role at the Centrosome: The Mother Centriole & Primary Cilia

4.1 Introduction

Whilst we were investigating the role of RASSF1A in differentiation, we were struck by the persistence of asymmetric RASSF1A accumulation at the centrosome. It is well known that the centrosomes themselves are inherently asymmetric, and display differing maturity levels with different biological functions (Nigg and Stearns, 2011).

The primary cilium is nucleated from the mother centriole in arguably one of its most important functions. The core of the cilium is comprised of microtubules (MTs) which are extensively post-translationally modified (Wloga et al., 2017). Interestingly, RASSF1A is a known stabiliser of MTs in a process that is thought to be linked to increased acetylation of α-Tubulin, an important PTM in the cilium (Dallol et al., 2004). Furthermore, the primary cilium has recently been implicated in the progression of tumourigenesis (Castresana, 2015) and has extensive ties with the cell cycle. We were intrigued by the asymmetric RASSF1A localisation at the centrosome and decided to investigate the possibility that RASSF1A may be associated with centriole/centrosome maturity and function.

4.2 RASSF1A Localises with the more mature centrosome and centriole in mESCs

As we were consistently seeing significant proportions of cells displaying asymmetry of RASSF1A, we sought to understand if this localisation pattern correlated with centrosome age. Using confocal microscopy with Airyscan to improve resolution, we examined the localisation of ZsRASSF1A within the centrosome, using Centrin-3 to mark centrioles and CEP164 as an indicator of their maturity (Figure 4.1).

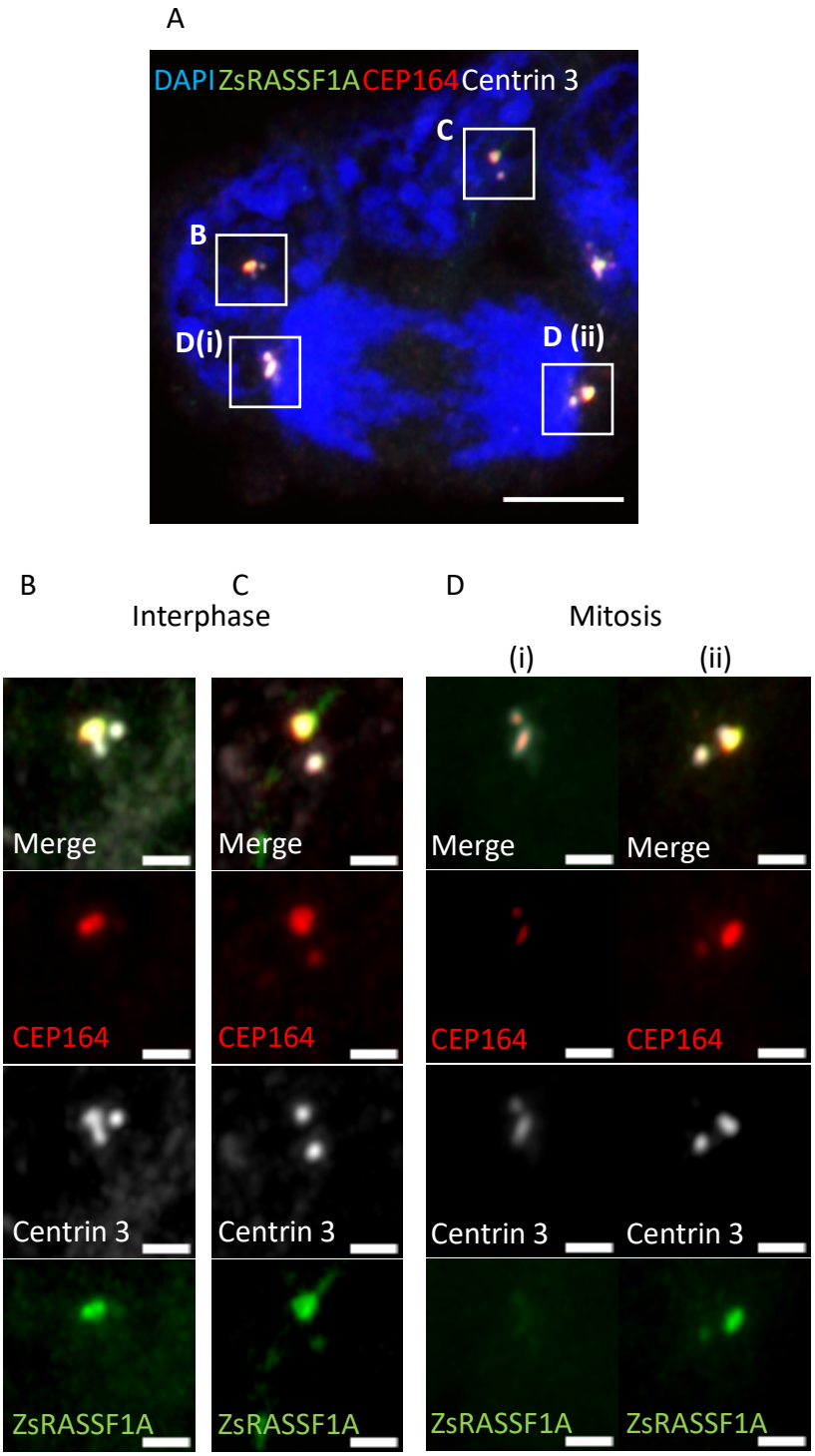


Figure 4. 1 RASSF1A localises preferentially with the more mature centriole. (A) Confocal imaging demonstrates that RASSF1A localises preferentially with the more mature centrosome, scale = 5μm. (B-D) AIRYSCAN imaging was used to demonstrate that within the centrosomes (indicated by boxed area in A) of interphase (B & C) and mitotic (D) cells, that RASSF1A preferentially localises with the more mature centriole, with D (i) and D (ii) representing the mother and daughter centrosomes of the same cell. Scale = 1 μm.

Here, we could identify the presence of ZsRASSF1A with the more mature centrosome in dividing cells (Figure 4.1) and we also observe an enrichment of ZsRASSF1A with the most mature centriole. Interestingly, we also saw this trend in interphase cells (Figure 4.1 A, B & C). In order to further evaluate this, we investigated the endogenous localisation pattern of RASSF1A with regards to CEP164 (Figure 4.2).

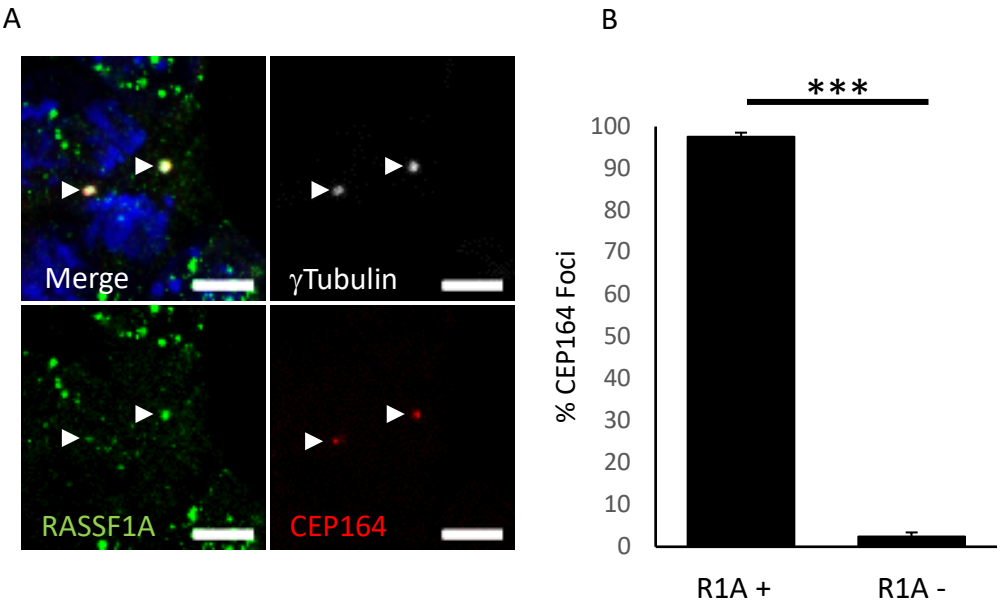


Figure 4. 2 RASSF1A localises with the mature centriole marker CEP164 in mESCs. (A) RASSF1A localises with CEP164 positive foci, arrows indicate corresponding locations in each channel, DAPI is shown in blue, scale = 5 μm. (B) Quantification of RASSF1A positive (R1A +) and negative (R1A -) foci, p = 0.000314.

RASSF1A was again observed to localise with CEP164 in mitotic mESCs (Figure 4.2 A), but as seen in the overexpression scenario, we also observed RASSF1A positive CEP164 foci in non-dividing cells as is quantified in Figure 4.2 B. Strikingly, the majority of CEP164 foci were associated with RASSF1A staining. To further explore this finding, we quantified the symmetry and asymmetry of RASSF1A localisation in relation to centriole maturity (Figure 4.3).

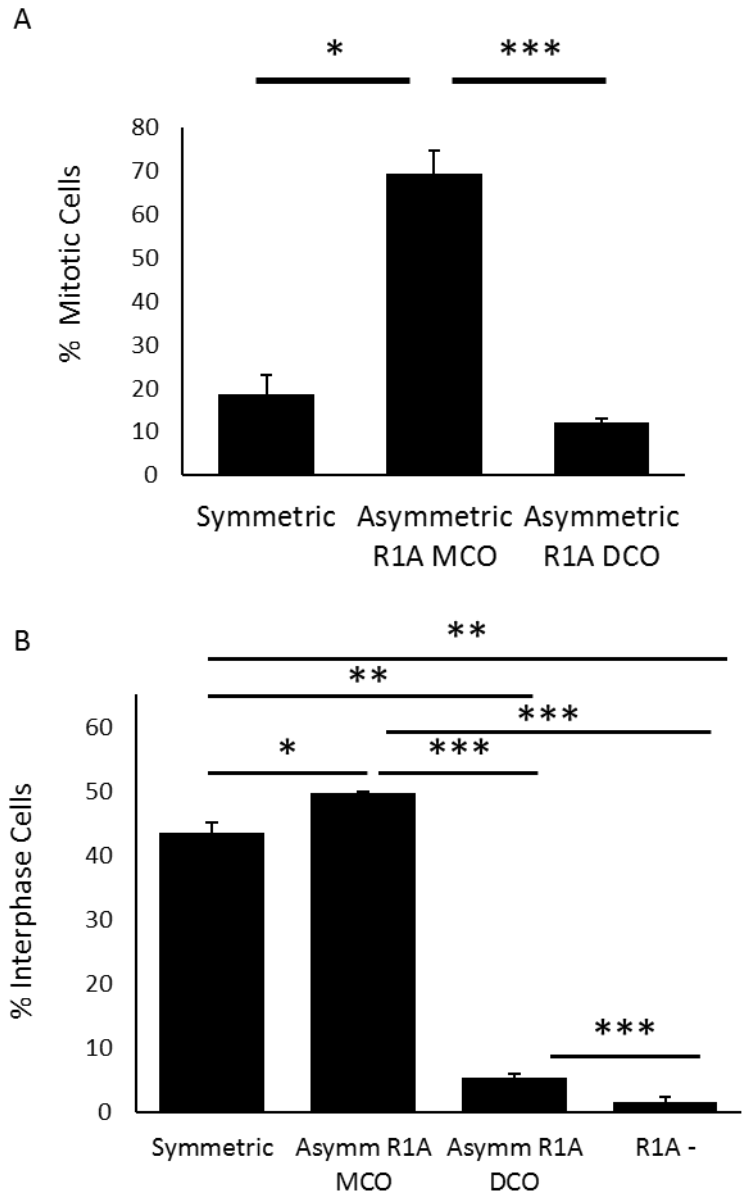


Figure 4. 3 RASSF1A localises symmetrically and asymmetrically within the centrosomes. Quantification of the fraction of cells displaying symmetric RASSF1A versus the fraction of cells displaying asymmetric RASSF1A at the Mother Centriole (*MCO*) and Daughter Centriole (*DCO*). (A) Quantification of events during mitosis where RASSF1A is either symmetrically localised; asymmetrically enriched at the mother centriole (*Asymmetric R1A MCO*) or; asymmetrically enriched at the daughter centriole (*Asymmetric R1A DCO*). P-values are as follows between each population: Symmetric RASSF1A – Asymmetric RASSF1A enriched at the Mother Centriole, p = 0.0262; Symmetric – Asymmetric R1A DCO, not significant p = 0.1232; Asymmetric R1A MCO – Asymmetric R1A DCO, p = 0.00921. Approx. 15 mitoses counted per experiment. (B) Quantification of the fraction of interphase cells displaying symmetric RASSF1A versus the fraction of cells displaying asymmetric RASSF1A where RASSF1A is enriched at the mother centriole (*Asymm R1A MCO*) or RASSF1A is enriched at the daughter centriole (*Asymm R1A DCO*) or is absent from the centrosome (R1A-). P-values are as follows between each population: Symmetric – Asymmetric R1A MCO, p = 0.0487; Symmetric – Asymmetric R1A DCO, p = 0.002816; Symmetric – No RASSF1A, p = 0.00258, Asymmetric R1A MCO – Asymmetric R1A DCO, p = 0.000145; Asymmetric R1A MCO – No RASSF1A, p = 0.000175, Asymmetric R1A DCO – No RASSF1A, p = 0.00075. Approx. 100 centrosomes counted per experiment.

With the pre-requisite that RASSF1A, CEP164 and γ-Tubulin must all be localised together, we quantified asymmetry based on centriole age. This analysis revealed that RASSF1A preferentially localises at the mother centrosome/centriole in mitotic mESCs (Figure 4.3 A), with significantly more cells displaying asymmetry where RASSF1A is localised with the most mature centriole (Asymmetric R1A MCO in Figure 4.3 A). Further, quantification of interphase centrosomes demonstrates that whilst there are more incidences of RASSF1A enrichment at the mother centriole in interphase mESCs, there is also a considerable proportion of cells displaying symmetric localisation of RASSF1A between centrioles (Figure 4.3 B). Of note here, is that due to the rare incidence of mitoses combined with the rules we set for scoring (where all three antibodies can be clearly seen), only a small number of mitotic asymmetries could be counted per experiment (Figure 4.3 A). Analysis of combined asymmetries are included in appendix Figure 7.1 whereby more mitoses could be examined per experiment due to the omission of CEP164 localisation consideration.

4.3 RASSF1A Localises with the Mother Centriole and Basal Body of ARPE19 cells

Arguably one of the most important roles of the mother centriole is the formation of the primary cilium. CEP164 is an essential regulator of ciliogenesis and mediates the docking of the mother centriole at the plasma membrane prior to the onset of cilium assembly (Schmidt et al., 2012). Given the association of RASSF1A with CEP164 reported here and previous reports that RASSF1A is important in MT stabilisation, we decided to investigate the possibility that RASSF1A may have a function at the primary cilium. We utilised the human retinal pigment epithelial (RPE) cell line, ARPE19. These cells are ideal for investigations into the primary cilium as they are a spontaneously arising, non-

transformed, primary cell line that readily assemble cilia. Firstly, we tested that the centrosomal localisation of RASSF1A persisted in these cells by co-staining for γ–Tubulin (Figure 4.4).

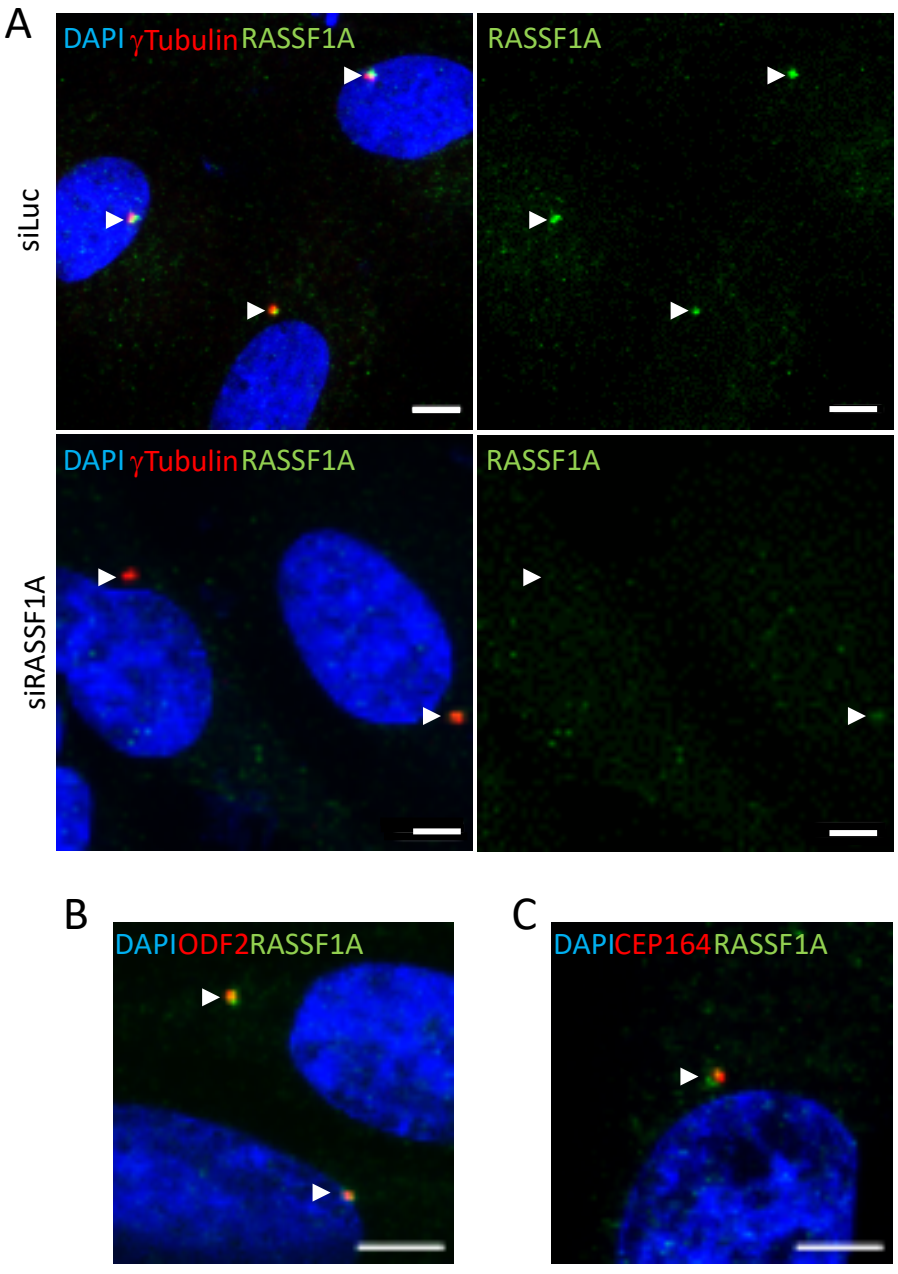


Figure 4. 4 RASSF1A localises with the centrosomes of human ARPE19 cells. (A) Human RASSF1A localises with the centrosomes (γTubulin, white arrow heads) of ARPE19 cells, scale = 10 μm. (B & C) RASSF1A localises with the mature centriole markers, ODF2 and CEP164, respectively, scale = 5 μm.

Indeed, we could see a similar colocalisation to that observed in mESCs (Figure 4.4 A), this localisation was confirmed by siRNA mediated knockdown of RASSF1A (Figure 4.4 A). We also demonstrate that RASSF1A can localise with the mother centriole in these cells, as it localises with both the mature appendage markers ODF2 and CEP164 (Figure 4.4 B & C, respectively).

Next, we explored the possibility that RASSF1A may be linked to the primary cilium by inducing ciliogenesis in the cells by serum starvation. We observed that RASSF1A localises at the basal body (marked by mother centriole appendage marker ODF2) of the cilium (marked with acetylated αTubulin) (Figure 4.5).

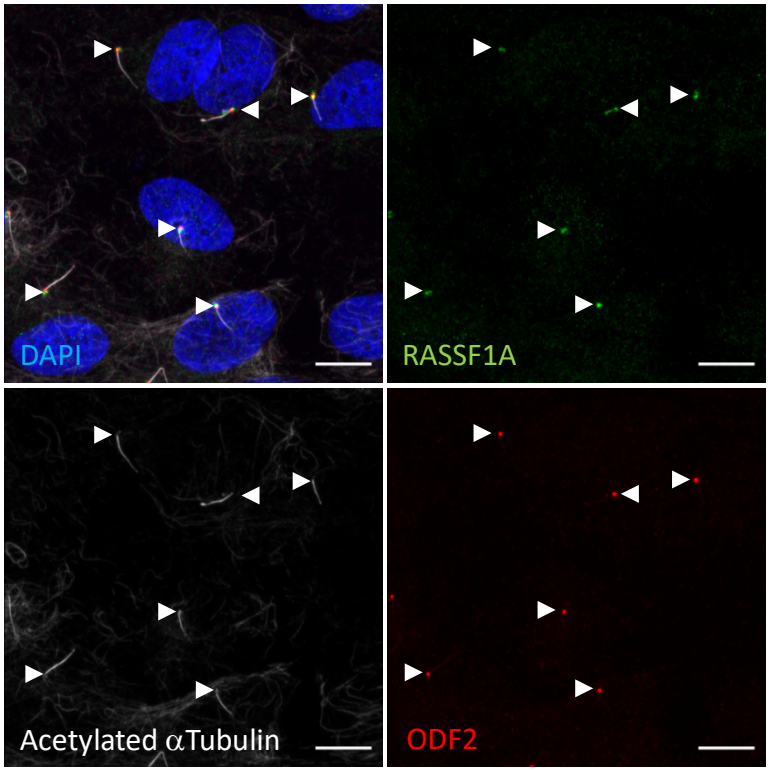


Figure 4. 5 RASSF1A localises at the basal body of the primary cilium. Serum starvation can induce ciliogenesis in cultured ARPE19 cells. RASSF1A can be visualised at the basal body (ODF2, red) of the primary cilium (Acetylated α-Tubulin, white). Scale = 10 μm.

4.4 RASSF1A Depletion Leads to Defects in Ciliogenesis

To explore a connection between RASSF1A and the cilium, we knocked down RASSF1A prior to the induction of ciliogenesis (Figure 4.6).

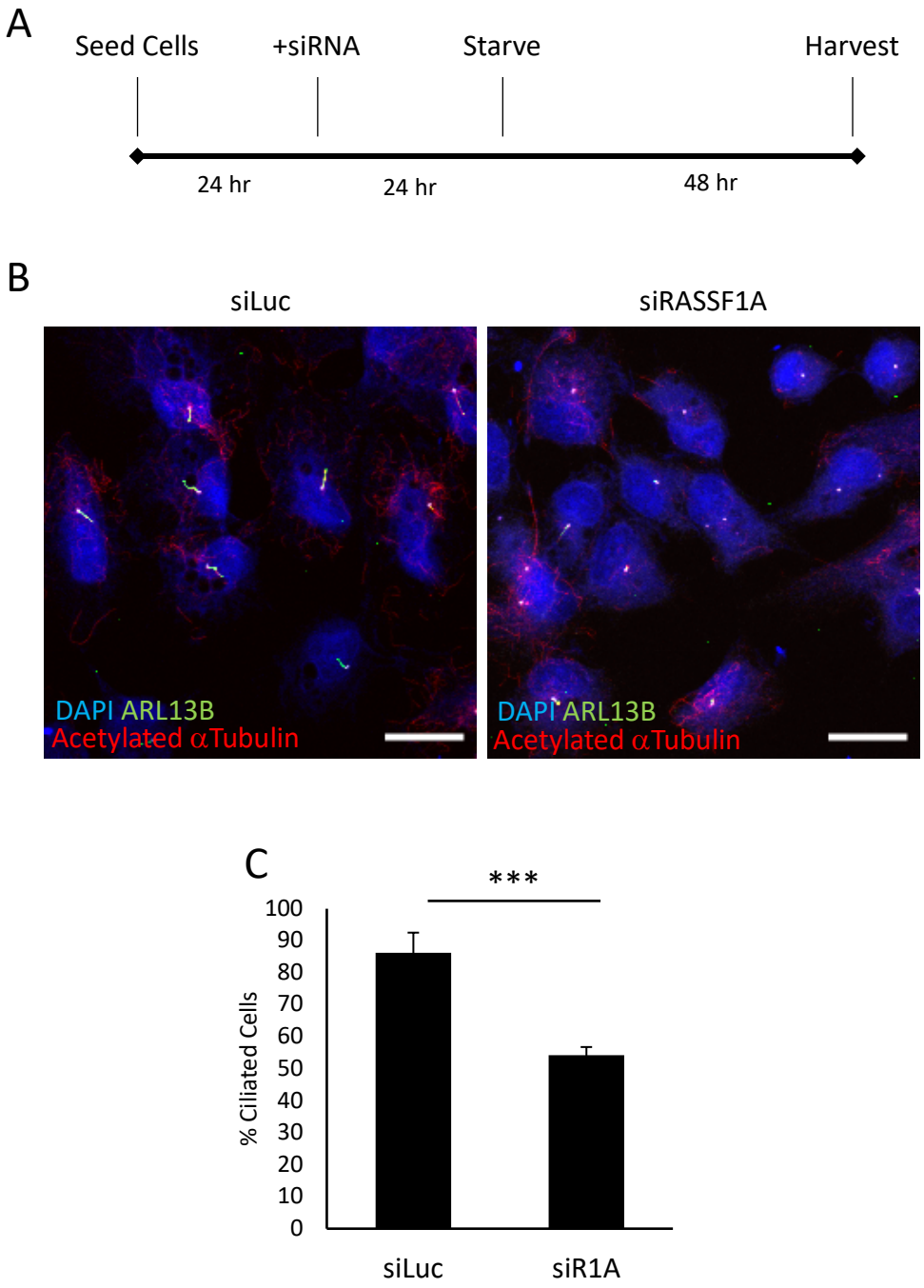


Figure 4. 6 RASSF1A depletion leads to a decrease in cilia numbers. (A) Schematic of experimental procedure. (B) Reduction in cilia (ARL13B, green & acetylated α-Tubulin, red) number was evident upon RASSF1A knockdown, scale = 20 μm. (C) Quantification of ciliated cells, p = 0.0049.

Transient knock down of RASSF1A led to a significant reduction in the number of cilia assembled as marked with the ciliary membrane marker, ARL13B, and axoneme marker, acetylated α-Tub (Figure 4.6 B & C). Upon closer inspection, we also noted that in the cells which did manage to assemble a cilium in the RASSF1A depleted cells, the formed cilia were abnormally shaped (Figure 4.7 A) and shorter (Figure 4.7 B). Western blotting revealed that RASSF1A knock down also affects the levels of important ciliary component proteins, namely, there is a decrease in acetylated α-Tubulin and IFT88 (Figure 4.7 C).

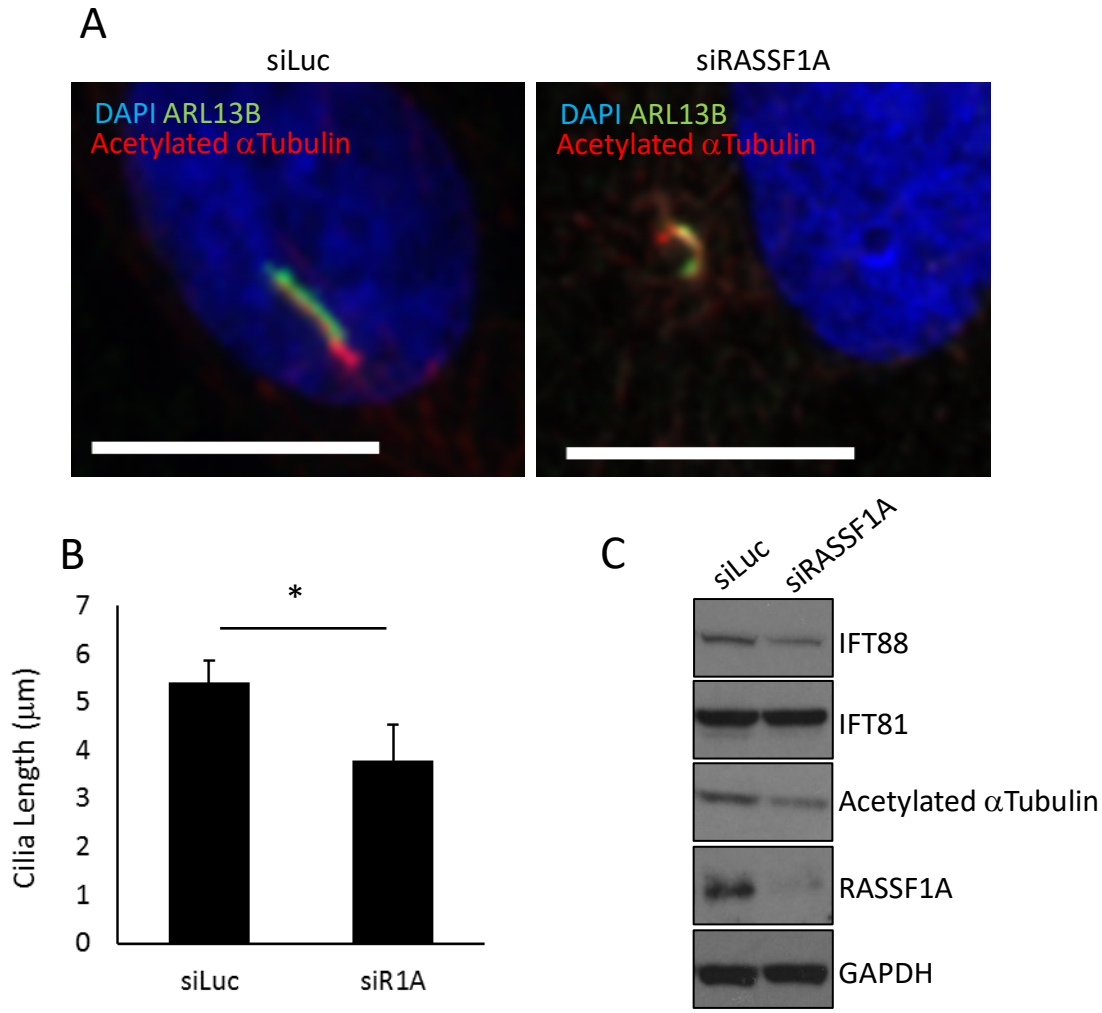


Figure 4. 7 RASSF1A depletion causes anomalies in ciliary shape and protein levels. (A) Upon siRNA mediated knock down of RASSF1A, observed cilia display defective shape, scale = 10 μm. (B) Cilia are shorter upon RASSF1A knock-down, p = 0.035. (C) Decreased levels of acetylated α–Tubulin and IFT88 are evident upon RASSF1A knock down & serum starvation. Western Blot analysis was carried out with the antibodies indicated to observe cilia related protein expression and GAPDH was used as a loading control.

4.5 RASSF1A Effect on Ciliation Levels Correlates with Changes in αTubulin Acetylation Independently of HDAC6

Previous studies have suggested that RASSF1A's role in microtubule stabilisation is a result of its ability to stabilise acetylated α–Tubulin (Dallol et al., 2004). Given the immunoblot results we obtained that suggested a decrease in the amount of acetylated α–Tubulin, we wondered if this may be the reason that RASSF1A depletion causes defective ciliation. To investigate this, we immunostained cells with acetylated αTubulin and observed a decrease in staining in the siRASSF1A conditions (Figure 4.8 A). Furthermore, we quantified the intensity of acetylated α–Tubulin fluorescence per cell and found that there was a general decrease (Figure 4.8 B).

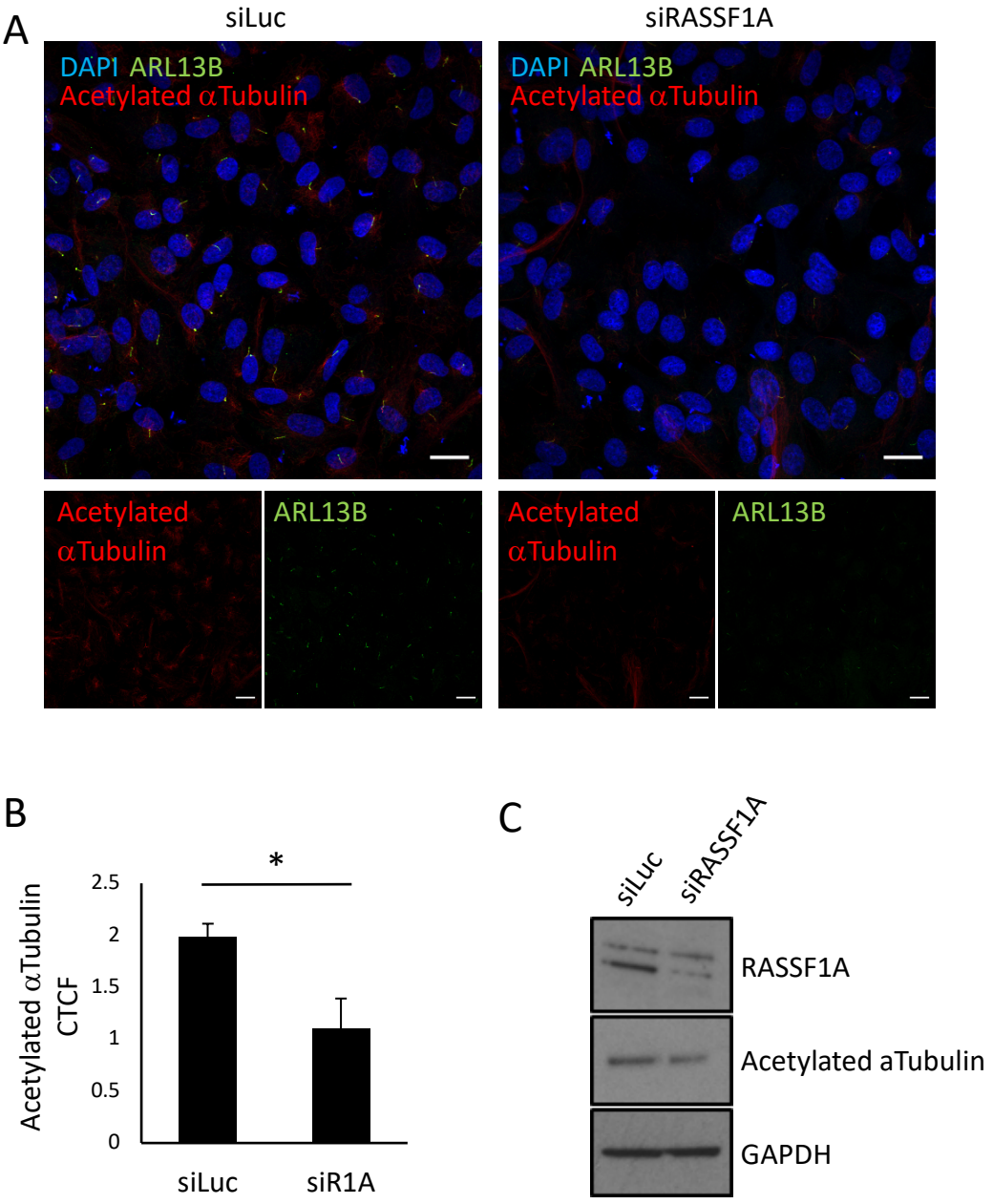


Figure 4. 8 Reduction of RASSF1A expression leads to a decrease of acetylated αTubulin signal. (A) RASSF1A knock down leads to a decrease in acetylate α-Tubulin, scale = 20μm, quantified corrected total cell fluorescence (CTCF) in (B), p = 0.05. (C) Western Blot analysis shows decreased levels of acetylated α–Tubulin are evident upon RASSF1A knock down & serum starvation. Western Blot analysis was carried out with the antibodies indicated, GAPDH was used as a loading control

We were curious as to how RASSF1A may be modulating this tubulin modification, to this end we expressed a FLAG-tagged version of RASSF1A in ARPE19 cells and performed co-immunoprecipitation experiments to examine the possibility that RASSF1A can physically associate with acetylated α–Tubulin (Figure 4.9).

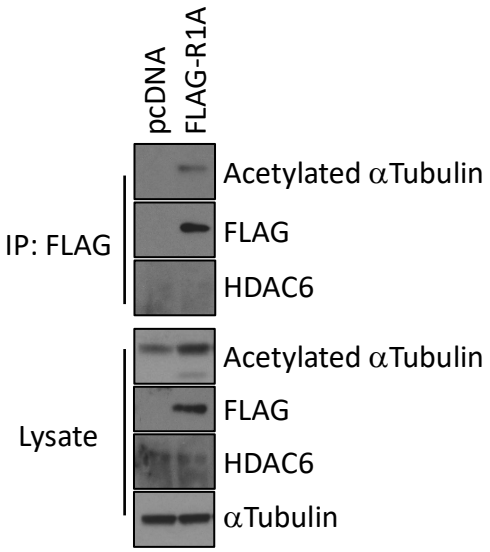


Figure 4. 9 RASSF1A is associated with Acetylated α-Tubulin. Immunoprecipitation of FLAG-RASSF1A expressing cell lysate demonstrates that RASSF1A can interact with acetylated αTubulin. Western Blot analysis was carried out with the antibodies indicated to examine the interaction partners for RASSF1A and the expression levels present in the lysate. αTubulin was used as a loading control for the lysate samples.

We showed that RASSF1A can interact with acetylated α–Tubulin (Figure 4.9, co-IP) and that overexpression of RASSF1A leads to an increase in the observed PTM levels (Figure 4.9, Lysate). We also assessed a possible interaction between RASSF1A and HDAC6 (Histone Deacetylase 6), an important regulator of tubulin acetylation. HDAC6 facilitates cilium disassembly by destabilising the central axoneme via deacetylation of tubulin (Pugacheva et al., 2007). It has been previously shown that RASSF1A is important in preventing HDAC6 activity towards acetylated α–Tubulin (Jung et al., 2013) and so we hypothesised that RASSF1A depletion may be detrimental to cilia stability due to

unlicensed functioning of HDAC6. We explored the possibility that RASSF1A could form a complex with both acetylated α–Tubulin and HDAC6, but our data indicates that this is not the case (Figure 4.9). Whilst RASSF1A and HDAC6 did not seem to interact, we also addressed what effect changes in RASSF1A expression may have on HDAC6 localisation (Figure 4.10).

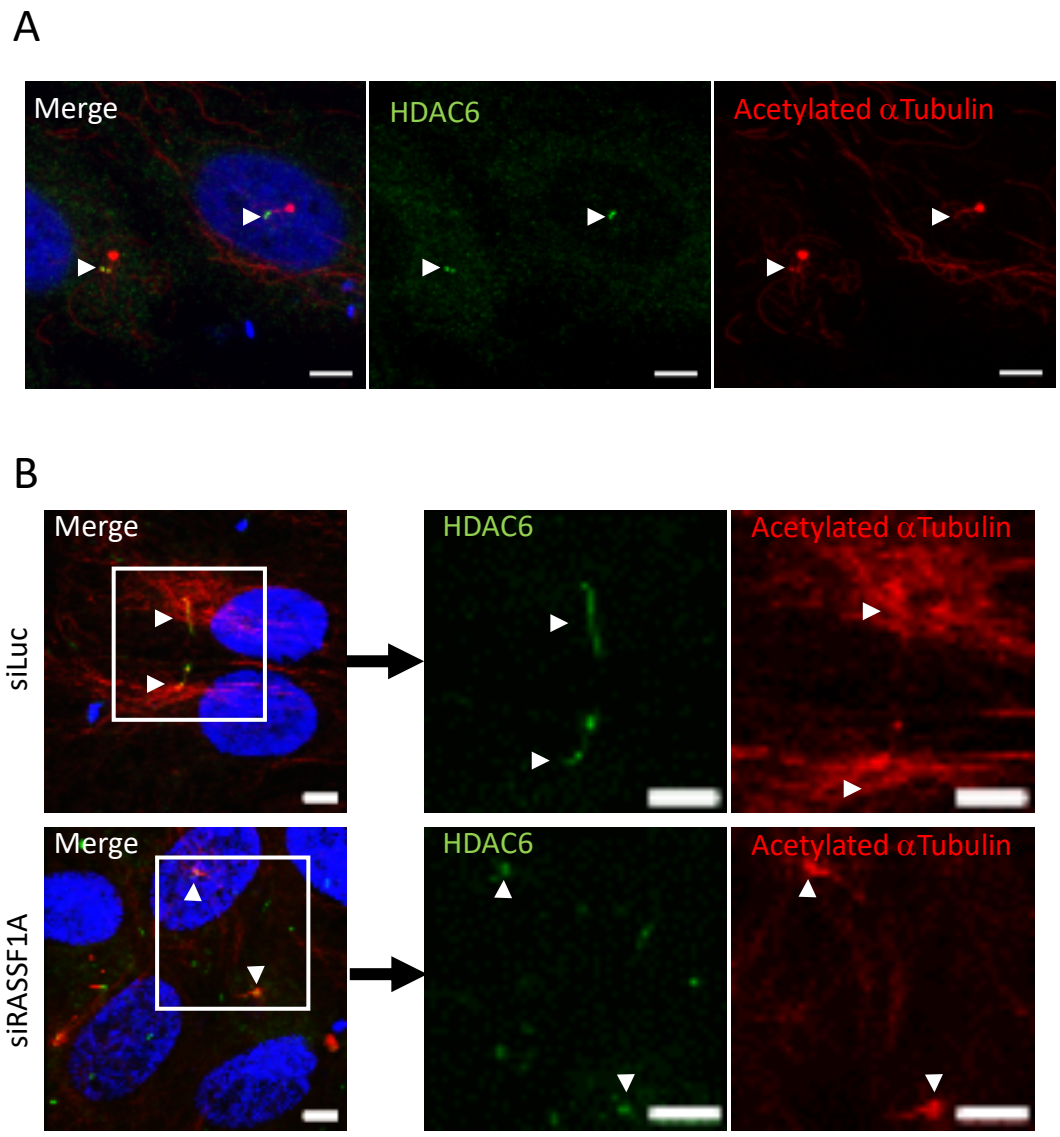


Figure 4. 10 HDAC6 localisation is independent of RASSF1A (A) HDAC6 localises with the primary cilium and (B) this localisation is not affected by RASSF1A expression. White arrows indicate HDAC6 localisation and corresponding locations in each image. DAPI is shown in blue, scale = 5 μm. (n = 2).

Firstly, we determined that, in line with published data (de Diego et al., 2014; Ran et al., 2015), HDAC6 can be visualised at the cilium and found that it is enriched at the basal body and can traverse the axoneme (Figure 4.10 A). Next, we depleted RASSF1A and found that loss of RASSF1A expression does not seem to influence the ability of HDAC6 to localise with acetylated α-Tubulin generally, or at the base of any stunted cilia (Figure 4.10 B).

In order to firmly establish if the defects we were observing in ciliogenesis upon RASSF1A knock down were related to HDAC6 function, we decided to utilise Tubacin (TUBA), a highly potent and selective inhibitor of HDAC6. In the presence of Tubacin (2 μm, 24 h) it has been shown that HDAC6 is unable to deacetylate tubulin (Haggarty et al., 2003), and so, if RASSF1A depletion induced cilia defects were indeed HDAC6 related, we would expect HDAC6 inhibition to rescue the phenotype.

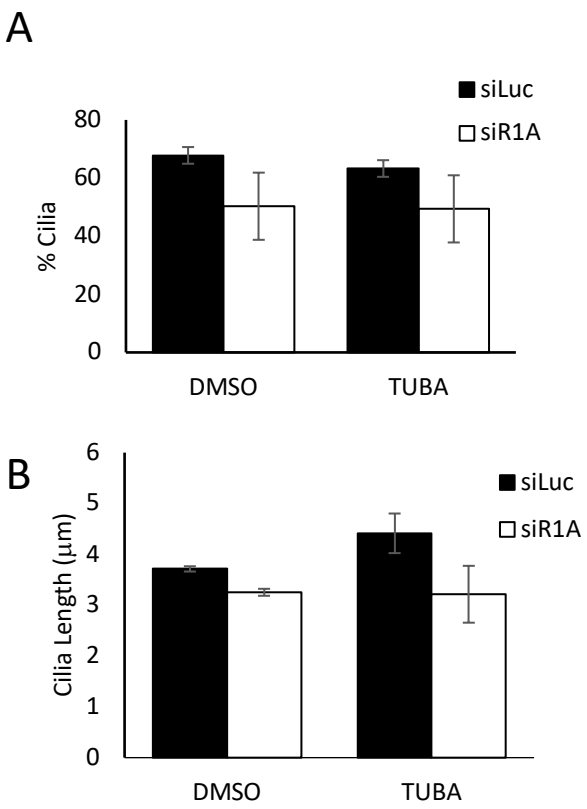


Figure 4. 11 Tubacin mediated inhibition of HDAC6 does not rescue the RASSF1A induced phenotype during ciliogenesis. In the presence of 2µm Tubacin (TUBA), *RASSF1A* knockdown still leads to a decrease in (A) cilia number and (B) cilia length in comparison to DMSO treated cells. (n = 2).

Our data indicate that HDAC6 inhibition in the presence of siRNA-mediated RASSF1A knockdown still causes a reduction of ciliation (Figure 4.11 A) and average cilium length (Figure 4.11 B), which led us to conclude that the ciliogenesis defects resulting from RASSF1A knockdown are not due to a heightened deacetylation activity of HDAC6. However, we have only performed two biological replicates of this experiment and so this needs to be further verified.

4.6 RASSF1A Depletion Leads to Defective Cilium Assembly Induction

Another important mediator of ciliation is the action of intraflagellar transport (IFT) proteins. IFT88 is an important component of the IFT-B complex which is required for proper cilium assembly and mutations in the *IFT88* gene can cause the ciliopathy, polycystic kidney disease (Pazour et al., 2000). When we were assessing the effect of RASSF1A knock down on cilium related proteins, we noted that IFT88 protein levels were reduced alongside that of RASSF1A (Figure 4.7 C). To that end, we wondered if the observed cilium defects were a result of IFT deregulation and evaluated IFT88 localisation (Figure 4.12).

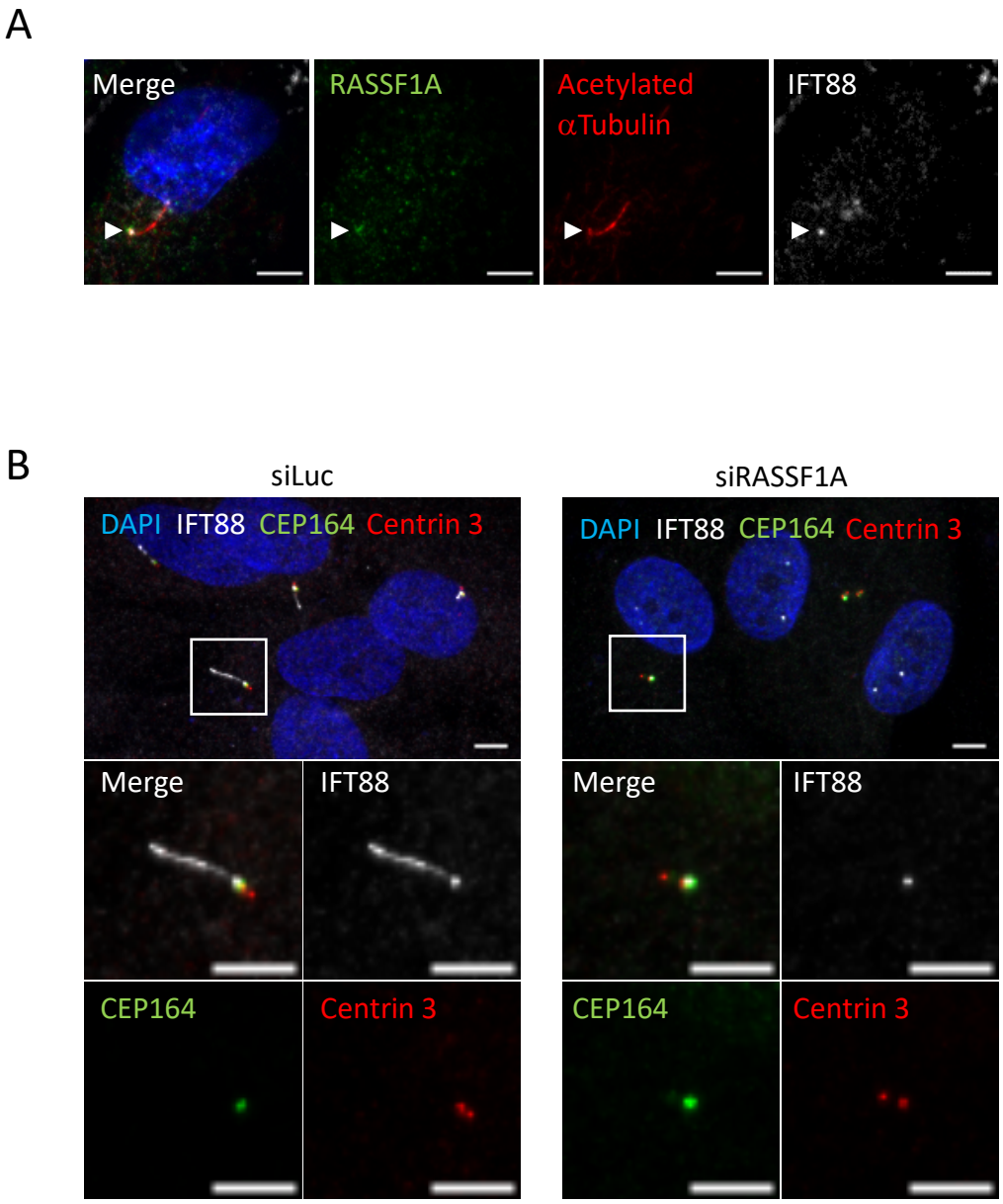


Figure 4. 12 RASSF1A and IFT88 colocalise at the basal body of the cilium. (A) IFT88 (white) is seen along the ciliary axoneme (acetylated α-tubulin, red) and white arrows indicate where it colocalises with RASSF1A at the ciliary base. (B) Upon the knock down of RASSF1A, IFT88 still localises with the basal body markers (CEP164, green) but no cilium is formed, white boxes indicate zoomed images in the bottom panels. Scale = 5μm.

As we expected, IFT88 was visualised on the ciliary axoneme and we found that it localises at the base of the cilium with RASSF1A (Figure 4.12 A). IFT88 enrichment at the ciliary base was confirmed to be at the basal body by co-staining with CEP164 (Figure 4. 12 B). Interestingly, when RASSF1A expression was depleted during serum starvation,

we were still able to detect a colocalisation of IFT88 with the mother centriole/basal body marker CEP164 (Figure 4.12 B, bottom panel). This suggests that RASSF1A knock down may lead to defects in the initiation of ciliogenesis. To further explore this hypothesis, we depleted RASSF1A expression post-cilium assembly (Figure 4.13 A).

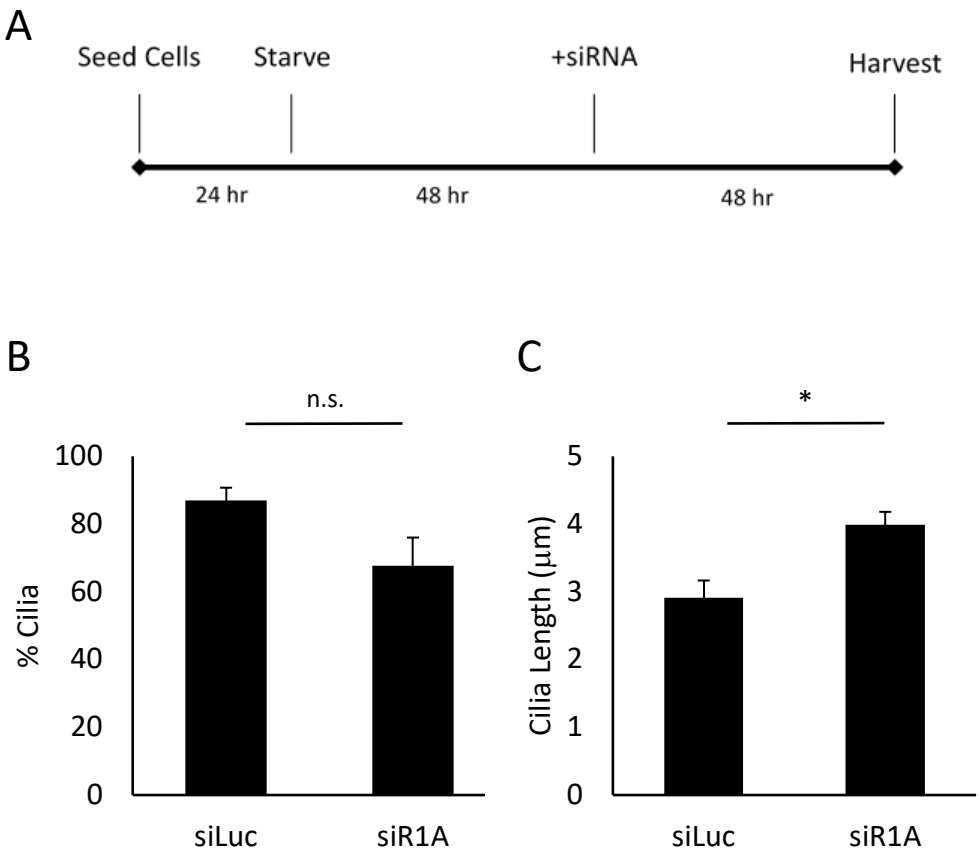


Figure 4. 13 RASSF1A does not affect ciliation levels or cilium length post-assembly. (A) Schematic of experimental procedure. (B) Knock down of RASSF1A does not cause a significant decrease in the number of ciliated cells, p-value = 0.095 but causes a significant increase in cilium length (C) p = 0.027.

When RASSF1A is knocked down in cells that already have cilia assembled, we couldn't see a significant reduction in the number of ciliated cells, however, we still observed an overall decrease (Figure 4.13 B). Interestingly, we saw a significant increase in cilium

length in this case (Figure 4.13 C) which is in opposition with what we see in RASSF1A knock down pre-induction of ciliogenesis (Figure 4.7 B).

4.7 RASSF1A Expression in LUAD Cell Lines Correlates with Ciliation

The primary cilium has been garnering increasing interest given its role in human pathology. Recently, these links to disease have extended to cancer. In the lab, we have a readily available panel of NCI-60 lung adenocarcinoma cells (LUAD) that possess different levels of *RASSF1A* promoter methylation and thus variations in the amount of RASSF1A expressed (Table 4.1).

NSCLC Cell Line	RASSF1A RNA Levels	% DNA Methylation
HOP_92	High	0
EKVX	Present	34
NCI_H460	Absent	58
NCI_H322M	Absent	77

Table 4. 1 LUAD Lines and their respective levels of RASSF1A RNA and promoter methylation. NCI LUAD line HOP-92 expresses high levels of RASSF1A RNA given the absence of methylation on the *RASSF1A* promoter. In the EKVX cell line, 34% of CpG island sites in the *RASSF1A* promoter are methylated but there are still detectable levels of *RASSF1A* RNA. In the NCI-H460/H322M LUAD cell lines, the *RASSF1A* promoter methylation is beyond the extent of which *RASSF1A* RNA can be detected. Data provided by Dr Anna Grawenda.

To see if natural variation of RASSF1A expression in human cancer derived cell lines reflected our results so far, we induced ciliogenesis with serum starvation in the LUAD lines, HOP_92, EKVX, NCI-H460 and NCI-H322M (Figure 4.13). Interestingly, when we induced ciliogenesis in each of these cell lines we observed differing levels of ciliation.

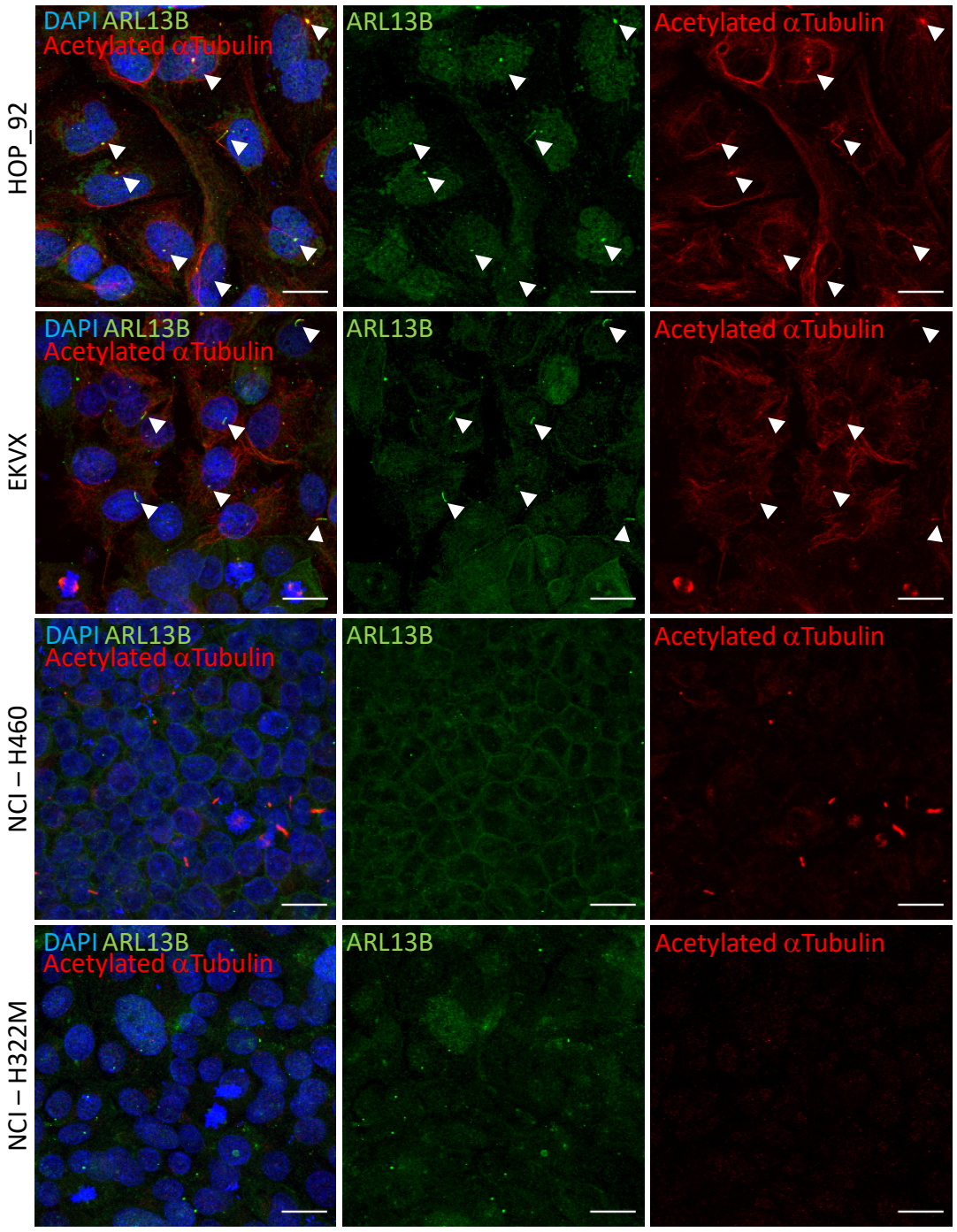


Figure 4. 14 Expression of RASSF1A correlates with ciliation in LUAD cell lines. Serum starvation in the the LUAD cell lines HOP_92, EKVX, NCI-H460 and NCI-H322M, which have decreasing levels of RASSF1A, demonstrated differential ciliation levels. White arrows indicate cilia, scale = 20 μm.

In accordance with our data in ARPE19 cells, the LUAD cell lines that do not express RASSF1A (NCI-H460/H322M) do not appear to have the capacity to assemble a cilium, whereas the cell lines that have maintained RASSF1A expression (HOP_92/EKVX) can.

4.8 Discussion

The primary cilium is a MT-based organelle that is responsible for mediating a broad range of signalling pathways and is essential for proper development. Here, we have demonstrated for the first time that the Hippo pathway regulator, RASSF1A, has a role in ciliogenesis.

In mouse ESCs, we observed that RASSF1A can localise with the mature centriole marker, CEP164, in mitotic and interphase cells (Figure 4.1 & 4.2). In addition to this, we observed that the localisation at the centrosome can be symmetric (RASSF1A on both centrioles in a pair) or asymmetric (RASSF1A on one centriole in the pair) (Figure 4.3). We hypothesised that RASSF1A may be important in the formation of the primary cilium, an essential organelle nucleated from the mother centriole. To investigate this, we decided to use a RPE cell line. Indeed, we confirmed that RASSF1A can localise at the mother centriole and, consequently, the basal body of the primary cilium (Figure 4.4 & 4.5). Interestingly, when we transiently knocked down RASSF1A expression in cells before the induction of ciliogenesis, we observed a significant decrease in the fraction of cells presenting cilia (Figure 4.6). Furthermore, we demonstrate here that within the siRASSF1A treated population, many cells that do assemble a cilium portray aberrant phenotypes, with the cilium often bearing an abnormal shape, and being overall, shorter (Figure 4.7).

Given the reduction in acetylated α-Tubulin levels observed upon RASSF1A knock down (Figure 4.7 & 4.8), we hypothesised that the reduction in ciliation may be due to a decrease in this ciliary stabilising PTM via deregulated action of HDAC6. However, while decreased levels of tubulin acetylation may still be contributing to the loss of cilia, our data suggests that this is unrelated to the action of HDAC6 (Figure 4.10 & 4.11).

Another interesting observation was that IFT88 levels are depleted when RASSF1A is transiently silenced (Figure 4.7). We established that IFT88 and RASSF1A colocalise at the basal body and that the recruitment of IFT88 to here is independent of RASSF1A expression (Figure 4.12). Whilst further exploration of this area is required to make a definitive hypothesis, we propose that RASSF1A may function in the initiation of ciliogenesis as the basal body still appears capable of assembling in the absence of RASSF1A expression. In addition to this, siRNA mediated knock down of RASSF1A post-cilium assembly was not found to reduce cilia numbers significantly, suggesting that RASSF1A's function is not in maintaining cilium stability (Figure 4.13 A). Paradoxically, in these experiments we report a general increase in cilium length when RASSF1A is silenced (Figure 4.13 B). Whilst this is in opposition with what we expected, it opens a new line of inquiry, as it suggests that RASSF1A may influence the ability of ciliary proteins to traffic in and out of the organelle. Of particular relevance to this theory is the existence of the transition zone (TZ), a specialised domain at the ciliary base that acts as a 'gate' that controls the entry and exit of proteins to the cilium (Garcia-Gonzalo et al., 2011). The TZ resides just above the basal body and it would be interesting to investigate if RASSF1A is in any way linked to the TZ.

We also demonstrate here that the expression of RASSF1A in LUAD cell lines correlates with the ability of the cells to form a cilium. This is of particular interest given the recent links being made between the cilium and cancer. It also is representative of the heterogeneity in the ciliation of CCs that has been reported in the literature. This is supportive of a dual role for cilia in tumourigenesis and it would be interesting to see if the RASSF1A expression correlates with ciliation across tumour types. Further, it would be important to see if these non-ciliated tumours are also more stem-like, given the data suggesting that RASSF1A loss leads to an increased ESC signature in cancer cells (Pefani et al., 2016).

Overall, this data leads us to propose that RASSF1A is an important regulator of ciliogenesis which may have critical implications in tumourigenesis.

Chapter 5

Results III

Investigating the Role of RASSF7

5.1 Introduction

RASSF7 is a member of the N-terminal group of RASSF family proteins. Like the other RASSFs in this group, not much is known about the function of RASSF7 and so further investigation is required. This is particularly important given the recent links between RASSF7 and tumourigenesis (Takahashi et al., 2011; Djos et al., 2012). To date, studies have suggested that RASSF7 may have roles in early development given its embryonic expression levels (Chalmers et al., 2006; Sherwood et al., 2008; Recino et al., 2010). It has been shown that RASSF7 expression is particularly pertinent in the brain. It functions in governing the cell divisions that occur in developing neural tube, and interacts with the brain protein DISC1 to regulate astrogenesis (Sherwood et al., 2008; Wang et al., 2016).

RASSF7 has been described to display similar characteristics to RASSF1A. RASSF7 also localises with the centrosomes and is a mitotic regulator that interacts with the MTs (Sherwood et al., 2008; Recino et al., 2010). Further to this, RASSF7 has been linked to the regulation of apoptosis, albeit as a negative regulator of the process (Takahashi et al., 2011). Like RASSF1A, RASSF7 can also interact with the core Hippo kinase MST2

(Chan et al., 2013) . However, unlike RASSF1A, RASSF7 is considered an oncogene with upregulation reported in a variety of cancers and promoter methylation is relatively rare (Djos et al., 2012; Gulsen et al., 2016).

Intrigued by the molecular similarities coupled with the functional disparities between RASSF1A and RASSF7, we decided to investigate the RASSF7 protein to see if we could discover more about its cellular role. In order to do so, we utilised the widely used HeLa cervical cancer cell line, as well as the pancreatic cell line, PANC1, due to the incidence of RASSF7 upregulation in pancreatic cancers (Lowe et al., 2007). All data shown is from HeLa cells and is representative of results obtained in both cell lines unless otherwise stated.

5.2 RASSF7 Dynamics

Previous studies showed the localisation of GFP-tagged RASSF7 in various organisms. To assess the localisation of RASSF7 in the utilised cancer cell lines (HeLa & Panc1), we cloned RASSF7 cDNA (provided by the Structural Genome Consortium, University of Oxford) into an empty pZsGreen plasmid (Figure 2.1). All five of the selected clones that were analysed by restriction digest gave a positive result for RASSF7 integration (Figure 2.2). Out of these, two were sent for sequencing and returned readings that confirmed the RASSF7 insert was present and in the correct orientation (data not shown). PZsGreen – RASSF7 clone #2 was selected and carried forward for study (herein ZsRASSF7).

To initially determine ZsRASSF7 staining, we transfected cells with the ZsRASSF7 plasmid and observed a dynamic localisation pattern (Figure 5.1).

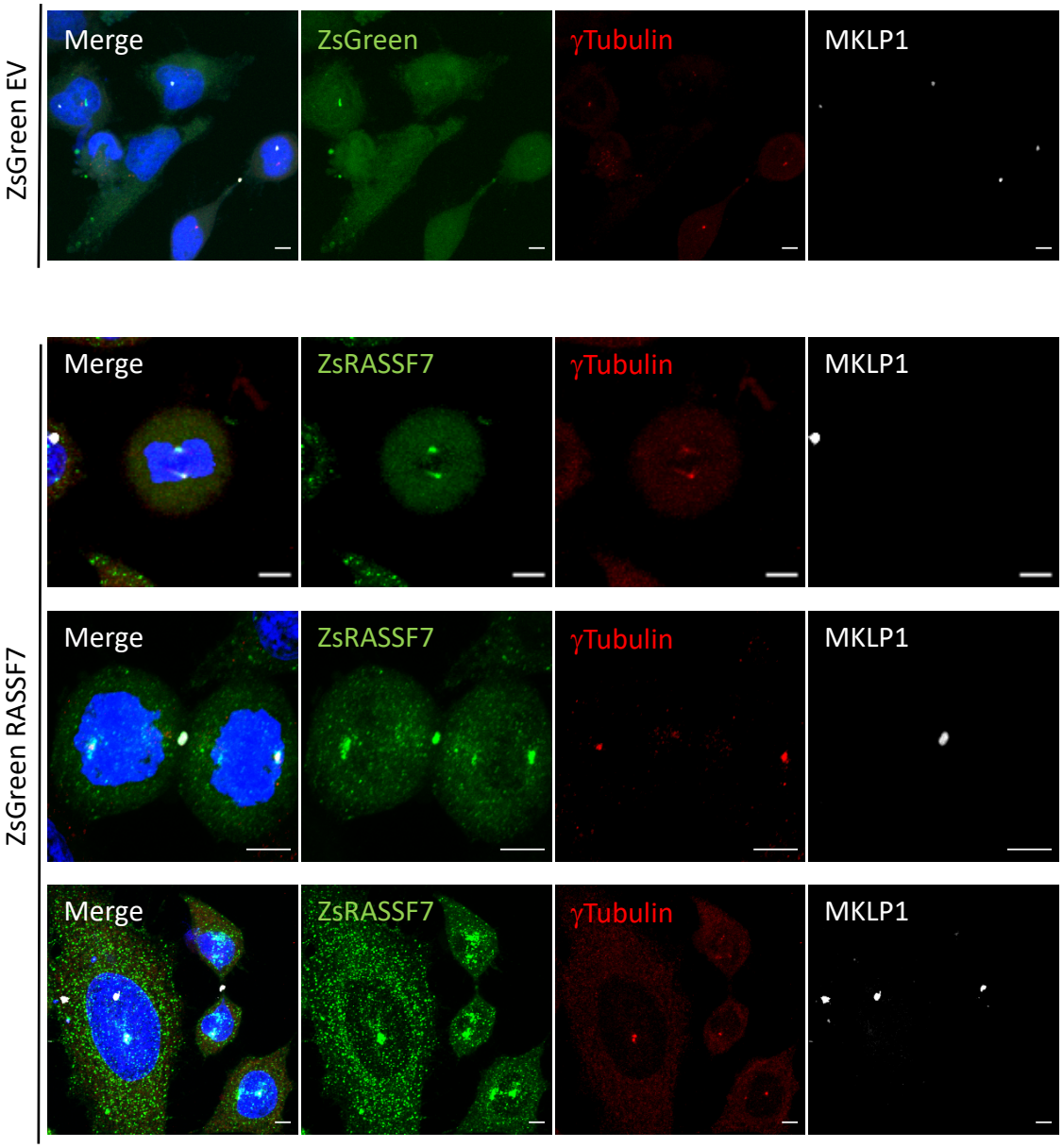


Figure 5. 1 ZsRASSF7 Displays a dynamic staining pattern throughout the cell cycle. ZsRASSF7 levels and localisation change throughout the cell cycle. During mitosis (top row, ZsGreenRASSF7 panel), the majority of the ZsRASSF7 signal colocalises with the centrosomes (γ-tubulin, red). As cells progress out of mitosis (bottom two rows, ZsGreenRASSF7 panel), ZsRASSF7 signal seems to increase. ZsRASSF7 persists at the centrosomes but can also be seen to localise with the midbody as marked with the midbody marker, MKLP1 (white). The remainder of the ZsRASSF7 signal is seen as punctate, vesicle-like structures. DAPI is shown in blue, scale = 5 μm.

ZsRASSF7 localisation changes drastically throughout the cell cycle. At metaphase, ZsRASSF7 is observed primarily at the centrosomes (marked with γ-tubulin, Figure 5.1), with expression elsewhere not visible. In agreement with published studies, ZsRASSF7

presence at the centrosome is visible throughout the cell cycle but as cells progress through M-phase towards cytokinesis, we observed a change in the localisation pattern. Interestingly, RASSF7 localises also at the midbody ring, as marked by MKLP1 (Figure 5.1 & 7.6). Post-anaphase, and throughout interphase, ZsRASSF7 is visualised as punctate vesicle-like structures.

Given this striking localisation, we wondered if endogenous RASSF7 behaved in a similar manner. To this end, we used a commercially available RASSF7 antibody and successfully verified its specificity using siRNA mediated knock down of RASSF7, alongside using siRNAs targeted to RASSF1A and the luciferase gene as a control (Figure 5.2 A). We also wanted to investigate the apparent change in RASSF7 levels throughout the cell cycle. To do so, we treated cells with 5 μm STLC (S-trityl-L-cysteine) for 16 hours to achieve a synchronous population of cells and follow RASSF7 expression levels upon release (Figure 5.2 B).

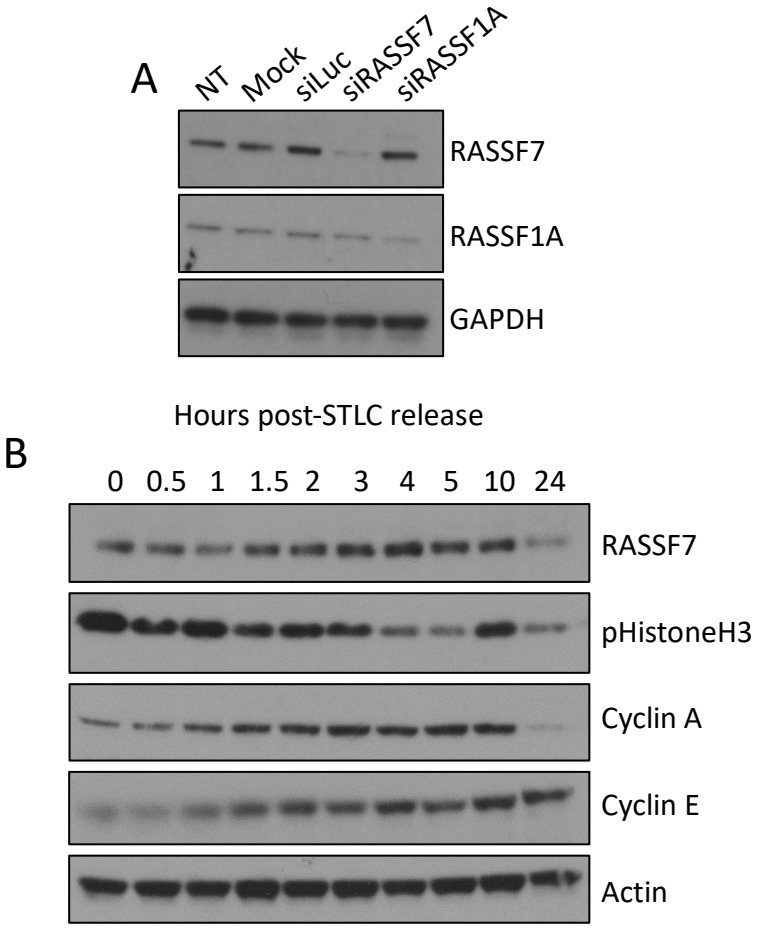


Figure 5. 2 Endogenous RASSF7 levels vary with the cell cycle. (A) RASSF7 antibody validation using siRNA mediated knock-down. NT = Non-treated. (B) Cell synchronisation with STLC confirms varying RASSF7 levels throughout the cell cycle. Western Blot analysis was carried out with the antibodies indicated. Phospho-Histone H3 (pHistone H3) was used to assess the presence of a mitotic cell population. Cyclin A & Cyclin E were used as indicators of cell cycle stage (G_2 and S phase, respectively). GAPDH & Actin were used as loading controls, and time post-STLC release is indicated in hours above corresponding band in (B).

STLC synchronisation works via the inhibition of the mitotic protein, Eg5, (Skoufias et al., 2006). Eg5 is a kinesin-related motor that is essential for the assembly of the bipolar spindle during mitosis (Blangy et al., 1995), and inhibition of its function effectively arrests cells in M-phase. Using this method, we can see that there are cell cycle dependent changes in RASSF7 expression, however, we cannot definitively conclude when these changes occur as the synchronisation observed does not seem to have worked sufficiently. Cyclin E expression is required for transition from G_1 to S phase (Lew et al., 1991; Dulić et al., 1992) and is an important initiator of the pre-replication complex (Coverley et al., 2002). Cyclin A expression increases through S phase and displaces Cyclin E from its partner, CDK2, leading to Cyclin E degradation (Clurman et al., 1996) and the initiation of DNA replication. Cyclin A peaks in G_2 phase (when Cyclin E should be absent), where it associates with CDK1 and reportedly activates mitotic Cyclin B before being degraded by the ubiquitin pathway (Glotzer et al., 1991; De Boer et al., 2008). However, in Figure 5.2 B, the western blot analysis appears to suggest the existence of divergent cell populations. This can be seen by the concomitant increase in both Cyclin A and Cyclin E expression, instead of the gradual degradation of Cyclin E that would be expected upon an increase in Cyclin A. However, the data in Figure 5.1 and 5.2 B taken together generally seem to indicate that RASSF7 is expressed throughout the cell cycle, with perhaps lower levels in mitosis than other cell cycle stages.

5.3 RASSF7 is Not Associated with the Endosome

The vesicular like appearance of ZsRASSF7 prompted us to hypothesise that RASSF7 may have links to vesicular trafficking within the cell. This theory was encouraged by the report that RASSF7 interacts with CHMP1B (Charged Multivesicular Body Protein 1B/

Chromatin Modifying Protein 1B), an essential component of ESCRT-III (endosomal sorting complex required for transport III) (Tsang et al., 2006). ESCRT-III is an endosome associated complex, important in membrane remodelling in the context of Multivesicular body (MVB) sorting (Babst et al., 2002; Babst, 2011). To explore this possibility, we initially sought to visualise ZsRASSF7 in live cells (Figure 5.3).

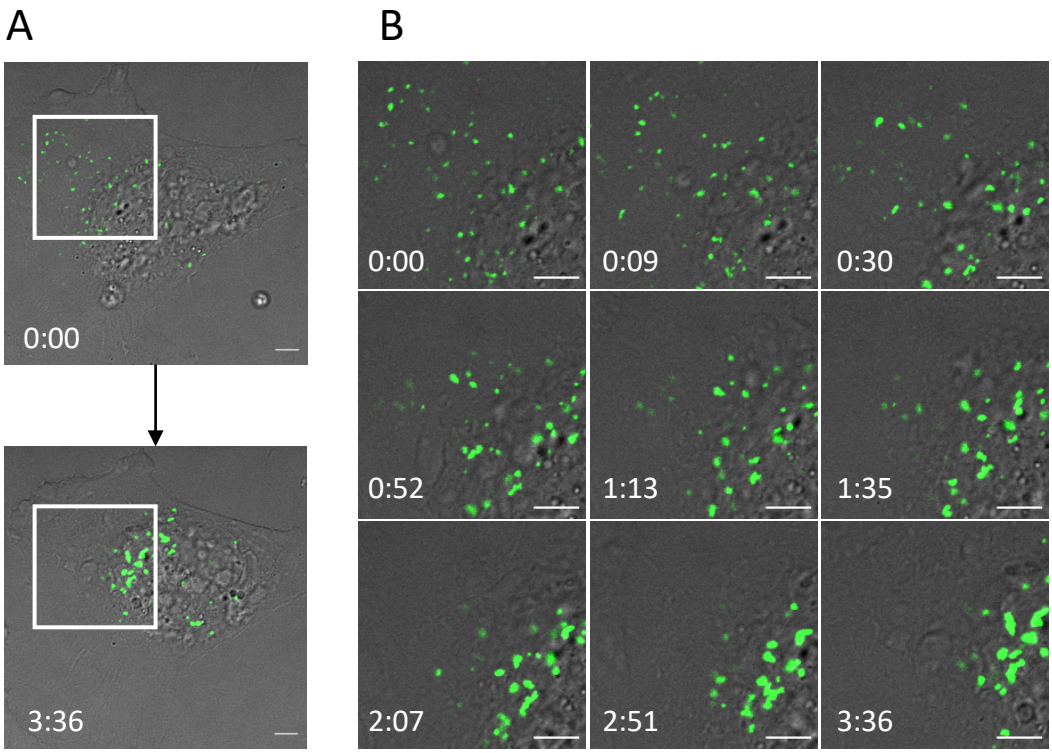


Figure 5. 3 ZsRASSF7 vesicles are motile. (A) Imaging of ZsRASSF7 transfected HeLa cells shows that the ZsRASSF7 vesicles are motile. (B) Enlarged still time frames from the enclosed regions indicated in (A) showing the movement of ZsRASSF7 positive puncta. Scale = 5 μm; time is shown in hh:mm format from first frame imaged.

Using live cell imaging we could demonstrate that the ZsRASSF7 positive vesicles are, in fact, motile. It is important to note that the time indicated in Figure 5.3 is not intended to reflect on the directionality of the ZsRASSF7 movement as this was not analysed. Overall, the movement of ZsRASSF7 supported our hypothesis that RASSF7 has a link to intracellular trafficking. To further test this, we investigated RASSF7 in association with endosomal markers (Figure 5.4 and Appendix Figure 2).

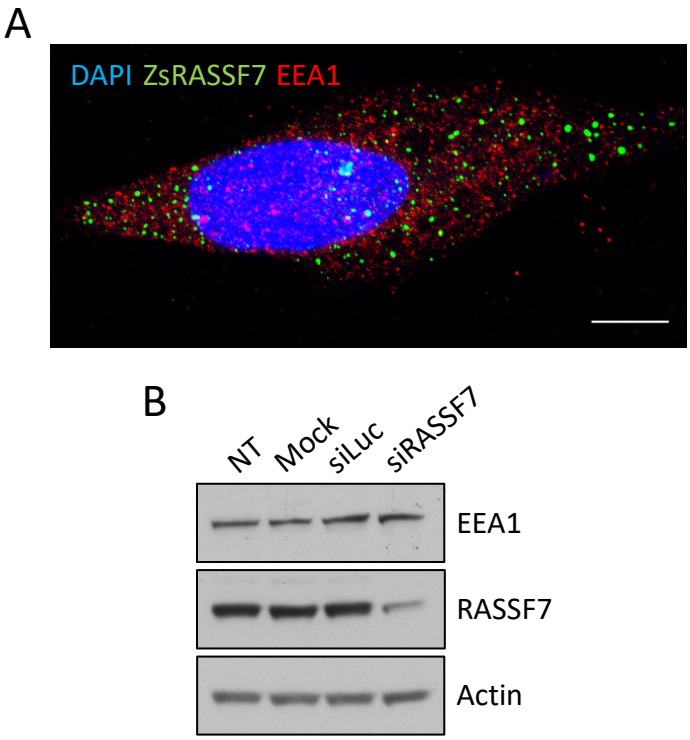


Figure 5. 4 ZsRASSF7 does not localise with tested MVB Markers. (A) Co-staining of RASSF7 with EEA1 revealed no obvious co-localisation of RASSF7 at the endosome. Scale, 10 μm; n=2. (B) Depletion of RASSF7 does not appear to affect EEA1 expression. Western Blot analysis was carried out with the indicated antibodies. Actin was used as a loading control. PANC1 results shown.

In our hands, RASSF7 displayed no consistent localisation with any of the vesicular markers tested. We co-stained cells expressing ZsRASSF7 with a variety of vesicular markers. EEA1 (early endosomal marker 1) an early-endosome protein, displayed no co-localisation with RASSF7 (Figure 5.4 A), nor did modulation of RASSF7 expression

influence EEA1 expression levels (Figure 5.4 B). Other endosomal proteins tested included Rab-5, -7 and -11, each of which are expressed and involved at various levels of endosomal function. However, these revealed no obvious correlations (Appendix Figure 7.2)

5.4 Exploring RASSF7 at the Nuclear Periphery

We noted that endogenous RASSF7 staining is enriched at the periphery of the nucleus and so we co-stained cells with Lamin A to examine if this localisation correlated to the position of the nuclear envelope. The nuclear envelope (NE) is a double membrane that surrounds the genome, compartmentalising it from the cytoplasm. Beneath this lies a network mesh of proteins, the nuclear lamina, which is mainly constituted from Lamin proteins. Lamin A is one of the major mammalian lamins and can be used to mark the boundary of the NE and the nucleus.

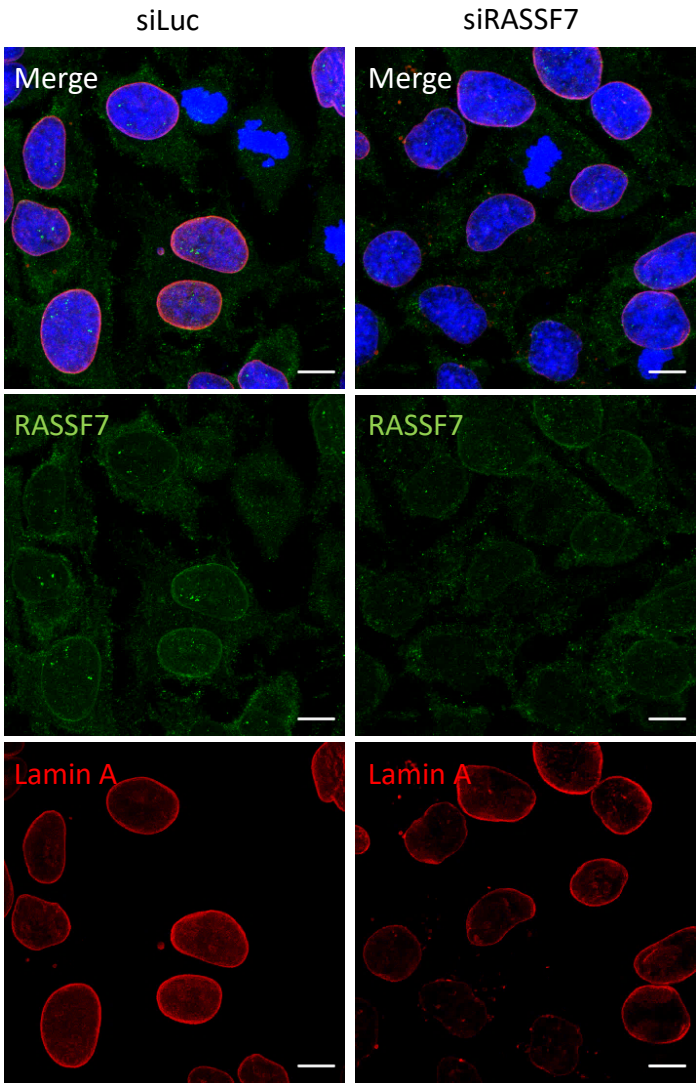


Figure 5. 5 RASSF7 localises at the periphery of the nuclear envelope. RASSF7 localises at the nuclear periphery, stained with Lamin A. Knock down of RASSF7 indicates a depletion of this localisation. Scale = 10 μm.

This demonstrated that RASSF7 co-localises with the nuclear envelope (Figure 5.5). Successful attempts were made to ensure this localisation wasn't the result of 'bleed-through' given the strong signal observed from the Lamin A antibody. This included separating the excitation values of the Alexa Fluor secondary antibodies as much as possible (i.e. Alexa Fluor-488 and -647 were used together) and reducing the intensity of the laser used to image the Lamin A antibody (data not shown). It was also striking

that the endogenous localisation pattern of RASSF7 was quite different to that of ZsRASSF7. Whilst we could still see the 'vesicle-like' RASSF7 staining and its centrosomal localisation in both the endogenous and overexpression scenarios, the visualisation of RASSF7 at the nuclear periphery was only apparent using endogenous staining. This highlights the importance of evaluating endogenous and exogenous expression, as any tags added to the exogenous protein may disrupt its normal localisation. Furthermore, we could confirm this endogenous localisation using siRNA mediated knock down of RASSF7.

Intrigued by this localisation, we wondered if RASSF7 might have a function at the nuclear envelope and so we examined NE integrity (described in Appendix Table 7.1) in siLuc and siRASSF7 treated HeLa cells (Figure 5.6).

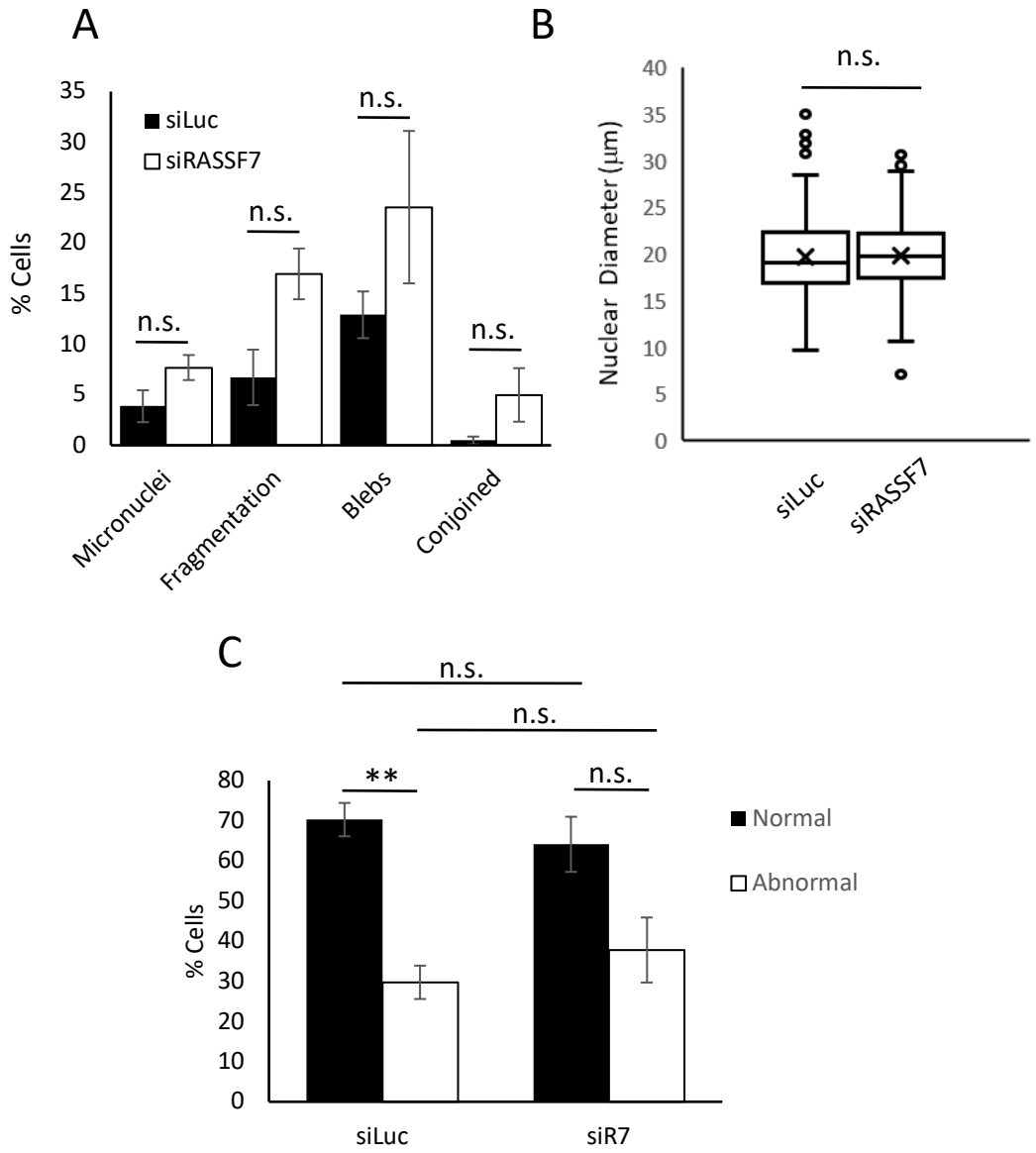


Figure 5. 6 RASSF7 depletion does not affect nuclear envelope integrity. Analysis of common nuclear envelope aberrations in cells +/- siRNA-mediated depletion of RASSF7. (A) Percentage of cells displaying indicated nuclear envelope phenotypes, p-values are as follows: Micronuclei, p = 0.153233; Fragmentation, p = 0.124779; Blebs, p = 0.229949; Conjoined, p = 0.165819. (B) Box and whisker plot of nuclear diameter at its largest point, the cross (x) represents the mean values and the line inside the box, the median. Boxes indicate the 25th and 75th percentiles and whiskers show 1st – 99th percentile. Hollow circles depict outliers from these parameters, p = 0.48606. (C) Fraction of cells with 'Normal' vs 'Abnormal' morphologies, p-values are as follows between 'Normal' and 'Abnormal' nuclear envelopes: siLuc, p= 0.00244; siRASSF7 p = 0.056399; and between siLuc and siRASSF7 'Normal', p= 0.282828, and 'Abnormal', p = 0.255164.

Whilst RASSF7 depletion appears to lead to a general increase in all phenotypes represented in Figure 5.6 A, none of these changes were statistically significant. Furthermore, there was no significant change in population nuclear diameter (Figure 5.6 B). Taken together, this suggests that RASSF7 depletion does not affect the overall NE phenotype. However, when the phenotypes from Figure 5.6 A are combined with morphological scoring of 'normal' vs 'abnormal' we see a change in the populations. Morphologically normal cells are those with a smooth, circular – oval appearance, whilst abnormal nuclear shapes include those that are irregularly shaped (for example 'heart'-shaped) and contain artefacts such as chromatin bridges. In control treated cells there is a significant difference between the number of cells that have normal and abnormal nuclei, but in the RASSF7 knockdown cells, this significance is lost (Figure 5.6 C). This suggests that RASSF7 may have a role in maintaining nuclear integrity but further investigation is necessary. Of note, there is no statistically significant difference in the fraction of abnormal cells between the siLuc and siRASSF7 conditions. All scoring of the nuclear envelope phenotypes was performed by eye and it would be ideal to repeat the analysis, therefore, using an automated system as this may increase the reliability of the results and may improve upon the statistical significance score achieved with manual analysis.

Simultaneously to the associations being drawn between RASSF7 and the NE, it was shown in the lab that the core Hippo kinase, MST2, is also enriched at the nuclear periphery (Appendix Figure 7.3, provided by Dr Dafni Pefani). Interestingly, it has been reported that RASSF7 interacts with MST kinases through its coiled-coil domain (Zheng et al., 2017). We wondered if RASSF7's presence at the NE may bear any relevance on

the localisation of MST2 here. To test this theory, we analysed the relationship between RASSF7 and MST2 (Figure 5.7).

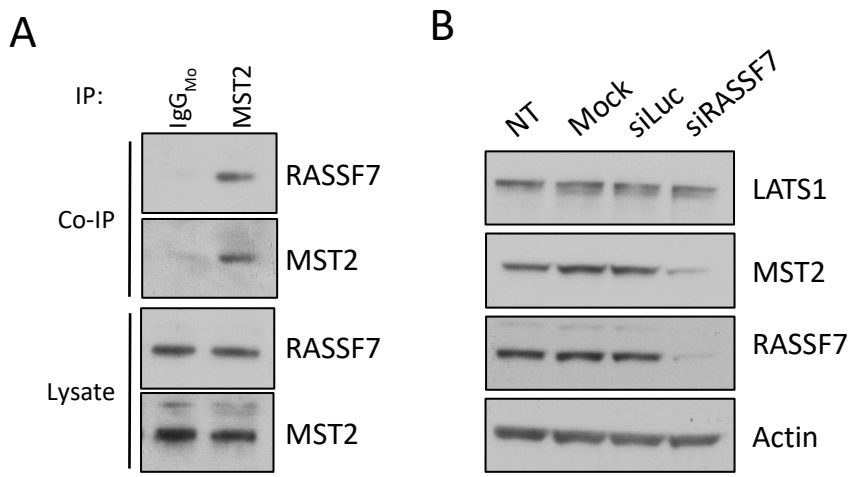


Figure 5. 7 RASSF7 & MST2 are associated with one another. (A) RASSF7 and MST2 co-immunoprecipitation demonstrates an interaction between the two proteins. (B) RASSF7 depletion leads to a decrease in MST2 levels. Western Blot analysis was carried out with the antibodies indicated. Actin was used as loading control, NT = Non-treated.

We confirmed that RASSF7 and MST2 can interact via immunoprecipitation of MST2 and immunoblotting for RASSF7 (Figure 5.7 A). The same relationship is observed when RASSF7 is immunoprecipitated (data not shown). To the best of our knowledge, we also demonstrate here for the first time that depletion of RASSF7 expression leads to a decrease in MST2 levels but does not affect LATS1 levels (Figure 5.7 B).

We then decided to explore the effect of RASSF7 knock down on MST2 localisation at the NE (Figure 5.8).

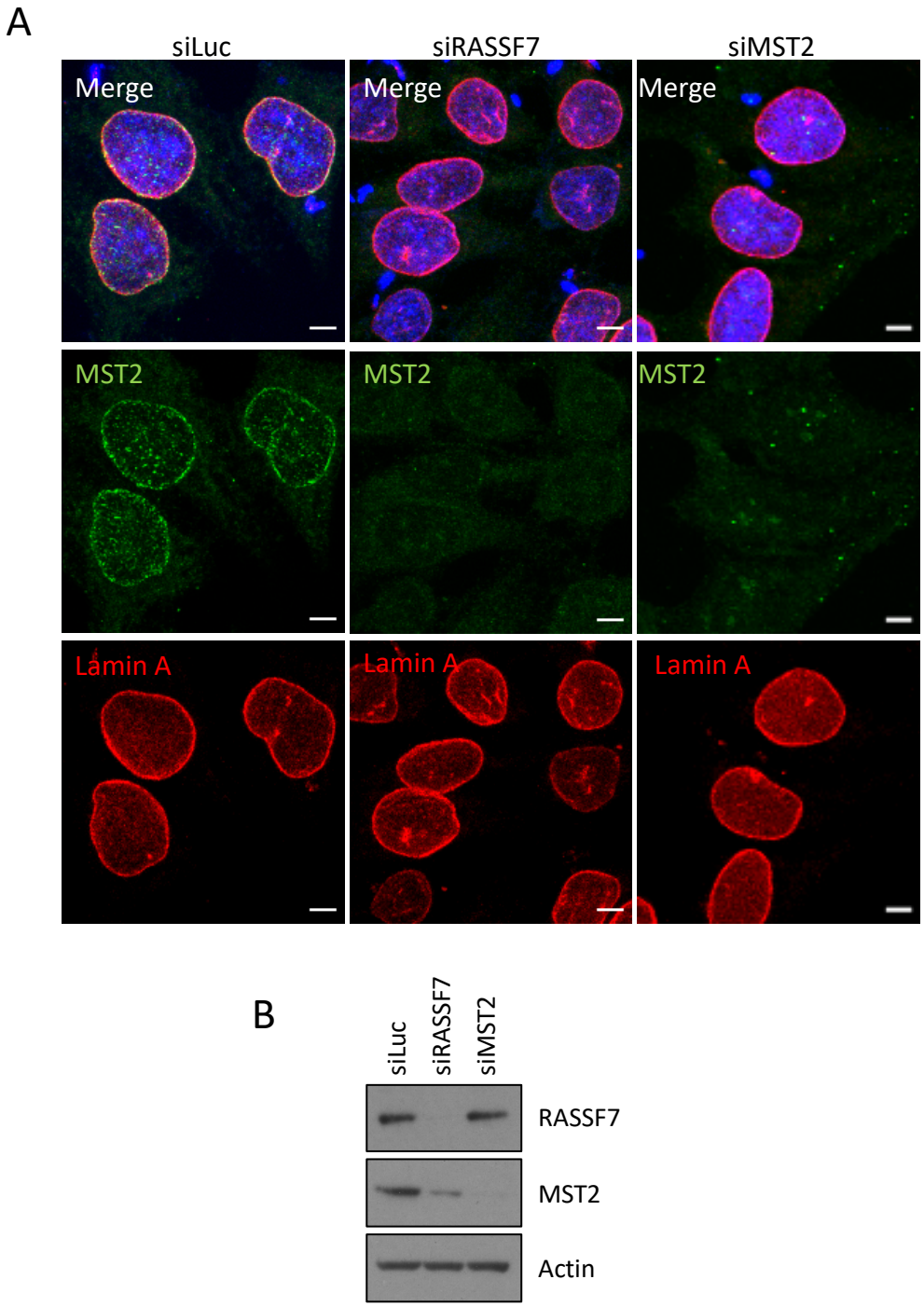


Figure 5. 8 Depletion of RASSF7 removes MST2 from the nuclear periphery. (A) MST2 (green) is enriched at the nuclear periphery, marked with Lamin A (red), in control treated cells. This localisation is lost along with the bulk of MST2 expression in siRASSF7 knock down. SiMST2 demonstrates MST2 antibody specificity. DAPI is shown in blue, scale = 5 μm. (B) RASSF7 expression knock down was confirmed by Western Blot analysis using the indicated antibodies. Actin was used as a loading control.

As shown by others in our group, MST2 localises at the nuclear periphery (Figure 5.8, first panel). Upon knock down of RASSF7, we can see the reduction in MST2 as suggested in Figure 5.7 B, however, the ability of any remaining MST2 to localise at the edge of the NE is lost. Taken together, our data suggests that RASSF7 is important in the expression of MST2 and further suggests that it has a role in directing MST2 to the nuclear periphery.

5.5 RASSF7 and Cancer

The main reason that we are interested in RASSF7 and its function, is because of the implications it may have in cancer. To date, reports of RASSF7 expression in cancers have varied, with reports of upregulation and silencing existing. By utilising an online tool to generate Kaplan-Meier plots (KM-plots), we were able to readily observe this (Figure 5.9) (Lánczky et al., 2016).

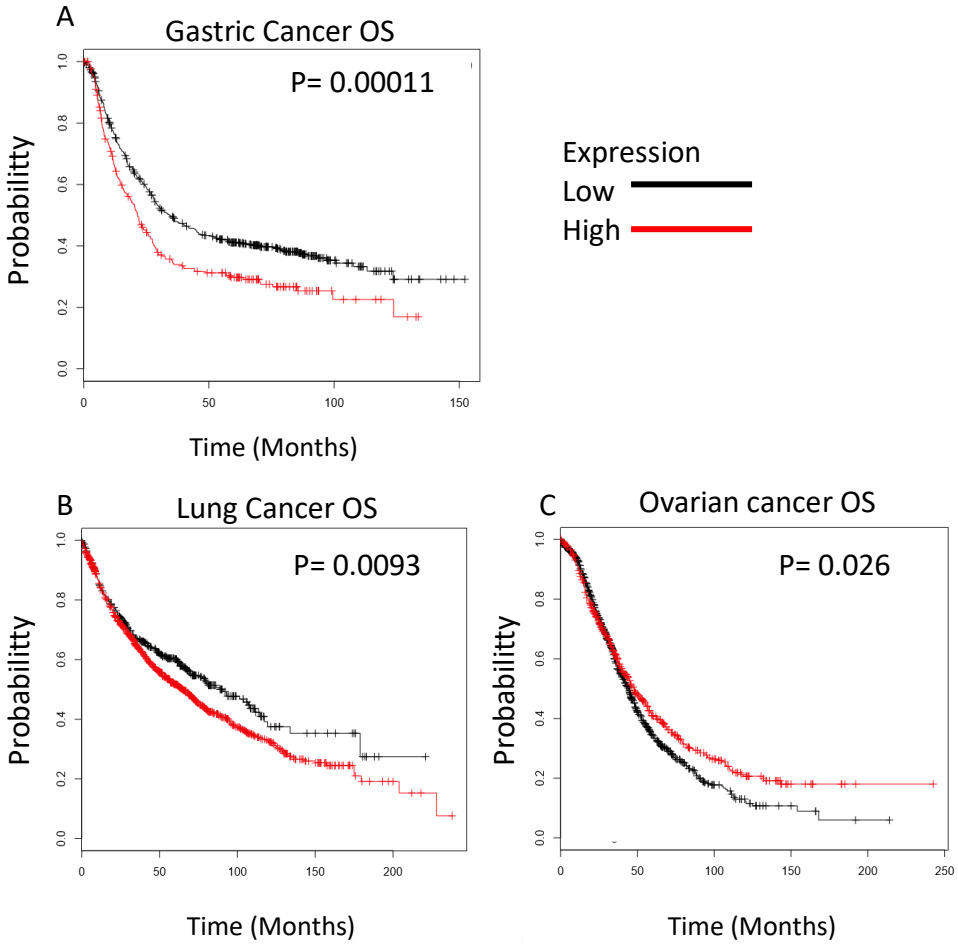


Figure 5. 9 RASSF7 Expression correlates differentially with overall survival in different cancers. KM-plots were generated using the online tool to observe overall survival (OS) of patients with gastric, lung and ovarian cancer. Black line demonstrates patients with low RASSF7 expression, and the red line is representative of patients with high RASSF7 expression. P-values are shown in their respective graphs.

Significant differences in survival were found in three of the available cancer types[2]. In gastric and lung cancer (Figure 5.9 A & B), high expression of RASSF7 is correlated with a poorer overall survival prognosis, however, in ovarian cancer the opposite is seen to be true (Figure 5.9 C).

[2] http://kmplot.com/analysis/

To further investigate the consequences of RASSF7 expression in cancer and to give us some indication of the processes RASSF7 is involved in, we decided to use GSEA to observe how gene signatures vary with RASSF7 expression. We used the FireBrowse[3] gene expression viewer to visualise RASSF7 expression across tumour types (Appendix Figure 7.4). From this we could see that RASSF7 expression is generally increased in the available tumour cohorts. We decided to analyse pancreatic adenocarcinoma (PAAD) and gastric Stomach adenocarcinoma (STAD) for different reasons. PAAD was selected due to the previous reports in the literature that RASSF7 expression is increased in pancreatic cancer patients and the FireBrowse plot confirmed this. We decided to also analyse STAD as to the best of our knowledge there has been no previous reports of RASSF7 expression in these cancers but there is an increase in RASSF7 expression in curated tumour samples (Appendix Figure 7.4) and high expression is correlated with poorer overall survival (Figure 5.9 A).

Using the GSEA software, we could see changes in oncogenic signatures as well as in gene ontology (GO) gene sets which were of interest to this project (Figure 5.10, Appendix Table 7.4 & 7.5).

[3] http://firebrowse.org/

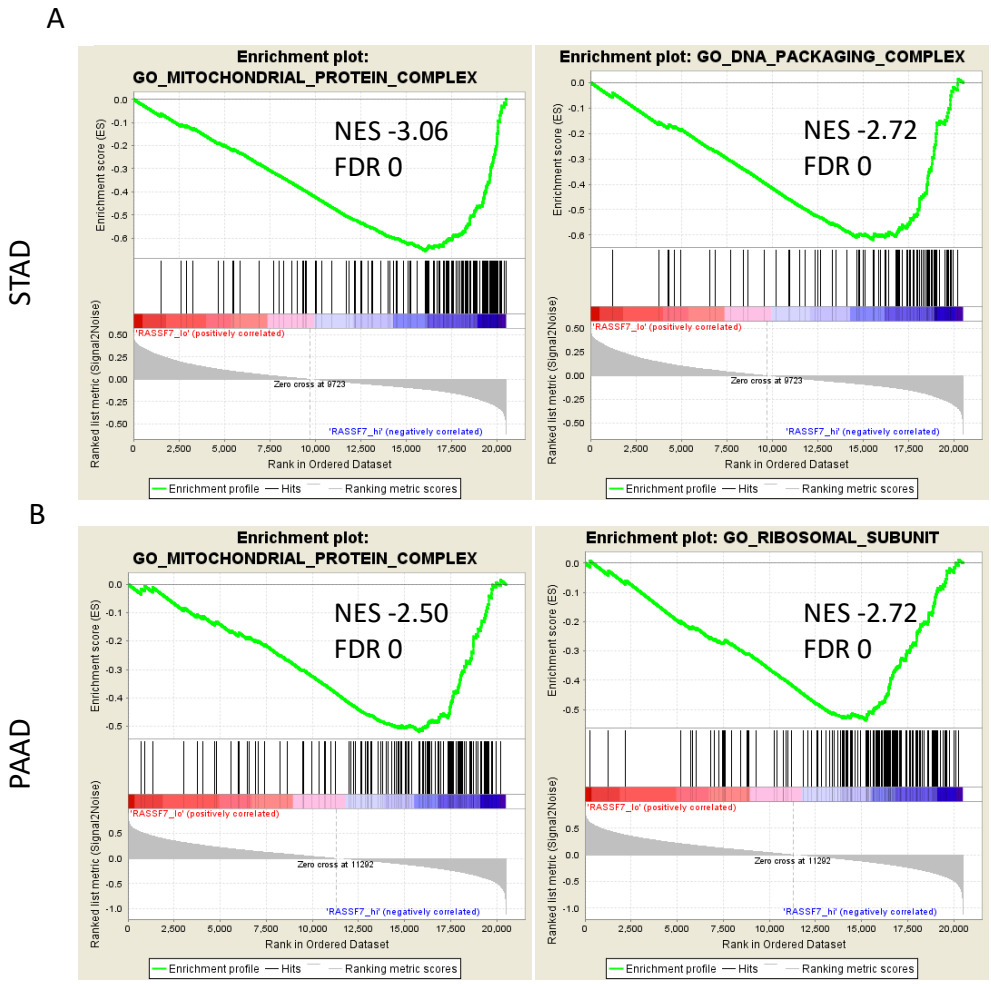


Figure 5. 10 RASSF7 Expression in STAD & PAAD correlates with changes in several types of gene signatures. Gene signatures related to the mitochondrion (left hand side) are significantly altered in STAD (A) and PAAD (B) tumour cohorts. Gene signatures related to heterochromatin are overrepresented in the STAD cohorts, whilst ribosomal gene sets are significantly altered in PAAD tumours.

High expression levels of RASSF7 were extensively correlated with a down-regulation of mitochondria-related gene sets (Figure 5.10, left panel; Appendix Table 7.2 & 7.3, yellow highlights). This is particularly interesting in the context of the punctate localisation of RASSF7, it would be worthwhile to investigate if these RASSF7 positive 'vesicles' displayed throughout this chapter are, in fact, linked to the mitochondria. Further, there was also downregulation of heterochromatin associated signatures (Figure 5.10 A, right panel; Appendix Table 7.2 & 7.3, green highlights), including the DNA-packaging complex and nucleolar gene sets. This is important in the context of cancer progression,

as high levels of RASSF7 may lead to relaxation of chromatin and unsuitable gene expression. In relation to the data presented here, this is quite interesting. Beneath the NE, there is a region of heterochromatin which can be marked by HP1α (Heterochromatin protein 1) expression. Recent work by others in our group has highlighted that MST2 localises with HP1α at the periphery of the NE (Appendix Figure 7.3). HP1α is a conserved protein with important roles in gene transcription regulation via heterochromatin formation (James and Elgin, 1986). Here, we report that RASSF7 and MST2 are localised at the nuclear envelope (Figure 5.8) and studies by others in our lab (Pefani et al., *In Revision*), have demonstrated a link between MST2 and heterochromatin. Therefore, it would be of interest to investigate if RASSF7 is involved in the regulation of heterochromatin via its interaction with MST2.

Of note, neither of these signatures are significantly altered in the low RASSF7 expression tumours, and so it would be important to perform more experiments with ZsRASSF7 overexpression to analyse the effects at a molecular level.

5.6 Discussion

As one of the newest members of the RASSF protein family, relatively little is known about the function of RASSF7. In this chapter, we present an explorative study of RASSF7 and its cellular function. Following the cloning of RASSF7 cDNA into a pZsGreen backbone, we report a dynamic localisation pattern for RASSF7 (Figure 5.1.). This pattern suggested variation in the levels of RASSF7 expressed during the cell cycle, which we confirmed for endogenous RASSF7 protein levels using cell synchronisation (Figure 5.2 B). The overexpression of RASSF7 displayed a punctate, vesicle – like appearance, although our efforts to link RASSF7 to several

endosome/exosome/trafficking proteins was unfruitful. However, we show here a visualised enrichment of RASSF7 at the nuclear periphery (Figure 5.5). Whilst this doesn't appear to be overtly linked to a nuclear function for RASSF7 (Figure 5.6), it may be important in the nuclear periphery localisation of MST2. MST2 is one of the core kinases of the Hippo pathway that has been previously shown to interact with RASSF7 (Chan et al., 2013). We confirm that interaction here, and further demonstrate that RASSF7 knockdown leads to a decrease in MST2 protein levels (Figure 5.7). Further, RASSF7 depletion also seemingly prevents the nuclear periphery localisation of MST2 (Figure 5.8), however, it is unclear if this is due to a depletion in levels or an incapability to localise here. Notably, upon knock down of MST2, the remaining protein that is expressed exhibits a very different staining pattern to that that observed upon RASSF7 depletion-mediated MST2 reduction. This indicates that RASSF7 may have an important role in the regulation of MST2 localisation.

We have also presented new analysis of RASSF7 expression in STAD and PAAD. RASSF7 expression is increased in both tumour types, as well as several others (Appendix Figure 7.4). Also, high expression levels of RASSF7 are correlated with poorer overall survival in patients with lung and gastric cancer (Figure 5.9). GSEA has allowed us to identify several avenues for future study, including the role of RASSF7 in the mitochondrion, as high RASSF7 expression levels were linked to suppression of a wide range of mitochondrial associated gene signatures in both tumour types (Figure 5.10 and Appendix Table 7.2 & 7.3). We also have highlighted that gene signatures related to heterochromatin control are altered in RASSF7 highly expressing tumours (Figure 5.10 and Appendix Table 7.2 & 7.3). Beyond these, there was also a huge variety of other

gene sets altered by RASSF7 expression, suggesting that there is still a wealth of information about RASSF7 to be discovered.

Chapter 6

Discussion

In this thesis, we investigated the role of RASSF1A at the centrosome and performed an explorative study of RASSF7 function. The RASSF proteins are an intriguing avenue of research given the various tumour suppressive roles that have been reported for several members of the family. The molecular mechanisms of these proteins, however, remain poorly understood. We sought to further elucidate these roles with an emphasis on the use of microscopy to study their spatial functions.

6.1 RASSF1A & Pluripotency

In the first chapter, we explored the role of RASSF1A in mESCs. The data presented support the previous findings in our group that RASSF1A is a player in the early specification of cell fate. We show here that RASSF1A expression increases as mESCs differentiate and that transient knock down of RASSF1A in pluripotent stem cells causes an increase in pluripotency markers and can delay differentiation (Figure 3.3). Previously, we demonstrated that this was due to the GATA-1 mediated activation of RASSF1A expression, which influenced the transcriptional output of YAP target genes (Papaspyropoulos et al., 2018). However, given the spatial localisation observed for RASSF1A (Figure 3.6 & 3.7), we hypothesised that RASSF1A may also play a structural

role in differentiation. This theory stemmed from the observation that RASSF1A localises asymmetrically at the centrosomes of dividing stem cells.

Interestingly, the staining pattern of RASSF1A localisation changes as mESCs differentiate. In pluripotent cells, RASSF1A can be seen at low levels within cells and its most apparent localisation is with the centrosome. However, as differentiation progresses, we see an enrichment of RASSF1A in the nucleus, this is supportive of previously reported roles for RASSF1A in DDR (Pefani et al., 2014). Further, we also see polarisation of RASSF1A, with cytoplasmic staining greatly reduced although with persistence of centrosomal localisation. These findings supported our original hypothesis that RASSF1A may have a role in ACD as both polarity establishment and the centrosome have a role in directional mitosis.

We were further encouraged by the finding that a subset of cells were asymmetrically distributing RASSF1A with the fate specification protein, Numb. The correlation between RASSF1A and Numb is a particularly intriguing finding from this project given the previously reported links between the two proteins. Numb localises at the cell membrane (Dho et al., 2006) and is asymmetrically inherited during differentiation of a number of cell types (Rhyu et al., 1994; Shen et al., 2002). The localisation of Numb with the membrane is in line with our similar findings for RASSF1A in spontaneously differentiating mESCs (Figure 3.9) and it would be interesting to investigate if they colocalise. Numb has been reported to permit differentiation in mouse neurogenesis via the inhibition of Notch signalling (Zhong et al., 1996), which correlates with our findings that RASSF1A promotes differentiation (Figure 3.2, 3.3 & 3.12) (Papaspyropoulos et al., 2018).

However, whilst we present evidence suggesting that RASSF1A has a role in ACD and directing SC fate in a spatial manner, further work is necessary to confirm if this is the case. It would be useful to investigate these findings in established ACD models to see if our findings have physiological significance. Possibilities include the system whereby ACD is induced in mESCs by the introduction of a 'Wnt microenvironment' (Habib et al., 2013; Lowndes et al., 2016), as well as more natural systems, such as organotypic brain slices where ACD in radial glial cells can be assessed (Bultje et al., 2009), or in meiotic mouse oocytes which divide asymmetrically (Verlhac et al., 2000). An important note to make from the data shown is the difficulty to identify enough events to achieve statistically significant data, further highlighting the need to establish a suitable system in which to study these phenomena.

From a cancer perspective, data from our lab demonstrates clearly that RASSF1A is important in preventing tumour progression (Grawenda and O'Neill, 2015; Pefani et al., 2016). The data presented in this thesis supports this notion and we demonstrate that re-expression of RASSF1A in cancer cell lines can restore a more differentiated phenotype. Further, we present new GSEA that displays an enrichment of ESC-linked gene expression in tumours that have lost RASSF1A expression (Figure 3.13). Here we demonstrate that loss of RASSF1A expression in glioblastoma Multiforme (GBM) is associated with an increased ESC signature. Cancer SCs have been reported in several studies of GBM and are implicated in the development, growth and persistence of tumours (Lathia et al., 2015).

6.1.1 Remaining Questions

The main question from this chapter remains, is RASSF1A driving asymmetric cell division or is it a passenger? Of interest is the association of RASSF1A with Numb inheritance. Given the important role of Numb in differentiation during neurogenesis, a system to assess the relationship between RASSF1A and Numb in this setting, for example using brain slice culture, would be of interest. Aurora-A has been shown to regulate Numb localisation via phosphorylation of the polarity regulating Par complex (Wirtz-Peitz et al., 2008), an important regulator of ACD (Betschinger et al., 2003). RASSF1A has been linked to both Aurora-A and polarity, therefore, this would be an interesting point of investigation.

An important query to address here would be to see if RASSF1A is involved in the regulation of Numb, or vice versa. If indeed RASSF1A is important in the segregation of Numb, then this control of ACD would be a novel mechanism by which it can promote differentiation. However, if RASSF1A is being segregated by Numb, this would provide a compelling demonstration that the cell is actively segregating RASSF1A to perform cell fate specifying roles in the inheriting daughter cell. A hypothetical model of the relationship between RASSF1A and Numb during ACD is proposed in Figure 6.1 and represents the relationships that we would investigate further if possible.

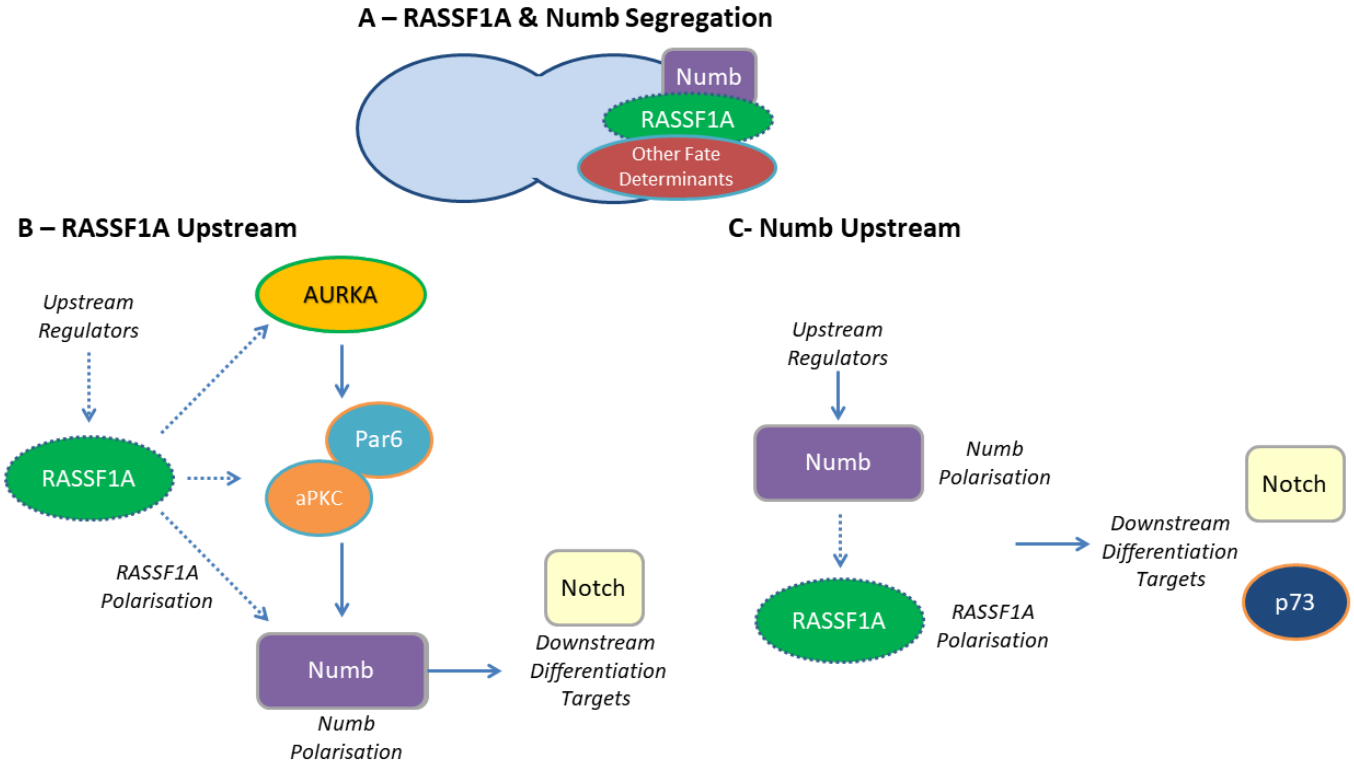


Figure 6. 1 Hypothetical model of RASSF1A and Numb associations during differentiation. (A) RASSF1A (green) is segregated asymmetrically with the fate determinant, Numb (purple). This may be accompanied by other fate determinants (red). (B) *RASSF1A may be an upstream regulator of numb*; here, hypothetical points of action for RASSF1A in the regulation of Numb are illustrated. RASSF1A has been previously reported to interact with and modulate other upstream regulators of Numb polarisation, including AURKA (yellow), Par6 (blue) and aPKC (orange). It is therefore possible that RASSF1A modulates Numb via its interactions with these proteins. It is also possible that RASSF1A can directly influence Numb. The polarisation of Numb modulates downstream differentiation targets including Notch (lemon). (C) *Numb may be an upstream regulator of RASSF1A*. To the best of our knowledge, Numb has not been reported to act upstream of any known RASSF1A interactors or modulators, however, Numb may still modulate RASSF1A activity and, therefore, the regulation of downstream differentiation targets such as Notch (lemon) by Numb and p73 (navy) by RASSF1A. Solid arrows depict previously reported interactions, dashed arrows are indicative of proposed associations.

RASSF1A is asymmetrically segregated with Numb in a subset of dividing mESCs. It is possible that this event may be accompanied by the asymmetric inheritance of other cell fate determinants (Figure 6.1 A), and so it would be of interest to explore this. It is tempting to favour a hypothesis in which RASSF1A regulates Numb localisation given its previously reported roles as a scaffolding protein. RASSF1A has been previously reported to interact with Aurora A (Rong et al., 2007; Liu et al., 2008) and has been implicated in the establishment of polarity (Arnette et al., 2014). Numb segregation has been linked to both also (Wirtz-Peitz et al., 2008), and therefore it is possible that RASSF1A may regulate this event via its interactions with upstream regulators of Numb (Figure 6.1 B). RASSF1A may also directly influence Numb (Figure 6.1 B), thus modulating its localisation and activity. In this scenario, the presence or absence of RASSF1A would influence differentiation capacity via ACD by modulating the polarisation of Numb and its downstream differentiation targets (Verdi et al., 1996; McGill and McGlade, 2003).

An alternative hypothesis would be that Numb regulates RASSF1A localisation (Figure 6.1 C). In this case, we hypothesise that Numb is important in the asymmetric inheritance of RASSF1A, ensuring that the differentiating daughter cell is enriched for RASSF1A expression. Thus, downstream differentiating targets of RASSF1A could be activated alongside those targets of Numb, such as p73 and Notch, respectively (McGill and McGlade, 2003; Papaspyropoulos et al., 2018). Interestingly, the knock down of Numb expression can lead to the epigenetic silencing of RASSF1A (Palakurthy et al., 2009). It is possible, therefore, that Numb may transcriptionally regulate RASSF1A expression, however this theory requires extensive further study.

To address these hypotheses, further work is necessary. Reciprocal knock downs of RASSF1A and Numb would be needed to evaluate the affect their expression exerts on one another and to see if this influences the frequency of asymmetric inheritance events. Notably, preliminary co-immunoprecipitation data suggests that RASSF1A and Numb may interact (data not shown) and the protein interaction predictor tool 'FpClass' (Kotlyar et al., 2015) suggests that they may, in fact, be interaction partners. It would also be of interest to further explore the transcriptional control of RASSF1A by Numb, as this could be a potential important feedback mechanism in the regulation of ACD and/or differentiation.

The relationship between RASSF1A and stemness is an interesting one, particularly in the context of cancer. It has been suggested in the past that RASSF1A could be used as a biomarker to diagnose and grade a variety of tumours, including tumours of the breast, lung, GI, endometrium and others (Zhang et al., 2014; Grawenda and O'Neill, 2015; Ye et al., 2017; Pabalan et al., 2017). Given the implications of a stem-like phenotype for cancer patients, a number of groups have been exploring a therapeutic route in which these CSCs are encouraged to differentiate, otherwise termed 'differentiation therapy' (Jin et al., 2017).

The concept of differentiation therapy arose from studies that demonstrated the ability of biological molecules (e.g. retinoic acid) to induce differentiation of certain cancer cell types (Lotem and Sachs, 1988; Huang et al., 1988). The induction of differentiation is suggested to deplete the cell pool capable of self-renewal, thereby allowing the clearance of the tumour bulk and preventing disease recurrence. Most current differentiation therapies exist for the treatment of different kinds of leukaemia (de Thé,

2017). As mentioned, retinoic acid (RA) is an important inducer of differentiation and it is utilised alongside epigenetic inhibitors or arsenic trioxides in the treatment of different types of Acute Myeloid Leukaemia (Schenk et al., 2012; Lo-Coco et al., 2013; McKeown et al., 2017). Other small molecules, including an Aurora kinase inhibitor, have also displayed efficacy in the clearance of Acute Megakaryocytic Leukaemia (Wen et al., 2015). Importantly, these therapies are now beginning to be introduced for other cancer types, with RA being used in the treatment of neuroblastoma (Matthay et al., 2009), and other small molecules such as a mutant isocitrate dehydrogenase inhibitors (IDHi) have been introduced in glioma therapies (Pusch et al., 2017). If current theories are correct and tumour resistance arises from CSC populations in certain cancers, then the study of RASSF1A's role in 'stem-like' properties may improve treatment outcome. On this vein, therefore, it would be worth investigating the possibility of reactivating RASSF1A expression, possibly via de-methylation of its promoter, and analysing if this can improve cancer therapy outcomes.

6.2 RASSF1A and the Cilium

In the last decade, research into the primary cilium has enjoyed a renaissance. Believed for years to be a vestigial and non-functional organelle, it has recently been shown to be a crucial signalling hub that can cause a wide range of developmental defects. Of interest, the primary cilium has also been linked to cancer progression.

In the first chapter, we noted the asymmetric localisation of RASSF1A at the centrosome, so in the second chapter, we explored the possibility that RASSF1A may function at the mother centriole. Here, we have presented evidence that RASSF1A is

asymmetric also within the centrosome and localises at the basal body of the primary cilium (Figure 4.1 – 4.5, model Figure 6.2).

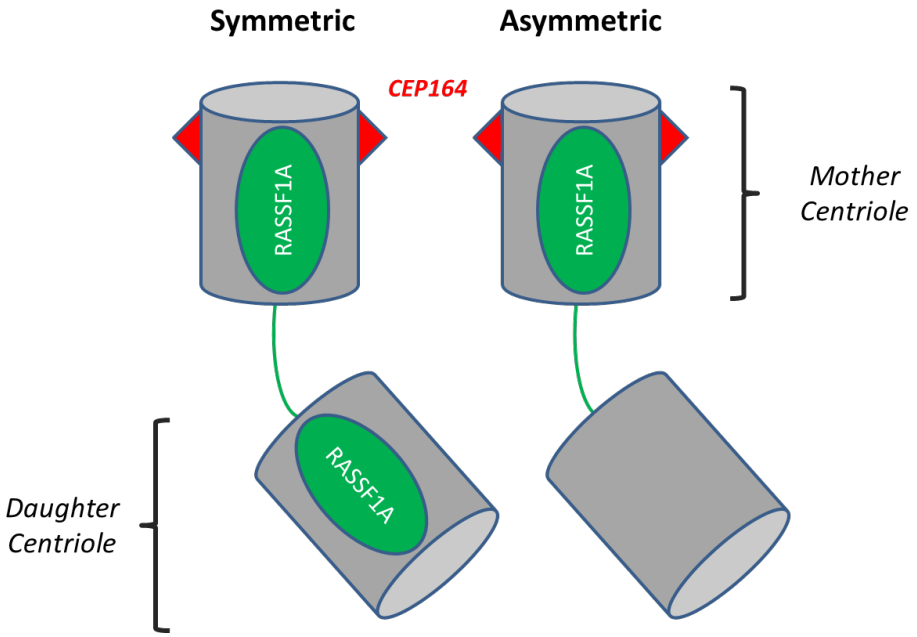


Figure 6. 2 Model of RASSF1A localisation within the centrosome. RASSF1A (Green) localises with the centrioles (grey). This localisation can be symmetric or asymmetric as indicated. However, when RASSF1A localises asymmetrically, it is associated with the more mature 'mother' centriole. The mother centriole can be distinguished by the presence of appendage proteins such as CEP164 (red).

Transient depletion of RASSF1A expression leads to a decrease in the ability of cells to present a primary cilium (Figure 4.6 & 4.7). Our data suggests that low levels of RASSF1A lead to a decrease in α-Tubulin acetylation, however, this appears to be independent of HDAC6, which has been shown to be important in the mediation of cilium assembly (Pugacheva et al., 2007) (Figure 4.8 – 4.11). This finding was surprising, as RASSF1A has been previously linked to the modulation of HDAC6 function (Jung et al., 2013; Tao et al., 2016), leading to our original hypothesis that the cilia defect observed may be due to unlicensed cilium disassembly. Furthermore, the study by Pugacheva et al. (2007)

demonstrated that the deacetylation action of HDAC6 at the cilium is regulated by Aurora-A. RASSF1A and Aurora-A have been previously shown to interact and modulate one another's activity (Rong et al., 2007; Liu et al., 2008). Considering the extensive links previously demonstrated between RASSF1A, HDAC6 and Aurora-A, we believe that the possibility that they cooperate at the cilium should not be disregarded and that further work, including siRNA mediated knock down of both HDAC6 and Aurora-A coupled with small molecule inhibition should help resolve this question.

Simultaneously, however, we also noted that RASSF1A knock down disrupts the levels of the intraflagellar transport (IFT) protein, IFT88 (Figure 4.7). This is another intriguing finding, as IFT88 is essential for the assembly and maintenance of the primary cilium. When we investigated IFT88 localisation using immunofluorescence, we observed IFT88, CEP164 and Centrin-3 can still localise, but there remains a lack of cilia present. We hypothesise that RASSF1A may, therefore, be an important player in the initiation event of ciliogenesis as the basal body is still able to assemble but the cilium does not form (Figure 4.12). Interestingly, localisation of activated pRASSF1A (Ser131) suggests that, unlike total RASSF1A, pRASSF1A can traverse the axoneme (Appendix Figure 7.5). This requires validation but suggests that it may be reasonable to test the ability of RASSF1A to traffic inside the ciliary axoneme.

In our initial efforts to test the theory that RASSF1A is important for the induction of ciliogenesis, we depleted RASSF1A after the cilium was assembled. In support of our hypothesis, this did not appear to cause a significant reduction in ciliation, suggesting that RASSF1A depletion does not overtly affect axoneme stability. Surprisingly, though, we saw an accompanied increase in cilium length, suggesting that there is a loss in

control of ciliary maintenance (Figure 4.13). Regulation of ciliary length is an important feature of cilium maintenance which is often reported as a measure of ciliary integrity, and relies heavily on the IFT system (Broekhuis et al., 2013). Whilst further investigation is necessary, it is possible that RASSF1A is important in the stabilisation of IFT88 and perhaps even its entry into the cilium. At the base of the primary cilium, distal to the basal body, there is a region known as the transition zone (TZ). The TZ is a specialised ciliary compartment which has been described as a gatekeeper and is necessary for proper cilia function as it modulates entry and exit of ciliary proteins (Gonçalves and Pelletier, 2017). An interesting theory to test, would be if RASSF1A functions at the TZ, and if its loss post-assembly restricts the exit of proteins already there.

Studies have demonstrated that the primary cilium is lost in a variety of cancers. This correlates well with our findings that RASSF1A loss, a frequent carcinogenic event, can lead to a decrease in cilia expression. Using a characterised panel of lung adenocarcinoma cells, we also present here that ciliation of cancer cell lines can correlate with the methylation status of the *RASSF1A* promoter, with cells that have lost RASSF1A expression being unable to form a cilium (Figure 4.14). It would be interesting to see if this observation persists in other cancer cell types.

Overall, we propose that RASSF1A is playing a role at the cilium, but further work is required to elucidate the mechanism of its action. We propose the following model for RASSF1A's role at the primary cilium (Figure 6.3).

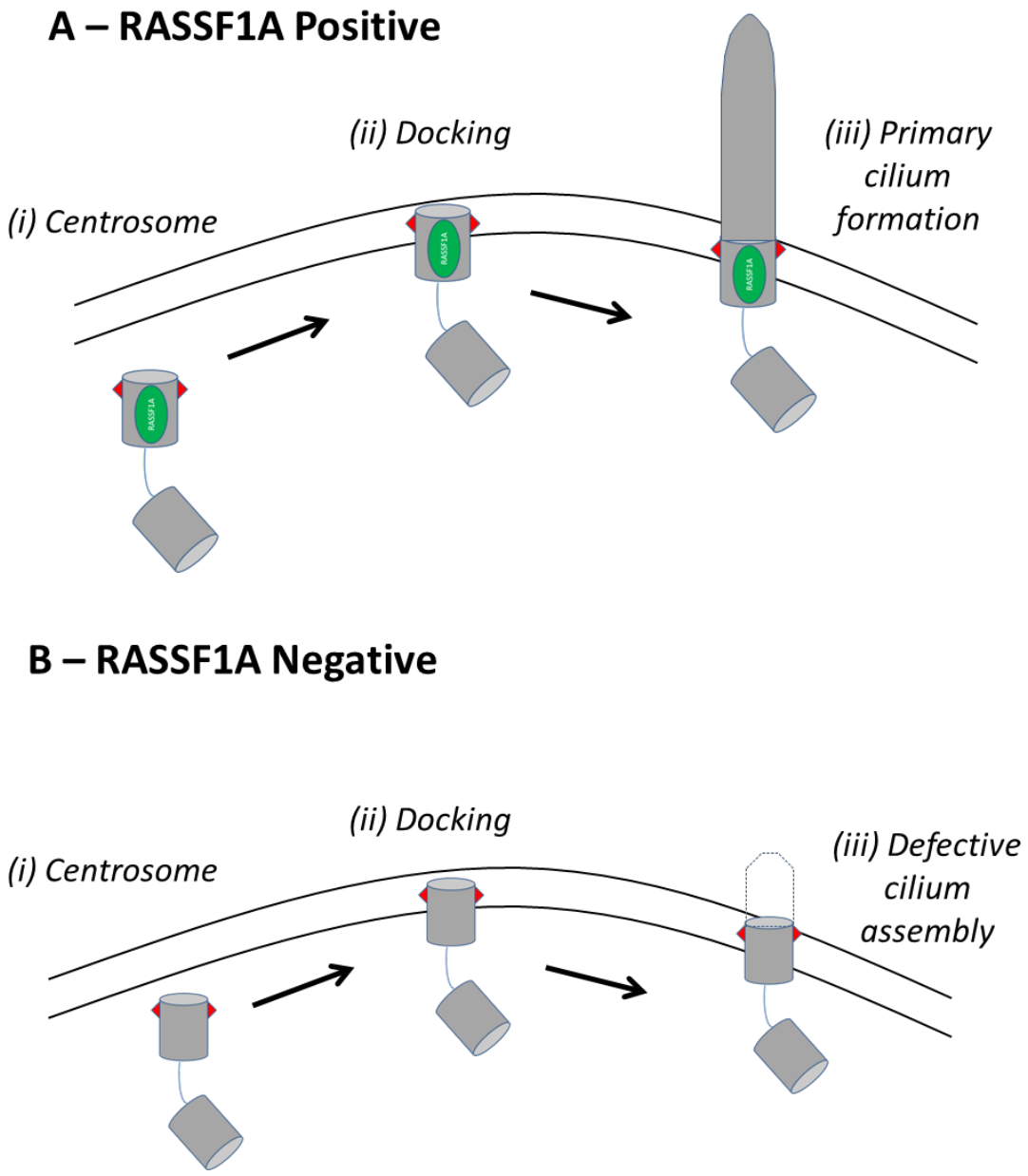


Figure 6. 3 Model of RASSF1A in the formation of the primary cilium. (A) When RASSF1A (green) is present, it can localise at the mother centriole (grey centriole marked with red CEP164 'appendages' as in Figure 6.1). Upon exit from the cell cycle and/or appropriate signalling cues, the centrosome migrates to the plasma membrane (double curved line) and the mother centriole docks. Once docked, the mother centriole transitions to a structure known as the basal body and nucleates the primary cilium. (B) In the absence of RASSF1A, the centrosome maintains the ability to reach step (ii) and a basal body can form, but primary cilia formation is defective.

6.2.1 Remaining Questions

A major question resulting from this work that needs to be addressed is the fact that RASSF1A seems to promote ciliogenesis and differentiation, two processes which are typically considered in opposition (Plaisant et al., 2009). RASSF1A activation in mESC differentiation is considered an early event (Papaspyropoulos et al., 2018). Interestingly, cilium presence has been documented throughout mouse embryonic development showing that ciliation is lineage specific (Bangs et al., 2015). Therefore, whilst there are reports highlighting the importance of the primary cilium for stem cell maintenance, the fact that several differentiated cell types are ciliated suggest presence of a cilium doesn't necessarily infer a stem cell phenotype and may also be important for proper differentiation.

Unpublished data from our group suggests that RASSF1A expression is also important in human SC differentiation (data not shown). To this end, it will be interesting to see if ciliation of mESCs and hESCs is linked with RASSF1A expression. There is also the possibility that the function of RASSF1A at the cilia presented in this thesis is cell-type and/or lineage specific. Therefore, as aforementioned, it will be essential to establish ciliation patterns alongside *RASSF1A* expression in hESCs as well as examining other tissue types. This will help determine if the discrepancy between ciliation and stemness is restricted to pluripotent versus differentiated cells in general or extends beyond this to tissue specificity.

Furthermore, the loss of cilia in several cancers is also in direct opposition with the dogma that cilia expression is a feature of a more stem-like phenotype, as many cancers display increased pluripotency. Clearly, there is much work needed to be done to define

the underlying mechanism, but the interplay between RASSF1A, the cilium and cancer formation presents a fascinating avenue for further study.

6.3 Connecting the Dots

Asymmetric cell division is important in the specification of cell fate and RASSF1A appears to be playing an important role. Whilst we haven't reached a definitive conclusion directly regarding ACD in this thesis, it is possible to draw links between this and the observation we make of RASSF1A being important in the formation of the primary cilium. The ability of a cell to assemble a primary cilium results in varying cell fates due to their ability to respond to differential signalling. Perhaps, therefore, there is a link between the asymmetric inheritance of RASSF1A and the ability to assemble a primary cilium, leading to differential cell fates.

6.4 RASSF7

In this thesis, we attempted to explore the role of RASSF7 to broaden knowledge on its function. Initially, we hypothesised that RASSF7 may be involved in vesicular trafficking, particularly in the endosome pathway, but our resulting data does not indicate that this is the case. From our preliminary imaging data (Figure 5.5), we also sought to investigate a link between RASSF7 and the nuclear envelope (NE) but RASSF7 loss does not appear to have a severe detrimental effect on this organelle (Figure 5.5). It would be prudent, however, not to completely dismiss the possibility that RASSF7 has a function at the NE. While none of the analysed phenotypes in Figure 5.6 was significantly different, there was an overall general increase in each upon RASSF7 knock down. Further, when the

results are pooled to normal vs abnormal nuclear architecture, there is a significant difference seen between the two labels in control cells. However, this significance is lost in RASSF7 depleted cells (Figure 5.6) – suggesting that, overall, RASSF7 may function in nuclear envelope integrity. Also, an important consideration is that nuclear envelope phenotypes were only measured in HeLa cells, so it would be interesting to see if there is a stronger defect in other cell types.

To the best of our knowledge, we demonstrate for the first time here that RASSF7 expression levels regulate the protein levels of MST2 (Figure 5.7 B). Further elucidation of this relationship is essential; to begin with, it would be helpful to know if RASSF7 depletion leads to a reduction in MST2 via a transcriptional or destabilisation mechanism. Given the scaffolding roles of the other RASSF proteins, it is most likely that RASSF7 acts as a stabilising platform on which MST2 functions. An ideal experiment to continue from here would be to evaluate MST2 expression upon RASSF7 knock down in the presence of a proteasome inhibitor. This would help determine if RASSF7 is stabilising MST2 protein levels by inhibiting proteolytic degradation in a manner similar to RASSF2 (Cooper et al., 2009). Furthermore, high levels of RASSF7 in stomach adenocarcinoma (STAD) and pancreatic adenocarcinoma (PAAD) correlates with significant changes in proteasome linked gene sets (Appendix Table 7.2 & 7.3).

Interestingly, the appearance of MST2 staining by immunofluorescence is punctate in nature (Figure 5.8), reminiscent of the vesicular-like appearance of RASSF7 (Figure 5.1 & 5.5). As stated, RASSF7 knockdown leads to a substantial reduction in MST2 levels but using siRNA-mediated depletion of MST2, we see a similar reduction in visualised MST2 but a very different localisation pattern (Figure 5.8). In the siMST2 scenario, the residual

MST2 is present in the same punctate manner as the siLuc condition – however, when RASSF7 expression is depleted any remaining visible MST2 is diffuse in nature. This raises questions about the relationship between RASSF7 and MST2 and it will be interesting to analyse what MST2-dependent functions are ablated upon RASSF7 loss, as well as any association with MST1 which has not been addressed here. Of note, RASSF7 depletion does not overtly affect LATS1 (another core Hippo kinase) levels (Figure 5.7) which suggests that RASSF7 can function through the non-canonical Hippo pathway. However, extensive studies are required to confirm and explore this statement. A hypothesised model for RASSF7 mediated regulation of MST2 follows (Figure 6.4).

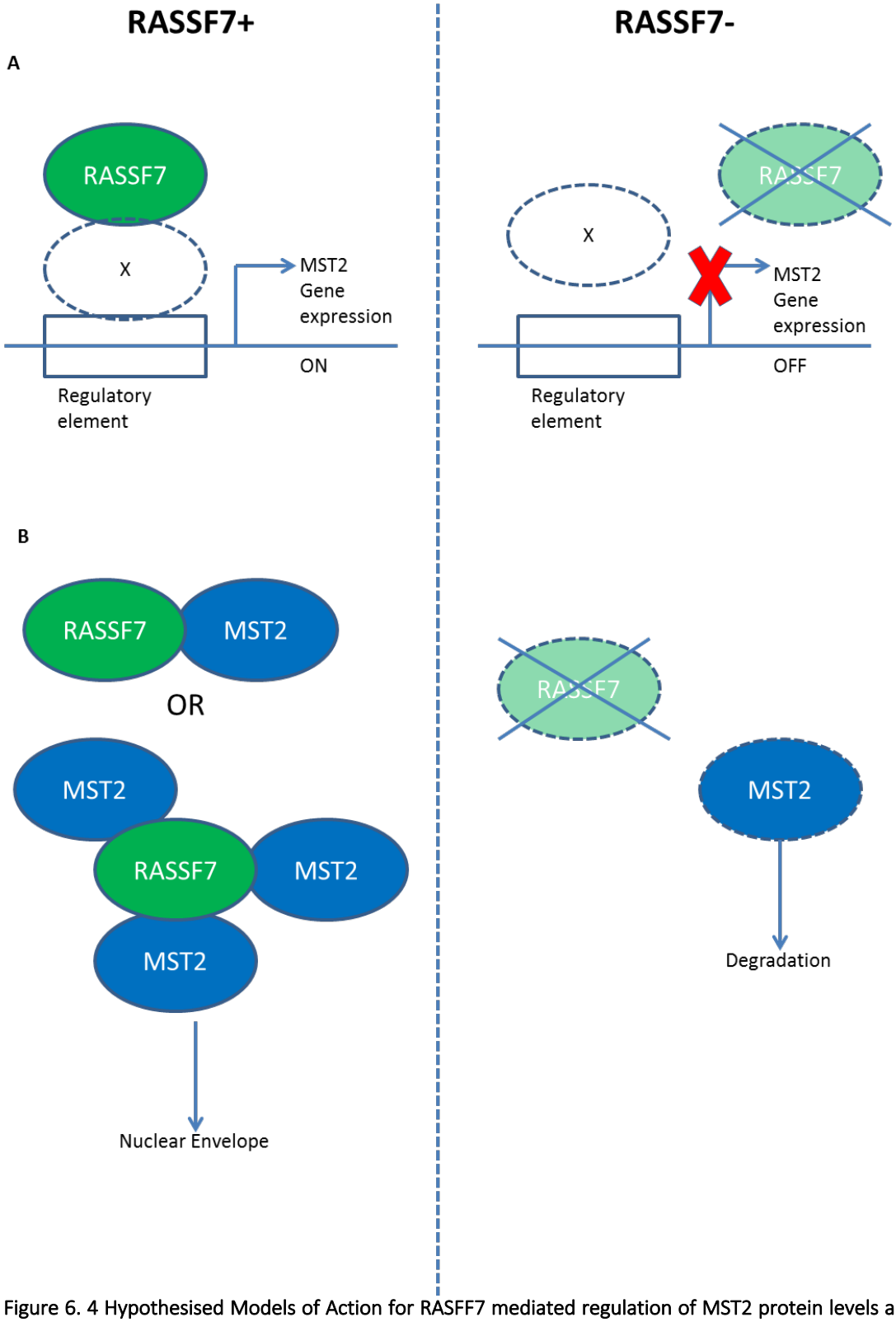


Figure 6. 4 Hypothesised Models of Action for RASFF7 mediated regulation of MST2 protein levels and localisation. (A) One possibility is that RASSF7 is in some way regulating expression of MST2 (transcriptionally depicted, but translationally is also possible). In the presence of RASSF7, MST2 is transcribed and translated, however, by unknown mechanisms, when RASSF7 is absent MST2 expression is not sustained. (B) Alternatively, RASSF7 may regulate MST2 at the protein level, which is more likely given the scaffolding roles of the RASSF protein family. In this scenario, we hypothesise that RASSF7 may scaffold one or more MST2 molecules and facilitate their localisation at the NE. In the absence of RASSF7, however, this aggregation of MST2 cannot occur and the protein is degraded.

6.4.1 Remaining Questions

The relationship between RASSF7 and MST2 at the nuclear periphery is an intriguing one. Whilst we report no obvious functionality for RASSF7 at the NE, it is possible that it may be important for a closely associated NE component, heterochromatin. As described in Chapter 5, MST2 localises with HP1α at the periphery of the nucleus (Appendix Figure 7.3). In relation to our findings here, HP1α interacts with the inner nuclear membrane and has been linked to NE reassembly (Kourmouli et al., 2000). Further to this, ESCRT-III has also been implicated in the sealing stage of NE reassembly (Vietri et al., 2015), and as mentioned in Chapter 5, RASSF7 has been reported as an interactor of this complex (Tsang et al., 2006). Considering the evidence thus discussed, it would be very interesting to investigate if there is any interplay between these proteins at the NE.

An observation which we would like to explore is that between RASSF7 and the midbody. RASSF7 localises at the midbody during cytokinesis (Appendix Figure 7.6). Interestingly, the ESCRT-III complex mediates membrane abscission via interactions with centralspindlin, an MKLP1 containing complex that is required for the completion of mitosis (Mishima et al., 2002). Our hypothesis that RASSF7 has a role in endosomal trafficking stemmed from the proposal of an interaction between RASSF7 and CHMP1B which was previously suggested in a high-throughput study (Tsang et al., 2006). However, our data did not support such a link. It may be worthwhile, however to explore the interaction between RASSF7 and CHMP1B/ESCRT-III in other biological processes such as cytokinesis and nuclear envelope resealing.

Our initial analysis of RASSF7 in stomach adenocarcinoma (STAD) and pancreatic adenocarcinoma (PAAD) presented in Chapter 5 also demonstrates that much more work is necessary to understand the role of RASSF7 in tumourigenesis. Of interest, would be to evaluate the relationship between RASSF7 and the mitochondria. High levels of RASSF7 in STAD and PAAD presented with variations in several gene sets related to the mitochondrion (Figure 5.10 and Appendix Table 7.2 & 7.3). Importantly, the gene sets are down-regulated, which suggests a potential inhibition of mitochondrial function. Mitochondria are key players in tumourigenesis, and have roles in stress detection and cellular adaptation to the environment (Vyas et al., 2016). It is possible, therefore, RASSF7 is important in the regulation of these organelles, and that deregulation of RASSF7 can cause transformation via mitochondrial dysfunction.

6.5 Concluding Remarks

In this thesis, we have presented an important role for RASSF1A asymmetry at the centrosome which may have far reaching implications in the determination of cell fate. The presence of RASSF1A in mESCs facilitates differentiation, perhaps through the RASSF1A mediated control of asymmetric cell division. This phenotype persists in cancer cells and may have important implications in the formation of tumours. Importantly, we have demonstrated that RASSF1A asymmetry and expression is positively correlated with the ability of cells to assemble a primary cilium, raising several interesting aspects for further study. Taken together, RASSF1A can be described as a cell fate determinant, as its presence and segregation is correlated with differential response in dividing daughter cells. Further, we explored RASSF7 function and propose an important role for RASSF7 in the regulation of MST2 stability and localisation at the nuclear envelope. Overall, this study has further highlighted the importance of the RASSF family proteins, RASSF1A and RASSF7, and is supportive of the need for further research into their functions.

Chapter 7 – Appendices

7.1 Appendix I

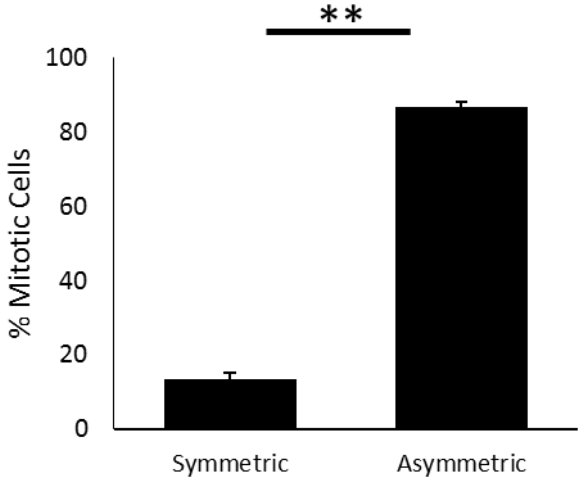


Figure 7. 1. Overall asymmetry of endogenous RASSF1A in mitotic mESCs. Approx. 20 mitoses counted per experiment, p = 0.001383.

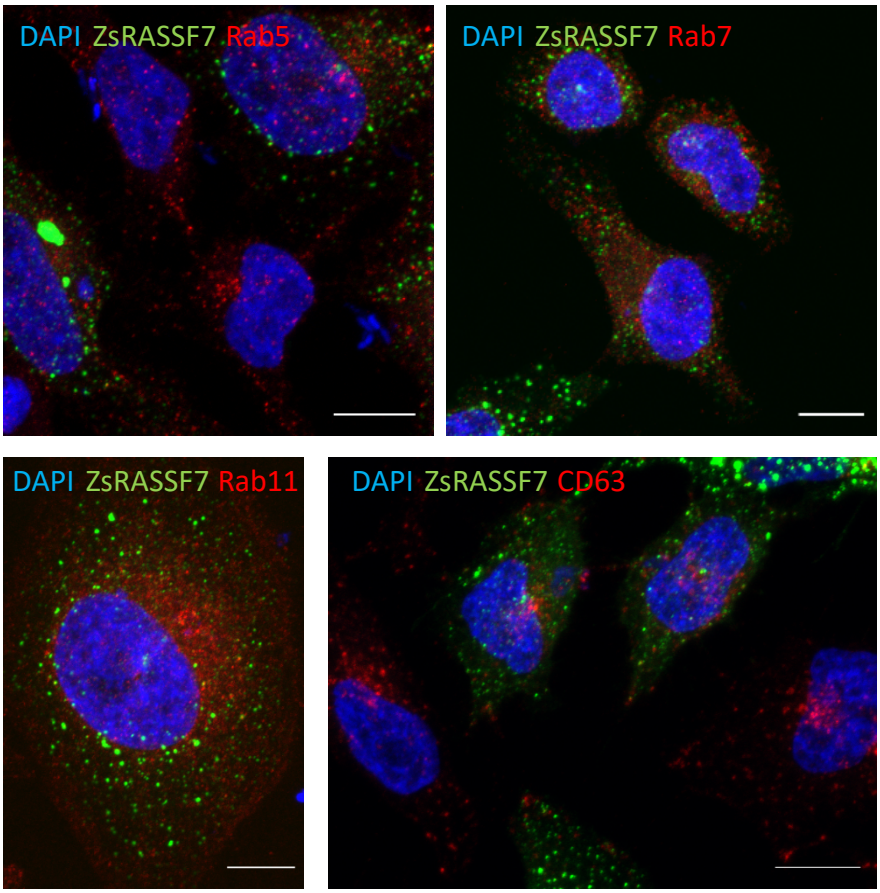


Figure 7. 2 RASSF1A does not exhibit any obvious correlation or localisation with endosomal markers. Antibodies tested include the early endosomal marker Rab5, late endosomal marker CD63 and the endocytic cycle linked markers Rab 7 and Rab 11. Scale = 10 μm.

Nuclear Envelope Phenotype	***Description***
Micronuclei	Rounded chromatin fragment surrounded by a nuclear envelope adjacent to the nucleus
Nuclear Fragmentation	Broken, extra-nuclear DNA lacking a nuclear envelope. Sign of apoptosis.
Nuclear Blebbing	Round/Oval protrusion of the nuclear envelope that remains connected to the nucleus
Conjoined cells	Cells that have completed mitosis but failed cytokinesis, the nuclei remain joined by a continuous nuclear envelope
Nuclear Diameter	This is the diameter of the nucleus at its largest point, measured three times and largest value taken.

Table 7. 1 Description of the Nuclear Envelope Phenotypes analysed in figure 5.6

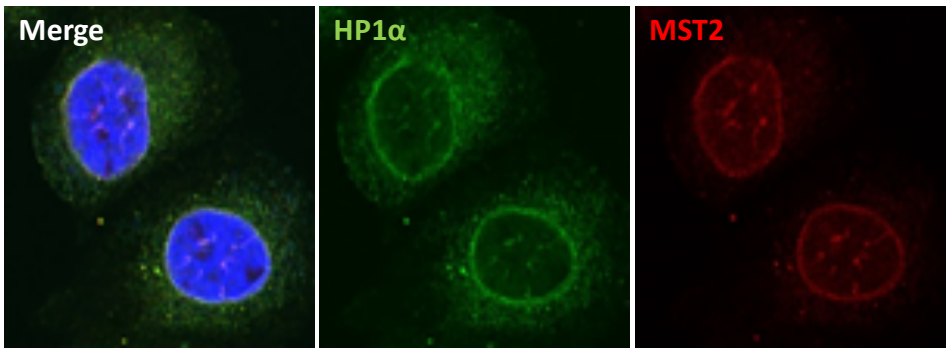


Figure 7. 3 MST2 localises with HP1a at the nuclear periphery. Image kindly provided by Dr Dafni Pefani.

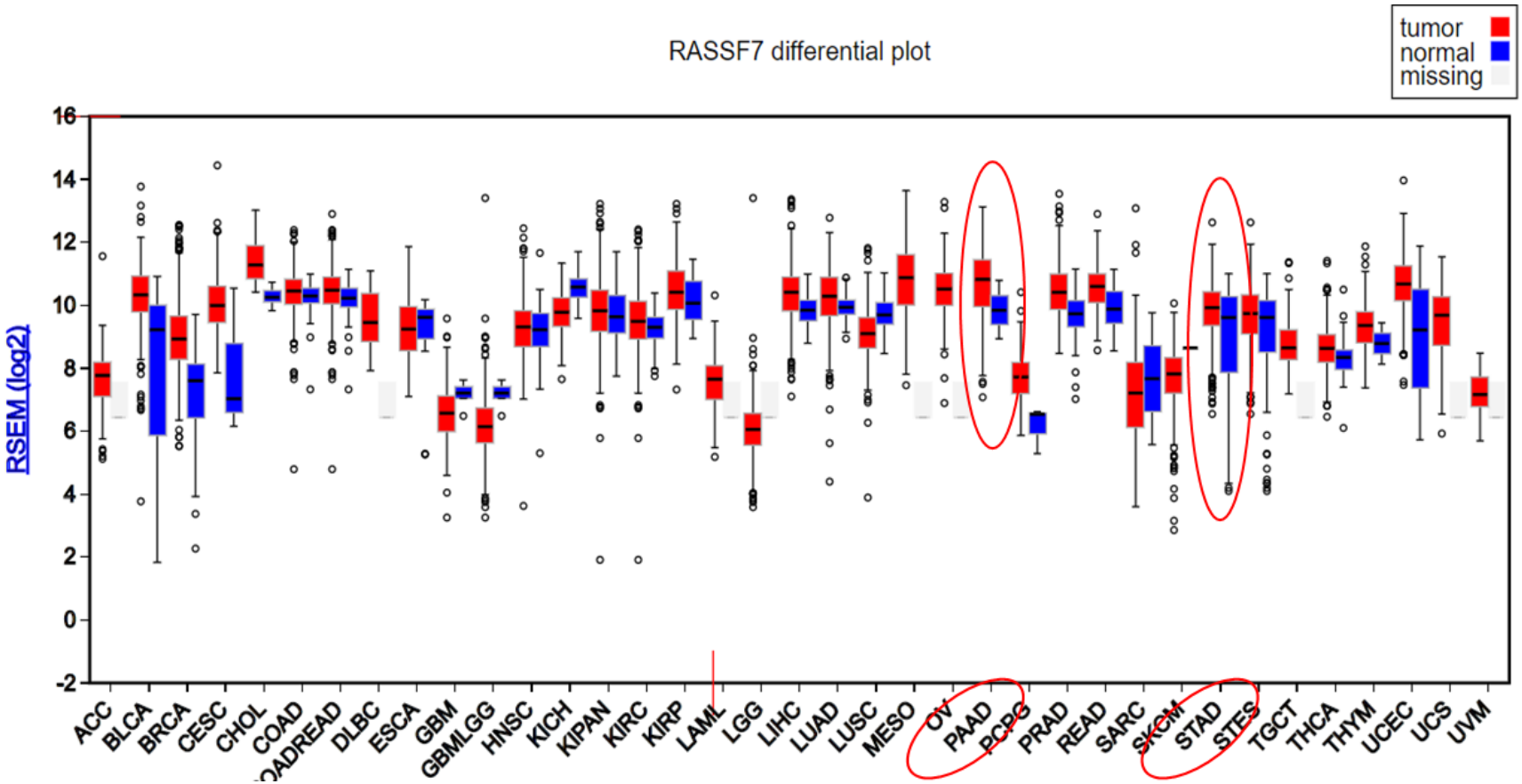


Figure 7. 4 RASSF7 Expression Data across human tumour types. RSEM (RNA-seq ahowa accurate quantification of RASSF7 expression across tumour types. RASSF7 expression is increased in many tumours (red boxes) compared to normal tissue (blue boxes). PAAD & STAD were chosen for further analysis (circled). http://firebrowse.org/viewGene.html?gene=rassf7

NAME	ES	NES	NOM p-val	FDR q-val
GO_INNER_MITOCHONDRIAL_MEMBRANE_PROTEIN_COMPLEX	-0.6967	-3.14532	0	0
GO_ORGANELLAR_RIBOSOME	-0.71592	-3.07855	0	0
GO_MITOCHONDRIAL_PROTEIN_COMPLEX	-0.65528	-3.05587	0	0
GO_RESPIRATORY_CHAIN	-0.6923	-2.96044	0	0
GO_MITOCHONDRIAL_MEMBRANE_PART	-0.60474	-2.92716	0	0
GO_RIBOSOME	-0.57373	-2.87454	0	0
GO_RIBOSOMAL_SUBUNIT	-0.59175	-2.83461	0	0
GO_NADH_DEHYDROGENASE_COMPLEX	-0.73381	-2.75514	0	0
GO_DNA_PACKAGING_COMPLEX	-0.61829	-2.71772	0	0
GO_ORGANELLAR_LARGE_RIBOSOMAL_SUBUNIT	-0.75043	-2.67396	0	0
GO_LARGE_RIBOSOMAL_SUBUNIT	-0.60045	-2.64772	0	0
GO_PROTEASOME_COMPLEX	-0.61967	-2.63949	0	0
GO_OXIDOREDUCTASE_COMPLEX	-0.59325	-2.61198	0	0

GO_NUCLEAR_NUCLEOSOME	-0.67637	-2.46464	0	0
GO_MITOCHONDRIAL_MATRIX	-0.46309	-2.45604	0	0
GO_SPLICEOSOMAL_COMPLEX	-0.50961	-2.42536	0	0
GO_SMALL_RIBOSOMAL_SUBUNIT	-0.58027	-2.38197	0	0
GO_CYTOSOLIC_RIBOSOME	-0.53087	-2.38195	0	0
GO_NUCLEOLAR_PART	-0.57867	-2.34465	0	0
GO_PROTEIN_DNA_COMPLEX	-0.48947	-2.34131	0	0
GO_PROTEASOME_ACCESSORY_COMPLEX	-0.7119	-2.33918	0	0
GO_ORGANELLAR_SMALL_RIBOSOMAL_SUBUNIT	-0.69069	-2.33698	0	0
GO_SMALL_NUCLEOLAR_RIBONUCLEOPROTEIN_COMPLEX	-0.74336	-2.33605	0	0
GO_SPLICEOSOMAL_TRI_SNRNP_COMPLEX	-0.70503	-2.32981	0	0
GO_PROTON_TRANSPORTING_ATP_SYNTHASE_COMPLEX	-0.71994	-2.30368	0	0
GO_U12_TYPE_SPLICEOSOMAL_COMPLEX	-0.67325	-2.29863	0	0
GO_SMALL_NUCLEAR_RIBONUCLEOPROTEIN_COMPLEX	-0.56983	-2.2857	0	0

GO_PRERIBOSOME_LARGE_SUBUNIT_PRECURSOR	-0.72313	-2.268	0	0
GO_PRECATALYTIC_SPLICEOSOME	-0.70089	-2.26111	0	0
GO_CYTOCHROME_COMPLEX	-0.70521	-2.24949	0	0
GO_CYTOSOLIC_LARGE_RIBOSOMAL_SUBUNIT	-0.56218	-2.24925	0	0
GO_PRERIBOSOME	-0.55045	-2.22215	0	0
GO_ORGANELLE_ENVELOPE_LUMEN	-0.50466	-2.17245	0	1.01E-04
GO_U4_U6_X_U5_TRI_SNRNP_COMPLEX	-0.68321	-2.13915	0	1.61E-04
GO_PROTON_TRANSPORTING_TWO_SECTOR_ATPASE_COMPLEX_PROTON_TRANSPORTING_DOMAIN	-0.66586	-2.13649	0	1.56E-04
GO_INTRINSIC_COMPONENT_OF_MITOCHONDRIAL_INNER_MEMBRANE	-0.68314	-2.12355	0	2.51E-04
GO_CATALYTIC_STEP_2_SPLICEOSOME	-0.49566	-2.11447	0	2.44E-04
GO_ESCRT_COMPLEX	-0.61733	-2.09561	0	2.67E-04
GO_INTRINSIC_COMPONENT_OF_MITOCHONDRIAL_MEMBRANE	-0.53855	-2.08779	0	2.60E-04
GO_CYTOSOLIC_SMALL_RIBOSOMAL_SUBUNIT	-0.53732	-2.08203	0	2.81E-04

GO_INTRINSIC_COMPONENT_OF_ENDOPLASMIC_RETICULUM_MEMBRANE	-0.44325	-2.05936	0	5.60E-04
GO_U2_SNRNP	-0.63021	-1.95313	0	0.001862
GO_PROTON_TRANSPORTING_TWO_SECTOR_ATPASE_COMPLEX	-0.50536	-1.91534	0.002786	0.002956
GO_CYTOSOLIC_PART	-0.38322	-1.90188	0	0.003276
GO_ROUGH_ENDOPLASMIC_RETICULUM_MEMBRANE	-0.59857	-1.89453	0	0.00353
GO_90S_PRERIBOSOME	-0.58994	-1.88572	0.002532	0.003576
GO_INTRINSIC_COMPONENT_OF_ORGANELLE_MEMBRANE	-0.36618	-1.86516	0	0.004641
GO_U1_SNRNP	-0.6196	-1.84986	0.002242	0.005239
GO_SMN_SM_PROTEIN_COMPLEX	-0.64229	-1.84033	0.004474	0.005554

Table 7. 2 Top 50 GO cellular component gene sets enriched with high RASSF7 expression in STAD. Name, Gene set enriched; ES, Enrichment Score; NES, Normalised Enrichment Score; Nom p-val, Nominal p-value; FDR q-val, False Discovery Rate q-value. Yellow highlight = Mitochondria related; Green highlight = chromatin link; Blue highlight = Proteasome link; Red = Other relevant links to this thesis

NAME	ES	NES	NOM p-val	FDR q-val
GO_RESPIRATORY_CHAIN	-0.6165	-2.77656	0	0
GO_ORGANELLAR_RIBOSOME	-0.63307	-2.75676	0	0
GO_RIBOSOMAL_SUBUNIT	-0.53706	-2.72636	0	0
GO_RIBOSOME	-0.51049	-2.66543	0	0
GO_INNER_MITOCHONDRIAL_MEMBRANE_PROTEIN_COMPLEX	-0.56435	-2.6651	0	0
GO_NADH_DEHYDROGENASE_COMPLEX	-0.65955	-2.56629	0	0
GO_LARGE_RIBOSOMAL_SUBUNIT	-0.54515	-2.52438	0	0
GO_MITOCHONDRIAL_PROTEIN_COMPLEX	-0.51825	-2.49968	0	0
GO_SMALL_RIBOSOMAL_SUBUNIT	-0.55379	-2.38117	0	0
GO_SPLICEOSOMAL_TRI_SNRNP_COMPLEX	-0.66551	-2.31722	0	0
GO_ORGANELLAR_LARGE_RIBOSOMAL_SUBUNIT	-0.62267	-2.2518	0	9.96E-05
GO_ORGANELLAR_SMALL_RIBOSOMAL_SUBUNIT	-0.6543	-2.25158	0	9.13E-05
GO_CYTOSOLIC_RIBOSOME	-0.47091	-2.23423	0	8.42E-05

GO_U1_SNRNP	-0.73447	-2.23145	0	7.82E-05
GO_MITOCHONDRIAL_MEMBRANE_PART	-0.44089	-2.22029	0	7.30E-05
GO_CORNIFIED_ENVELOPE	-0.55915	-2.21708	0	6.85E-05
GO_CYTOCHROME_COMPLEX	-0.6528	-2.16088	0	4.79E-04
GO_ESCRT_COMPLEX	-0.62102	-2.10535	0	0.001301
GO_SMALL_NUCLEAR_RIBONUCLEOPROTEIN_COMPLEX	-0.47891	-2.06609	0	0.001657
GO_CYTOSOLIC_LARGE_RIBOSOMAL_SUBUNIT	-0.49186	-2.06533	0	0.001574
GO_NUCLEOLAR_PART	-0.48208	-2.0588	0	0.001499
GO_U12_TYPE_SPLICEOSOMAL_COMPLEX	-0.58666	-2.04238	0	0.001862
GO_PROTEASOME_ACCESSORY_COMPLEX	-0.58092	-2.02893	0	0.001981
GO_OXIDOREDUCTASE_COMPLEX	-0.42898	-1.9991	0	0.002332
GO_U4_U6_X_U5_TRI_SNRNP_COMPLEX	-0.59879	-1.96234	0	0.003695
GO_DNA_PACKAGING_COMPLEX	-0.42261	-1.94913	0	0.004004
GO_CYTOSOLIC_SMALL_RIBOSOMAL_SUBUNIT	-0.50284	-1.94611	0	0.003984

GO_PROTEASOME_COMPLEX	-0.44002	-1.9406	0	0.004012
GO_U2_SNRNP	-0.5931	-1.91711	0.007614	0.004564
GO_PRESPLICEOSOME	-0.58571	-1.91394	0.005634	0.004452
GO_U2_TYPE_SPLICEOSOMAL_COMPLEX	-0.52036	-1.89715	0.003067	0.005039
GO_PRERIBOSOME_LARGE_SUBUNIT_PRECURSOR	-0.56587	-1.87737	0.00838	0.005744
GO_MITOCHONDRIAL_MATRIX	-0.33164	-1.85452	0	0.006903
GO_NUCLEAR_NUCLEOSOME	-0.49093	-1.85261	0	0.006733
GO_PROTON_TRANSPORTING_ATP_SYNTHASE_COMPLEX	-0.54796	-1.85058	0.002639	0.006683
GO_LATERAL_PLASMA_MEMBRANE	-0.44368	-1.80004	0	0.010509
GO_KERATIN_FILAMENT	-0.39214	-1.78111	0	0.012144
GO_ORGANELLE_ENVELOPE_LUMEN	-0.39011	-1.73128	0	0.017827
GO_SMALL_NUCLEOLAR_RIBONUCLEOPROTEIN_COMPLEX	-0.52411	-1.72679	0.005587	0.017975
GO_U2_TYPE_PRESPLICEOSOME	-0.56363	-1.68908	0.01847	0.023821
GO_PRERIBOSOME	-0.38804	-1.63578	0.003906	0.035584

GO_SPLICEOSOMAL_COMPLEX	-0.323	-1.62323	0	0.037456
GO_DNA_DIRECTED_RNA_POLYMERASE_II_CORE_COMPLEX	-0.51673	-1.61964	0.023599	0.037618
GO_U5_SNRNP	-0.52096	-1.61897	0.023684	0.036899
GO_90S_PRERIBOSOME	-0.47206	-1.61085	0.03096	0.038169
GO_CYTOSOLIC_PART	-0.30751	-1.59536	0	0.042216
GO_SMN_SM_PROTEIN_COMPLEX	-0.51875	-1.58243	0.030303	0.045138
GO_PROTEIN_DNA_COMPLEX	-0.31667	-1.58237	0	0.044222
GO_NUCLEAR_EXOSOME_RNASE_COMPLEX_	-0.5421	-1.57907	0.033898	0.044389

Table 7. 3 Top 50 GO cellular component gene sets enriched with high RASSF7 expression in PAAD. Name, Gene set enriched; ES, Enrichment Score; NES, Normalised Enrichment Score; Nom p-val, Nominal p-value; FDR q-val, False Discovery Rate q-value. Yellow highlight = Mitochondria related; Green highlight = chromatin link; Blue highlight = Proteasome link; Red = Other relevant links to this thesis

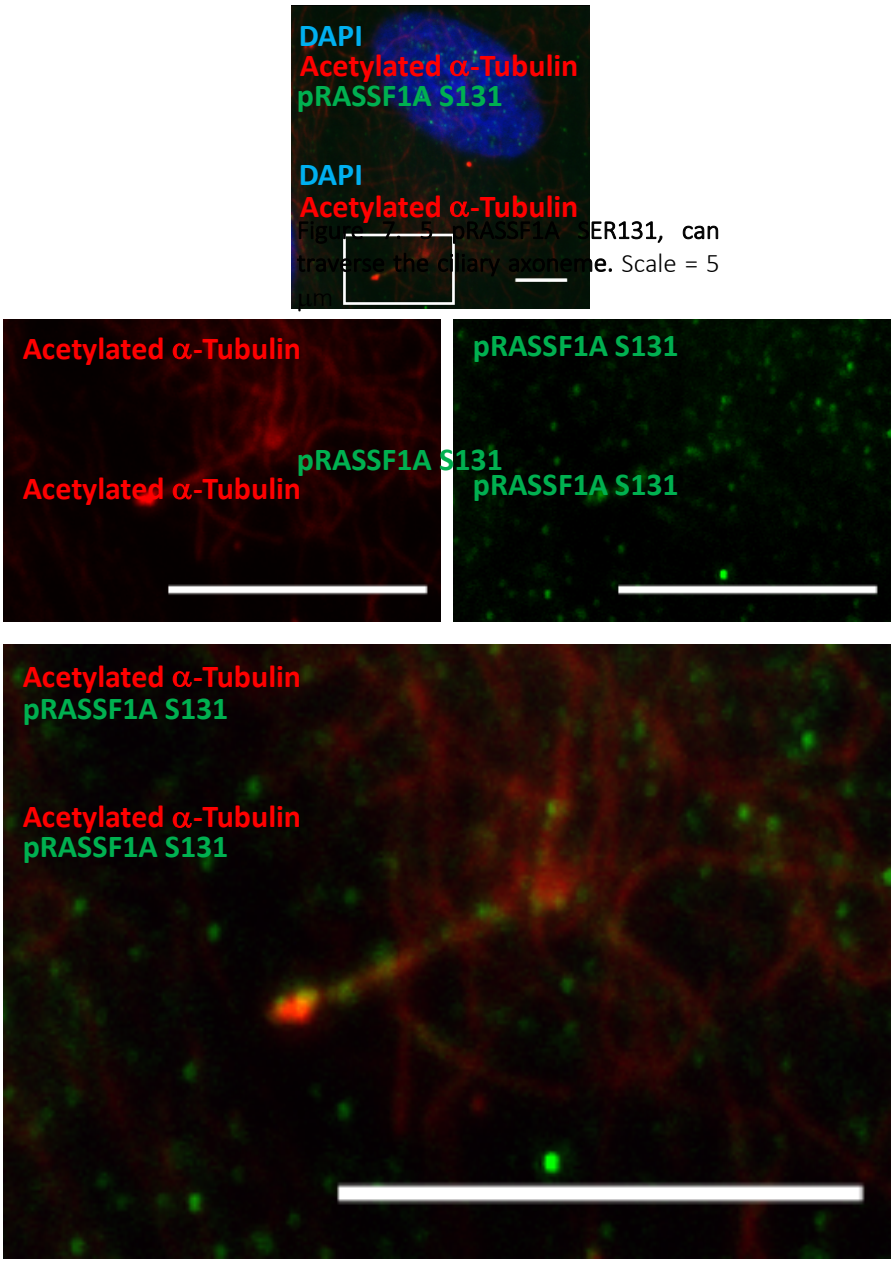


Figure 7. 5 pRASSF1A SER131, can traverse the ciliary axoneme. Scale = 5 μm

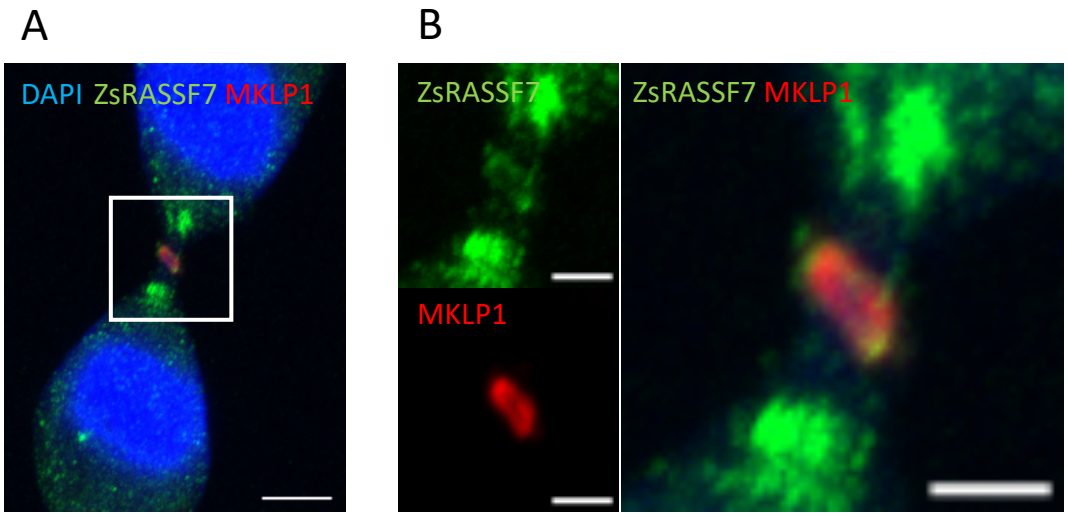


Figure 7. 6 RASSF7 localises at the midbody ring of cytokinetic cells, as markerd with the centralspindlin componenet MKLP1. (A) Scale = 5 μm. (B) Magnified image of boxed area in A, scale = 2 μm.

7.2 Appendix II

Publications from this thesis

1) Papaspyropoulos, A., **Bradley, L.**, Thapa, A., Leung, C.Y., Toskas, K., Koennig, D., Pefani, D.E., Raso, C., Grou, C., Hamilton, G., Vlahov, N., Grawenda, A., Haider, S., Chauhan, J., Buti, L., Kanapin, A., Lu, X., Buffa, F., Dianov, G., Von Kriegsheim, A., Matallanas, D., Samsonova, A., Zernicka-Goetz, M., O'Neill, E., 2018. RASSF1A uncouples Wnt from Hippo signalling and promotes YAP mediated differentiation via p73. Nature Communications 9. doi:10.1038/s41467-017-02786-5

2) **Bradley L.,** Koennig D., Tognoli M.L., van der Vaart J., O'Neill E. (2018) RASSF Family. In: Choi S. (eds) *Encyclopedia of Signaling Molecules*. Springer, Cham

3) Vlahov, N., S. Scrace, M.S. Soto, A.M. Grawenda, **L. Bradley**, D. Pankova, A. Papaspyropoulos, K.S. Yee, F. Buffa, C.R. Goding, P. Timpson, N. Sibson, and E. O'Neill. 2015. Alternate RASSF1 Transcripts Control SRC Activity, E-Cadherin Contacts, and YAP-Mediated Invasion. *Curr. Biol.* 1–16. doi:10.1016/j.cub.2015.09.072.

7.3 Appendix III – Original Copyright Notices

Figure 1.1

ELSEVIER LICENSE
TERMS AND CONDITIONS

Dec 30, 2017

This Agreement between Miss. Leanne Bradley ("You") and Elsevier ("Elsevier") consists of your license details and the terms and conditions provided by Elsevier and Copyright Clearance Center.

License Number	4258810423115
License date	Dec 30, 2017
Licensed Content Publisher	Elsevier
Licensed Content Publication	Cell
Licensed Content Title	Hallmarks of Cancer: The Next Generation
Licensed Content Author	Douglas Hanahan,Robert A. Weinberg
Licensed Content Date	Mar 4, 2011
Licensed Content Volume	144
Licensed Content Issue	5
Licensed Content Pages	29
Start Page	646
End Page	674
Type of Use	reuse in a thesis/dissertation
Portion	figures/tables/illustrations
Number of figures/tables/illustrations	1
Format	both print and electronic
Are you the author of this Elsevier article?	No
Will you be translating?	No
Original figure numbers	Figure 6
Title of your thesis/dissertation	Exploring the Roles of the Centrosomal RASSF Proteins, RASSF1A & RASSF7, in Stem Cells & Cancer
Expected completion date	Jan 2018
Estimated size (number of pages)	200

Requestor Location	Miss. Leanne Bradley 213 Shore Road Magherafelt, Derry BT45 6LW United Kingdom Attn: Miss. Leanne Bradley
Publisher Tax ID	GB 494 6272 12
Total	0.00 GBP
Terms and Conditions	

INTRODUCTION

1. The publisher for this copyrighted material is Elsevier. By clicking "accept" in connection with completing this licensing transaction, you agree that the following terms and conditions apply to this transaction (along with the Billing and Payment terms and conditions established by Copyright Clearance Center, Inc. ("CCC"), at the time that you opened your Rightslink account and that are available at any time at http://myaccount.copyright.com).

GENERAL TERMS

2. Elsevier hereby grants you permission to reproduce the aforementioned material subject to the terms and conditions indicated.

3. Acknowledgement: If any part of the material to be used (for example, figures) has appeared in our publication with credit or acknowledgement to another source, permission must also be sought from that source. If such permission is not obtained then that material may not be included in your publication/copies. Suitable acknowledgement to the source must be made, either as a footnote or in a reference list at the end of your publication, as follows:

"Reprinted from Publication title, Vol /edition number, Author(s), Title of article / title of chapter, Pages No., Copyright (Year), with permission from Elsevier [OR APPLICABLE SOCIETY COPYRIGHT OWNER]." Also Lancet special credit - "Reprinted from The Lancet, Vol. number, Author(s), Title of article, Pages No., Copyright (Year), with permission from Elsevier."

4. Reproduction of this material is confined to the purpose and/or media for which permission is hereby given.

5. Altering/Modifying Material: Not Permitted. However figures and illustrations may be altered/adapted minimally to serve your work. Any other abbreviations, additions, deletions and/or any other alterations shall be made only with prior written authorization of Elsevier Ltd. (Please contact Elsevier at permissions@elsevier.com). No modifications can be made to any Lancet figures/tables and they must be reproduced in full.

6. If the permission fee for the requested use of our material is waived in this instance, please be advised that your future requests for Elsevier materials may attract a fee.

7. Reservation of Rights: Publisher reserves all rights not specifically granted in the combination of (i) the license details provided by you and accepted in the course of this licensing transaction, (ii) these terms and conditions and (iii) CCC's Billing and Payment terms and conditions.

8. License Contingent Upon Payment: While you may exercise the rights licensed immediately upon issuance of the license at the end of the licensing process for the transaction, provided that you have disclosed complete and accurate details of your proposed use, no license is finally effective unless and until full payment is received from you (either by publisher or by CCC) as provided in CCC's Billing and Payment terms and conditions. If full payment is not received on a timely basis, then any license preliminarily granted shall be deemed automatically revoked and shall be void as if never granted. Further, in the event that you breach any of these terms and conditions or any of CCC's Billing and Payment terms and conditions, the license is automatically revoked and shall be void as if never granted. Use of materials as described in a revoked license, as well as any use of the materials beyond the scope of an unrevoked license, may constitute copyright infringement and publisher reserves the right to take any and all action to protect its copyright in the materials.
9. Warranties: Publisher makes no representations or warranties with respect to the licensed material.
10. Indemnity: You hereby indemnify and agree to hold harmless publisher and CCC, and their respective officers, directors, employees and agents, from and against any and all claims arising out of your use of the licensed material other than as specifically authorized pursuant to this license.
11. No Transfer of License: This license is personal to you and may not be sublicensed, assigned, or transferred by you to any other person without publisher's written permission.
12. No Amendment Except in Writing: This license may not be amended except in a writing signed by both parties (or, in the case of publisher, by CCC on publisher's behalf).
13. Objection to Contrary Terms: Publisher hereby objects to any terms contained in any purchase order, acknowledgment, check endorsement or other writing prepared by you, which terms are inconsistent with these terms and conditions or CCC's Billing and Payment terms and conditions. These terms and conditions, together with CCC's Billing and Payment terms and conditions (which are incorporated herein), comprise the entire agreement between you and publisher (and CCC) concerning this licensing transaction. In the event of any conflict between your obligations established by these terms and conditions and those established by CCC's Billing and Payment terms and conditions, these terms and conditions shall control.
14. Revocation: Elsevier or Copyright Clearance Center may deny the permissions described in this License at their sole discretion, for any reason or no reason, with a full refund payable to you. Notice of such denial will be made using the contact information provided by you. Failure to receive such notice will not alter or invalidate the denial. In no event will Elsevier or Copyright Clearance Center be responsible or liable for any costs, expenses or damage incurred by you as a result of a denial of your permission request, other than a refund of the amount(s) paid by you to Elsevier and/or Copyright Clearance Center for denied permissions.

LIMITED LICENSE

The following terms and conditions apply only to specific license types:

15. **Translation**: This permission is granted for non-exclusive world **English** rights only unless your license was granted for translation rights. If you licensed translation rights you may only translate this content into the languages you requested. A professional translator must perform all translations and reproduce the content word for word preserving the integrity of the article.
16. **Posting licensed content on any Website**: The following terms and conditions apply as follows: Licensing material from an Elsevier journal: All content posted to the web site must maintain the copyright information line on the bottom of each image; A hyper-text must be included to the Homepage of the journal from which you are licensing at http://www.sciencedirect.com/science/journal/xxxxx or the Elsevier homepage for books at http://www.elsevier.com; Central Storage: This license does not include permission for a scanned version of the material to be stored in a central repository such as that provided by Heron/XanEdu. Licensing material from an Elsevier book: A hyper-text link must be included to the Elsevier homepage at http://www.elsevier.com . All content posted to the web site must maintain the copyright information line on the bottom of each image.

Posting licensed content on Electronic reserve: In addition to the above the following clauses are applicable: The web site must be password-protected and made available only to bona fide students registered on a relevant course. This permission is granted for 1 year only. You may obtain a new license for future website posting.
17. **For journal authors:** the following clauses are applicable in addition to the above:
Preprints:
A preprint is an author's own write-up of research results and analysis, it has not been peer-reviewed, nor has it had any other value added to it by a publisher (such as formatting, copyright, technical enhancement etc.).
Authors can share their preprints anywhere at any time. Preprints should not be added to or enhanced in any way in order to appear more like, or to substitute for, the final versions of articles however authors can update their preprints on arXiv or RePEc with their Accepted Author Manuscript (see below).
If accepted for publication, we encourage authors to link from the preprint to their formal publication via its DOI. Millions of researchers have access to the formal publications on ScienceDirect, and so links will help users to find, access, cite and use the best available version. Please note that Cell Press, The Lancet and some society-owned have different preprint policies. Information on these policies is available on the journal homepage.
Accepted Author Manuscripts: An accepted author manuscript is the manuscript of an article that has been accepted for publication and which typically includes author-incorporated changes suggested during submission, peer review and editor-author communications.
Authors can share their accepted author manuscript:

- immediately
    - via their non-commercial person homepage or blog

    - by updating a preprint in arXiv or RePEc with the accepted manuscript
    - via their research institute or institutional repository for internal institutional uses or as part of an invitation-only research collaboration work-group
    - directly by providing copies to their students or to research collaborators for their personal use
    - for private scholarly sharing as part of an invitation-only work group on commercial sites with which Elsevier has an agreement
- After the embargo period
    - via non-commercial hosting platforms such as their institutional repository
    - via commercial sites with which Elsevier has an agreement

In all cases accepted manuscripts should:

- link to the formal publication via its DOI
- bear a CC-BY-NC-ND license - this is easy to do
- if aggregated with other manuscripts, for example in a repository or other site, be shared in alignment with our hosting policy not be added to or enhanced in any way to appear more like, or to substitute for, the published journal article.

Published journal article (JPA): A published journal article (PJA) is the definitive final record of published research that appears or will appear in the journal and embodies all value-adding publishing activities including peer review co-ordination, copy-editing, formatting, (if relevant) pagination and online enrichment.
Policies for sharing publishing journal articles differ for subscription and gold open access articles:
Subscription Articles: If you are an author, please share a link to your article rather than the full-text. Millions of researchers have access to the formal publications on ScienceDirect, and so links will help your users to find, access, cite, and use the best available version.
Theses and dissertations which contain embedded PJAs as part of the formal submission can be posted publicly by the awarding institution with DOI links back to the formal publications on ScienceDirect.
If you are affiliated with a library that subscribes to ScienceDirect you have additional private sharing rights for others' research accessed under that agreement. This includes use for classroom teaching and internal training at the institution (including use in course packs and courseware programs), and inclusion of the article for grant funding purposes.
Gold Open Access Articles: May be shared according to the author-selected end-user license and should contain a CrossMark logo, the end user license, and a DOI link to the formal publication on ScienceDirect.
Please refer to Elsevier's posting policy for further information.
18. **For book authors** the following clauses are applicable in addition to the above: Authors are permitted to place a brief summary of their work online only. You are not allowed to download and post the published

electronic version of your chapter, nor may you scan the printed edition to create an electronic version. **Posting to a repository:** Authors are permitted to post a summary of their chapter only in their institution's repository.

19. **Thesis/Dissertation**: If your license is for use in a thesis/dissertation your thesis may be submitted to your institution in either print or electronic form. Should your thesis be published commercially, please reapply for permission. These requirements include permission for the Library and Archives of Canada to supply single copies, on demand, of the complete thesis and include permission for Proquest/UMI to supply single copies, on demand, of the complete thesis. Should your thesis be published commercially, please reapply for permission. Theses and dissertations which contain embedded PJAs as part of the formal submission can be posted publicly by the awarding institution with DOI links back to the formal publications on ScienceDirect.

Elsevier Open Access Terms and Conditions

You can publish open access with Elsevier in hundreds of open access journals or in nearly 2000 established subscription journals that support open access publishing. Permitted third party re-use of these open access articles is defined by the author's choice of Creative Commons user license. See our open access license policy for more information.

Terms & Conditions applicable to all Open Access articles published with Elsevier:

Any reuse of the article must not represent the author as endorsing the adaptation of the article nor should the article be modified in such a way as to damage the author's honour or reputation. If any changes have been made, such changes must be clearly indicated.

The author(s) must be appropriately credited and we ask that you include the end user license and a DOI link to the formal publication on ScienceDirect.

If any part of the material to be used (for example, figures) has appeared in our publication with credit or acknowledgement to another source it is the responsibility of the user to ensure their reuse complies with the terms and conditions determined by the rights holder.

Additional Terms & Conditions applicable to each Creative Commons user license:

CC BY: The CC-BY license allows users to copy, to create extracts, abstracts and new works from the Article, to alter and revise the Article and to make commercial use of the Article (including reuse and/or resale of the Article by commercial entities), provided the user gives appropriate credit (with a link to the formal publication through the relevant DOI), provides a link to the license, indicates if changes were made and the licensor is not represented as endorsing the use made of the work. The full details of the license are available at http://creativecommons.org/licenses/by/4.0.

CC BY NC SA: The CC BY-NC-SA license allows users to copy, to create extracts, abstracts and new works from the Article, to alter and revise the Article, provided this is not done for commercial purposes, and that the user gives appropriate credit (with a link to the formal publication through

the relevant DOI), provides a link to the license, indicates if changes were made and the licensor is not represented as endorsing the use made of the work. Further, any new works must be made available on the same conditions. The full details of the license are available at http://creativecommons.org/licenses/by-nc-sa/4.0.
CC BY NC ND: The CC BY-NC-ND license allows users to copy and distribute the Article, provided this is not done for commercial purposes and further does not permit distribution of the Article if it is changed or edited in any way, and provided the user gives appropriate credit (with a link to the formal publication through the relevant DOI), provides a link to the license, and that the licensor is not represented as endorsing the use made of the work. The full details of the license are available at http://creativecommons.org/licenses/by-nc-nd/4.0. Any commercial reuse of Open Access articles published with a CC BY NC SA or CC BY NC ND license requires permission from Elsevier and will be subject to a fee.
Commercial reuse includes:

- Associating advertising with the full text of the Article
- Charging fees for document delivery or access
- Article aggregation
- Systematic distribution via e-mail lists or share buttons

Posting or linking by commercial companies for use by customers of those companies.

20. **Other Conditions**:

v1.9

Questions? customercare@copyright.com or +1-855-239-3415 (toll free in the US) or +1-978-646-2777.

References

Akella, J.S., D. Wloga, J. Kim, N.G. Starostina, S. Lyons-Abbott, N.S. Morrissette, S.T. Dougan, E.T. Kipreos, and J. Gaertig. 2010. MEC-17 is an α-tubulin acetyltransferase. *Nature*. 467:218–222. doi:10.1038/nature09324.

Al-Hajj, M., M.S. Wicha, A. Benito-Hernandez, S.J. Morrison, and M.F. Clarke. 2003. Prospective identification of tumorigenic breast cancer cells. *Proc. Natl. Acad. Sci.* 100:3983–3988. doi:10.1073/pnas.0530291100.

Alves-Cruzeiro, J.M. da C., R. Nogales-Cadenas, and A.D. Pascual-Montano. 2014. CentrosomeDB: a new generation of the centrosomal proteins database for *Human* and *Drosophila melanogaster*. *Nucleic Acids Res.* 42:D430–D436. doi:10.1093/nar/gkt1126.

Andersen, J.S., C.J. Wilkinson, T. Mayor, P. Mortensen, E.A. Nigg, and M. Mann. 2003. Proteomic characterization of the human centrosome by protein correlation profiling. *Nature*. 426:570–574. doi:10.1038/nature02166.

Anderson, C.T., and T. Stearns. 2009. Centriole age underlies asynchronous primary cilium growth in mammalian cells. *Curr. Biol.* 19:1498–502. doi:10.1016/j.cub.2009.07.034.

Arce, C.A., and H.S. Barra. 1983. Association of tubulinyl-tyrosine carboxypeptidase with microtubules. *FEBS Lett.* 157:75–78. doi:10.1016/0014-5793(83)81119-3.

Arnette, C., N. Efimova, X. Zhu, G.J. Clark, and I. Kaverina. 2014. Microtubule segment stabilization by RASSF1A is required for proper microtubule dynamics and Golgi integrity. *Mol. Biol. Cell*. 25:800–10. doi:10.1091/mbc.E13-07-0374.

Arquint, C., and E.A. Nigg. 2014. STIL Microcephaly Mutations Interfere with APC/C-Mediated Degradation and Cause Centriole Amplification. *Curr. Biol.* 24:351–360. doi:10.1016/J.CUB.2013.12.016.

Arrighi, N., K. Lypovetska, C. Moratal, S. Giorgetti-Peraldi, C.A. Dechesne, C. Dani, and P. Peraldi. 2017. The primary cilium is necessary for the differentiation and the maintenance of human adipose progenitors into myofibroblasts. *Sci. Rep.* 7:15248. doi:10.1038/s41598-017-15649-2.

Babst, M. 2011. MVB vesicle formation: ESCRT-dependent, ESCRT-independent and everything in between. *Curr. Opin. Cell Biol.* 23:452–7. doi:10.1016/j.ceb.2011.04.008.

Babst, M., D.J. Katzmann, E.J. Estepa-Sabal, T. Meerloo, and S.D. Emr. 2002. Escrt-III: an endosome-associated heterooligomeric protein complex required for mvb sorting. *Dev. Cell*. 3:271–82.

Bahe, S., Y.-D. Stierhof, C.J. Wilkinson, F. Leiss, and E.A. Nigg. 2005. Rootletin forms centriole-associated filaments and functions in centrosome cohesion. *J. Cell Biol.* 171:27–33. doi:10.1083/jcb.200504107.

Bai, H., N. Zhang, Y. Xu, Q. Chen, M. Khan, J.J. Potter, S.K. Nayar, T. Cornish, G. Alpini, S. Bronk, D. Pan, and R.A. Anders. 2012. Yes-associated protein regulates the hepatic response after bile duct ligation. *Hepatology*. 56:1097–1107. doi:10.1002/hep.25769.

Bakkenist, C.J., and M.B. Kastan. 2003. DNA damage activates ATM through intermolecular autophosphorylation and dimer dissociation. *Nature*. 421:499–506. doi:10.1038/nature01368.

Baksh, S., S. Tommasi, S. Fenton, V.C. Yu, L.M. Martins, G.P. Pfeifer, F. Latif, J. Downward, and B.G. Neel. 2005. The Tumor Suppressor RASSF1A and MAP-1 Link Death Receptor Signaling to Bax Conformational Change and Cell Death. *Mol. Cell*. 18:637–650. doi:10.1016/j.molcel.2005.05.010.

Bangs, F.K., N. Schrode, A.-K. Hadjantonakis, and K. V. Anderson. 2015. Lineage specificity of primary cilia in the mouse embryo. *Nat. Cell Biol.* 17:113–122. doi:10.1038/ncb3091.

Basiri, M.L., A. Ha, A. Chadha, N.M. Clark, A. Polyanovsky, B. Cook, and T. Avidor-Reiss. 2014. A Migrating Ciliary Gate Compartmentalizes the Site of Axoneme Assembly in Drosophila Spermatids. *Curr. Biol.* 24:2622–2631. doi:10.1016/j.cub.2014.09.047.

Basto, R., K. Brunk, T. Vinadogrova, N. Peel, A. Franz, A. Khodjakov, and J.W. Raff. 2008. Centrosome amplification can initiate tumorigenesis in flies. *Cell*. 133:1032–42. doi:10.1016/j.cell.2008.05.039.

Basto, R., J. Lau, T. Vinogradova, A. Gardiol, C.G. Woods, A. Khodjakov, and J.W. Raff. 2006. Flies without Centrioles. *Cell*. 125:1375–1386. doi:10.1016/j.cell.2006.05.025.

Ben-Porath, I., M.W. Thomson, V.J. Carey, R. Ge, G.W. Bell, A. Regev, and R.A. Weinberg. 2008. An embryonic stem cell–like gene expression signature in poorly differentiated aggressive human tumors. *Nat. Genet.* 40:499–507. doi:10.1038/ng.127.

van Beneden, E., and A. Neyt. 1887. Nouvelle recherches sur la fécondation et la division mitosique chez l'Ascaride mégalocéphale. *Bull. Acad. R. Belgique 3éme sér*. 14:215–295.

ten Berge, D., D. Kurek, T. Blauwkamp, W. Koole, A. Maas, E. Eroglu, R.K. Siu, and R. Nusse. 2011. Embryonic stem cells require Wnt proteins to prevent differentiation to epiblast stem cells. *Nat. Cell Biol.* 13:1070–1075. doi:10.1038/ncb2314.

Bergqvist, J., A. Latif, S.A. Roberts, K.D. Hadfield, F. Lalloo, A. Howell, D.G. Evans, and W.G. Newman. 2010. RASSF1A polymorphism in familial breast cancer. *Fam. Cancer*. 9:263–265. doi:10.1007/s10689-010-9335-8.

Bernstein, B.E., T.S. Mikkelsen, X. Xie, M. Kamal, D.J. Huebert, J. Cuff, B. Fry, A. Meissner, M. Wernig, K. Plath, R. Jaenisch, A. Wagschal, R. Feil, S.L. Schreiber, and E.S. Lander. 2006. A Bivalent Chromatin Structure Marks Key Developmental Genes in Embryonic Stem Cells. *Cell*. 125:315–326. doi:10.1016/j.cell.2006.02.041.

Betschinger, J., K. Mechtler, and J.A. Knoblich. 2003. The Par complex directs asymmetric cell division by phosphorylating the cytoskeletal protein Lgl. *Nature*. 422:326–330. doi:10.1038/nature01486.

Bettencourt-Dias, M., A. Rodrigues-Martins, L. Carpenter, M. Riparbelli, L. Lehmann, M.K. Gatt, N. Carmo, F. Balloux, G. Callaini, and D.M. Glover. 2005. SAK/PLK4 Is Required for Centriole Duplication and Flagella Development. *Curr. Biol.* 15:2199–2207. doi:10.1016/j.cub.2005.11.042.

Bhat, K.P.L., K.L. Salazar, V. Balasubramaniyan, K. Wani, L. Heathcock, F. Hollingsworth, J.D. James, J. Gumin, K.L. Diefes, S.H. Kim, A. Turski, Y. Azodi, Y. Yang, T. Doucette, H. Colman, E.P. Sulman, F.F. Lang, G. Rao, S. Copray, B.D. Vaillant, and K.D. Aldape. 2011. The transcriptional coactivator TAZ regulates mesenchymal differentiation in malignant glioma. *Genes Dev.* 25:2594–2609. doi:10.1101/gad.176800.111.

Bienkowska, D., and C.R. Cowan. 2012. Centrosomes Can Initiate a Polarity Axis from Any Position within One-Cell C. elegans Embryos. *Curr. Biol.* 22:583–589. doi:10.1016/J.CUB.2012.01.064.

Blachon, S., J. Gopalakrishnan, Y. Omori, A. Polyanovsky, A. Church, D. Nicastro, J. Malicki, and T. Avidor-Reiss. 2008. Drosophila asterless and Vertebrate Cep152 Are Orthologs Essential for Centriole Duplication. *Genetics*. 180:2081–2094. doi:10.1534/genetics.108.095141.

Blangy, A., H.A. Lane, P. D 'herin, M. Harper, M. Kress, and E.A. Nigg. 1995. Phosphorylation by ~34~~~~ Regulates Spindle Association of Human Eg5, a Kinesin-Related Motor Essential for Bipolar Spindle Formation In Vivo. *Cell*. 63:1159–169.

Bodle, J.C., C.D. Rubenstein, M.E. Phillips, S.H. Bernacki, J. Qi, A.J. Banes, and E.G. Loboa. 2013. Primary Cilia: The Chemical Antenna Regulating Human Adipose-Derived Stem Cell Osteogenesis. *PLoS One*. 8:e62554. doi:10.1371/journal.pone.0062554.

De Boer, L., V. Oakes, H. Beamish, N. Giles, F. Stevens, M. Somodevilla-Torres, C. DeSouza, and B. Gabrielli. 2008. Cyclin A/cdk2 coordinates centrosomal and nuclear mitotic events. *Oncogene*. 27:4261–4268. doi:10.1038/onc.2008.74.

Bonnet, D., and J.E. Dick. 1997. Human acute myeloid leukemia is organized as a hierarchy that originates from a primitive hematopoietic cell. *Nat. Med.* 3:730–7.

Boveri, T. 1887. Ueber den Antheil des Spermatozoon an der Teilung des Eies. *Sitzungsber. Ges. Morph. Physiol. München*. 3:151–164.

Brandt, R., R. Grützmann, A. Bauer, R. Jesnowski, J. Ringel, M. Löhr, C. Pilarsky, and J.D. Hoheisel. 2004. DNA microarray analysis of pancreatic malignancies. *Pancreatology*. 4:587–597. doi:10.1159/000082241.

van Breugel, M., M. Hirono, A. Andreeva, H. Yanagisawa, S. Yamaguchi, Y. Nakazawa, N. Morgner, M. Petrovich, I.-O. Ebong, C. V Robinson, C.M. Johnson, D. Veprintsev, and B. Zuber. 2011. Structures of SAS-6 suggest its organization in centrioles. *Science*. 331:1196–9. doi:10.1126/science.1199325.

Broekhuis, J.R., W.Y. Leong, and G. Jansen. 2013. Regulation of Cilium Length and

Intraflagellar Transport. *Int. Rev. Cell Mol. Biol.* 303:101–138. doi:10.1016/B978-0-12-407697-6.00003-9.

Bultje, R.S., D.R. Castaneda-Castellanos, L.Y. Jan, Y.-N. Jan, A.R. Kriegstein, and S.-H. Shi. 2009. Mammalian Par3 regulates progenitor cell asymmetric division via notch signaling in the developing neocortex. *Neuron*. 63:189–202. doi:10.1016/j.neuron.2009.07.004.

Čajánek, L., and E.A. Nigg. 2014. Cep164 triggers ciliogenesis by recruiting Tau tubulin kinase 2 to the mother centriole. *Proc. Natl. Acad. Sci. U. S. A.* 111:E2841-50. doi:10.1073/pnas.1401777111.

Campbell, P.K., K.G. Waymire, R.L. Heier, C. Sharer, D.E. Day, H. Reimann, J.M. Jaje, G.A. Friedrich, M. Burmeister, T.J. Bartness, L.D. Russell, L.J. Young, M. Zimmer, D.E. Jenne, and G.R. MacGregor. 2002. Mutation of a novel gene results in abnormal development of spermatid flagella, loss of intermale aggression and reduced body fat in mice. *Genetics*. 162:307–20.

Castresana, J. 2015. Cancer as a Ciliopathy: The Primary Cilium as a New Therapeutic Target. *J. Carcinog. Mutagen.* 6:1–3. doi:10.4172/2157-2518.1000e119.

Caussinus, E., and C. Gonzalez. 2005. Induction of tumor growth by altered stem-cell asymmetric division in Drosophila melanogaster. *Nat. Genet.* 37:1125–1129. doi:10.1038/ng1632.

Cevik, S., Y. Hori, O.I. Kaplan, K. Kida, T. Toivenon, C. Foley-Fisher, D. Cottell, T. Katada, K. Kontani, and O.E. Blacque. 2010. Joubert syndrome Arl13b functions at ciliary membranes and stabilizes protein transport in Caenorhabditis elegans. *J. Cell Biol.* 188:953–69. doi:10.1083/jcb.200908133.

Chalmers, A.D., K. Lachani, Y. Shin, V. Sherwood, K.W.Y. Cho, and N. Papalopulu. 2006. Grainyhead-like 3, a transcription factor identified in a microarray screen, promotes the specification of the superficial layer of the embryonic epidermis. *Mech. Dev.* 123:702–718. doi:10.1016/J.MOD.2006.04.006.

Chan, J.J., D. Flatters, F. Rodrigues-Lima, J. Yan, K. Thalassinos, and M. Katan. 2013. Comparative analysis of interactions of RASSF1-10. *Adv. Biol. Regul.* 53:190–201. doi:10.1016/j.jbior.2012.12.001.

Chang, J.C. 2016. Cancer stem cells. *Medicine (Baltimore).* 95:S20–S25. doi:10.1097/MD.0000000000004766.

Chiou, S.-H., M.-L. Wang, Y.-T. Chou, C.-J. Chen, C.-F. Hong, W.-J. Hsieh, H.-T. Chang, Y.-S. Chen, T.-W. Lin, H.-S. Hsu, and C.-W. Wu. 2010. Coexpression of Oct4 and Nanog enhances malignancy in lung adenocarcinoma by inducing cancer stem cell-like properties and epithelial-mesenchymal transdifferentiation. *Cancer Res.* 70:10433–44. doi:10.1158/0008-5472.CAN-10-2638.

Cizmecioglu, O., M. Arnold, R. Bahtz, F. Settele, L. Ehret, U. Haselmann-Weiß, C. Antony, and I. Hoffmann. 2010. Cep152 acts as a scaffold for recruitment of Plk4 and CPAP to the centrosome. *J. Cell Biol.* 191:731–739. doi:10.1083/jcb.201007107.

Clurman, B.E., R.J. Sheaff, K. Thress, M. Groudine, and J.M. Roberts. 1996. Turnover of

cyclin E by the ubiquitin-proteasome pathway is regulated by cdk2 binding and cyclin phosphorylation. *Genes Dev.* 10:1979–90. doi:10.1101/GAD.10.16.1979.

Colaluca, I.N., D. Tosoni, P. Nuciforo, F. Senic-Matuglia, V. Galimberti, G. Viale, S. Pece, and P.P. Di Fiore. 2008. NUMB controls p53 tumour suppressor activity. *Nature*. 451:76–80. doi:10.1038/nature06412.

Conduit, P.T., and J.W. Raff. 2010. Cnn dynamics drive centrosome size asymmetry to ensure daughter centriole retention in Drosophila neuroblasts. *Curr. Biol.* 20:2187–92. doi:10.1016/j.cub.2010.11.055.

Cooper, W.N., L.B. Hesson, D. Matallanas, A. Dallol, A. von Kriegsheim, R. Ward, W. Kolch, and F. Latif. 2009. RASSF2 associates with and stabilizes the proapoptotic kinase MST2. *Oncogene*. 28:2988–2998. doi:10.1038/onc.2009.152.

Cordenonsi, M., F. Zanconato, L. Azzolin, M. Forcato, A. Rosato, C. Frasson, M. Inui, M. Montagner, A.R. Parenti, A. Poletti, M.G. Daidone, S. Dupont, G. Basso, S. Bicciato, and S. Piccolo. 2011. The Hippo Transducer TAZ Confers Cancer Stem Cell-Related Traits on Breast Cancer Cells. *Cell*. 147:759–772. doi:10.1016/j.cell.2011.09.048.

Couturier, L., N. Vodovar, and F. Schweisguth. 2012. Endocytosis by Numb breaks Notch symmetry at cytokinesis. *Nat. Cell Biol.* 14:131–139. doi:10.1038/ncb2419.

Coverley, D., H. Laman, and R.A. Laskey. 2002. Distinct roles for cyclins E and A during DNA replication complex assembly and activation. *Nat. Cell Biol.* 4:523–528. doi:10.1038/ncb813.

Cowan, C.R., and A.A. Hyman. 2004. Centrosomes direct cell polarity independently of microtubule assembly in C. elegans embryos. *Nature*. 431:92–96. doi:10.1038/nature02825.

Cueva, J.G., J. Hsin, K.C. Huang, and M.B. Goodman. 2012. Posttranslational Acetylation of α-Tubulin Constrains Protofilament Number in Native Microtubules. *Curr. Biol.* 22:1066–1074. doi:10.1016/j.cub.2012.05.012.

D'Angiolella, V., V. Donato, S. Vijayakumar, A. Saraf, L. Florens, M.P. Washburn, B. Dynlacht, and M. Pagano. 2010. SCFCyclin F controls centrosome homeostasis and mitotic fidelity through CP110 degradation. *Nature*. 466:138–142. doi:10.1038/nature09140.

Dallol, A., A. Agathanggelou, S.L. Fenton, J. Ahmed-choudhury, L. Hesson, M.D. Vos, G.J. Clark, J. Downward, E.R. Maher, and F. Latif. 2004. RASSF1A Interacts with Microtubule-Associated Proteins and Modulates Microtubule Dynamics RASSF1A Interacts with Microtubule-Associated Proteins and Modulates Microtubule Dynamics. 4112–4116.

Dallol, A., L.B. Hesson, D. Matallanas, W.N. Cooper, E. O'Neill, E.R. Maher, W. Kolch, and F. Latif. 2009. RAN GTPase is a RASSF1A effector involved in controlling microtubule organization. *Curr. Biol.* 19:1227–32. doi:10.1016/j.cub.2009.05.064.

Dammann, R., C. Li, J.-H. Yoon, P.L. Chin, S. Bates, and G.P. Pfeifer. 2000. Epigenetic inactivation of a RAS association domain family protein from the lung tumour suppressor locus 3p21.3. *Nat Genet*. 25:315–319.

Dammann, R., U. Schagdarsurengin, L. Liu, N. Otto, O. Gimm, H. Dralle, B.O. Boehm, G.P. Pfeifer, and C. Hoang-Vu. 2003a. Frequent RASSF1A promoter hypermethylation and K-ras mutations in pancreatic carcinoma. *Oncogene*. 22:3806–3812. doi:10.1038/sj.onc.1206582.

Dammann, R., U. Schagdarsurengin, M. Strunnikova, M. Rastetter, C. Seidel, L. Liu, S. Tommasi, and G.P. Pfeifer. 2003b. Epigenetic inactivation of the Ras-association domain family 1 (RASSF1A) gene and its function in human carcinogenesis. *Histol. Histopathol.* 18:665–77.

Das, R.M., and K.G. Storey. 2014. Apical abscission alters cell polarity and dismantles the primary cilium during neurogenesis. *Science*. 343:200–4. doi:10.1126/science.1247521.

Deane, J.A., D.G. Cole, E.S. Seeley, D.R. Diener, and J.L. Rosenbaum. 2001. Localization of intraflagellar transport protein IFT52 identifies basal body transitional fibers as the docking site for IFT particles. *Curr. Biol.* 11:1586–90.

Delling, M., A.A. Indzhykulian, X. Liu, Y. Li, T. Xie, D.P. Corey, and D.E. Clapham. 2016. Primary cilia are not calcium-responsive mechanosensors. *Nature*. 531:656–660. doi:10.1038/nature17426.

Dho, S.E., J. Trejo, D.P. Siderovski, and C.J. McGlade. 2006. Dynamic regulation of mammalian numb by G protein-coupled receptors and protein kinase C activation: Structural determinants of numb association with the cortical membrane. *Mol. Biol. Cell*. 17:4142–55. doi:10.1091/mbc.E06-02-0097.

de Diego, A.S., A. Alonso Guerrero, C. Martínez-A, and K.H.M. van Wely. 2014. Dido3-dependent HDAC6 targeting controls cilium size. *Nat. Commun.* 5:3500. doi:10.1038/ncomms4500.

Djos, A., T. Martinsson, P. Kogner, and H. Carén. 2012. The RASSF gene family members RASSF5, RASSF6 and RASSF7 show frequent DNA methylation in neuroblastoma. *Mol. Cancer*. 11:40. doi:10.1186/1476-4598-11-40.

Dong, J., G. Feldmann, J. Huang, S. Wu, N. Zhang, S.A. Comerford, M.F. Gayyed, R.A. Anders, A. Maitra, and D. Pan. 2007. Elucidation of a Universal Size-Control Mechanism in Drosophila and Mammals. *Cell*. 130:1120–1133. doi:10.1016/j.cell.2007.07.019.

Donninger, H., J.A. Clark, M.K. Monaghan, M.L. Schmidt, M. Vos, and G.J. Clark. 2014. Cell cycle restriction is more important than apoptosis induction for RASSF1A protein tumor suppression. *J. Biol. Chem.* 289:31287–95. doi:10.1074/jbc.M114.609537.

Donninger, H., J. Clark, F. Rinaldo, N. Nelson, T. Barnoud, M.L. Schmidt, K.R. Hobbing, M.D. Vos, B. Sils, and G.J. Clark. 2015. The RASSF1A tumor suppressor regulates XPA-mediated DNA repair. *Mol Cell Biol*. 35:277–287. doi:10.1128/MCB.00202-14.

Donninger, H., M.D. Vos, and G.J. Clark. 2007. The RASSF1A tumor suppressor. *J. Cell Sci.* 120:3163–3172. doi:10.1242/jcs.010389.

Driessens, G., B. Beck, A. Caauwe, B.D. Simons, and C. Blanpain. 2012. Defining the mode

of tumour growth by clonal analysis. *Nature*. 488:527–530. doi:10.1038/nature11344.

Duan, C., M. Liu, J. Zhang, and R. Ma. 2013. RASSF1A: A potential novel therapeutic target against cardiac hypertrophy. *Prog. Biophys. Mol. Biol.* 113:284–288. doi:10.1016/j.pbiomolbio.2013.07.004.

Dulić, V., E. Lees, and S.I. Reed. 1992. Association of human cyclin E with a periodic G1-S phase protein kinase. *Science*. 257:1958–61. doi:10.1126/SCIENCE.1329201.

Dylewski, D.P., and T.W. Keenan. 1984. Centrioles in the mammary epithelium of the rat. *J. Cell Sci.* 72.

Dzhindzhev, N.S., Q.D. Yu, K. Weiskopf, G. Tzolovsky, I. Cunha-Ferreira, M. Riparbelli, A. Rodrigues-Martins, M. Bettencourt-Dias, G. Callaini, and D.M. Glover. 2010. Asterless is a scaffold for the onset of centriole assembly. *Nature*. 467:714–718. doi:10.1038/nature09445.

Elbediwy, A., Z.I. Vincent-Mistiaen, B. Spencer-Dene, R.K. Stone, S. Boeing, S.K. Wculek, J. Cordero, E.H. Tan, R. Ridgway, V.G. Brunton, E. Sahai, H. Gerhardt, A. Behrens, I. Malanchi, O.J. Sansom, and B.J. Thompson. 2016. Integrin signalling regulates YAP and TAZ to control skin homeostasis. *Development*. 143:1674–1687. doi:10.1242/dev.133728.

Emoto, K., Y. Masugi, K. Yamazaki, K. Effendi, H. Tsujikawa, M. Tanabe, Y. Kitagawa, and M. Sakamoto. 2014. Presence of primary cilia in cancer cells correlates with prognosis of pancreatic ductal adenocarcinoma. *Hum. Pathol.* 45:817–25. doi:10.1016/j.humpath.2013.11.017.

Estrabaud, E., I. Lassot, G. Blot, E. Le Rouzic, V. Tanchou, E. Quemeneur, L. Daviet, F. Margottin-Goguet, and R. Benarous. 2007. RASSF1C, an Isoform of the Tumor Suppressor RASSF1A, Promotes the Accumulation of -Catenin by Interacting with TrCP. *Cancer Res.* 67:1054–1061. doi:10.1158/0008-5472.CAN-06-2530.

Evans, M.J., and M.H. Kaufman. 1981. Establishment in culture of pluripotential cells from mouse embryos. *Nature*. 292:154–6.

Evans, T., and G. Felsenfeld. 1989. The erythroid-specific transcription factor Eryf1: a new finger protein. *Cell*. 58:877–85.

Feldman, J.L., and J.R. Priess. 2012. A Role for the Centrosome and PAR-3 in the Hand-Off of MTOC Function during Epithelial Polarization. *Curr. Biol.* 22:575–582. doi:10.1016/J.CUB.2012.02.044.

Feng, Z., A. Caballe, A. Wainman, S. Johnson, A.F.M. Haensele, M.A. Cottee, P.T. Conduit, S.M. Lea, and J.W. Raff. 2017. Structural Basis for Mitotic Centrosome Assembly in Flies. *Cell*. 169:1078–1089.e13. doi:10.1016/j.cell.2017.05.030.

Fernandez-L, A., P.A. Northcott, J. Dalton, C. Fraga, D. Ellison, S. Angers, M.D. Taylor, and A.M. Kenney. 2009. YAP1 is amplified and up-regulated in hedgehog-associated medulloblastomas and mediates Sonic hedgehog-driven neural precursor proliferation. *Genes Dev.* 23:2729–41. doi:10.1101/gad.1824509.

Font-Burgada, J., B. Sun, and M. Karin. 2016. Obesity and Cancer: The Oil that Feeds the Flame. *Cell Metab.* 23:48–62. doi:10.1016/J.CMET.2015.12.015.

Frank, V., S. Habbig, M.P. Bartram, T. Eisenberger, H.E. Veenstra-Knol, C. Decker, R.A.C. Boorsma, H. Göbel, G. Nürnberg, A. Griessmann, M. Franke, L. Borgal, P. Kohli, L.A. Völker, J. Dötsch, P. Nürnberg, T. Benzing, H.J. Bolz, C. Johnson, E.H. Gerkes, B. Schermer, and C. Bergmann. 2013. Mutations in NEK8 link multiple organ dysplasia with altered Hippo signalling and increased c-MYC expression. *Hum. Mol. Genet.* 22:2177–2185. doi:10.1093/hmg/ddt070.

Friess, H., J. Ding, J. Kleeff, L. Fenkell, J.A. Rosinski, A. Guweidhi, J.F. Reidhaar-Olson, M. Korc, J. Hammer, and M.W. Büchler. 2003. Microarray-based identification of differentially expressed growth- and metastasis-associated genes in pancreatic cancer. *Cell. Mol. Life Sci. C.* 60:1180–1199. doi:10.1007/s00018-003-3036-5.

Frise, E., J.A. Knoblich, S. Younger-shepherd, L.Y. Jan, and Y. Nung Jan. 1996. The Drosophila Numb protein inhibits signaling of the Notch receptor during cell-cell interaction in sensory organ lineage. *Neurobiology*. 93:11925–11932.

Fruman, D.A., H. Chiu, B.D. Hopkins, S. Bagrodia, L.C. Cantley, and R.T. Abraham. 2017. The PI3K Pathway in Human Disease. doi:10.1016/j.cell.2017.07.029.

Fruman, D.A., and C. Rommel. 2014. PI3K and cancer: lessons, challenges and opportunities. *Nat. Rev. Drug Discov.* 13:140–56. doi:10.1038/nrd4204.

Fu, J., M. Bian, Q. Jiang, and C. Zhang. 2007. Roles of Aurora Kinases in Mitosis and Tumorigenesis. *Mol. Cancer Res.* . 5:1–10. doi:10.1158/1541-7786.MCR-06-0208.

Fu, W., P. Asp, B. Canter, and B.D. Dynlacht. 2014. Primary cilia control hedgehog signaling during muscle differentiation and are deregulated in rhabdomyosarcoma. *Proc. Natl. Acad. Sci.* 111:9151–9156. doi:10.1073/pnas.1323265111.

Fukasawa, K., T. Choi, R. Kuriyama, S. Rulong, and G.F. Vande Woude. 1996. Abnormal centrosome amplification in the absence of p53. *Science*. 271:1744–7.

Gadadhar, S., S. Bodakuntla, K. Natarajan, and C. Janke. 2017a. The tubulin code at a glance. *J. Cell Sci.* 130:1347–1353. doi:10.1242/jcs.199471.

Gadadhar, S., H. Dadi, S. Bodakuntla, A. Schnitzler, I. Bièche, F. Rusconi, and C. Janke. 2017b. Tubulin glycylation controls primary cilia length. *J. Cell Biol.* 216:2701–2713. doi:10.1083/jcb.201612050.

Ganem, N.J., S.A. Godinho, and D. Pellman. 2009. A mechanism linking extra centrosomes to chromosomal instability. *Nature*. 460:278–282. doi:10.1038/nature08136.

Gao, B.N., X.J. Xie, C.X. Huang, D.S. Shames, T.T.L. Chen, C.M. Lewis, A.H. Bian, B.F. Zhang, O.I. Olopade, J.E. Garber, D.M. Euhus, G.E. Tomlinson, and J.D. Minna. 2008. RASSF1A polymorphism A133S is associated with early onset breast cancer in BRCA1/2 mutation carriers. *Cancer Res*. 68:22–25. doi:10.1158/0008-5472.Can-07-5183.

Garcia-Gonzalo, F.R., K.C. Corbit, M.S. Sirerol-Piquer, G. Ramaswami, E.A. Otto, T.R.

Noriega, A.D. Seol, J.F. Robinson, C.L. Bennett, D.J. Josifova, J.M. García-Verdugo, N. Katsanis, F. Hildebrandt, and J.F. Reiter. 2011. A transition zone complex regulates mammalian ciliogenesis and ciliary membrane composition. *Nat. Genet.* 43:776–784. doi:10.1038/ng.891.

Ginestier, C., M.H. Hur, E. Charafe-Jauffret, F. Monville, J. Dutcher, M. Brown, J. Jacquemier, P. Viens, C.G. Kleer, S. Liu, A. Schott, D. Hayes, D. Birnbaum, M.S. Wicha, and G. Dontu. 2007. ALDH1 Is a Marker of Normal and Malignant Human Mammary Stem Cells and a Predictor of Poor Clinical Outcome. *Cell Stem Cell*. 1:555–567. doi:10.1016/J.STEM.2007.08.014.

Giovinazzi, S., C.R. Lindsay, V.M. Morozov, E. Escobar-Cabrera, M.K. Summers, H.S. Han, L.P. McIntosh, and a M. Ishov. 2012. Regulation of mitosis and taxane response by Daxx and Rassf1. *Oncogene*. 31:13–26. doi:10.1038/onc.2011.211.

Glotzer, M., A.W. Murray, and M.W. Kirschner. 1991. Cyclin is degraded by the ubiquitin pathway. *Nature*. 349:132–138. doi:10.1038/349132a0.

Goetz, S.C., and K. V Anderson. 2010. The primary cilium: a signalling centre during vertebrate development. *Nat Rev Genet*. 11:331–344.

Golsteyn, R.M., K.E. Mundt, A.M. Fry, and E.A. Nigg. 1995. Cell cycle regulation of the activity and subcellular localization of Plk1, a human protein kinase implicated in mitotic spindle function. *J. Cell Biol.* 129:1617–28.

Gómez-López, S., R.G. Lerner, and C. Petritsch. 2014. Asymmetric cell division of stem and progenitor cells during homeostasis and cancer. *Cell. Mol. Life Sci.* 71:575–97. doi:10.1007/s00018-013-1386-1.

Gonçalves, J., and L. Pelletier. 2017. The Ciliary Transition Zone: Finding the Pieces and Assembling the Gate. *Mol. Cells*. 40:243–253. doi:10.14348/molcells.2017.0054.

Gopalan, G., C.S. Chan, and P.J. Donovan. 1997. A novel mammalian, mitotic spindle-associated kinase is related to yeast and fly chromosome segregation regulators. *J. Cell Biol.* 138:643–56.

Gould, R.R., and G.G. Borisy. 1977. The pericentriolar material in Chinese hamster ovary cells nucleates microtubule formation. *J. Cell Biol.* 73:601–15. doi:10.1083/JCB.73.3.601.

Graser, S., Y.-D. Stierhof, S.B. Lavoie, O.S. Gassner, S. Lamla, M. Le Clech, and E.A. Nigg. 2007a. Cep164, a novel centriole appendage protein required for primary cilium formation. *J. Cell Biol.* 179:321–30. doi:10.1083/jcb.200707181.

Graser, S., Y.-D. Stierhof, and E.A. Nigg. 2007b. Cep68 and Cep215 (Cdk5rap2) are required for centrosome cohesion. *J. Cell Sci.* 120:4321–4331. doi:10.1242/jcs.020248.

Grawenda, A.M., and E. O'Neill. 2015. Clinical utility of RASSF1A methylation in human malignancies. *Br. J. Cancer*. 113:372–81. doi:10.1038/bjc.2015.221.

Grote, H.J., V. Schmiemann, H. Geddert, A. Bocking, R. Kappes, H.E. Gabbert, and M. Sarbia. 2006. Methylation of RAS association domain family protein 1A as a

biomarker of lung cancer. *Cancer*. 108:129–134. doi:10.1002/cncr.21717.

Gulsen, T., I. Hadjicosti, Y. Li, X. Zhang, P.R. Whitley, and A.D. Chalmers. 2016. Truncated RASSF7 promotes centrosomal defects and cell death. *Dev. Biol.* 409:502–517. doi:10.1016/j.ydbio.2015.11.001.

Guo, C., S. Tommasi, L. Liu, J.-K. Yee, R. Dammann, and G.P. Pfeifer. 2007. RASSF1A is part of a complex similar to the Drosophila Hippo/Salvador/Lats tumor-suppressor network. *Curr. Biol.* 17:700–5. doi:10.1016/j.cub.2007.02.055.

Habbig, S., M.P. Bartram, R.U. Müller, R. Schwarz, N. Andriopoulos, S. Chen, J.G. Sägmüller, M. Hoehne, V. Burst, M.C. Liebau, H.C. Reinhardt, T. Benzing, and B. Schermer. 2011. NPHP4, a cilia-associated protein, negatively regulates the Hippo pathway. *J. Cell Biol.* 193:633–42. doi:10.1083/jcb.201009069.

Habedanck, R., Y.-D. Stierhof, C.J. Wilkinson, and E.A. Nigg. 2005. The Polo kinase Plk4 functions in centriole duplication. *Nat. Cell Biol.* 7:1140–1146. doi:10.1038/ncb1320.

Habib, S.J., B.-C. Chen, F.-C. Tsai, K. Anastassiadis, T. Meyer, E. Betzig, and R. Nusse. 2013. A localized Wnt signal orients asymmetric stem cell division in vitro. *Science*. 339:1445–8. doi:10.1126/science.1231077.

Haggarty, S.J., K.M. Koeller, J.C. Wong, C.M. Grozinger, and S.L. Schreiber. 2003. Domain-selective small-molecule inhibitor of histone deacetylase 6 (HDAC6)-mediated tubulin deacetylation. *Proc. Natl. Acad. Sci. U. S. A.* 100:4389–94. doi:10.1073/pnas.0430973100.

Hamilton, G., K.S. Yee, S. Scrace, and E. O'Neill. 2009. ATM regulates a RASSF1A-dependent DNA damage response. *Curr Biol*. 19:2020–2025. doi:10.1016/j.cub.2009.10.040.

Han, Y.-G., H.J. Kim, A.A. Dlugosz, D.W. Ellison, R.J. Gilbertson, and A. Alvarez-Buylla. 2009. Dual and opposing roles of primary cilia in medulloblastoma development. *Nat. Med.* 15:1062–1065. doi:10.1038/nm.2020.

Hanahan, D., and R.A. Weinberg. 2011. Hallmarks of cancer: The next generation. *Cell*. 144:646–674.

Hannak, E., M. Kirkham, A.A. Hyman, and K. Oegema. 2001. Aurora-A kinase is required for centrosome maturation in Caenorhabditis elegans. *J. Cell Biol.* 155:1109–16. doi:10.1083/jcb.200108051.

Harvey, K.F., C.M. Pfleger, and I.K. Hariharan. 2003. The Drosophila Mst Ortholog, hippo, Restricts Growth and Cell Proliferation and Promotes Apoptosis. *Cell*. 114:457–467. doi:10.1016/S0092-8674(03)00557-9.

Hatch, E.M., A. Kulukian, A.J. Holland, D.W. Cleveland, and T. Stearns. 2010. Cep152 interacts with Plk4 and is required for centriole duplication. *J. Cell Biol.* 191:721–9. doi:10.1083/jcb.201006049.

Hermann, P.C., S.L. Huber, T. Herrler, A. Aicher, J.W. Ellwart, M. Guba, C.J. Bruns, and C. Heeschen. 2007. Distinct Populations of Cancer Stem Cells Determine Tumor

Growth and Metastatic Activity in Human Pancreatic Cancer. *Cell Stem Cell*. 1:313–323. doi:10.1016/J.STEM.2007.06.002.

Hesson, L.B., W.N. Cooper, and F. Latif. 2007. The role of RASSF1A methylation in cancer. *Dis Markers*. 23. doi:10.1155/2007/291538.

Hochedlinger, K., Y. Yamada, C. Beard, and R. Jaenisch. 2005. Ectopic Expression of Oct-4 Blocks Progenitor-Cell Differentiation and Causes Dysplasia in Epithelial Tissues. *Cell*. 121:465–477. doi:10.1016/j.cell.2005.02.018.

Hong, J.-H., E.S. Hwang, M.T. McManus, A. Amsterdam, Y. Tian, R. Kalmukova, E. Mueller, T. Benjamin, B.M. Spiegelman, P.A. Sharp, N. Hopkins, and M.B. Yaffe. 2005. TAZ, a Transcriptional Modulator of Mesenchymal Stem Cell Differentiation. *Science (80-.).* 309:1074–1078. doi:10.1126/science.1110955.

Hornick, J.E., C.C. Mader, E.K. Tribble, C.C. Bagne, K.T. Vaughan, S.L. Shaw, and E.H. Hinchcliffe. 2011. Amphiastral Mitotic Spindle Assembly in Vertebrate Cells Lacking Centrosomes. *Curr. Biol.* 21:598–605. doi:10.1016/j.cub.2011.02.049.

Howes, S.C., G.M. Alushin, T. Shida, M. V Nachury, and E. Nogales. 2014. Effects of tubulin acetylation and tubulin acetyltransferase binding on microtubule structure. *Mol. Biol. Cell*. 25:257–66. doi:10.1091/mbc.E13-07-0387.

Huang, M.E., Y.C. Ye, S.R. Chen, J.R. Chai, J.X. Lu, L. Zhoa, L.J. Gu, and Z.Y. Wang. 1988. Use of all-trans retinoic acid in the treatment of acute promyelocytic leukemia. *Blood*. 72:567–72.

Huang, Z., J. Hu, J. Pan, Y. Wang, G. Hu, J. Zhou, L. Mei, and W.-C. Xiong. 2016. YAP stabilizes SMAD1 and promotes BMP2-induced neocortical astrocytic differentiation. *Development*. 143:2398–2409. doi:10.1242/dev.130658.

Huangfu, D., A. Liu, A.S. Rakeman, N.S. Murcia, L. Niswander, and K. V. Anderson. 2003. Hedgehog signalling in the mouse requires intraflagellar transport proteins. *Nature*. 426:83–87. doi:10.1038/nature02061.

Hubbert, C., A. Guardiola, R. Shao, Y. Kawaguchi, A. Ito, A. Nixon, M. Yoshida, X.-F. Wang, and T.-P. Yao. 2002. HDAC6 is a microtubule-associated deacetylase. *Nature*. 417:455–458. doi:10.1038/417455a.

Hung, J., Y. Kishimoto, K. Sugio, A. Virmani, D.D. McIntire, J.D. Minna, and A.F. Gazdar. 1995. Allele-specific chromosome 3p deletions occur at an early stage in the pathogenesis of lung carcinoma. *JAMA*. 273:558–63.

Hurt, E.M., B.T. Kawasaki, G.J. Klarmann, S.B. Thomas, and W.L. Farrar. 2008. CD44+CD24− prostate cells are early cancer progenitor/stem cells that provide a model for patients with poor prognosis. *Br. J. Cancer*. 98:756–765. doi:10.1038/sj.bjc.6604242.

Ito, T., H.Y. Kwon, B. Zimdahl, K.L. Congdon, J. Blum, W.E. Lento, C. Zhao, A. Lagoo, G. Gerrard, L. Foroni, J. Goldman, H. Goh, S.-H. Kim, D.-W. Kim, C. Chuah, V.G. Oehler, J.P. Radich, C.T. Jordan, and T. Reya. 2010. Regulation of myeloid leukaemia by the cell-fate determinant Musashi. *Nature*. 466:765–768. doi:10.1038/nature09171.

Izumi, H., and Y. Kaneko. 2012. Evidence of asymmetric cell division and centrosome inheritance in human neuroblastoma cells. *Proc. Natl. Acad. Sci. U. S. A.* 109:18048–53. doi:10.1073/pnas.1205525109.

Jackman, M., C. Lindon, E.A. Nigg, and J. Pines. 2003. Active cyclin B1–Cdk1 first appears on centrosomes in prophase. *Nat. Cell Biol.* 5:143–148. doi:10.1038/ncb918.

James, T.C., and S.C. Elgin. 1986. Identification of a nonhistone chromosomal protein associated with heterochromatin in Drosophila melanogaster and its gene. *Mol. Cell. Biol.* 6:3862–72.

Janke, C., K. Rogowski, D. Wloga, C. Regnard, A. V Kajava, J.-M. Strub, N. Temurak, J. van Dijk, D. Boucher, A. van Dorsselaer, S. Suryavanshi, J. Gaertig, and B. Eddé. 2005. Tubulin Polyglutamylase Enzymes Are Members of the TTL Domain Protein Family. *Science (80-.).* 308:1758–1762. doi:10.1126/science.1113010.

Januschke, J., S. Llamazares, J. Reina, and C. Gonzalez. 2011. Drosophila neuroblasts retain the daughter centrosome. *Nat. Commun.* 2:243. doi:10.1038/ncomms1245.

Jerónimo, C., R. Henrique, M.O. Hoque, E. Mambo, F.R. Ribeiro, G. Varzim, J. Oliveira, M.R. Teixeira, C. Lopes, and D. Sidransky. 2004. A quantitative promoter methylation profile of prostate cancer. *Clin. Cancer Res.* 10:8472–8. doi:10.1158/1078-0432.CCR-04-0894.

Jin, X., X. Jin, and H. Kim. 2017. Cancer stem cells and differentiation therapy. *Tumor Biol.* 39:101042831772993. doi:10.1177/1010428317729933.

Jones, C., V.C. Roper, I. Foucher, D. Qian, B. Banizs, C. Petit, B.K. Yoder, and P. Chen. 2008. Ciliary proteins link basal body polarization to planar cell polarity regulation. *Nat. Genet.* 40:69–77. doi:10.1038/ng.2007.54.

Jung, H.-Y., J.S. Jung, Y.M. Whang, and Y.H. Kim. 2013. RASSF1A Suppresses Cell Migration through Inactivation of HDAC6 and Increase of Acetylated alpha-Tubulin. *Cancer Res. Treat.* 45:134–144. doi:10.4143/crt.2013.45.2.134.

Jung Hae-Yun Jung Jun Seok, W.Y.M.K.Y.H. 2013. RASSF1A Suppresses Cell Migration through Inactivation of HDAC6 and Increase of Acetylated alpha-Tubulin. *Cancer Res Treat*. 45:134–144. doi:10.4143/crt.2013.45.2.134.

Kalebic, N., S. Sorrentino, E. Perlas, G. Bolasco, C. Martinez, and P.A. Heppenstall. 2013. αTAT1 is the major α-tubulin acetyltransferase in mice. *Nat. Commun.* 4:1962. doi:10.1038/ncomms2962.

Kanzaki, H., H. Hanafusa, H. Yamamoto, Y. Yasuda, K. Imai, M. Yano, M. Aoe, N. Shimizu, K. Nakachi, M. Ouchida, and K. Shimizu. 2006. Single nucleotide polymorphism at codon 133 of the RASSF1 gene is preferentially associated with human lung adenocarcinoma risk. *Cancer Lett*. 238:128–134. doi:10.1016/j.canlet.2005.07.006.

Kaverina, I., and A. Straube. 2011. Regulation of cell migration by dynamic microtubules. *Semin. Cell Dev. Biol.* 22:968–74. doi:10.1016/j.semcdb.2011.09.017.

Khayyeri, H., S. Barreto, and D. Lacroix. 2015. Primary cilia mechanics affects cell mechanosensation: A computational study. *J. Theor. Biol.* 379:38–46.

doi:10.1016/J.JTBI.2015.04.034.

Khodjakov, A., R.W. Cole, B.R. Oakley, and C.L. Rieder. 2000. Centrosome-independent mitotic spindle formation in vertebrates. *Curr. Biol.* 10:59–67.

Kim, G.-W., L. Li, M. Gorbani, L. You, and X.-J. Yang. 2013a. Mice lacking α-tubulin acetyltransferase 1 are viable but display α-tubulin acetylation deficiency and dentate gyrus distortion. *J. Biol. Chem.* 288:20334–50. doi:10.1074/jbc.M113.464792.

Kim, J., H. Jo, H. Hong, M.H. Kim, J.M. Kim, J.-K. Lee, W. Do Heo, and J. Kim. 2015a. Actin remodelling factors control ciliogenesis by regulating YAP/TAZ activity and vesicle trafficking. *Nat. Commun.* 6. doi:10.1038/ncomms7781.

Kim, M., M. Kim, M.-S. Lee, C.-H. Kim, and D.-S. Lim. 2014. The MST1/2-SAV1 complex of the Hippo pathway promotes ciliogenesis. 5:5370.

Kim, S., K. Lee, J.-H. Choi, N. Ringstad, and B.D. Dynlacht. 2015b. Nek2 activation of Kif24 ensures cilium disassembly during the cell cycle. *Nat. Commun.* 6:8087. doi:10.1038/ncomms9087.

Kim, T.-S., J.-E. Park, A. Shukla, S. Choi, R.N. Murugan, J.H. Lee, M. Ahn, K. Rhee, J.K. Bang, B.Y. Kim, J. Loncarek, R.L. Erikson, and K.S. Lee. 2013b. Hierarchical recruitment of Plk4 and regulation of centriole biogenesis by two centrosomal scaffolds, Cep192 and Cep152. *Proc. Natl. Acad. Sci.* 110:E4849–E4857. doi:10.1073/pnas.1319656110.

Kimble, J.E., and J.G. White. 1981. On the control of germ cell development in Caenorhabditis elegans. *Dev. Biol.* 81:208–219. doi:10.1016/0012-1606(81)90284-0.

King, R.W., J.-M. Peters, S. Tugendreich, M. Rolfe, P. Hieter, and M.W. Kirschner. 1995. A 20s complex containing CDC27 and CDC16 catalyzes the mitosis-specific conjugation of ubiquitin to cyclin B. *Cell*. 81:279–288. doi:10.1016/0092-8674(95)90338-0.

Kiprilov, E.N., A. Awan, R. Desprat, M. Velho, C.A. Clement, A.G. Byskov, C.Y. Andersen, P. Satir, E.E. Bouhassira, S.T. Christensen, and R.E. Hirsch. 2008. Human embryonic stem cells in culture possess primary cilia with hedgehog signaling machinery. *J. Cell Biol.* 180:897–904. doi:10.1083/jcb.200706028.

Kitagawa, D., I. Vakonakis, N. Olieric, M. Hilbert, D. Keller, V. Olieric, M. Bortfeld, M.C. Erat, I. Flückiger, P. Gönczy, and M.O. Steinmetz. 2011. Structural Basis of the 9-Fold Symmetry of Centrioles. *Cell*. 144:364–375. doi:10.1016/j.cell.2011.01.008.

Klajic, J., T. Fleischer, E. Dejeux, H. Edvardsen, F. Warnberg, I. Bukholm, P.E. Lønning, H. Solvang, A.-L. Børresen-Dale, J. Tost, and V.N. Kristensen. 2013. Quantitative DNA methylation analyses reveal stage dependent DNA methylation and association to clinico-pathological factors in breast tumors. *BMC Cancer*. 13:456. doi:10.1186/1471-2407-13-456.

Kok, K., S.L. Naylor, and C.H. Buys. 1997. Deletions of the short arm of chromosome 3 in solid tumors and the search for suppressor genes. *Adv. Cancer Res.* 71:27–92.

Kolch, W., G. Heidecker, P. Lloyd, and U.R. Rapp. 1991. Raf-1 protein kinase is required for growth of induced NIH/3T3 cells. *Nature*. 349:426–428. doi:10.1038/349426a0.

Konno, A., K. Ikegami, Y. Konishi, H.-J. Yang, M. Abe, M. Yamazaki, K. Sakimura, I. Yao, K. Shiba, K. Inaba, and M. Setou. 2016. Ttll9-/- mice sperm flagella show shortening of doublet 7, reduction of doublet 5 polyglutamylation and a stall in beating. *J. Cell Sci.* 129:2757–66. doi:10.1242/jcs.185983.

Kotlyar, M., C. Pastrello, F. Pivetta, A. Lo Sardo, C. Cumbaa, H. Li, T. Naranian, Y. Niu, Z. Ding, F. Vafaee, F. Broackes-Carter, J. Petschnigg, G.B. Mills, A. Jurisicova, I. Stagljar, R. Maestro, and I. Jurisica. 2015. In silico prediction of physical protein interactions and characterization of interactome orphans. *Nat. Methods*. 12:79–84. doi:10.1038/nmeth.3178.

Kourmouli, N., P.A. Theodoropoulos, G. Dialynas, A. Bakou, A.S. Politou, I.G. Cowell, P.B. Singh, and S.D. Georgatos. 2000. Dynamic associations of heterochromatin protein 1 with the nuclear envelope. *EMBO J.* 19:6558–6568. doi:10.1093/emboj/19.23.6558.

Kozminski, K.G., K.A. Johnson, P. Forscher, and J.L. Rosenbaum. 1993. A motility in the eukaryotic flagellum unrelated to flagellar beating. *Proc. Natl. Acad. Sci. U. S. A.* 90:5519–23.

Lánczky, A., Á. Nagy, G. Bottai, G. Munkácsy, A. Szabó, L. Santarpia, and B. Győrffy. 2016. miRpower: a web-tool to validate survival-associated miRNAs utilizing expression data from 2178 breast cancer patients. *Breast Cancer Res. Treat.* 160:439–446. doi:10.1007/s10549-016-4013-7.

Lapidot, T., C. Sirard, J. Vormoor, B. Murdoch, T. Hoang, J. Caceres-Cortes, M. Minden, B. Paterson, M.A. Caligiuri, and J.E. Dick. 1994. A cell initiating human acute myeloid leukaemia after transplantation into SCID mice. *Nature*. 367:645–648. doi:10.1038/367645a0.

Lathia, J.D., S.C. Mack, E.E. Mulkearns-Hubert, C.L.L. Valentim, and J.N. Rich. 2015. Cancer stem cells in glioblastoma. *Genes Dev.* 29:1203–17. doi:10.1101/gad.261982.115.

Lawrence, M.S., P. Stojanov, C.H. Mermel, J.T. Robinson, L.A. Garraway, T.R. Golub, M. Meyerson, S.B. Gabriel, E.S. Lander, and G. Getz. 2014. Discovery and saturation analysis of cancer genes across 21 tumour types. *Nature*. 505:495–501. doi:10.1038/nature12912.

Lee, D.-H., J.O. Park, T.-S. Kim, S.-K. Kim, T. Kim, M. Kim, G.S. Park, J.-H. Kim, S. Kuninaka, E.N. Olson, H. Saya, S.-Y. Kim, H. Lee, and D.-S. Lim. 2016. LATS-YAP/TAZ controls lineage specification by regulating TGFβ signaling and Hnf4α expression during liver development. *Nat. Commun.* 7:11961. doi:10.1038/ncomms11961.

Lee, J.-H., T.-S. Kim, T.-H. Yang, B.-K. Koo, S.-P. Oh, K.-P. Lee, H.-J. Oh, S.-H. Lee, Y.-Y. Kong, J.-M. Kim, and D.-S. Lim. 2008. A crucial role of WW45 in developing epithelial tissues in the mouse. *EMBO J.* 27:1231–1242. doi:10.1038/emboj.2008.63.

Leicht, D.T., V. Balan, A. Kaplun, V. Singh-Gupta, L. Kaplun, M. Dobson, and G. Tzivion.

2007. Raf kinases: Function, regulation and role in human cancer. *Biochim. Biophys. Acta - Mol. Cell Res.* 1773:1196–1212. doi:https://doi.org/10.1016/j.bbamcr.2007.05.001.

Lerman, M.I., and J.D. Minna. 2000. The 630-kb lung cancer homozygous deletion region on human chromosome 3p21.3: identification and evaluation of the resident candidate tumor suppressor genes. The International Lung Cancer Chromosome 3p21.3 Tumor Suppressor Gene Consortium. *Cancer Res.* 60:6116–33.

Lew, D.J., V. Dulić, and S.I. Reed. 1991. Isolation of three novel human cyclins by rescue of G1 cyclin (cln) function in yeast. *Cell*. 66:1197–1206. doi:10.1016/0092-8674(91)90042-W.

Li, C., D.G. Heidt, P. Dalerba, C.F. Burant, L. Zhang, V. Adsay, M. Wicha, M.F. Clarke, and D.M. Simeone. 2007. Identification of Pancreatic Cancer Stem Cells. *Cancer Res.* 67:1030–1037. doi:10.1158/0008-5472.CAN-06-2030.

Li, J., V. D'Angiolella, E.S. Seeley, S. Kim, T. Kobayashi, W. Fu, E.I. Campos, M. Pagano, and B.D. Dynlacht. 2013a. USP33 regulates centrosome biogenesis via deubiquitination of the centriolar protein CP110. *Nature*. 495:255–259. doi:10.1038/nature11941.

Li, X., G. Zhao, Y. Wang, J. Zhang, Z. Duan, and S. Xin. 2013b. RASSF7 and RASSF8 proteins are predictive factors for development and metastasis in malignant thyroid neoplasms. *J. Cancer Res. Ther.* 9 Suppl:S173-7. doi:10.4103/0973-1482.122519.

Lian, I., J. Kim, H. Okazawa, J. Zhao, B. Zhao, J. Yu, A. Chinnaiyan, M.A. Israel, L.S.B. Goldstein, R. Abujarour, S. Ding, and K.-L. Guan. 2010. The role of YAP transcription coactivator in regulating stem cell self-renewal and differentiation. *Genes Dev.* 24:1106–18. doi:10.1101/gad.1903310.

Limin Liu, Katrin Baier, R.H.D.& G.P.P. 2007. The Tumor Suppressor RASSF1A Does not Interact with Cdc20, an Activator of the AnaphasePromoting Complex. *Cell Cycle*. 6:1663–1665.

Lin, Z., A. von Gise, P. Zhou, F. Gu, Q. Ma, J. Jiang, A.L. Yau, J.N. Buck, K.A. Gouin, P.R.R. van Gorp, B. Zhou, J. Chen, J.G. Seidman, D.-Z. Wang, and W.T. Pu. 2014. Cardiac-Specific YAP Activation Improves Cardiac Function and Survival in an Experimental Murine MI Model. *Circ. Res.* 115:354–363. doi:10.1161/CIRCRESAHA.115.303632.

Lingle, W.L., S.L. Barrett, V.C. Negron, A.B. D'Assoro, K. Boeneman, W. Liu, C.M. Whitehead, C. Reynolds, and J.L. Salisbury. 2002. Centrosome amplification drives chromosomal instability in breast tumor development. *Proc. Natl. Acad. Sci.* 99:1978–1983. doi:10.1073/pnas.032479999.

Liu, J., C. Sato, M. Cerletti, and A. Wagers. 2010. Notch Signaling in the Regulation of Stem Cell Self-Renewal and Differentiation. *In* Current topics in developmental biology. 367–409.

Liu, L., C. Guo, R. Dammann, S. Tommasi, and G.P. Pfeifer. 2008. RASSF1A interacts with and activates the mitotic kinase Aurora-A. *Oncogene*. 27:6175–6186. doi:10.1038/onc.2008.220.

Liu, L., S. Tommasi, D.-H. Lee, R. Dammann, and G.P. Pfeifer. 2003. Control of microtubule stability by the RASSF1A tumor suppressor. *Oncogene*. 22:8125–8136. doi:10.1038/sj.onc.1206984.

Liu, Z.-H., J.-L. Huo, Z.-G. Wu, Z. Sun, F. Bai, D. Samartzis, B. Gantenbein, S.-D. Fan, and H.-Q. Wang. 2015. RASSF7 expression and its regulatory roles on apoptosis in human intervertebral disc degeneration. *Int. J. Clin. Exp. Pathol.* 8:16097–103.

Lo-Coco, F., G. Avvisati, M. Vignetti, C. Thiede, S.M. Orlando, S. Iacobelli, F. Ferrara, P. Fazi, L. Cicconi, E. Di Bona, G. Specchia, S. Sica, M. Divona, A. Levis, W. Fiedler, E. Cerqui, M. Breccia, G. Fioritoni, H.R. Salih, M. Cazzola, L. Melillo, A.M. Carella, C.H. Brandts, E. Morra, M. von Lilienfeld-Toal, B. Hertenstein, M. Wattad, M. Lübbert, M. Hänel, N. Schmitz, H. Link, M.G. Kropp, A. Rambaldi, G. La Nasa, M. Luppi, F. Ciceri, O. Finizio, A. Venditti, F. Fabbiano, K. Döhner, M. Sauer, A. Ganser, S. Amadori, F. Mandelli, H. Döhner, G. Ehninger, R.F. Schlenk, and U. Platzbecker. 2013. Retinoic Acid and Arsenic Trioxide for Acute Promyelocytic Leukemia. *N. Engl. J. Med.* 369:111–121. doi:10.1056/NEJMoa1300874.

Logsdon, C.D., D.M. Simeone, C. Binkley, T. Arumugam, J.K. Greenson, T.J. Giordano, D.E. Misek, R. Kuick, and S. Hanash. 2003. Molecular profiling of pancreatic adenocarcinoma and chronic pancreatitis identifies multiple genes differentially regulated in pancreatic cancer. *Cancer Res.* 63:2649–57.

Lotem, J., and L. Sachs. 1988. In vivo control of differentiation of myeloid leukemic cells by recombinant granulocyte-macrophage colony-stimulating factor and interleukin 3. *Blood*. 71:375–82.

Lowe, A.W., M. Olsen, Y. Hao, S.P. Lee, K. Taek Lee, X. Chen, M. van de Rijn, and P.O. Brown. 2007. Gene Expression Patterns in Pancreatic Tumors, Cells and Tissues. *PLoS One*. 2:1–11. doi:10.1371/journal.pone.0000323.

Lowndes, M., M. Rotherham, J.C. Price, A.J. El Haj, and S.J. Habib. 2016. Immobilized WNT Proteins Act as a Stem Cell Niche for Tissue Engineering. *Stem Cell Reports*. 7:126–137. doi:10.1016/j.stemcr.2016.06.004.

Mansour, S.J., W.T. Matten, A.S. Hermann, J.M. Candia, S. Rong, K. Fukasawa, G.F. Vande Woude, and N.G. Ahn. 1994. Transformation of mammalian cells by constitutively active MAP kinase kinase. *Science*. 265:966–70. doi:10.1126/science.8052857.

Markiewicz, E., M. Ledran, and C.J. Hutchison. 2005. Remodelling of the nuclear lamina and nucleoskeleton is required for skeletal muscle differentiation in vitro. *J. Cell Sci.* 118:409–20. doi:10.1242/jcs.01630.

Marthiens, V., M.A. Rujano, C. Pennetier, S. Tessier, P. Paul-Gilloteaux, and R. Basto. 2013. Centrosome amplification causes microcephaly. *Nat. Cell Biol.* 15. doi:10.1038/ncb2746.

Matallanas, D., D. Romano, K. Yee, K. Meissl, L. Kucerova, D. Piazzolla, M. Baccarini, J.K. Vass, W. Kolch, and E. O'Neill. 2007. RASSF1A elicits apoptosis through an MST2 pathway directing proapoptotic transcription by the p73 tumor suppressor protein. *Mol Cell*. 27. doi:10.1016/j.molcel.2007.08.008.

Matthay, K.K., C.P. Reynolds, R.C. Seeger, H. Shimada, E.S. Adkins, D. Haas-Kogan, R.B. Gerbing, W.B. London, and J.G. Villablanca. 2009. Long-term results for children with high-risk neuroblastoma treated on a randomized trial of myeloablative therapy followed by 13-cis-retinoic acid: a children's oncology group study. *J. Clin. Oncol.* 27:1007–13. doi:10.1200/JCO.2007.13.8925.

May-Simera, H.L., R.S. Petralia, M. Montcouquiol, Y.-X. Wang, K.B. Szarama, Y. Liu, W. Lin, M.R. Deans, G.J. Pazour, and M.W. Kelley. 2015. Ciliary proteins Bbs8 and Ift20 promote planar cell polarity in the cochlea. *Development*. 142:555–66. doi:10.1242/dev.113696.

Mayor, T., Y.D. Stierhof, K. Tanaka, A.M. Fry, and E.A. Nigg. 2000. The centrosomal protein C-Nap1 is required for cell cycle-regulated centrosome cohesion. *J. Cell Biol.* 151:837–46.

McGill, M.A., and C.J. McGlade. 2003. Mammalian numb proteins promote Notch1 receptor ubiquitination and degradation of the Notch1 intracellular domain. *J. Biol. Chem.* 278:23196–203. doi:10.1074/jbc.M302827200.

McKeown, M.R., M.R. Corces, M.L. Eaton, C. Fiore, E. Lee, J.T. Lopez, M.W. Chen, D. Smith, S.M. Chan, J.L. Koenig, K. Austgen, M.G. Guenther, D.A. Orlando, J. Lovén, C.C. Fritz, and R. Majeti. 2017. Superenhancer Analysis Defines Novel Epigenomic Subtypes of Non-APL AML, Including an RARα Dependency Targetable by SY-1425, a Potent and Selective RARα Agonist. *Cancer Discov.* 7:1136–1153. doi:10.1158/2159-8290.CD-17-0399.

Meloche, S., and J. Pouysségur. 2007. The ERK1/2 mitogen-activated protein kinase pathway as a master regulator of the G1- to S-phase transition. *Oncogene*. 26:3227–3239. doi:10.1038/sj.onc.1210414.

Meraldi, P., R. Honda, and E.A. Nigg. 2002. Aurora-A overexpression reveals tetraploidization as a major route to centrosome amplification in p53-/- cells. *EMBO J.* 21:483–92. doi:10.1093/EMBOJ/21.4.483.

Mikkelsen, T.S., M. Ku, D.B. Jaffe, B. Issac, E. Lieberman, G. Giannoukos, P. Alvarez, W. Brockman, T.-K. Kim, R.P. Koche, W. Lee, E. Mendenhall, A. O'Donovan, A. Presser, C. Russ, X. Xie, A. Meissner, M. Wernig, R. Jaenisch, C. Nusbaum, E.S. Lander, and B.E. Bernstein. 2007. Genome-wide maps of chromatin state in pluripotent and lineage-committed cells. *Nature*. 448:553–560. doi:10.1038/nature06008.

Mikule, K., B. Delaval, P. Kaldis, A. Jurcyzk, P. Hergert, and S. Doxsey. 2007. Loss of centrosome integrity induces p38—p53—p21-dependent G1—S arrest. *Nat. Cell Biol.* 9:160–170. doi:10.1038/ncb1529.

Mishima, M., S. Kaitna, and M. Glotzer. 2002. Central Spindle Assembly and Cytokinesis Require a Kinesin-like Protein/RhoGAP Complex with Microtubule Bundling Activity. *Dev. Cell*. 2:41–54.

Mo, J.-S., H. Woo Park, and K.-L. Guan. 2014. The Hippo signaling pathway in stem cell biology and cancer Introduction: The Hippo signaling pathway. *EMBO Rep.* 15:642–656. doi:10.15252/embr.201438638.

Morin-Kensicki, E.M., B.N. Boone, M. Howell, J.R. Stonebraker, J. Teed, J.G. Alb, T.R. Magnuson, W. O'Neal, and S.L. Milgram. 2006. Defects in Yolk Sac Vasculogenesis, Chorioallantoic Fusion, and Embryonic Axis Elongation in Mice with Targeted Disruption of Yap65. *Mol. Cell. Biol.* 26:77–87. doi:10.1128/MCB.26.1.77-87.2006.

Moritz, M., M.B. Braunfeld, J.W. Sedat, B. Alberts, and D.A. Agard. 1995. Microtubule nucleation by γ-tubulin-containing rings in the centrosome. *Nature*. 378:638–640. doi:10.1038/378638a0.

Morrisont, D.K., D.R. Kaplant, U. Rapp, and T.M. Robertst. 1988. Signal transduction from membrane to cytoplasm: Growth factors and membrane-bound oncogene products increase Raf-1 phosphorylation and associated protein kinase activity. *Biochemistry*. 85:8855–8859.

Müsch, A. 2004. Microtubule organization and function in epithelial cells. *Traffic*. 5:1–9.

Mutter, G.L., J.P.A. Baak, J.T. Fitzgerald, R. Gray, D. Neuberg, G.A. Kust, R. Gentleman, S.R. Gullans, L.-J. Wei, and M. Wilcox. 2001. Global Expression Changes of Constitutive and Hormonally Regulated Genes during Endometrial Neoplastic Transformation. *Gynecol. Oncol.* 83:177–185. doi:10.1006/GYNO.2001.6352.

Nagai, T., and K. Mizuno. 2017. Jasplakinolide induces primary cilium formation through cell rounding and YAP inactivation. *PLoS One*. 12:e0183030. doi:10.1371/journal.pone.0183030.

Nakagawa, Y., Y. Yamane, T. Okanoue, S. Tsukita, and S. Tsukita. 2001. Outer dense fiber 2 is a widespread centrosome scaffold component preferentially associated with mother centrioles: its identification from isolated centrosomes. *Mol. Biol. Cell*. 12:1687–97. doi:10.1091/MBC.12.6.1687.

Nakakura, T., A. Asano-Hoshino, T. Suzuki, K. Arisawa, H. Tanaka, Y. Sekino, Y. Kiuchi, K. Kawai, and H. Hagiwara. 2015. The elongation of primary cilia via the acetylation of α-tubulin by the treatment with lithium chloride in human fibroblast KD cells. *Med. Mol. Morphol.* 48:44–53. doi:10.1007/s00795-014-0076-x.

Nathwani, B.B., C.H. Miller, T.-L.T. Yang, J.L. Solimano, and J.-C. Liao. 2014. Morphological Differences of Primary Cilia Between Human Induced Pluripotent Stem Cells and Their Parental Somatic Cells. *Stem Cells Dev.* 23:115–123. doi:10.1089/scd.2013.0162.

Nauli, S.M., F.J. Alenghat, Y. Luo, E. Williams, P. Vassilev, X. Li, A.E.H. Elia, W. Lu, E.M. Brown, S.J. Quinn, D.E. Ingber, and J. Zhou. 2003. Polycystins 1 and 2 mediate mechanosensation in the primary cilium of kidney cells. doi:10.1038/ng1076.

Nigg, E.A., and T. Stearns. 2011. The centrosome cycle: Centriole biogenesis, duplication and inherent asymmetries. *Nat. Cell Biol.* 13:1154–60. doi:10.1038/ncb2345.

Nigg, E. a, and J.W. Raff. 2009. Centrioles, centrosomes, and cilia in health and disease. *Cell*. 139:663–78. doi:10.1016/j.cell.2009.10.036.

Nishioka, N., K. Inoue, K. Adachi, H. Kiyonari, M. Ota, A. Ralston, N. Yabuta, S. Hirahara, R.O. Stephenson, N. Ogonuki, R. Makita, H. Kurihara, E.M. Morin-Kensicki, H. Nojima, J. Rossant, K. Nakao, H. Niwa, and H. Sasaki. 2009. The Hippo Signaling

Pathway Components Lats and Yap Pattern Tead4 Activity to Distinguish Mouse Trophectoderm from Inner Cell Mass. *Dev. Cell*. 16:398–410. doi:10.1016/j.devcel.2009.02.003.

North, B.J., B.L. Marshall, M.T. Borra, J.M. Denu, and E. Verdin. 2003. The human Sir2 ortholog, SIRT2, is an NAD+-dependent tubulin deacetylase. *Mol. Cell*. 11:437–44.

O'Brien, C.A., A. Pollett, S. Gallinger, and J.E. Dick. 2007. A human colon cancer cell capable of initiating tumour growth in immunodeficient mice. *Nature*. 445:106–110. doi:10.1038/nature05372.

O'Hagan, R., and M.M. Barr. 2012. Regulation of tubulin glutamylation plays cell-specific roles in the function and stability of sensory cilia. *Worm*. 1:155–9. doi:10.4161/worm.19539.

Oh, H.J., K.-K. Lee, S.J. Song, M.S. Jin, M.S. Song, J.H. Lee, C.R. Im, J.-O. Lee, S. Yonehara, and D.-S. Lim. 2006. Role of the Tumor Suppressor RASSF1A in Mst1-Mediated Apoptosis. *Cancer Res.* 66:2562–2569. doi:10.1158/0008-5472.CAN-05-2951.

Oozeer, F., L.L. Yates, C. Dean, and C.J. Formstone. 2017. A role for core planar polarity proteins in cell contact-mediated orientation of planar cell division across the mammalian embryonic skin. *Sci. Rep.* 7:1880. doi:10.1038/s41598-017-01971-2.

Otto, E.A., B. Schermer, T. Obara, J.F. O'Toole, K.S. Hiller, A.M. Mueller, R.G. Ruf, J. Hoefele, F. Beekmann, D. Landau, J.W. Foreman, J.A. Goodship, T. Strachan, A. Kispert, M.T. Wolf, M.F. Gagnadoux, H. Nivet, C. Antignac, G. Walz, I.A. Drummond, T. Benzing, and F. Hildebrandt. 2003. Mutations in INVS encoding inversin cause nephronophthisis type 2, linking renal cystic disease to the function of primary cilia and left-right axis determination. *Nat. Genet.* 34:413–420. doi:10.1038/ng1217.

Pabalan, N., A. Kunjantarachot, C. Ruangpratheep, H. Jarjanazi, D.M. Christofolini, C.P. Barbosa, and B. Bianco. 2017. Potential of RASSF1A promoter methylation as biomarker for endometrial cancer: A systematic review and meta-analysis. *Gynecol. Oncol.* 146:603–608. doi:10.1016/J.YGYNO.2017.06.017.

Palakurthy, R.K., N. Wajapeyee, M.K. Santra, C. Gazin, L. Lin, S. Gobeil, and M.R. Green. 2009. Epigenetic Silencing of the RASSF1A Tumor Suppressor Gene through HOXB3-Mediated Induction of DNMT3B Expression. *Mol. Cell*. 36:219–230. doi:10.1016/J.MOLCEL.2009.10.009.

Papaspyropoulos, A., L. Bradley, A. Thapa, C.Y. Leung, K. Toskas, D. Koennig, D.-E. Pefani, C. Raso, C. Grou, G. Hamilton, N. Vlahov, A. Grawenda, S. Haider, J. Chauhan, L. Buti, A. Kanapin, X. Lu, F. Buffa, G. Dianov, A. von Kriegsheim, D. Matallanas, A. Samsonova, M. Zernicka-Goetz, and E. O'Neill. 2018. RASSF1A uncouples Wnt from Hippo signalling and promotes YAP mediated differentiation via p73. *Nat. Commun.* 9:424. doi:10.1038/s41467-017-02786-5.

Paridaen, J.T.M.L., M. Wilsch-Bräuninger, and W.B. Huttner. 2013. Asymmetric inheritance of centrosome-associated primary cilium membrane directs ciliogenesis after cell division. *Cell*. 155:333–44. doi:10.1016/j.cell.2013.08.060.

Park, R., U.Y. Moon, J.Y. Park, L.J. Hughes, R.L. Johnson, S.-H. Cho, and S. Kim. 2016. Yap

is required for ependymal integrity and is suppressed in LPA-induced hydrocephalus. *Nat. Commun.* 7:10329. doi:10.1038/ncomms10329.

Parker, A.L., M. Kavallaris, and J.A. McCarroll. 2014. Microtubules and their role in cellular stress in cancer. *Front. Oncol.* 4:153. doi:10.3389/fonc.2014.00153.

Pazour, G.J., B.L. Dickert, Y. Vucica, E.S. Seeley, J.L. Rosenbaum, G.B. Witman, and D.G. Cole. 2000. Chlamydomonas IFT88 and its mouse homologue, polycystic kidney disease gene tg737, are required for assembly of cilia and flagella. *J. Cell Biol.* 151:709–18.

Pece, S., M. Serresi, E. Santolini, M. Capra, E. Hulleman, V. Galimberti, S. Zurrida, P. Maisonneuve, G. Viale, and P.P. Di Fiore. 2004. Loss of negative regulation by Numb over Notch is relevant to human breast carcinogenesis. *J. Cell Biol.* 167:215–221. doi:10.1083/jcb.200406140.

Pefani, D.-E., R. Latusek, I. Pires, A.M. Grawenda, K.S. Yee, G. Hamilton, L. van der Weyden, F. Esashi, E.M. Hammond, and E. O'Neill. 2014. RASSF1A–LATS1 signalling stabilizes replication forks by restricting CDK2-mediated phosphorylation of BRCA2. *Nat Cell Biol*. 16:962–971.

Pefani, D.E., D. Pankova, A.G. Abraham, A.M. Grawenda, N. Vlahov, S. Scrace, and O.N. E. 2016. TGF-beta Targets the Hippo Pathway Scaffold RASSF1A to Facilitate YAP/SMAD2 Nuclear Translocation. *Mol Cell*. 63:156–166. doi:10.1016/j.molcel.2016.05.012.

Pelletier, L., E. O'Toole, A. Schwager, A.A. Hyman, and T. Müller-Reichert. 2006. Centriole assembly in Caenorhabditis elegans. *Nature*. 444:619–623. doi:10.1038/nature05318.

Pepper, A.S.-R., T.W. Lo, D.J. Killian, D.H. Hall, and E.J.A. Hubbard. 2003. The establishment of Caenorhabditis elegans germline pattern is controlled by overlapping proximal and distal somatic gonad signals. *Dev. Biol.* 259:336–50.

Peters, J.-M. 2006. The anaphase promoting complex/cyclosome: a machine designed to destroy. *Nat. Rev. Mol. Cell Biol.* 7:644–656. doi:10.1038/nrm1988.

Pihan, G.A., J. Wallace, Y. Zhou, and S.J. Doxsey. 2003. Centrosome abnormalities and chromosome instability occur together in pre-invasive carcinomas. *Cancer Res.* 63:1398–404.

Piperno, G., and M.T. Fuller. 1985. Monoclonal antibodies specific for an acetylated form of alpha-tubulin recognize the antigen in cilia and flagella from a variety of organisms. *J. Cell Biol.* 101:2085–94.

Plaisant, M., C. Fontaine, W. Cousin, N. Rochet, C. Dani, and P. Peraldi. 2009. Activation of Hedgehog Signaling Inhibits Osteoblast Differentiation of Human Mesenchymal Stem Cells. *Stem Cells*. 27:703–713. doi:10.1634/stemcells.2008-0888.

Plotnikova, O. V., A.S. Nikonova, Y. V. Loskutov, P.Y. Kozyulina, E.N. Pugacheva, and E.A. Golemis. 2012. Calmodulin activation of Aurora-A kinase (AURKA) is required during ciliary disassembly and in mitosis. *Mol. Biol. Cell*. 23:2658–2670. doi:10.1091/mbc.E11-12-1056.

Praetorius, H.A., and K.R. Spring. 2001. Bending the MDCK cell primary cilium increases intracellular calcium. *J. Membr. Biol.* 184:71–9.

Praskova, M., A. Khoklatchev, S. Ortiz-Vega, and J. Avruch. 2004. Regulation of the MST1 kinase by autophosphorylation, by the growth inhibitory proteins, RASSF1 and NORE1, and by Ras. *Biochem J*. 381. doi:10.1042/BJ20040025.

Prior, I.A., P.D. Lewis, and C. Mattos. 2012. A comprehensive survey of Ras mutations in cancer. *Cancer Res.* 72:2457–2467. doi:10.1158/0008-5472.CAN-11-2612.

Pugacheva, E.N., S.A. Jablonski, T.R. Hartman, E.P. Henske, and E.A. Golemis. 2007. HEF1-Dependent Aurora A Activation Induces Disassembly of the Primary Cilium. *Cell*. 129:1351–1363. doi:10.1016/J.CELL.2007.04.035.

Pusch, S., S. Krausert, V. Fischer, J. Balss, M. Ott, D. Schrimpf, D. Capper, F. Sahm, J. Eisel, A.-C. Beck, M. Jugold, V. Eichwald, S. Kaulfuss, O. Panknin, H. Rehwinkel, K. Zimmermann, R.C. Hillig, J. Guenther, L. Toschi, R. Neuhaus, A. Haegebart, H. Hess-Stumpp, M. Bauser, W. Wick, A. Unterberg, C. Herold-Mende, M. Platten, and A. von Deimling. 2017. Pan-mutant IDH1 inhibitor BAY 1436032 for effective treatment of IDH1 mutant astrocytoma in vivo. *Acta Neuropathol.* 133:629–644. doi:10.1007/s00401-017-1677-y.

Quintyne, N.J., J.E. Reing, D.R. Hoffelder, S.M. Gollin, and W.S. Saunders. 2005. Spindle multipolarity is prevented by centrosomal clustering. *Science*. 307:127–9. doi:10.1126/science.1104905.

Rajalingam, K., R. Schreck, U.R. Rapp, and Š. Albert. 2007. Ras oncogenes and their downstream targets. *Biochim. Biophys. Acta - Mol. Cell Res.* 1773:1177–1195. doi:https://doi.org/10.1016/j.bbamcr.2007.01.012.

Ran, J., Y. Yang, D. Li, M. Liu, and J. Zhou. 2015. Deacetylation of α-tubulin and cortactin is required for HDAC6 to trigger ciliary disassembly. *Sci. Rep.* 5:12917. doi:10.1038/srep12917.

Rebollo, E., P. Sampaio, J. Januschke, S. Llamazares, H. Varmark, and C. González. 2007. Functionally Unequal Centrosomes Drive Spindle Orientation in Asymmetrically Dividing Drosophila Neural Stem Cells. *Dev. Cell*. 12:467–474. doi:10.1016/J.DEVCEL.2007.01.021.

Recino, A., V. Sherwood, A. Flaxman, W.N. Cooper, F. Latif, A. Ward, and A.D. Chalmers. 2010. Human RASSF7 regulates the microtubule cytoskeleton and is required for spindle formation, Aurora B activation and chromosomal congression during mitosis. *Biochem. J.* 430:207–13. doi:10.1042/BJ20100883.

Reeves, M.E., M. Firek, S.-T. Chen, and Y. Amaar. 2013. The RASSF1 Gene and the Opposing Effects of the RASSF1A and RASSF1C Isoforms on Cell Proliferation and Apoptosis. *Mol. Biol. Int.* 2013:145096. doi:10.1155/2013/145096.

Regnard, C., D. Fesquet, C. Janke, D. Boucher, E. Desbruyéres, A. Koulakoff, C. Insina, P. Travo, and B. Eddé. 2003. Characterisation of PGs1, a subunit of a protein complex co-purifying with tubulin polyglutamylase. *J. Cell Sci.* 116:4181–90. doi:10.1242/jcs.00743.

Reilova-Velez, J., and M.W. Seiler. 1984. Abnormal cilia in a breast carcinoma. An ultrastructural study. *Arch. Pathol. Lab. Med.* 108:795–7.

Ren, F., B. Wang, T. Yue, E.-Y. Yun, Y.T. Ip, and J. Jiang. 2010. Hippo signaling regulates Drosophila intestine stem cell proliferation through multiple pathways. *Proc. Natl. Acad. Sci.* 107:21064–21069. doi:10.1073/pnas.1012759107.

Rhyu, M.S., L.Y. Jan, and Y.N. Jan. 1994. Asymmetric distribution of numb protein during division of the sensory organ precursor cell confers distinct fates to daughter cells. *Cell*. 76:477–91.

Ricci-Vitiani, L., D.G. Lombardi, E. Pilozzi, M. Biffoni, M. Todaro, C. Peschle, and R. De Maria. 2007. Identification and expansion of human colon-cancer-initiating cells. *Nature*. 445:111–115. doi:10.1038/nature05384.

Richter, A.M., G.P. Pfeifer, and R.H. Dammann. 2009. The RASSF proteins in cancer; from epigenetic silencing to functional characterization.

Roghi, C., R. Giet, R. Uzbekov, N. Morin, I. Chartrain, R. Le Guellec, A. Couturier, M. Dorée, M. Philippe, and C. Prigent. 1998. The Xenopus protein kinase pEg2 associates with the centrosome in a cell cycle-dependent manner, binds to the spindle microtubules and is involved in bipolar mitotic spindle assembly. *J. Cell Sci.* 111 (Pt 5):557–72.

Rogowski, K., F. Juge, J. van Dijk, D. Wloga, J.-M. Strub, N. Levilliers, D. Thomas, M.-H. Bré, A. Van Dorsselaer, J. Gaertig, and C. Janke. 2009. Evolutionary Divergence of Enzymatic Mechanisms for Posttranslational Polyglycylation. *Cell*. 137:1076–1087. doi:10.1016/j.cell.2009.05.020.

Rong, R., L.Y. Jiang, M.S. Sheikh, and Y. Huang. 2007. Mitotic kinase Aurora-A phosphorylates RASSF1A and modulates RASSF1A-mediated microtubule interaction and M-phase cell cycle regulation. *Oncogene*. 26:7700–7708. doi:10.1038/sj.onc.1210575.

Rong, R., W. Jin, J. Zhang, M. Saeed Sheikh, and Y. Huang. 2004. Tumor suppressor RASSF1A is a microtubule-binding protein that stabilizes microtubules and induces G2/M arrest. *Oncogene*. 23:8216–8230. doi:10.1038/sj.onc.1207901.

Ross, A.J., H. May-Simera, E.R. Eichers, M. Kai, J. Hill, D.J. Jagger, C.C. Leitch, J.P. Chapple, P.M. Munro, S. Fisher, P.L. Tan, H.M. Phillips, M.R. Leroux, D.J. Henderson, J.N. Murdoch, A.J. Copp, M.-M. Eliot, J.R. Lupski, D.T. Kemp, H. Dollfus, M. Tada, N. Katsanis, A. Forge, and P.L. Beales. 2005. Disruption of Bardet-Biedl syndrome ciliary proteins perturbs planar cell polarity in vertebrates. *Nat. Genet.* 37:1135–1140. doi:10.1038/ng1644.

Sato, N., L. Meijer, L. Skaltsounis, P. Greengard, and A.H. Brivanlou. 2004. Maintenance of pluripotency in human and mouse embryonic stem cells through activation of Wnt signaling by a pharmacological GSK-3-specific inhibitor. *Nat. Med.* 10:55–63. doi:10.1038/nm979.

Sawada, A., H. Kiyonari, K. Ukita, N. Nishioka, Y. Imuta, and H. Sasaki. 2008. Redundant Roles of Tead1 and Tead2 in Notochord Development and the Regulation of Cell

Proliferation and Survival. *Mol. Cell. Biol.* 28:3177–3189. doi:10.1128/MCB.01759-07.

Scheel, H., and K. Hofmann. 2003. A novel inter action motif, SARAH, connects three classes of tumor suppressor. *Curr. Biol.* 13:R899–R900. doi:10.1016/j.cub.2003.11.007.

Schenk, T., W.C. Chen, S. Göllner, L. Howell, L. Jin, K. Hebestreit, H.-U. Klein, A.C. Popescu, A. Burnett, K. Mills, R.A. Casero, L. Marton, P. Woster, M.D. Minden, M. Dugas, J.C.Y. Wang, J.E. Dick, C. Müller-Tidow, K. Petrie, and A. Zelent. 2012. Inhibition of the LSD1 (KDM1A) demethylase reactivates the all-trans-retinoic acid differentiation pathway in acute myeloid leukemia. *Nat. Med.* 18:605–611. doi:10.1038/nm.2661.

Schlegelmilch, K., M. Mohseni, O. Kirak, J. Pruszak, J.R. Rodriguez, D. Zhou, B.T. Kreger, V. Vasioukhin, J. Avruch, T.R. Brummelkamp, and F.D. Camargo. 2011. Yap1 Acts Downstream of α-Catenin to Control Epidermal Proliferation. *Cell*. 144:782–795. doi:10.1016/j.cell.2011.02.031.

Schmidt, K.N., S. Kuhns, A. Neuner, B. Hub, H. Zentgraf, and G. Pereira. 2012. Cep164 mediates vesicular docking to the mother centriole during early steps of ciliogenesis. *J. Cell Biol.* 199:1083–1101. doi:10.1083/jcb.201202126.

Schmidt, T.I., J. Kleylein-Sohn, J. Westendorf, M. Le Clech, S.B. Lavoie, Y.-D. Stierhof, and E.A. Nigg. 2009. Control of Centriole Length by CPAP and CP110. *Curr. Biol.* 19:1005–1011. doi:10.1016/j.cub.2009.05.016.

Schneider, L., C.A. Clement, S.C. Teilmann, G.J. Pazour, E.K. Hoffmann, P. Satir, and S.T. Christensen. 2005. PDGFRαα Signaling Is Regulated through the Primary Cilium in Fibroblasts. *Curr. Biol.* 15:1861–1866. doi:10.1016/j.cub.2005.09.012.

Schraml, P., I.J. Frew, C.R. Thoma, G. Boysen, K. Struckmann, W. Krek, and H. Moch. 2009. Sporadic clear cell renal cell carcinoma but not the papillary type is characterized by severely reduced frequency of primary cilia. *Mod. Pathol.* 22:31–36. doi:10.1038/modpathol.2008.132.

Schurov, I.L., E.J. Handford, N.J. Brandon, and P.J. Whiting. 2004. Expression of disrupted in schizophrenia 1 (DISC1) protein in the adult and developing mouse brain indicates its role in neurodevelopment. *Mol. Psychiatry*. 9:1100–1110. doi:10.1038/sj.mp.4001574.

Sekido, Y., M. Ahmadian, I.I. Wistuba, F. Latif, S. Bader, M.-H. Wei, F.-M. Duh, A.F. Gazdar, M.I. Lerman, and J.D. Minna. 1998. Cloning of a breast cancer homozygous deletion junction narrows the region of search for a 3p21.3 tumor suppressor gene. *Oncogene*. 16:3151–3157. doi:10.1038/sj.onc.1201858.

Serwas, D., T.Y. Su, M. Roessler, S. Wang, and A. Dammermann. 2017. Centrioles initiate cilia assembly but are dispensable for maturation and maintenance in C. elegans. *J. Cell Biol.* 216:1659–1671. doi:10.1083/jcb.201610070.

Shah, A.S., Y. Ben-Shahar, T.O. Moninger, J.N. Kline, and M.J. Welsh. 2009. Motile cilia of human airway epithelia are chemosensory. *Science*. 325:1131–4.

doi:10.1126/science.1173869.

Sharma, N., J. Bryant, D. Wloga, R. Donaldson, R.C. Davis, M. Jerka-Dziadosz, and J. Gaertig. 2007. Katanin regulates dynamics of microtubules and biogenesis of motile cilia. *J. Cell Biol.* 178:1065–79. doi:10.1083/jcb.200704021.

Shaw, R.L., A. Kohlmaier, C. Polesello, C. Veelken, B.A. Edgar, and N. Tapon. 2010. The Hippo pathway regulates intestinal stem cell proliferation during Drosophila adult midgut regeneration. *Development*. 137:4147–4158. doi:10.1242/dev.052506.

Shen, Q., W. Zhong, Y.N. Jan, and S. Temple. 2002. Asymmetric Numb distribution is critical for asymmetric cell division of mouse cerebral cortical stem cells and neuroblasts. *Development*. 129:4843–53.

Sherwood, V., R. Manbodh, C. Sheppard, and A.D. Chalmers. 2008. RASSF7 is a member of a new family of RAS association domain-containing proteins and is required for completing mitosis. *Mol Biol Cell*. 19. doi:10.1091/mbc.E07-07-0652.

Shida, T., J.G. Cueva, Z. Xu, M.B. Goodman, and M. V Nachury. 2010. The major alpha-tubulin K40 acetyltransferase alphaTAT1 promotes rapid ciliogenesis and efficient mechanosensation. *Proc. Natl. Acad. Sci. U. S. A.* 107:21517–22. doi:10.1073/pnas.1013728107.

Shinawi, T., V. Hill, A. Dagklis, P. Baliakas, K. Stamatopoulos, A. Agathanggelou, T. Stankovic, E.R. Maher, P. Ghia, and F. Latif. 2012. *KIBRA* gene methylation is associated with unfavorable biological prognostic parameters in chronic lymphocytic leukemia. *Epigenetics*. 7:211–215. doi:10.4161/epi.7.3.19222.

Shivakumar, L., J. Minna, T. Sakamaki, R. Pestell, and M.A. White. 2002. The RASSF1A tumor suppressor blocks cell cycle progression and inhibits cyclin D1 accumulation. *Mol. Cell. Biol.* 22:4309–18.

Simons, M., J. Gloy, A. Ganner, A. Bullerkotte, M. Bashkurov, C. Krönig, B. Schermer, T. Benzing, O.A. Cabello, A. Jenny, M. Mlodzik, B. Polok, W. Driever, T. Obara, and G. Walz. 2005. Inversin, the gene product mutated in nephronophthisis type II, functions as a molecular switch between Wnt signaling pathways. *Nat. Genet.* 37:537–543. doi:10.1038/ng1552.

Singh, S.K., C. Hawkins, I.D. Clarke, J.A. Squire, J. Bayani, T. Hide, R.M. Henkelman, M.D. Cusimano, and P.B. Dirks. 2004. Identification of human brain tumour initiating cells. *Nature*. 432:396–401. doi:10.1038/nature03128.

Sir, J.-H., M. Pütz, O. Daly, C.G. Morrison, M. Dunning, J. V Kilmartin, and F. Gergely. 2013. Loss of centrioles causes chromosomal instability in vertebrate somatic cells. *J. Cell Biol.* 203:747–56. doi:10.1083/jcb.201309038.

Sirajuddin, M., L.M. Rice, and R.D. Vale. 2014. Regulation of microtubule motors by tubulin isotypes and post-translational modifications. *Nat. Cell Biol.* 16:335–344. doi:10.1038/ncb2920.

Skoufias, D.A., S. DeBonis, Y. Saoudi, L. Lebeau, I. Crevel, R. Cross, R.H. Wade, D. Hackney, and F. Kozielski. 2006. S-trityl-L-cysteine is a reversible, tight binding inhibitor of the human kinesin Eg5 that specifically blocks mitotic progression. *J.*

Biol. Chem. 281:17559–69. doi:10.1074/jbc.M511735200.

Song, S.J., M.S. Song, S.J. Kim, S.Y. Kim, S.H. Kwon, J.G. Kim, D.F. Calvisi, D. Kang, and D.-S. Lim. 2009. Aurora A Regulates Prometaphase Progression by Inhibiting the Ability of RASSF1A to Suppress APC-Cdc20 Activity. *Cancer Res.* 69.

Sonnen, K.F., A.-M. Gabryjonczyk, E. Anselm, Y.-D. Stierhof, and E.A. Nigg. 2013. Human Cep192 and Cep152 cooperate in Plk4 recruitment and centriole duplication. *J. Cell Sci.* 126:3223–3233. doi:10.1242/jcs.129502.

Sorokin, S.P. 1968. Reconstructions of Centriole Formation and Ciliogenesis in Mammalian Lungs. *J. Cell Sci.* 3.

Spektor, A., W.Y. Tsang, D. Khoo, and B.D. Dynlacht. 2007. Cep97 and CP110 Suppress a Cilia Assembly Program. *Cell*. 130:678–690. doi:10.1016/j.cell.2007.06.027.

Strano, S., O. Monti, N. Pediconi, A. Baccarini, G. Fontemaggi, E. Lapi, F. Mantovani, A. Damalas, G. Citro, A. Sacchi, G. Del Sal, M. Levrero, and G. Blandino. 2005. The transcriptional coactivator Yes-associated protein drives p73 gene-target specificity in response to DNA Damage. *Mol Cell*. 18:447–459. doi:10.1016/j.molcel.2005.04.008.

Sugiarto, S., A.I. Persson, E.G. Munoz, M. Waldhuber, C. Lamagna, N. Andor, P. Hanecker, J. Ayers-Ringler, J. Phillips, J. Siu, D.A. Lim, S. Vandenberg, W. Stallcup, M.S. Berger, G. Bergers, W.A. Weiss, and C. Petritsch. 2011. Asymmetry-Defective Oligodendrocyte Progenitors Are Glioma Precursors. *Cancer Cell*. 20:328–340. doi:10.1016/J.CCR.2011.08.011.

Sundaresan, V., P. Ganly, P. Hasleton, R. Rudd, G. Sinha, N.M. Bleehen, and P. Rabbitts. 1992. p53 and chromosome 3 abnormalities, characteristic of malignant lung tumours, are detectable in preinvasive lesions of the bronchus. *Oncogene*. 7:1989–97.

Sup Song, M., S. Jeong Song, N.G. Ayad, J. Sook Chang, J. Hyun Lee, H. Kyung Hong, H. Lee, N. Choi, J. Kim, H. Kim, J. Woo Kim, E.-J. Choi, M.W. Kirschner, and D.-S. Lim. 2004a. The tumour suppressor RASSF1A regulates mitosis by inhibiting the APC–Cdc20 complex. *Nat. Cell Biol.* 6. doi:10.1038/ncb1091.

Sup Song, M., J. Sook Chang, S. Jeong Song, T. Hong Yang, H. Lee, and D.-S. Lim. 2004b. The Centrosomal Protein RAS Association Domain Family Protein 1A (RASSF1A)-binding Protein 1 Regulates Mitotic Progression by Recruiting RASSF1A to Spindle Poles*. doi:10.1074/jbc.M409115200.

Takahashi, S., a Ebihara, H. Kajiho, K. Kontani, H. Nishina, and T. Katada. 2011. RASSF7 negatively regulates pro-apoptotic JNK signaling by inhibiting the activity of phosphorylated-MKK7. *Cell Death Differ.* 18:645–55. doi:10.1038/cdd.2010.137.

Tan, D.S.P., M.B.K. Lambros, S. Rayter, R. Natrajan, R. Vatcheva, Q. Gao, C. Marchiò, F.C. Geyer, K. Savage, S. Parry, K. Fenwick, N. Tamber, A. Mackay, T. Dexter, C. Jameson, W.G. McCluggage, A. Williams, A. Graham, D. Faratian, M. El-Bahrawy, A.J. Paige, H. Gabra, M.E. Gore, M. Zvelebil, C.J. Lord, S.B. Kaye, A. Ashworth, and J.S. Reis-Filho. 2009. PPM1D is a potential therapeutic target in ovarian clear cell

carcinomas. *Clin. Cancer Res.* 15:2269–80. doi:10.1158/1078-0432.CCR-08-2403.

Tang, T.K. 2013. Centriole biogenesis in multiciliated cells. *Nat. Cell Biol.* 15:1400–1402. doi:10.1038/ncb2892.

Tao, H., J.-J. Yang, W. Hu, K.-H. Shi, and J. Li. 2016. HDAC6 Promotes Cardiac Fibrosis Progression through Suppressing RASSF1A Expression. *Cardiology*. 133:18–26.

Teng, I.W., P.C. Hou, K.D. Lee, P.Y. Chu, K.T. Yeh, V.X. Jin, M.J. Tseng, S.J. Tsai, Y.S. Chang, C.S. Wu, H.S. Sun, K.D. Tsai, L.B. Jeng, K.P. Nephew, T.H.M. Huang, S.H. Hsiao, and Y.W. Leu. 2011. Targeted Methylation of Two Tumor Suppressor Genes Is Sufficient to Transform Mesenchymal Stem Cells into Cancer Stem/Initiating Cells. *Cancer Res*. 71:4653–4663. doi:10.1158/0008-5472.Can-10-3418.

Thaler, S., P.S. Hähnel, A. Schad, R. Dammann, and M. Schuler. 2009. RASSF1A Mediates p21Cip1/Waf1-Dependent Cell Cycle Arrest and Senescence through Modulation of the Raf-MEK-ERK Pathway and Inhibition of Akt. *Cancer Res.* 69.

de Thé, H. 2017. Differentiation therapy revisited. *Nat. Publ. Gr.* 18. doi:10.1038/nrc.2017.103.

Therizols, P., R.S. Illingworth, C. Courilleau, S. Boyle, A.J. Wood, and W.A. Bickmore. 2014. Chromatin decondensation is sufficient to alter nuclear organization in embryonic stem cells. *Science (80-.).* 346:1238–1242. doi:10.1126/science.1259587.

Tommasi, S., R. Dammann, Z. Zhang, Y. Wang, L. Liu, W.M. Tsark, S.P. Wilczynski, J. Li, M. You, and G.P. Pfeifer. 2005. Tumor Susceptibility of Rassf1a Knockout Mice. *Cancer Res.* 65:92 LP-98.

Toriyama, M., C. Lee, S.P. Taylor, I. Duran, D.H. Cohn, A.-L. Bruel, J.M. Tabler, K. Drew, M.R. Kelly, S. Kim, T.J. Park, D.A. Braun, G. Pierquin, A. Biver, K. Wagner, A. Malfroot, I. Panigrahi, B. Franco, H.A. Al-lami, Y. Yeung, Y.J. Choi, Y. Duffourd, L. Faivre, J.-B. Rivière, J. Chen, K.J. Liu, E.M. Marcotte, F. Hildebrandt, C. Thauvin-Robinet, D. Krakow, P.K. Jackson, J.B. Wallingford, and J.B. Wallingford. 2016. The ciliopathy-associated CPLANE proteins direct basal body recruitment of intraflagellar transport machinery. *Nat. Genet.* 48:648–656. doi:10.1038/ng.3558.

Tritarelli, A., E. Oricchio, M. Ciciarello, R. Mangiacasale, A. Palena, P. Lavia, S. Soddu, and E. Cundari. 2004. p53 localization at centrosomes during mitosis and postmitotic checkpoint are ATM-dependent and require serine 15 phosphorylation. *Mol. Biol. Cell*. 15:3751–7. doi:10.1091/mbc.E03-12-0900.

Trotta, N., G. Orso, M.G. Rossetto, A. Daga, and K. Broadie. 2004. The Hereditary Spastic Paraplegia Gene, spastin, Regulates Microtubule Stability to Modulate Synaptic Structure and Function. *Curr. Biol.* 14:1135–1147. doi:10.1016/j.cub.2004.06.058.

Tsai, S.-F., D.I.K. Martin, L.I. Zon, A.D. D'Andrea, G.G. Wong, and S.H. Orkin. 1989. Cloning of cDNA for the major DNA-binding protein of the erythroid lineage through expression in mammalian cells. *Nature*. 339:446–451. doi:10.1038/339446a0.

Tsang, H.T.H., J.W. Connell, S.E. Brown, A. Thompson, E. Reid, and C.M. Sanderson.

2006. A systematic analysis of human CHMP protein interactions: Additional MIT domain-containing proteins bind to multiple components of the human ESCRT III complex. *Genomics*. 88:333–346. doi:10.1016/J.YGENO.2006.04.003.

Tsou, M.-F.B., W.-J. Wang, K.A. George, K. Uryu, T. Stearns, and P. V. Jallepalli. 2009. Polo Kinase and Separase Regulate the Mitotic Licensing of Centriole Duplication in Human Cells. *Dev. Cell*. 17:344–354. doi:10.1016/j.devcel.2009.07.015.

Tummala, P., E.J. Arnsdorf, and C.R. Jacobs. 2010. The Role of Primary Cilia in Mesenchymal Stem Cell Differentiation: A Pivotal Switch in Guiding Lineage Commitment. *Cell. Mol. Bioeng.* 3:207–212. doi:10.1007/s12195-010-0127-x.

Udan, R.S., M. Kango-Singh, R. Nolo, C. Tao, and G. Halder. 2003. Hippo promotes proliferation arrest and apoptosis in the Salvador/Warts pathway. *Nat. Cell Biol.* 5:914–920. doi:10.1038/ncb1050.

Varelas, X., R. Sakuma, P. Samavarchi-Tehrani, R. Peerani, B.M. Rao, J. Dembowy, M.B. Yaffe, P.W. Zandstra, and J.L. Wrana. 2008. TAZ controls Smad nucleocytoplasmic shuttling and regulates human embryonic stem-cell self-renewal. *Nat Cell Biol*. 10:837–848. doi:10.1038/ncb1748.

Vavvas, D., X. Li, J. Avruch, and X.-F. Zhang. 1998. Identification of Nore1 as a Potential Ras Effector. *J. Biol. Chem.* 273:5439–5442. doi:10.1074/jbc.273.10.5439.

Verdi, J.M., R. Schmandt, A. Bashirullah, S. Jacob, R. Salvino, C.G. Craig, A.E. Program, H.D. Lipshitz, and C.J. McGlade. 1996. Mammalian NUMB is an evolutionarily conserved signaling adapter protein that specifies cell fate. *Curr. Biol.* 6:1134–1145. doi:10.1016/S0960-9822(02)70680-5.

Verlhac, M.-H., C. Lefebvre, P. Guillaud, P. Rassinier, and B. Maro. 2000. Asymmetric division in mouse oocytes: with or without Mos. *Curr. Biol.* 10:1303–1306. doi:10.1016/S0960-9822(00)00753-3.

Vichalkovski, A., E. Gresko, H. Cornils, A. Hergovich, D. Schmitz, and B.A. Hemmings. 2008. NDR Kinase Is Activated by RASSF1A/MST1 in Response to Fas Receptor Stimulation and Promotes Apoptosis. *Curr. Biol.* 18:1889–1895. doi:10.1016/J.CUB.2008.10.060.

Vietri, M., K.O. Schink, C. Campsteijn, C.S. Wegner, S.W. Schultz, L. Christ, S.B. Thoresen, A. Brech, C. Raiborg, and H. Stenmark. 2015. Spastin and ESCRT-III coordinate mitotic spindle disassembly and nuclear envelope sealing. *Nature*. 522:231–235. doi:10.1038/nature14408.

Vining, K.H., and D.J. Mooney. 2017. Mechanical forces direct stem cell behaviour in development and regeneration. *Nat. Rev. Mol. Cell Biol.* 18:728–742. doi:10.1038/nrm.2017.108.

Vlahov, N., S. Scrace, M.S. Soto, A.M. Grawenda, L. Bradley, D. Pankova, A. Papaspyropoulos, K.S. Yee, F. Buffa, C.R. Goding, P. Timpson, N. Sibson, and E. O'Neill. 2015. Alternate RASSF1 Transcripts Control SRC Activity, E-Cadherin Contacts, and YAP-Mediated Invasion. *Curr. Biol.* 1–16. doi:10.1016/j.cub.2015.09.072.

Volodko, N., M. Gordon, M. Salla, H.A. Ghazaleh, and S. Baksh. 2014. RASSF tumor suppressor gene family: Biological functions and regulation. *FEBS Lett.* 588:2671–2684. doi:10.1016/j.febslet.2014.02.041.

Vorobjev, I.A., and C. Chentsov YuS. 1982. Centrioles in the cell cycle. I. Epithelial cells. *J. Cell Biol.* 93:938–49. doi:10.1083/JCB.93.3.938.

Vos, M.D., A. Dallol, K. Eckfeld, N.P. Allen, H. Donninger, L.B. Hesson, D. Calvisi, F. Latif, and G.J. Clark. 2006. The RASSF1A tumor suppressor activates Bax via MOAP-1. *J Biol Chem*. 281. doi:10.1074/jbc.M512128200.

Vos, M.D., A. Martinez, C. Elam, A. Dallol, B.J. Taylor, F. Latif, and G.J. Clark. 2004. A Role for the RASSF1A Tumor Suppressor in the Regulation of Tubulin Polymerization and Genomic Stability. *Cancer Res.* 64.

Vyas, S., E. Zaganjor, and M.C. Haigis. 2016. Mitochondria and Cancer. *Cell*. 166:555–566. doi:10.1016/j.cell.2016.07.002.

Wahab, A.H.A., H.A. El-mezayen, H. Sharad, S.A. Rahman, H. Sharad, and S. Abdel Rahman. 2011. Promoter hypermethylation of RASSF1A, MGMT, and HIC-1 genes in benign and malignant colorectal tumors. *Tumor Biol.* 32:845–852. doi:10.1007/s13277-011-0156-7.

Wang, S., Q. Liang, H. Qiao, H. Li, T. Shen, F. Ji, and J. Jiao. 2016. DISC1 regulates astrogenesis in the embryonic brain via modulation of RAS/MEK/ERK signaling through RASSF7. *Development*. 143:2732–2740. doi:10.1242/dev.133066.

Wang, X., J.-W. Tsai, J.H. Imai, W.-N. Lian, R.B. Vallee, and S.-H. Shi. 2009. Asymmetric centrosome inheritance maintains neural progenitors in the neocortex. *Nature*. 461:947–955. doi:10.1038/nature08435.

Watanabe, D., Y. Saijoh, S. Nonaka, G. Sasaki, Y. Ikawa, T. Yokoyama, and H. Hamada. 2003. The left-right determinant Inversin is a component of node monocilia and other 9+0 cilia. *Development*. 130:1725–34. doi:10.1242/DEV.00407.

Weitzel, J.N., A. Kasperczyk, C. Mohan, and T.G. Krontiris. 1992. The HRAS1 gene cluster: two upstream regions recognizing transcripts and a third encoding a gene with a leucine zipper domain. *Genomics*. 14:309—319. doi:10.1016/s0888-7543(05)80221-6.

Wen, Q.J., Q. Yang, B. Goldenson, S. Malinge, T. Lasho, R.K. Schneider, L.J. Breyfogle, R. Schultz, L. Gilles, P. Koppikar, O. Abdel-Wahab, A. Pardanani, B. Stein, S. Gurbuxani, A. Mullally, R.L. Levine, A. Tefferi, and J.D. Crispino. 2015. Targeting megakaryocytic-induced fibrosis in myeloproliferative neoplasms by AURKA inhibition. *Nat. Med.* 21:1473–80. doi:10.1038/nm.3995.

Wennerberg, K., K.L. Rossman, and C.J. Der. 2005. The Ras superfamily at a glance. *J. Cell Sci.* 118:843 LP-846.

Westlake, C.J., L.M. Baye, M. V Nachury, K.J. Wright, K.E. Ervin, L. Phu, C. Chalouni, J.S. Beck, D.S. Kirkpatrick, D.C. Slusarski, V.C. Sheffield, R.H. Scheller, and P.K. Jackson. 2011. Primary cilia membrane assembly is initiated by Rab11 and transport protein particle II (TRAPPII) complex-dependent trafficking of Rabin8 to the centrosome.

Proc. Natl. Acad. Sci. U. S. A. 108:2759–64. doi:10.1073/pnas.1018823108.

Weyden, L. v. a. n. d. e. r., and D.J. Adams. 2007. The Ras-association domain family (RASSF) members and their role in human tumourigenesis. *Biochim Biophys Acta*. 1776.

Weyden, L. Van Der, K.K. Tachibana, M.A. Gonzalez, D.J. Adams, B.L. Ng, R. Petty, A.R. Venkitaraman, M.J. Arends, A. Bradley, C.C. Unit, H. Mrc, H. Road, and U. Kingdom. 2005. The RASSF1A Isoform of RASSF1 Promotes Microtubule Stability and Suppresses Tumorigenesis. 25:8356–8367. doi:10.1128/MCB.25.18.8356.

Whang, Y.M., Y.H. Kim, J.S. Kim, and Y. Do Yoo. 2005. RASSF1A Suppresses the c-Jun-NH 2 -Kinase Pathway and Inhibits Cell Cycle Progression. *Cancer Res*. 65:3682–90.

Williams, R.L., D.J. Hilton, S. Pease, T.A. Willson, C.L. Stewart, D.P. Gearing, E.F. Wagner, D. Metcalf, N.A. Nicola, and N.M. Gough. 1988. Myeloid leukaemia inhibitory factor maintains the developmental potential of embryonic stem cells. *Nature*. 336:684–687.

Wirtz-Peitz, F., T. Nishimura, and J.A. Knoblich. 2008. Linking Cell Cycle to Asymmetric Division: Aurora-A Phosphorylates the Par Complex to Regulate Numb Localization. *Cell*. 135:161–173. doi:10.1016/j.cell.2008.07.049.

Wistuba, I.I., C. Behrens, A.K. Virmani, G. Mele, S. Milchgrub, L. Girard, J.W. Fondon, H.R. Garner, B. McKay, F. Latif, M.I. Lerman, S. Lam, A.F. Gazdar, and J.D. Minna. 2000. High resolution chromosome 3p allelotyping of human lung cancer and preneoplastic/preinvasive bronchial epithelium reveals multiple, discontinuous sites of 3p allele loss and three regions of frequent breakpoints. *Cancer Res.* 60:1949–60.

Wloga, D., E. Joachimiak, P. Louka, and J. Gaertig. 2017. Posttranslational Modifications of Tubulin and Cilia. *Cold Spring Harb. Perspect. Biol.* 9:a028159. doi:10.1101/cshperspect.a028159.

Wloga, D., K. Rogowski, N. Sharma, J. Van Dijk, C. Janke, B. Eddé, M.-H. Bré, N. Levilliers, V. Redeker, J. Duan, M.A. Gorovsky, M. Jerka-Dziadosz, and J. Gaertig. 2008. Glutamylation on alpha-tubulin is not essential but affects the assembly and functions of a subset of microtubules in Tetrahymena thermophila. *Eukaryot. Cell*. 7:1362–72. doi:10.1128/EC.00084-08.

Wloga, D., D.M. Webster, K. Rogowski, M.-H. Bré, N. Levilliers, M. Jerka-Dziadosz, C. Janke, S.T. Dougan, and J. Gaertig. 2009. TTLL3 Is a Tubulin Glycine Ligase that Regulates the Assembly of Cilia. *Dev. Cell*. 16:867–876. doi:10.1016/j.devcel.2009.04.008.

Wong, S.Y., A.D. Seol, P.-L. So, A.N. Ermilov, C.K. Bichakjian, E.H. Epstein, A.A. Dlugosz, and J.F. Reiter. 2009. Primary cilia can both mediate and suppress Hedgehog pathway–dependent tumorigenesis. *Nat. Med.* 15:1055–1061. doi:10.1038/nm.2011.

Wu, S., J. Huang, J. Dong, and D. Pan. 2003. hippo Encodes a Ste-20 Family Protein Kinase that Restricts Cell Proliferation and Promotes Apoptosis in Conjunction with

salvador and warts. *Cell*. 114:445–456. doi:10.1016/S0092-8674(03)00549-X.

Wynshaw-Boris, A., and M.J. Gambello. 2001. LIS1 and dynein motor function in neuronal migration and development. *Genes Dev.* 15:639–651. doi:10.1101/gad.886801.

Yagi, R., M.J. Kohn, I. Karavanova, K.J. Kaneko, D. Vullhorst, M.L. DePamphilis, and A. Buonanno. 2007. Transcription factor TEAD4 specifies the trophectoderm lineage at the beginning of mammalian development. *Development*. 134:3827–3836. doi:10.1242/dev.010223.

Yamashita, Y.M., D.L. Jones, and M.T. Fuller. 2003. Orientation of asymmetric stem cell division by the APC tumor suppressor and centrosome. *Science*. 301:1547–50. doi:10.1126/science.1087795.

Yamashita, Y.M., A.P. Mahowald, J.R. Perlin, and M.T. Fuller. 2007. Asymmetric inheritance of mother versus daughter centrosome in stem cell division. *Science*. 315:518–21. doi:10.1126/science.1134910.

Yang, X.-R., Y. Xu, B. Yu, J. Zhou, S.-J. Qiu, G.-M. Shi, B.-H. Zhang, W.-Z. Wu, Y.-H. Shi, B. Wu, G.-H. Yang, Y. Ji, and J. Fan. 2010. High expression levels of putative hepatic stem/progenitor cell biomarkers related to tumour angiogenesis and poor prognosis of hepatocellular carcinoma. *Gut*. 59:953–62. doi:10.1136/gut.2008.176271.

Ye, M., T. Huang, C. Ni, P. Yang, and S. Chen. 2017. Diagnostic Capacity of RASSF1A Promoter Methylation as a Biomarker in Tissue, Brushing, and Blood Samples of Nasopharyngeal Carcinoma. *EBioMedicine*. 18:32–40. doi:10.1016/j.ebiom.2017.03.038.

Ying, Q.-L., J. Wray, J. Nichols, L. Batlle-Morera, B. Doble, J. Woodgett, P. Cohen, and A. Smith. 2008. The ground state of embryonic stem cell self-renewal. *Nature*. 453:519–523. doi:10.1038/nature06968.

Yuan, K., N. Frolova, Y. Xie, D. Wang, L. Cook, Y.-J. Kwon, A.D. Steg, R. Serra, and A.R. Frost. 2010. Primary Cilia Are Decreased in Breast Cancer: Analysis of a Collection of Human Breast Cancer Cell Lines and Tissues. *J. Histochem. Cytochem.* 58:857–870. doi:10.1369/jhc.2010.955856.

Zack, T.I., S.E. Schumacher, S.L. Carter, A.D. Cherniack, G. Saksena, B. Tabak, M.S. Lawrence, C.-Z. Zhang, J. Wala, C.H. Mermel, C. Sougnez, S.B. Gabriel, B. Hernandez, H. Shen, P.W. Laird, G. Getz, M. Meyerson, and R. Beroukhim. 2013. Pan-cancer patterns of somatic copy number alteration. *Nat. Genet.* 45:1134–1140. doi:10.1038/ng.2760.

Zhang, C.-Y., Y.-X. Zhao, R.-H. Xia, J. Han, B.-S. Wang, Z. Tian, L.-Z. Wang, Y.-H. Hu, and J. Li. 2014. RASSF1A Promoter Hypermethylation Is a Strong Biomarker of Poor Survival in Patients with Salivary Adenoid Cystic Carcinoma in a Chinese Population. *PLoS One*. 9:e110159. doi:10.1371/journal.pone.0110159.

Zhang, N., H. Bai, K.K. David, J. Dong, Y. Zheng, J. Cai, M. Giovannini, P. Liu, R.A. Anders, and D. Pan. 2010. The Merlin/NF2 Tumor Suppressor Functions through the YAP

Oncoprotein to Regulate Tissue Homeostasis in Mammals. *Dev. Cell*. 19:27–38. doi:10.1016/j.devcel.2010.06.015.

Zhang, W., and H.T. Liu. 2002. MAPK signal pathways in the regulation of cell proliferation in mammalian cells. *Cell Res.* 12:9–18. doi:10.1038/sj.cr.7290105.

Zhao, B., X. Wei, W. Li, R.S. Udan, Q. Yang, J. Kim, J. Xie, T. Ikenoue, J. Yu, L. Li, P. Zheng, K. Ye, A. Chinnaiyan, G. Halder, Z.-C. Lai, and K.-L. Guan. 2007. Inactivation of YAP oncoprotein by the Hippo pathway is involved in cell contact inhibition and tissue growth control. *Genes Dev.* 21:2747–61. doi:10.1101/gad.1602907.

Zhao, J., Y. Ren, Q. Jiang, and J. Feng. 2003. Parkin is recruited to the centrosome in response to inhibition of proteasomes. *J. Cell Sci.* 116:4011–4019. doi:10.1242/jcs.00700.

Zheng, X., Q. Dong, X. Zhang, Q. Han, X. Han, Y. Han, J. Wu, X. Rong, and E. Wang. 2017. The coiled-coil domain of oncogene RASSF 7 inhibits hippo signaling and promotes non-small cell lung cancer. *Oncotarget*. 8:78734–78748. doi:10.18632/oncotarget.20223.

Zhong, W., J.N. Feder, M.-M. Jiang, L.Y. Jan, and Y.N. Jan. 1996. Asymmetric Localization of a Mammalian Numb Homolog during Mouse Cortical Neurogenesis. *Neuron*. 17:43–53. doi:10.1016/S0896-6273(00)80279-2.